Characterisation of a gene encoding a transcript localised during oogenesis in *Drosophila melanogaster*

Angela M^{c}Cormack

Thesis presented for the degree of PhD

University of Edinburgh

1998

Abstract

The processes and interactions involved in oogenesis, the formation of the oocyte, are a fundamental concern of developmental biology. The accessible genetics and manipulability of the fruit fly *Drosophila melanogaster* make it an ideal organism in which to study the cellular and molecular events of oogenesis. In this lab a P-element enhancer trap approach was adopted to identify genes with interesting spatial and temporal expression patterns during oogenesis. In the course of such an enhancer trap screen, a cDNA was isolated which corresponded to a transcript which was localised during oogenesis but which was unrelated to any enhancer trap pattern. The transcript was localised to the oocyte from the early stages of oogenesis, then became localised within the oocyte as a band at the anterior cortex. In late stage egg chambers the transcript was expressed strongly in the degenerating nurse cells then transported to the oocyte so that anterior localisation was lost. The localisation of maternal transcripts is known to play an important role in axis determination and pattern formation of the developing oocyte and embryo, so it was important that this transcript and its corresponding gene should be studied further. The entire gene was subsequently cloned and sequenced and found to encode a class V unconventional myosin and was therefore termed *myosinV*.

A developmental profile indicated that the *myosinV* transcript was also present in testes and early embryos. The early embryo transcript was initially presumed to be maternally encoded transcript, laid down during oogenesis. *in situ* hybridisation revealed that the transcript was distributed throughout early embryos but was concentrated at sites of epithelial morphogenesis. The testes transcript was smaller than the ovarian transcript and was localised to the developing sperm heads. The expression of the gene in only the germ line cells of the ovary and the testes suggested that expression was germ line specific, however, an RT-PCR approach identified low levels of the transcript in other tissues.

Much of the work of this project focused on the localisation of the *myosinV* transcript. In an attempt to establish the position of the gene within the genetic

pathways of oogenesis, the localisation pattern of the transcript was assessed in flies mutant for genes involved in various aspects of oogenesis. The correct localisation of the *myosinV* transcript was found to require genes involved in oocyte determination, anterior patterning, posterior patterning, and also neurogenic genes involved in oocyte-follicle cell signalling.

The localisation of maternal transcripts has been found in several instances, to depend on a signal in the 3'UTR of the transcript. A P-element mediated germline transformation approach was used to determine whether the 3'UTR of the *myosinV* transcript was capable of directing localisation. Work presented in this thesis indicates that the *myosinV* 3'UTR does not direct transcript localisation. However, localisation was found to depend upon the integrity of the microtubules.

The *myosinV* gene had previously been located to position 43BC on the right arm of the second chromosome. A genetic analysis of the *myosinV* gene suggested that it corresponds to *l(2)43Cc*, a locus identified as having several embryonic lethal alleles. The embryonic lethal phenotype indicates that there must normally be some transcription from the zygotic genome. The arrested embryos show segmentation defects in the dorsal region of the embryos due to a failure in dorsal closure. These dorsal closure defects suggest that the MyosinV protein might be required for epithelial morphogenesis.

In the course of studying the *myosinV* gene, two other genes were identified - one encoding a putative zinc finger transcriptional regulator and the other encoding a putative sodium-dependent inorganic phosphate cotransporter. The isolation and preliminary characterisation of these genes will also be discussed.

Acknowledgements

I would like to thank my supervisor, Professor Mary Bownes for her advice and encouragement throughout the course of this PhD. I would also like to thank all members of the Bownes group, past and present, especially Bryce, Kathleen, Diane, Debbie, Colin, Claudia, Simone and Debiao for their help and friendship. Thanks are also due to the support staff at ICMB, in particular to Frances for providing flyfood and to Helen for providing plenty of clean glassware. I also wish to acknowledge those outside Edinburgh who provided me with plasmids, fly stocks and advice, in particular John Roote and Kellie Whittaker. I am grateful to those who helped me put this thesis together, especially Kathleen for being an endless source of information, Nigel for his expert computing assistance and Irene whose PC I borrowed for slightly longer than anticipated. I want to thank all the friends and flatmates who helped make my time in Edinburgh so enjoyable, especially my partners in crime, Kerrie and Jill. Thanks also to all the friends whom I've neglected while I've been writing up. I want to say a special thank you to my husband Neil, who was crazy enough to marry a PhD student - I don't know how I would have got through without all his love, understanding and cups of tea! Finally, I would like to thank my family for their support, both emotional and financial, throughout my long years as a student, and for their love and encouragement at all times.

List of Abbreviations

A	adenine
amp	ampicillin
AP	alkaline phosphatase
ATP	adenosine-5'-triphosphate
bp	base pair
C	cytosine
°C	degrees Celcius
cDNA	complementary DNA
Ci	Curies
cm	centimetre
(d)dATP	2'(3'-di) deoxyadenosine-5'-triphosphate
(d)dCTP	2'(3'-di) deoxycytosine-5'-triphosphate
(d)dGTP	2'(3'-di) deoxyguanosine-5'-triphosphate
(d)dTTP	2'(3'-di) deoxythymidine-5'-triphosphate
dH_2O	distilled water
DNA	deoxyribonucleic acid
DNase	deoxyribonuclease
dNTP	deoxyribonucleotide-5'-triphosphate
DTT	dithiothreitol
EDTA	ethylene diaminetetra-acetic acid
EGTA	ethylene glycol tetra acetic acid
fs	female sterile
g	gram
G	guanine
HEPES	N-(2-Hydroxyethyl)piperazine-N'-(2-ethanesulphonic acid)
HRP	horse radish peroxidase
IPTG	isopropyl-β-D-thio-galactopyranoside

kb	kilobase
λ	Lambda bacteriophage
l	litre
LB	Luria broth
μCi	microCurie
μg	microgram
μl	microlitre
μM	micromolar
M	molar
mg	milligram
min	minutes
ml	millilitre
mM	millimolar
mol	moles
MOPS	morpholinepropanesulphonic acid
mRNA	messenger ribonucleic acid
ng	nanogram
OD	optical density
p	prefix for plasmid
pmol	picomoles
PBS	phosphate buffered saline
PCR	polymerase chain reaction
pfu	plaque forming units
PIPES	piperazinediethanesulphonic acid
polyA$^+$ RNA	polyadenylated ribonucleic acid
psi	pounds per square inch
RNA	ribonucleic acid
RNase	ribonuclease
rpm	revolutions per minute
RT	reverse transcriptase
SDS	sodium dodecyl sulphate

sec	seconds
T	Thymine
TEMED	tetraethylmethylenediamine
Tris	Tris (hydroxymethyl) aminomethane
U	Uracil
UTR	untranslated region
UV	ultraviolet
X-Gal	5-bromo-4-chloro-3-indolyl-β-galactopyranoside
Y	thymine or cytosine

Table of Contents

Chapter 1

Introduction

1.1 Introduction

Oogenesis is the process by which an oocyte, or egg cell is formed. The oocyte is commonly the largest and most complex cell a given species can produce and often contains all the information and components necessary for growth and pattern formation in the early embryo. The events involved in oogenesis are therefore of fundamental concern to developmental biology.

During embryonic development of the fruit fly *Drosophila melanogaster*, there is no significant transcription from the zygotic genome until the formation of the blastoderm. At the point of fertilisation, the oocyte must therefore already contain all the RNA, protein and positional information essential for pre-blastoderm development, which includes axis specification, germ cell determination and 13 rounds of mitotic division. The accessible genetics and manipulability of *Drosophila* make it an ideal organism in which to study the cellular and molecular interactions involved in the formation of the oocyte.

1.2 Morphology of *Drosophila* Oogenesis

The morphology of oogenesis has been described in detail by King (1970) and reviewed in Bownes and Dale (1982). *Drosophila* adult females have a pair of ovaries connected to a common oviduct. Each ovary contains 15-20 ovarioles, consisting of a succession of egg chambers increasing in developmental age as they pass from germarium to oviduct (fig 1.1). The ovaries are surrounded by the peritoneal sheath - a network of muscle fibres which contract rhythmically to push the developing egg chambers posteriorly towards the oviduct. The germarium is at the anterior tip of each ovariole and contains two to four stem cells (Weischaus and Szabad, 1979). Each stem cell can divide producing a daughter cell and a cystoblast. The cystoblast divides a further four times with incomplete cytokinesis to produce a

16 cell cyst inter-connected with cytoplasmic bridges or ring canals. Only two of these cystocytes have the maximum of four ring canals and it is always one of these cells which becomes the oocyte (Koch *et al*, 1967), while the remaining 15 cystocytes become nurse cells. These 16 cells become surrounded by a layer of somatically derived follicle cells to form an egg chamber.

The pro-oocyte normally takes up position as the most posterior germ-line cell in the egg chamber (Koch *et al*, 1967). Newly formed egg chambers leave the germarium and are connected to each other by short chains of follicular stalk cells as they mature and progress towards the oviduct. The 15 nurse cells become polyploid and can replicate up to 2096 copies of their DNA as they produce large quantities of RNA and protein to be transferred to the growing oocyte via the ring canals. The extent of the polyploidism is graded such that those cells closest to the oocyte undergo more rounds of replication and so contribute more gene products to the developing oocyte than those further away (Jacob and Sirlin, 1959). The follicle cells also become polyploid in the later stages of oogenesis.

The developing egg chambers have been divided into 14 distinct morphological stages (King, 1970) (fig 1.1). The oocyte increases in size around 10 000 fold during the 14 stages. In stage 1-7 egg chambers the nurse cells and the oocyte are of similar size, however at stage 8, vitellogenesis or the process of yolk deposition begins. Yolk proteins are synthesised by the fat body and the follicle cells and secreted into the haemolymph. The oocyte takes up the yolk proteins by pinocytosis from the haemolymph, causing a dramatic increase in oocyte volume between stages 8 and 10.

The follicle cells undergo their own complex series of morphological movements during oogenesis. The stage 1 egg chamber is surrounded by around 80 follicle cells. From stages 2-5 the follicle cells proliferate to produce around 1200 cells which at stages 6 and 7 form a continuous sheath around the egg chamber. From stages 7-13 the follicle cells migrate such that the oocyte becomes completely surrounded by

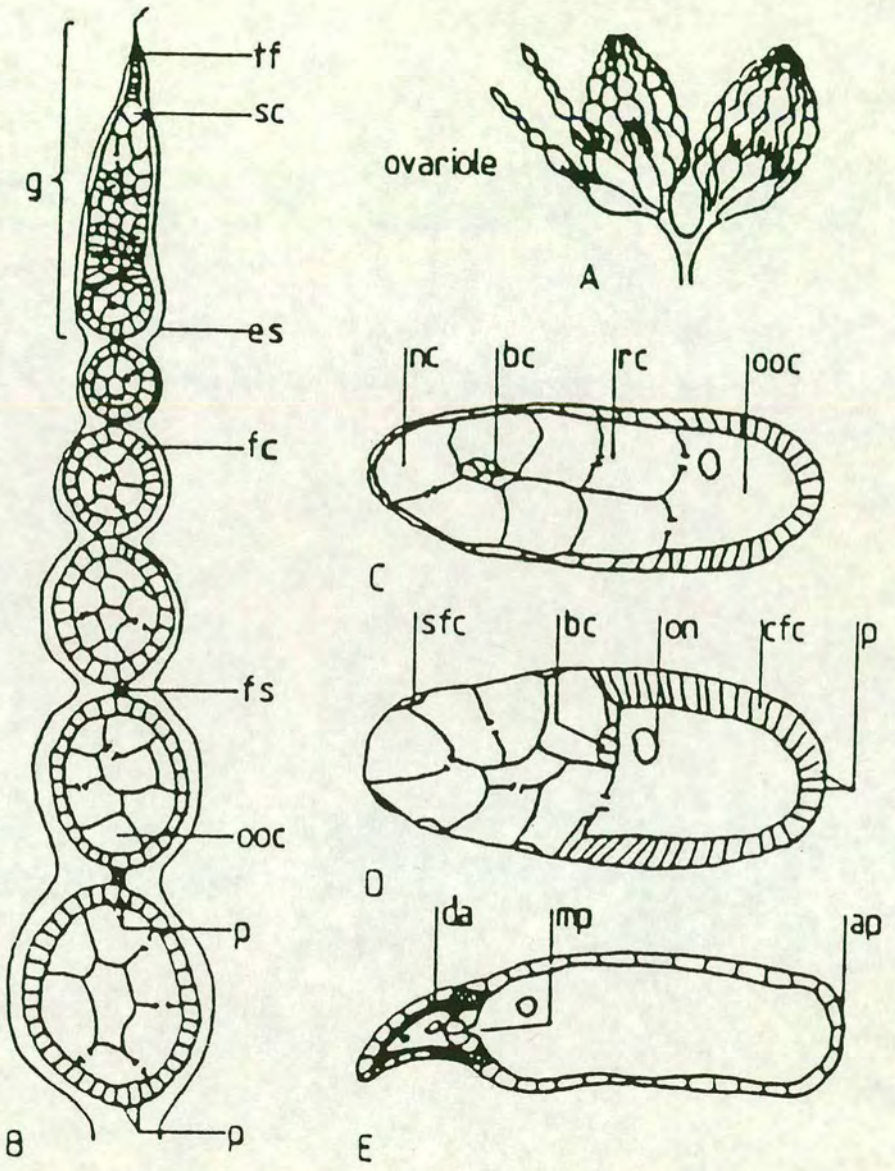

Figure 1.1 A) Pair of *Drosophila* ovaries showing two separated ovarioles. B) Pre-vitellogenic stages of oogenesis. C) Stage 9 egg chamber. D) Stage 10 egg chamber. E) stage 13 egg chamber. g: germarium, tf: terminal filament, sc: stem cell, es: epithelial sheet, fc: follicle cell, ooc: oocyte, p: polar cells, nc: nurse cells, bc: border cells, rc: ring canal, sfc: squamous follicle cell, on: oocyte nucleus, cfc: columnar follicle cell, da: dorsal appendages, mp: micropyle, ap: aeropyle. From King (1970).

columnar follicle cells, while only a few squamous follicle cells remain associated with the nurse cells. At stage 9, a group of six to ten follicle cells originally located at the anterior of the egg chamber, leave the monolayer and migrate posteriorly through the nurse cells to form the anterior border cells. These then migrate dorsally along the nurse cell - oocyte border and come to lie opposite the oocyte nucleus where they are later involved in the formation of the micropyle (King and Koch, 1963).

Around stages 9 and 10 the polar granules become distinguishable. These are complexes of RNA and protein in the cytoplasm at the posterior pole of the oocyte. After fertilisation, any nuclei entering this region of cytoplasm are induced to become germ cells (Illmensee *et al*, 1976).

Also at stages 9 and 10 the follicle cells surrounding the oocyte secrete the vitelline membrane - the inner protective layer of the egg. The uptake of yolk by the oocyte ceases as the vitelline membrane is completed. From stage 10b the nurse cells rapidly transfer almost their entire cytoplasmic contents into the oocyte via the ring canals. Meanwhile from stages 11 to 14 the follicle cells secrete the chorion including two specialised anterior structures - the micropylar apparatus to allow sperm entry and the dorsal appendages which facilitate embryonic respiration. As the chorion is completed the follicle cells and nurse cells degenerate leaving behind the mature egg.

1.3 Molecular Genetics of Drosophila Oogenesis

1.3.1 Introduction

Oogenesis in *Drosophila* is a complex process which involves the determination of cell type, cell to cell signalling, axis specification, intercellular and intracellular transport and the establishment of positional information. The genetic interactions which underlie the events of oogenesis have long been the focus of intensive research.

The application of modern molecular techniques has greatly advanced the study of oogenesis with the result that some of the molecular genetic events of oogenesis are now well understood. Presented below is a review of those areas of oogenesis relevant to the work of this thesis. A fully comprehensive review of the molecular genetics of *Drosophila* oogenesis can be found in Lasko (1994).

1.3.2 Screens for Genes Involved in Oogenesis

A number of extensive genetic screens have been performed in *Drosophila* to identify mutations which affect oogenesis (e.g. Bakken, 1973; Gans *et al*, 1975; Mohler, 1977; Schupbach and Weischaus 1986, 1989, 1991). Mutations affecting genes specifically involved in oogenesis result in one of two phenotypes, (i) female sterility, where either egg production is abortive or the eggs that are produced are defective and so cannot be fertilised, or (ii) maternal-effect lethality, where eggs are laid and fertilised but lack maternal components necessary for normal development so that the resultant embryos develop abnormally and do not reach adulthood. As a result of such screens many of the genes involved in oogenesis have been identified and characterised. For example, many of the genes involved in establishing the anterioposterior and dorso-ventral polarities of the embryo have been identified in genetic screens for maternal effect mutations that alter the cuticular pattern of the first instar larvae (e.g. Schupbach and Wieschaus, 1986; Frohnhofer and Nusslein-Volhard, 1986). Some of these genes will be discussed in sections 1.3.4 and 1.3.5.

Mutations in approximately 400 *Drosophila* genes have been reported which result in female sterility or maternal-effect lethality (reviewed in Lasko, 1994). A number of researchers have posed the question of how many genes in total are required for oogenesis. On the basis of an extensive analysis of the second chromosome for female sterile and maternal-effect mutations, Schupbach and Wieschaus (1989, 1991) calculate that approximately 300 genes are exclusively required for oogenesis. However, many of the genes involved in oogenesis are also required throughout

development and are therefore essential for viability (Perrimon *et al*, 1986). The generation of germ-line mosaics to screen for zygotic lethals with maternal-effect lethal phenotypes led Chou and Perrimon (1992) to suggest that an additional 800 essential loci are required maternally for specific events in oogenesis or embryogenesis.

Genes which are required for oogenesis but which have earlier essential functions may not be recognised by classical genetic screens because mutations in such genes will cause homozygous females to die before reaching adulthood so the effects on oogenesis and subsequent embryonic development cannot be assessed. These essential genes will only be picked up in genetic screens for female sterile mutants if they have hypomorphic alleles that affect oogenesis. Classical genetic screens will also fail to detect genes with redundant functions as mutations will be complemented by other genes such that no phenotype is observed. A further limitation of the classical genetic screen is the difficulty in assigning a functional role to a gene when its mutation results in a phenotype which cannot easily be interpreted. A comprehensive analysis of the genes involved in oogenesis therefore requires a screening method which is not primarily based on the recognition of a mutant phenotype.

1.3.2.1 Enhancer-Trap Analysis

An alternative method for the investigation of genes involved in *Drosophila* oogenesis is the reverse genetic approach of enhancer-trap analysis or P-element mediated enhancer detection (O'Kane and Gehring, 1987). In this technique, a P-element in which the *transposase* gene has been replaced by the *E.coli lacZ* reporter gene, is introduced into the *Drosophila* genome by germline transformation. The P-element is subsequently mobilised by crossing the transformed flies to other flies carrying a P-element which produces active transposase but has defective ends so cannot itself transpose. The transposing P-element is stably and heritably integrated at random

sites in the genome of the resulting progeny. The *lacZ* gene is under the control of the P-element promoter, which is constitutive but weak, giving a low background level of expression in all cells throughout development. However, if the P-element inserts in close proximity to a *Drosophila* enhancer element, then the pattern of expression of the reporter gene will reveal the spatial and temporal expression of the gene normally under the influence of that enhancer. The expression of *lacZ* can be easily assayed by histochemical staining for its product - β-galactosidase. Those fly lines which show a developmentally interesting pattern of *lacZ* expression can be selected and the P-element used as a tag to clone the corresponding gene from flanking sequences. Enhancer-trap analysis is therefore termed a reverse genetic approach in that a gene can be cloned and sequenced without any knowledge of its mutant phenotype.

A number of studies have validated the enhancer trap approach. In a study by Bellen *et al* (1989), on over 500 lines carrying single P-element insertions, 65% of insertion strains (or transposants) showed some degree of specific embryonic staining. P-element insertion was found to occur at diverse locations to produce a wide array of spatially and temporally regulated β-gal staining patterns, with a large fraction of transposants showing complex expression patterns in the embryonic nervous system. In a number of transposants specific internal tissues or cells were stained, allowing the potential study of previously inaccessible embryonic structures. In some cases the β-gal expression patterns were found to correlate well with the expression patterns of genes which map nearby, indicating that the detected regulatory elements do control nearby genes. Wilson *et al* (1989) confirmed this at the molecular level by using genomic DNA flanking the inserted P-elements as probes for *in situ* hybridisation to gene transcripts in the embryo. In a number of cases studied, the β-gal staining pattern was indeed found to match the expression pattern of the flanking gene as revealed by *in situ* hybridisation.

Grossniklaus *et al* (1989) applied P-element mediated enhancer detection to the study of oogenesis. Over 600 independent lines were screened for their *lacZ* expression

pattern and ~47% were found to show β-gal staining in one or more ovarian cell. The majority of these staining patterns were spatially and temporally regulated throughout oogenesis. Several expression patterns revealed differences between morphologically indistinguishable cells indicating that all nurse cells are not transcriptionally equivalent and that subsets of follicle cells are functionally different to their neighbours. A number of insertion-linked mutants that were either sterile or aberrant in oogenesis were also identified in the screen and a correlation was noted between these mutations affecting oogenesis and a specific β-gal expression in the nurse cells.

The enhancer trap approach has made it possible to identify genes required for oogenesis without knowledge of mutant phenotype and even when the genes have earlier essential functions. A further advantage of the enhancer trap is that mutations can subsequently be generated in identified genes by local P-element hopping to cause insertional inactivation or by imprecise excision (Zhang and Spradling, 1993). A second generation of enhancer trap elements have provided an even more potent tool for the analysis of identified genes (Brand and Perrimon, 1993). This system employs two P-elements, one encoding the yeast transcriptional activator GAL4 and a secondary reporter element in which the *lacZ* gene is placed under the control of a GAL4 dependent promoter. Activation of the GAL4 by a nearby enhancer element results in expression of the reporter gene in a pattern reflecting enhancer activity. The advantage of the GAL4 system is that the secondary reporter gene can be replaced by sequences encoding toxins for targeted cell killing or by antisense constructs which specifically prevent translation. An existing bank of GAL4 lines allows the potential for targeted gene expression in a wide range of spatially and temporally specific patterns.

1.3.3 Oocyte determination

Determination of the *Drosophila* oocyte occurs within the germarium (fig 1.2). The germarium can be divided into four cytologically distinct regions of sequential

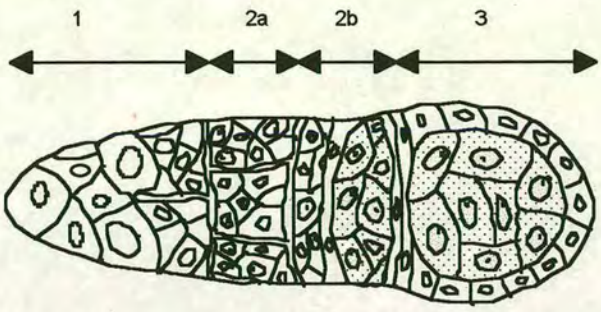

Figure 1.2 The Drosophila germarium – subdivided into its four regions. After Christerson and McKearin, (1994).

development - region 1, region 2a, region 2b and region 3 (Koch and King, 1966; Mahowald and Kambysellis, 1980). Oogenesis begins in region 1 with the asymmetric division of a germline stem cell to produce another stem cell and a cystoblast. The cystoblast undergoes a further four synchronous rounds of mitotic divisions, characterised by incomplete cytokinesis, to produce a 16 cell cyst interconnected by the ring canals. In region 2a, somatically derived follicle cells start to migrate around the newly formed 16 cell cysts. By region 2b, one cell of the 16 cell cyst has been determined as the oocyte while the remaining 15 become nurse cells. At this stage the oocyte is morphologically distinct from the nurse cells and has a characteristic position at the centre of the lens shaped cyst (Koch *et al*, 1967). By germarial region 3 the oocyte is located at the posterior of the cyst which has become surrounded by a monolayer of follicle cells to form a stage 1 egg chamber.

The pattern of the four incomplete cystoblast divisions is highly ordered leading to the production of a 16 cell cyst containing two cells with four ring canals, two cells with three ring canals, four cells with two ring canals and eight cells with a single ring canal. It is always one of the cells with four ring canals that becomes the oocyte (Koch *et al*, 1967) indicating that specification of the oocyte is linked to this cystocyte

division pattern. The precise geometry of the cystoblast divisions appears to depend on a structure called the fusome (Storto and King, 1989). The fusome is composed of mitotic spindle remnants arising from the four rounds of cystoblast division. At the completion of each division, spindle residues fuse with the remnants from previous mitoses to form a continuous branching network that passes through and completely fills each ring canal within region 1 cysts. The fusome forms a region of cytoplasm rich in vesicles and membrane-associated cytoskeletal proteins but deficient in ribosomes and mitochondria. During each mitosis, the association of the fusome with one spindle pole of the dividing cystoblast determines the mitotic cleavage plane. The fusome therefore directly influences the geometry of cystoblast division and the development of asymmetry within the cyst that leads to oocyte determination (Lin *et al*, 1994).

One component of both the ring canals and fusome is the product of the *hu-li tai shao* gene (Yue and Spradling, 1992), also known as *Adducin-like* (Ding *et al*, 1993a). The *hu-li tai shao* gene encodes a homologue of the mammalian cytoskeletal protein adducin, which promotes the association of F-actin and spectrin (Mische *et al*, 1987). *hu-li tai shao* mRNA is first readily detectable in region 2b of the germarium and accumulates within the oocyte in stage 2 - 5 egg chambers. From stage 6, the mRNA is localised to the anterior margin of the oocyte dependent on the function of the *swallow* gene (Ding *et al*, 1993a). Mutations in *hu-li tai shao* completely eliminate the fusome resulting in abnormal cysts containing an average of four cells and only rarely do one of these differentiate into an oocyte (Lin *et al*, 1994). In addition, *hu-li tai shao* mutant egg chambers have no actin on their ring canals (Yue and Spradling, 1992).

The formation of the 16 cell cyst and subsequent differentiation of the oocyte requires the function of the *orb* gene (Lantz *et al*, 1994). *orb* encodes a germ-line specific RNA binding protein that is also required for anterioposterior and dorsoventral patterning (Lantz *et al*, 1992; Christerson and McKearin, 1994). Both the *orb* transcript and Orb protein preferentially accumulate in the presumptive oocyte of

region 2 cysts (Lantz *et al*, 1992, 1994). In the most severe mutant alleles of *orb*, cystoblast division arrests at the 8 cell stage and the cells then degenerate rather than differentiate. In weaker alleles, the 16 cell cyst is formed and oocyte differentiation is initiated but several mRNAs fail to properly localise to the presumptive oocyte. Furthermore, the presumptive oocyte fails to localise to the posterior of the cyst and overall morphology becomes aberrant leading to an arrest in development. This phenotype is consistent with a role for *orb* in the localisation of mRNAs whose proteins mediate the reorganisation and further differentiation of the oocyte (Lantz *et al*, 1994).

The differentiation of one of the four ring canal cells of the 16 cell cyst into the oocyte appears to depend on the formation of a polarised microtubule cytoskeleton and the accumulation of several maternal mRNAs within the pro-oocyte. Within region 2a, a prominent microtubule organising centre (MTOC) is established within the pro-oocyte and a single microtubule network extends through the ring canals into all the nurse cells (Theurkauf *et al*, 1993). Treatment of flies with the microtubule depolymerising drug colchicine disrupts the formation of this MTOC and polarised cytoskeleton and results in the production of egg chambers that contain 16 nurse cells and no oocyte. The germline microtubule cytoskeleton therefore appears to play a critical role in oocyte differentiation. Time course studies with microtubule inhibitors indicate that the functional requirement for microtubules in oocyte differentiation is specific to germarial region 2 and is therefore temporally correlated with the morphological differentiation of the pro-oocyte from the nurse cells (Theurkauf *et al*, 1993).

Two genes, *Bicaudal-D* and *egalitarian*, have been identified as being specifically required for oocyte differentiation (Mohler and Weischaus, 1986; Schupbach and Weischaus, 1991) and appear to be involved in formation and maintenance of the polarised microtubule cytoskeleton (Theurkauf *et al*, 1993). Recessive mutations in either of these loci result in female sterility because of the formation of egg chambers with 16 nurse cells and no oocyte. In *egalitarian* mutant germaria, reorganisation of the microtubules is initiated normally to form an MTOC in a single cell of a region 2a

cyst, however, this MTOC is unstable and breaks down with the result that microtubules are evenly distributed in region 2b and 3 cysts. This indicates that the establishment and maintenance of the polarised microtubule array are two independent processes and that *egalitarian* function is not required for MTOC establishment but is required for maintenance in region 2b and later cysts (Theurkauf *et al*, 1993).

In contrast, *Bic-D* function appears to be required to initiate microtubule reorganisation in region 2a cysts. Recessive mutations in *Bic-D* block establishment of the MTOC and polarised microtubule array and ultimately lead to the failure of oocyte differentiation (Theurkauf *et al*, 1993). *Bic-D* has been shown to encode a protein with an extensive region of coiled-coil α-helix, similar to the tail regions of kinesin and type II myosins (Wharton and Struhl, 1989; Suter *et al*, 1989). *Bic-D* mRNA and the Bicaudal-D protein both accumulate in the pro-oocyte of region 2a cysts. Localisation of *Bic-D* mRNA to the pro-oocyte requires the function of the *Bic-D* gene itself as its accumulation is abolished in 16-nurse cell *Bic-D* mutants (Suter and Steward, 1991). Phosphorylation of the Bicaudal-D protein appears to be important for its localisation to the pro-oocyte as a mutation in *Bic-D* that abolishes phosphorylation of its protein results in no accumulation in the pro-oocyte and a consequent failure of oocyte differentiation (Suter and Steward, 1991). In $Bic\text{-}D^{R26}$ mutant germaria, although establishment of the polarised microtubule array is blocked, initial oocyte specification appears to take place in that both *oskar* mRNA and mutant Bicaudal-D protein accumulate in a single cell of each cyst (Suter and Steward, 1991). This indicates that microtubule reorganisation is downstream of initial oocyte specification and that a polarised microtubule cytoskeleton is not required for the localisation of Bicaudal-D protein.

Based on the data presented above, a three step model has been proposed for oocyte differentiation (Theurkauf *et al*, 1993; Cooley and Theurkauf, 1994). Firstly, an initial asymmetry is established within the cyst which specifies the cytoplasmic compartment that will form the oocyte. This step is thought to occur during the cystoblast divisions under the influence of the fusome. Secondly, the germline microtubules reorganise to

form a polarised array with the MTOC in the pro-oocyte. Establishment of this polarised array requires *Bic-D* function while its maintenance requires *egalitarian* function. Thirdly, mRNAs and proteins are transported to the oocyte along the polarised microtubule cytoskeleton where their accumulation ultimately leads to the biochemical and cytological differentiation of the oocyte.

1.3.4 Axis determination

1.3.4.1 Dorso-ventral axis

Signalling between the oocyte and the follicle cells has long been known to be a crucial factor in specifying the dorso-ventral (DV) axis of the *Drosophila* oocyte and embryo (Schupbach, 1987; reviewed in Morisato and Anderson, 1995). Using genetic mosaics, Schupbach (1987) demonstrated that dorsal follicle cell fate and the dorso-ventral pattern of the embryo depend on the function of the *torpedo* gene in the follicle cells. The *torpedo* gene encodes the *Drosophila* homologue of the vertebrate epidermal growth factor (EGF) receptor - a membrane bound tyrosine kinase (Price *et al*, 1989). Function of the *gurken* gene is required in the germ-line where it encodes a transforming growth factor (TGF)-α-like protein (Neuman-Silberberg and Schupbach, 1993). Dorsally localised Gurken protein is proposed to directly bind to the Torpedo EGF receptor in the adjacent follicle cells to activate a receptor tyrosine kinase signal transduction pathway that results in the cells taking a dorsal pathway of development rather than the default ventral pathway (Neuman-Silberberg and Schupbach, 1993; Brand and Perrimon, 1994). The polarised follicle cells subsequently signal back to the germ line to establish the dorso-ventral axis of the embryo (Chasan and Anderson, 1993). Mutations in both *gurken* and *torpedo* cause all of the follicle cells to adopt a ventral fate leading to the development of eggs with ventralised chorions which, if fertilised, give rise to ventralised embryos.

Localisation of *gurken* mRNA appears to be crucial for defining the dorso-ventral

polarity of the egg and embryo. *gurken* mRNA is localised to the oocyte beginning in germarial region 2b, then from stages 1-7 is concentrated to the oocyte's posterior end (Neuman-Silberberg and Schupbach, 1993). At stage 8 the oocyte's microtubule cytoskeleton re-organises to form a polarised array with the plus end extending towards the posterior (Theurkauf *et al*, 1992). Soon thereafter, the oocyte nucleus moves from the posterior to the anterio-dorsal corner of the oocyte - the first visible dorso-ventral asymmetry in the egg chamber (Mahowald and Kambysellis, 1980). Around this time *gurken* mRNA relocalises first to the anterior margin of the oocyte, then by stage 9 becomes spatially restricted to the anterio-dorsal side of the oocyte nucleus (Neuman-Silberberg and Schupbach, 1993). Translation of this spatially restricted mRNA results in dorsally localised Gurken protein which signals to the adjacent follicle cells to adopt a dorsal fate.

The final stage of *gurken* mRNA localisation to the anterio-dorsal corner of the oocyte requires the function of the *cappuccino*, *spire*, and *fs(1)K10* genes (Neuman-Silberberg and Schupbach, 1993). Mutations in any of these genes causes *gurken* mRNA to remain in a ring at the anterior margin of the oocyte rather than localise to the anterio-dorsal corner. This failure to restrict the Gurken signal leads to dorsalisation of all the follicle cells - the opposite phenotype to that caused by mutations in *gurken* or *torpedo*. *fs(1)K10* encodes a protein that bears homology to DNA and RNA binding proteins and which is confined to the interior of the oocyte nucleus where it proposed to activate an anchor for *gurken* mRNA (Serano *et al*, 1995). Mutations in *cappuccino* and *spire* lead to missing abdominal segments and lack of pole cells in addition to dorsalisation, indicating that these genes are also involved in posterior patterning (Manseau and Schupbach, 1989). *cappuccino* has recently been cloned and found to be closely related to the vertebrate limb deformity locus and to share regions of homology with pattern formation genes of yeast and *Aspergillus* (Emmons *et al*, 1995). The phenotypes of *cappuccino* and *spire* mutants have been proposed to be due to the displacement of localised mRNAs as a result of the premature initiation of microtubule-based cytoplasmic streaming which occurs in these mutants (Theurkauf *et al*, 1994b). However, the premature induction of

cytoplasmic streaming in wild-type oocytes has revealed that cytoplasmic streaming is sufficient to displace Staufen protein from the posterior pole but not sufficient to displace *gurken* mRNA from around the nucleus, suggesting that *cappuccino* and *spire* play some other role in gurken mRNA localisation (Emmons *et al*, 1995).

A maternal effect lethal allele of *orb* also prevents the final stage of *gurken* mRNA localisation but interestingly leads to a ventralised phenotype (Christerson and McKearin, 1994). *orb* encodes an RNA binding protein which is also required for RNA localisation events during oocyte determination and posterior patterning, thus mutations in *orb* lead to a complex phenotype (Lantz *et al*, 1994).

1.3.4.2 Anterior-posterior axis

The anterior-posterior (AP) axis of the *Drosophila* embryo is established during oogenesis by the localisation of the mRNAs for the anterior determinant *bicoid* and the posterior group gene *oskar* to opposite poles of the oocyte (reviewed in St Johnstone and Nusslein-Volhard, 1992; see also 1.3.5). The transport and anchoring of these mRNAs is dependent on the oocyte's microtubule cytoskeleton which, at the time these mRNAs first localise, displays a clear AP asymmetry with the microtubules nucleating at the anterior of the oocyte and extending their plus ends towards the posterior pole (Theurkauf *et al*, 1992; see also 1.4.3.3). Anterior-posterior polarity within the oocyte is therefore defined by the organisation of its microtubule cytoskeleton.

Anterior-posterior polarity was initially proposed to originate in the follicle cells because loss of *Notch* or *Delta* function in the follicle cells results in oocytes with two anterior poles such that *bicoid* mRNA accumulates at both ends of the oocyte whereas *oskar* mRNA and Staufen protein mislocalise to the centre of the oocyte (Ruohola *et al*, 1991). Gonzalez-Reyes and St Johnston (1994) subsequently proposed that AP polarity arises with the movement of the oocyte to the posterior of

the 16 cell cyst, the first visible asymmetry in egg chamber development. They demonstrated that in *spindle-C* mutant egg chambers, where the oocyte fails to move to the posterior and instead remains in the centre of the nurse cells to form bipolar egg chambers, the posterior follicle cells duplicate the behaviour of the anterior follicle cells by forming border cells, centripetal cells and a second micropyle. These results indicate that the position of the oocyte at the posterior of the egg chamber is required for acquisition of posterior follicle cell fate. Furthermore, in *spindle-C* bipolar egg chambers, *bicoid* mRNA was found to localise to both poles of the oocyte while *oskar* mRNA and Staufen protein localise to the centre instead of the posterior pole. A chimeric protein, consisting of the plus-end directed microtubule motor kinesin fused to β-galactosidase (kin:β-gal, Clark *et al*, 1994), was subsequently used as a marker for microtubule polarity. In wild type egg chambers this chimeric protein localises to the plus-ends of microtubules at the oocyte's posterior pole, however it accumulates at the centre of *spindle-C* bipolar oocytes indicating that the altered arrangement of nurse cells and oocyte causes a new mirror-symmetric organisation of the microtubule cytoskeleton (Gonzalez-Reyes and St Johnstone, 1994). AP polarity within the oocyte is therefore specified by the position of the oocyte within the egg chamber. To reconcile this model with the earlier mentioned requirement for *Notch* and *Delta* in the follicle cells, Gonzalez-Reyes and St Johnston (1994) proposed that the oocyte first signals to the adjacent posterior follicle cells to induce posterior fate, then the follicle cells signal back to reorganise the microtubule cytoskeleton and thus define AP polarity.

The original description of the *gurken* phenotype noted anterior-posterior defects such as a duplicated micropyle, as well as the more obvious dorso-ventral defects (Schupbach, 1987). However, it was not until 1995 that Gonzalez-Reyes *et al* showed that this was due to a failure to specify posterior follicle cell fate and the resulting duplication of anterior follicle cell fate. In addition, they demonstrated that *bicoid* mRNA, *oskar* mRNA, Staufen protein and the kin:β-gal fusion protein all mislocalise in *gurken* mutant egg chambers indicating that *gurken* function is required for the proper re-organisation of the microtubule cytoskeleton. The TGF-α-like

product of the *gurken* gene was therefore identified as the key signalling molecule in the acquisition of posterior follicle cell fate and the establishment of AP polarity in the oocyte (Gonzalez-Reyes *et al*, 1995). Function of the *torpedo* gene is again required in the follicle cell layer to transduce the Gurken signal and activate posterior fate and reorganisation of the cytoskeleton. Thus both major body axes of *Drosophila* are established by Gurken-Torpedo signalling (Gonzalez-Reyes *et al*, 1995). Function of the neurogenic genes *Notch* and *Delta* is also required in the follicle cells to mediate the *gurken* signal. *Notch* and *Delta* are both essential genes, however temperature sensitive alleles have been used to demonstrate their requirement during oogenesis (Ruohola *et al*, 1991; Xu *et al*, 1992). *Notch* and *Delta* both encode large transmembrane proteins containing numerous epidermal growth factor (EGF)-like repeats (Wharton *et al*, 1985; Kopczynski *et al*, 1988). Cell-cell signalling via Notch and Delta appears to be required throughout development to mediate cell fate choices among equivalent groups of cells (Fehon *et al*, 1990; Artavanis-Tsakonas and Simpson, 1991).

The current model for axis specification is therefore as depicted in figure 1.3. Between stages 1 and 6 the oocyte nucleus and *gurken* mRNA are localised to the posterior of the oocyte, leading to the posterior production of extracellular Gurken. This then binds to the Torpedo receptor in adjacent uncommitted polar follicle cells to activate a tyrosine kinase signalling pathway that results in the determination of posterior follicle cell fate. The posterior follicle cells subsequently signal back to the oocyte to reorganise their microtubule cytoskeleton. The resulting polarised array of microtubules directs the localisation of *bicoid* mRNA and *oskar* mRNA to opposite poles of the oocyte, thereby defining the AP axis of the embryo. Formation of the polarised microtubule cytoskeleton is also required for the correct movement of the oocyte nucleus to the anterio-dorsal region of the oocyte at stage 8, which is in turn required for the spatial restriction of *gurken* mRNA to the anterio-dorsal corner. The resulting localised synthesis of Gurken induces the adjacent follicle cells to adopt a dorsal fate and subsequent signalling from the follicle cells back to the germ-line establishes the DV pattern of the embryo (Gonzalez-Reyes *et al*, 1995). The

formation of the DV axis depends on the prior specification of the AP axis, therefore the AP axis is the primary axis in *Drosophila*.

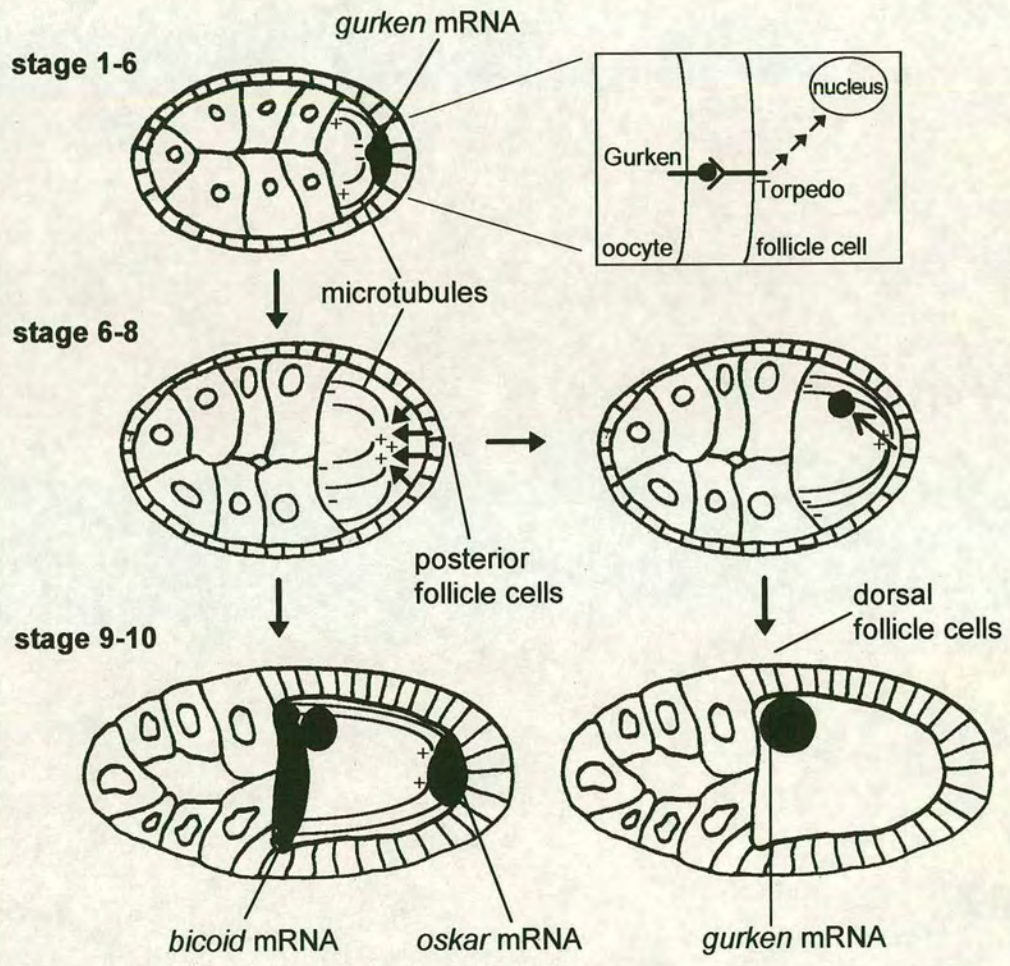

Figure 1.3 Establishment of AP polarity and DV polarity in the *Drosophila* oocyte. See text for full explanation. After Gonzalez-Reyes *et al*, (1995).

1.3.5 Maternal genes and embryonic pattern formation

Once the *Drosophila* egg is fertilised the early stages of embryonic development occur very rapidly because the initial mitotic divisions are not coupled to cell division. Instead the early embryo is a single syncitial cell. After nine mitotic cycles the zygotic nuclei migrate to the periphery of the embryo forming the syncitial blastoderm. Three or four of these nuclei enter the pole plasm at the posterior of the embryo and go on to form pole cells, the precursors of the germline. The remaining nuclei divide a further four times at the surface before being surrounded by cell membranes to form the ~6000 cells of the cellular blastoderm. Soon after this occurs gastrulation begins. From fertilised egg to hatching of the first-instar larva takes only 24 hours.

In *Drosophila*, significant transcription from the zygotic genome does not begin until the blastoderm stage of development. All the information for pre-blastoderm development must therefore be laid down during oogenesis. As a result of the extensive genetic screens discussed earlier, many of the maternal signals that define the basic organisation and polarity of the embryo are now well understood (reviewed in St Johnston and Nusslein-Volhard, 1992). In particular, pattern formation along the anterior-posterior axis of the embryo is defined by two localised maternal determinants - the anterior determinant and the posterior determinant.

Evidence that the *Drosophila* egg contains localised cytoplasmic determinants comes from experiments where the egg is pricked so that a small amount of cytoplasm leaks out (Bownes and Sang, 1974; Frohnhofer *et al*, 1986). Loss of anterior cytoplasm leads to the development of larvae with severely reduced head and thoracic structures, similar to those produced by mutations in the anterior group gene *bicoid*. Loss of posterior cytoplasm leads to abdominal defects, similar to those produced by mutations in posterior group genes. These results implied the existence of two localised signals at opposite poles of the egg. Further evidence to support this theory came from the discovery that *bicoid* mutants could be rescued by injecting anterior cytoplasm from wild-type eggs into the anterior pole of mutant eggs (Frohnhofer and

Nusslein-Volhard, 1986). Similarly, transplantation of posterior cytoplasm (or pole plasm) was found to rescue defects caused by mutations in posterior group genes, although for best results the pole plasm has to be injected into the abdominal region (Lehmann and Nusslein-Volhard, 1986). The pole plasm therefore appears to contain a localised posterior determinant which acts at a distance to determine abdomen formation. In addition the pole plasm is responsible for the formation of the pole cells which ultimately form the germ-line (Illmensee & Mahowald, 1974).

1.3.5.1 The Anterior Determinant

The anterior determinant is encoded by the *bicoid* gene. The Bicoid protein is a homeodomain containing transcriptional regulator that determines anterior pattern by the direct regulation of zygotic genes (Frigerio *et al*, 1986; Berleth *et al*, 1988). Mutations in *bicoid*, which normally result in embryos with head and thoracic defects, can be rescued by anterior injection of synthetic *bicoid* mRNA (Driever *et al*, 1990). Injection of synthetic *bicoid* mRNA into other positions in the embryo results in the formation of ectopic head and thoracic structures. In wild type flies, *bicoid* mRNA is synthesised in the nurse cells and transported to the oocyte where it is ultimately localised to the anterior cytoplasm of the mature egg (Berleth *et al*, 1988). After fertilisation, Bicoid protein is synthesised from this localised mRNA and diffuses posteriorly to form a protein gradient that extends over the anterior two thirds of the embryo and controls the expression of zygotic genes in a concentration dependent manner (Struhl *et al*, 1989).

The primary role of the Bicoid transcription factor is activation of the zygotic gap gene *hunchback* in the anterior region of the embryo (Driever and Nusslein-Volhard, 1989a). The *hunchback* gene also encodes a transcriptional regulator which controls the expression of other gap genes and pair-rule genes to determine pattern formation in the head and thorax (Lehmann and Nusslein-Volhard, 1987). Zygotic expression of *hunchback* is only activated in the anterior region of the embryo where

the level of Bicoid protein is above a certain threshold. The importance of the Bicoid protein gradient is demonstrated in experiments where the number of maternal copies of the *bicoid* gene is increased. As more RNA and protein are produced, the resulting posterior shift in the protein gradient causes a corresponding shift in the expression domains of *hunchback* and the other gap and pair-rule genes (Driever and Nusslein-Volhard, 1988b; Struhl *et al*, 1989). The promoter region of the *hunchback* gene contains a number of high affinity and low affinity Bicoid-binding sites (Driever and Nusslein-Volhard, 1989b). This region of *hunchback* is sufficient to direct the Bicoid-dependent expression of a reporter gene in the anterior region of the embryo. Bicoid is proposed to exert its concentration dependent effect via differential affinity for the sites in the promoter region - high concentrations of Bicoid will activate both high and low affinity sites whereas low concentrations of Bicoid will only activate high affinity sites (Driever and Nusslein-Volhard, 1989b). The *hunchback* gene also has a maternal promoter which is active during oogenesis resulting in a uniform distribution of *hunchback* mRNA throughout the mature egg (Schroeder *et al*, 1988). The primary function of the posterior group gene *nanos* is to repress translation of hunchback mRNA at the posterior of the embryo to further limit *hunchback* activity to the anterior region of the embryo (Tautz and Pfeifle, 1989; Irish *et al*, 1989) (see 1.3.5.2).

The embryonic gradient of Bicoid protein depends on the correct localisation of *bicoid* mRNA to the anterior cytoplasm of the mature egg. The anterior localisation of *bicoid* mRNA occurs in a stepwise fashion and requires the function of at least three maternal genes - *exuperantia, swallow and staufen* (St Johnston *et al*, 1989) (see also 1.4.3.2). The *exuperantia* gene is required for the localisation of *bicoid* to the anterior of the oocyte at stages 8-9 and to the apical regions of the nurse cells at stages 9-11, whereas the *swallow* gene is required for maintenance at the anterior cortex from stage 10b-12. Mutations in *exuperantia* or *swallow* lead to an almost uniform distribution of *bicoid* mRNA and give rise to embryos with head and thoracic defects (Berleth *et al*, 1988; Frohnhofer and Nusslein-Volhard, 1987). The final redistribution of *bicoid* mRNA in the anterior cytoplasm requires the function of

staufen, a gene also required for posterior patterning and pole plasm assembly (St Johnston *et al*, 1989). Mutations in *staufen* therefore give rise to embryos with mild head region defects in addition to abdominal defects and lack of pole cells (Schupbach and Wieschaus, 1986).

1.3.5.2 The Posterior Determinant

The pole plasm at the posterior of the *Drosophila* oocyte contains two localised signals - the posterior determinant required to specify posterior somatic patterning and a second signal required to specify the development of the pole cells. The posterior group genes *oskar, staufen, cappuccino, spire, vasa, tudor, valois* and *mago nashi* are all required for both abdominal patterning and pole cell formation, whereas two other posterior group genes *nanos* and *pumilio* are specifically required for the determination of the abdomen. The *oskar, staufen, vasa, tudor* and *nanos* genes all produce mRNAs and/or proteins which localise to the posterior pole of the egg. Localisation of these molecules occurs in a stepwise fashion with the products of *oskar* and *staufen* the first to localise, followed by *vasa, tudor* and *nanos*, with each subsequent localisation dependent on the function of the preceding genes (fig 1.4) (reviewed in Lasko, 1994).

The *nanos* gene encodes the posterior determinant critical for specifying posterior somatic pattern and *nanos* mRNA is highly concentrated at the posterior pole of the mature egg (Wang and Lehmann, 1991). Females mutant for *nanos* produce embryos which lack abdominal segments but which have normal pole cells (Nusslein-Volhard *et al*, 1987). The abdominal phenotype caused by mutations in *oskar, staufen, cappuccino, spire, vasa, tudor, valois* and *mago nashi* occur as a consequence of failure to localise *nanos* mRNA to the posterior pole (Sander and Lehmann, 1988, Lehmann and Nusslein-Volhard, 1991). Injection of *in vitro* synthesised *nanos* mRNA into the abdominal region can not only restore normal abdomen development in *nanos* mutants but can also rescue the abdominal defects produced by mutations in

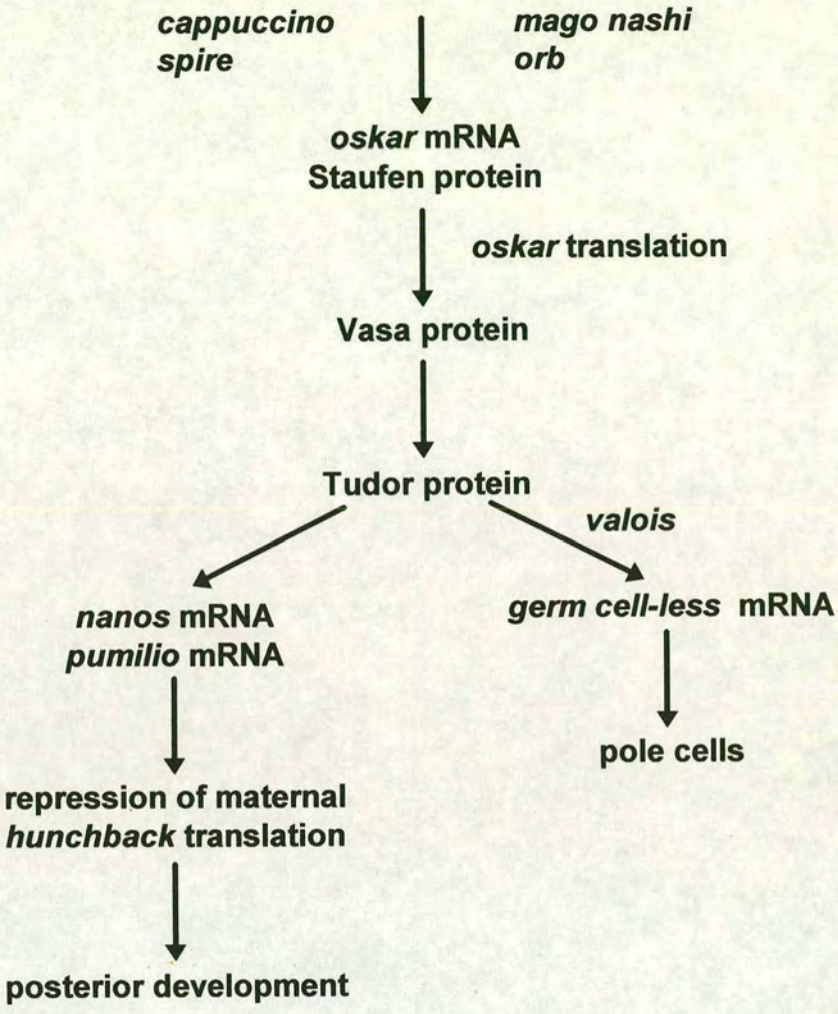

Figure 1.4 The functional and temporal hierarchy of pole plasm assembly. Each molecule in the pathway localises to the pole plasm dependent upon the localisation of the preceding molecule. After Lasko, (1994).

all the other posterior group genes (Wang and Lehmann, 1991).

The primary function of *nanos* is to repress the translation of the maternal *hunchback* transcript in the posterior region of the embryo (Tautz and Pfeifle, 1989; Irish *et al*, 1989). The *hunchback* gene product is therefore localised to the anterior of the embryo by two different mechanisms - transcriptional activation by *bicoid* in the anterior region of the embryo and translational repression by *nanos* in the posterior

region. Posterior elimination of *hunchback* allows the expression of the gap genes *knirps* and *giant* in the abdominal region of the embryo which would otherwise be repressed by the hunchback transcription factor. Translational control of *hunchback* by *nanos* has been shown to be mediated via short sequences in the 3' untranslated region (3'UTR) of *hunchback* mRNA. Wharton and Struhl (1991) demonstrated that a transgenic copy of *hunchback* lacking these sequences, termed *nanos*-response elements (NRE's), is translated throughout the embryo. NRE's are also sufficient to confer *nanos*-dependent posterior translational repression on other mRNAs (Wharton and Struhl, 1991). Translational repression of *hunchback* in the posterior of the embryo appears to be the only role of the Nanos protein in posterior determination. Use of germline clones has allowed the production of embryos which lack both maternal *hunchback* and *nanos* but which still develop normal abdomens, indicating that in the absence of maternal *hunchback*, *nanos* activity is dispensable (Struhl, 1989; Hulskamp *et al*, 1989). More recently, *nanos* activity has been found to be additionally required for the correct migration of the germ cells to the gonads (Kobayashi *et al*, 1996).

The product of the *oskar* gene plays a critical organising role in posterior embryonic patterning and pole cell formation. *oskar* mRNA is one of the first molecules to localise to the posterior of the embryo where it defines the site of pole plasm assembly and thus the site of *nanos* mRNA localisation (Ephrussi *et al*, 1991). This is demonstrated when *oskar* mRNA is mislocalised to the anterior pole by means of an *oskar* transgene fused to the 3'UTR of *bicoid* mRNA (see 1.4.3.1), resulting in the formation of bicaudal, double abdomen embryos with pole cells at both ends (Ephrussi and Lehmann, 1992). *oskar* induced ectopic abdomen and pole cell formation requires the functions of the *tudor* and *vasa* genes whereas the functions of *cappuccino*, *spire*, *staufen* and *valois* are dispensable (Ephrussi and Lehmann, 1992). An increase in the gene dosage of *oskar* leads to an increase in the levels of Vasa and Staufen protein and *nanos* mRNA localised to the posterior pole indicating that *oskar* is the limiting factor in pole plasm assembly. Furthermore, the number of pole cells which form in the blastoderm embryo is directly proportional to the number of

maternal copies of the *oskar* gene (Ephrussi and Lehmann, 1992).

oskar encodes a basic protein with hydrophobic amino and carboxy terminal domains separated by a hydrophilic region (Ephrussi *et al*, 1991). The *oskar* transcript has been discovered to possess two potential translational start sites which can give rise to proteins of 54 kDa or 69kDa, respectively referred to as ShortOskar and LongOskar (Markussen *et al*, 1995). Mutational analysis of the translational start sites revealed that ShortOskar is capable of rescuing the *oskar* mutant phenotype but LongOskar is not, despite its tight association with the posterior pole.

Localisation of the *oskar* transcript to the posterior pole of the oocyte is a complex process that occurs in a number of discrete steps (Ephrussi *et al*, 1991; Kim-Ha *et al*, 1991). *oskar* mRNA is synthesised in the nurse cells and transferred to the oocyte where it is first detectable in germarial region 2b. This accumulation of *oskar* mRNA is one of the first markers for oocyte differentiation and is abolished in *egalitarian* and *Bic-D* mutants. *oskar* mRNA is detectable in the apical regions of the nurse cells before transport to the oocyte where it is uniformly distributed until stage 7 when it becomes transiently localised to the anterior margin of the oocyte. Between stages 7 and 9 *oskar* mRNA also accumulates at the posterior pole to give a biphasic pattern of localisation. As oogenesis progresses the anterior localisation disappears and the posterior localisation increases such that beyond stage 9 *oskar* mRNA is strictly localised to the posterior pole (Ephrussi *et al*, 1991; Kim-Ha *et al*, 1991, 1993).

The final stage of *oskar* mRNA localisation to the posterior pole requires the functions of the *staufen*, *cappuccino*, *spire* and *orb* genes (Ephrussi *et al*, 1991; Christerson and McKearin, 1994). Mutations in any of these genes leads to abdominal defects and missing pole cells as a consequence of failure to localise *oskar* activity. Staufen protein appears to be important for the transport of *oskar* mRNA from the anterior margin to the posterior pole, as in *staufen* mutants *oskar* mRNA persists longer at the anterior and fails to accumulate at the posterior (Ephrussi *et al*, 1991). Staufen is proposed to associate with the 3'UTR of *oskar* mRNA to mediate

its microtubule dependent transport to the posterior pole (see 1.4.3.2). In *cappuccino*, *spire* and *orb* mutants, *oskar* mRNA fails to accumulate at the posterior pole and instead is diffuse throughout the oocyte. *orb* encodes an RNA binding protein that is proposed to be part of the multiprotein complex required to localise *oskar* mRNA (Christerson and McKearin, 1994). Failure of *oskar* mRNA localisation in *cappuccino* and *spire* mutants is thought to be due to the premature onset of cytoplasmic streaming which occurs in these mutants (Theurkauf *et al*, 1994b). Maintenance of *oskar* mRNA localisation at the posterior pole also requires Oskar protein. Kim-Ha *et al* (1991) showed that *oskar* mutations which give rise to premature stop codons result in the loss of *oskar* mRNA localisation beyond stage 10, whereas mis-sense mutations do not, indicating that the presence, but not the complete wild-type function of Oskar protein is required to anchor *oskar* mRNA in the pole plasm.

The *vasa* gene encodes a germ-line specific protein that localises to the pole plasm at stages 9-10a and becomes sequestered into the pole cells as they form. Vasa protein is localised to the pole plasm dependent on the functions of *cappuccino*, *spire*, *oskar* and *staufen* (Hay *et al*, 1988, 1990; Lasko and Ashburner, 1990). Localisation of Vasa appears to require *oskar* activity as both nonsense and mis-sense mutations of *oskar* abolish Vasa localisation (Hay *et al*, 1988, 1990). Interestingly, maintenance of Oskar protein at the posterior pole requires the function of *vasa*, suggesting a positive feedback mechanism is involved in pole plasm assembly (Markussen *et al*, 1995). In the early stages of oogenesis, Vasa protein is localised to the perinuclear regions of the nurse cells, dependent on its own function but independent of the functions of *cappuccino*, *spire*, *oskar* and *staufen* (Liang *et al*, 1994). These two distinct stages of Vasa localisation suggests two independent roles for Vasa. Correspondingly, *vasa* mutations fall into two phenotypic classes - a posterior group class which results in embryos with abdominal defects and missing pole cells and an oogenesis class where oogenesis does not proceed beyond stage 9 (Lasko and Ashburner, 1988).

vasa encodes a DEAD box protein with ATP-dependent RNA helicase activity (Hay

et al, 1988). Mutations in *vasa* which abolish its RNA binding and unwinding activities do not prevent localisation of Vasa protein to the posterior pole, indicating that localisation occurs independent of helicase activity. Such mutations do however prevent the formation of the pole cells, indicating that helicase activity is essential for Vasa's role in pole cell formation (Liang *et al*, 1994). Expression of *vasa* requires the function of the *pipsqueak* gene. In *pipsqueak* mutants Vasa protein is decreased to 1% of wild type although the expression of *bicoid*, *nanos* and *germ cell-less* is unaffected (Siegel *et al*, 1993). *oskar* mRNA and Staufen protein are still localised to the posterior in *pipsqueak* mutants but *nanos* mRNA is not, resulting in the posterior group phenotype.

Of the posterior group genes, only the functions of *oskar*, *vasa* and *tudor* are required for the formation of *oskar*-induced pole cells at the anterior pole (Ephrussi and Lehmann, 1992). The *tudor* gene encodes a large protein which has no obvious homologies to other proteins (Golumbeski *et al*, 1991). *tudor* mRNA is concentrated in the oocyte from germarial region 2 and persists until stage 8, after which it also accumulates to high levels in the nurse cells (Golumbeski *et al*, 1991). Tudor protein is localised to the perinuclear regions of the nurse cells during early oogenesis, and is also abundant throughout the oocyte where it transiently localises to the anterior pole between stages 4-6. Tudor protein becomes concentrated to the posterior pole during stages 9-10, concurrent with, and dependent upon, the localisation of Vasa (Bardsley *et al*, 1993). After fertilisation, posteriorly localised Tudor is incorporated into the pole cells while residual cytoplasmic Tudor becomes associated with the somatic nuclei of the syncitial blastoderm. It has been proposed that the Tudor protein localised to the posterior pole plasm is essential for pole cell formation while Tudor protein associated with the somatic nuclei is involved in abdominal pattern formation (Bardsley *et al*, 1993).

The *valois* gene is required for normal abdominal patterning and pole cell formation but is not required for the formation of *oskar*-induced ectopic pole cells at the anterior pole (Schupbach and Wieschaus, 1986; Ephrussi and Lehmann, 1992). Despite being

dispensable in ectopic pole cell formation, *valois* is thought to function relatively late in pole cell formation as mutations in *valois* do not affect the localisation of any known pole plasm components. In addition to the posterior group phenotype, embryos from *valois* mothers often fail to complete cellularisation, indicating that *valois* plays a further role in embryonic development (Schupbach and Wieschaus, 1986).

The *mago nashi* gene was originally identified by its posterior group phenotype by Boswell *et al*, (1991). The *mago nashi* gene encodes a small protein of 147 amino acids, which has no known function although it is conserved from plants to animals (Newmark and Boswell, 1994). The first identified allele of *mago nashi* was found to prevent pole plasm assembly as a consequence of failure to localise *oskar* mRNA and Staufen protein to the posterior pole (Newmark and Boswell, 1994). More recently, *mago nashi* has been demonstrated to play an important role in axis formation during oogenesis. After the induction of posterior follicle cell fate by posteriorly localised Gurken protein, the *mago nashi* product is required in the germ line to transduce the return signal from the follicle cells and bring about reorganisation of the cytoskeleton (Micklem *et al*, 1997; Newmark *et al*, 1997).

The *germ cell-less* gene is required for the formation of the pole cells but not for abdominal patterning (Jongens *et al*, 1992). Expression of a transgene encoding antisense *germ cell-less* RNA results in reduction or loss of pole cells, while increased expression results in additional pole cells. *germ cell-less* mRNA is localised to the pole plasm dependent on all the genes required for *nanos* mRNA localisation. The *germ cell-less* gene encodes a protein of 569 amino acids which is found to associate with nuclear pores (Jongens *et al*, 1994). Additional components of the pole plasm include *cyclin B*, *orb* and *Hsp83* mRNAs, mitochondrial large ribosomal RNA and *fat facets* protein (Raff *et al*, 1990; Lantz *et al*, 1992; Ding *et al*, 1993; Kobayashi *et al*, 1993; Fischer-Vize *et al*, 1992) Again, the accumulation of these molecules in the pole plasm is dependent on the functions of upstream, posterior group genes.

Pattern formation along the anterior-posterior axis of the *Drosophila* embryo is defined by cytoplasmic determinants localised to opposite poles of the mature egg. These centres of organising activity are largely established by the localisation of maternal mRNAs - a phenomenon found to be increasingly widespread in development. Although superficially similar, the anterior determinant and posterior determinant act in quite different ways. The anterior determinant *bicoid*, encodes a protein which regulates zygotic gene expression directly. In contrast, the function of the posterior determinant *nanos*, is to repress translation of the transcription factor *hunchback*, encoded by a ubiquitous maternal mRNA. The fact that *nanos* is not required in the absence of *hunchback* raises the question of why these two separate systems evolved when they both essentially act to restrict *hunchback* expression to the same anterior region of the embryo. It is possible that the posterior system is the more primitive of the two but has survived, despite the evolution of the anterior system, because it is inextricably linked to the formation of the pole cells.

1.4 Localisation of Messenger RNA

1.4.1 Introduction

As discussed in previous sections, the localisation of maternal mRNAs plays an important role in *Drosophila* development. The process of oocyte determination requires the localisation of the *Bic-D* and *orb* transcripts to the pro-oocyte (Suter and Steward, 1991; Lantz *et al*, 1994), localisation of the *gurken* transcript is required to establish both major body axes (Gonzalez-Reyes *et al*, 1995) and localisation of the anterior and posterior determinants *bicoid* and *nanos,* is essential for embryonic pattern formation (reviewed in St Johnston and Nusslein-Volhard, 1992). However, the phenomenon of mRNA localisation is not restricted to *Drosophila* maternal mRNAs. Localised mRNAs have also been described in the oocytes of *Xenopus laevis* and also in the somatic cells of both *Drosophila* and vertebrates (reviewed in

Ding and Lipshitz, 1993; St Johnstone, 1995).

In *Xenopus*, several maternal mRNAs have been shown to localise to either the animal or vegetal pole of unfertilised oocytes, such that they are inherited by a subset of the blastomeres of the early embryo. The mRNAs of *Vg1* and *Xwnt11* are localised to the vegetal cortex (Melton, 1987; Ku and Melton, 1993). These mRNAs encode growth factor-like proteins and are postulated to be responsible for the mesoderm-inducing and dorsal axis-inducing properties of the vegetal blastomeres (Weeks and Melton, 1987a; Ku and Melton, 1993). In contrast, *An1*, *An2* and *An3* transcripts are localised to the animal pole of *Xenopus* oocytes. *An3* encodes an RNA binding protein, while *An2* encodes a subunit of the mitochondrial ATPase and has been proposed to be involved in generating a respiration gradient (Weeks and Melton, 1987b).

In the *Drosophila* developing embryo, several zygotically transcribed, localised mRNAs have been reported. Examples include the localisation of the *sevenless* transcript to the apical regions of developing photoreceptor cells (Banerjee *et al*, 1987) and the localisation of pair-rule transcripts, such as *hairy* and *fushi-tarazu*, to the cortical side of the nuclei in the syncytial blastoderm (Ingham *et al*, 1985; Weir and Kornberg, 1985). In vertebrates, the mRNAs of several cytoskeletal proteins exhibit subcellular localisation. β-actin mRNA is localised to the leading edge of chick fibroblasts where the actin it encodes is required for lamellipodial extension (Lawrence and Singer, 1986), myosin heavy chain mRNA is localised to the peripheral regions of developing chick muscle cells (Pomeroy *et al*, 1991) and the mRNA for MAP-2 (microtubule-associated protein-2) is localised to the dendrites of rat neuronal cells (Garner *et al*, 1988). A further example of mRNA localisation in vertebrates is the localisation of the mRNA for myelin basic protein (MBP) to the dendritic processes of rat neurons (Trapp *et al*, 1987). MBP is involved in the formation of myelin sheaths around axons and reacts strongly with membranes, causing them to compact. The problem of transporting this protein from the cell body to the dendrites is therefore circumvented by the localisation of MBP mRNA.

1.4.2 Functions of mRNA Localisation

The intracellular localisation of mRNAs allows proteins to be synthesised in the particular subcellular regions where they are required. As many protein molecules can be translated from a single mRNA molecule, mRNA localisation appears to be a more efficient means of protein targeting than localisation of the proteins themselves. This localisation of mRNA and subsequent concentration of protein translation can serve several purposes. For example, in the *Drosophila* embryo, the localised translation and subsequent diffusion of the Bicoid protein forms a morphogenic gradient of the Bicoid transcription factor (Berleth *et al*, 1988), which then switches on zygotic genes in a concentration dependent manner (Driever and Nusslein-Volhard, 1988a). In the *Drosophila* oocyte, the embryonic axes are established by localised cell signalling between the oocyte and the surrounding follicle cells, achieved by the localised translation of the TGFα–like encoding *gurken* transcript (Gonzalez-Reyes *et al*, 1995). The localisation of an mRNA within an oocyte can also specify cell fate by the differential inheritance of the mRNA or its protein by the cells of the developing embryo, as is the case for *germ cell-less* (*gcl*) in *Drosophila* (Jongens *et al*, 1992) and *Vg1* in *Xenopus* (Weeks and Melton, 1987a). *gcl* mRNA is localised to the posterior of the oocyte where it is translated after fertilisation and becomes associated with the nuclei of the germ-line pole cells that form at the posterior of the oocyte. The localisation of *gcl* is essential for the formation of the pole cells, however it is not sufficient to direct formation. In contrast, the localisation of *oskar* mRNA is necessary and sufficient to determine both the site of pole plasm assembly and the site of posterior embryonic patterning (Ephrussi and Lehmann, 1992).

Localised mRNAs can also serve a variety of purposes in somatic cells. In chick embryonic fibroblasts, the localisation of β-actin transcripts to the leading lamellae appears to be important for the establishment and maintenance of cell polarity. If the localisation of the β-actin mRNA is disrupted, then despite the overall levels of mRNA and protein being unaffected, the lamellae collapse and the cell becomes symmetrical (Kislauskis *et al*, 1994). Another function of mRNA localisation is to

prevent the inappropriate expression of a protein in the wrong regions of the cell, as would appear to be the case for the above mentioned localisation of MBP mRNA to the dendritic processes of oligodendrocytes. Similarly, the localised expression of different protein subunit isoforms may prevent the inappropriate formation of heteromultimers. Thus the localisation of β-actin mRNA to the leading lamellae of developing myoblasts, while α- and γ-actin mRNAs localise perinuclearly, may be important in determining the composition of actin filaments (Hill and Gunning, 1993). The localisation of mRNAs and subsequent protein translation also provides the possibility of localised translational control. This has been postulated to be the case for mRNAs which localise to the post-synaptic sites of neurons, where regulation of translation at individual post-synaptic sites could potentially contribute towards synaptic plasticity (Steward and Banker, 1992).

1.4.3 Mechanisms of mRNA Localisation

The localisation of an mRNA species within a cell can potentially be achieved by several different mechanisms. One possible mechanism is the spatial control of mRNA stability, whereby transcripts at the correct localisation site are stabilised while unlocalised transcripts are degraded. This rather inefficient mechanism appears to be responsible for the localisation of *hsp83* mRNA to the posterior pole of the *Drosophila* embryo (Ding *et al*, 1993b). In the mature egg the *hsp83* transcript is uniform throughout the cytoplasm, but by the time of pole cell formation the transcript has been degraded everywhere except the pole plasm. Posterior stabilisation seems to be a property of the pole plasm itself, as *hsp83* mRNA is degraded at the posterior of embryos which lack pole plasm but is stabilised at the anterior pole when pole plasm is induced to form there ectopically.

An alternative mechanism for the localisation of mRNA without active transport is the anchoring of transcripts to localised binding sites. This mechanism has been postulated to be responsible for the localisation of *nanos*, *germ cell-less* and *cyclin B*

transcripts to the posterior of the *Drosophila* oocyte (St Johnston, 1995). The fact that posterior accumulation of these three transcripts requires the previous localisation of the *oskar* transcript and Oskar, Staufen and Vasa proteins, indicates that these transcripts bind to pole plasm components which have already been localised (Wang *et al*, 1994; Jongens *et al*, 1992; Raff *et al*, 1990). At the stage of oogenesis when the *nanos*, *gcl* and *cyclin B* mRNAs localise, the cytoskeleton is no longer polarised but instead has reorganised so as to drive a flow of cytoplasm around the egg (Theurkauf *et al*, 1992). This cytoplasmic streaming appears to be sufficient to circulate these mRNAs around the oocyte until they are bound by already localised components of the pole plasm.

A third possible mechanism of mRNA localisation is the vectorial nuclear export of nascent mRNAs. This is the mechanism proposed to account for the localisation of the pair-rule gene transcripts *even-skipped*, *hairy*, *runt* and *fushi tarazu* to the apical side of nuclei in the blastoderm embryo, where their lateral diffusion is prevented by the invaginations of the plasma membrane as cellularisation proceeds (Davis and Ish-Horowicz, 1991; Davis *et al*, 1993). The short, six minute half life and low diffusion rate of the pair-rule transcripts make it unlikely that apical localisation is achieved by differential stability or localised anchoring (Edgar *et al*, 1986). This, in addition to the fact that transcripts are never detected in the basal cytoplasm, has led to the suggestion that apical localisation occurs via vectorial mRNA export from the apical side of the nuclei (Davis *et al*, 1993; Francis-Lang *et al*, 1996). Evidence to support this theory comes from recent work on mutant embryos where a proportion of the cortical layer nuclei become internalised. Francis-Lang *et al* (1996) demonstrated that internalised nuclei maintain their apico-basal orientation and still localise pair-rule transcripts to their apical side. Furthermore, internalised nuclei lack the apical basket of microtubules which lies adjacent to cortical nuclei, indicating that apical localisation of pair-rule transcripts does not require this cytoskeletal structure. The mechanisms responsible for vectorial nuclear export are not understood, however, apical localisation is known to depend on sequences within the 3'UTRs of the localised transcripts (Davis and Ish-Horowicz, 1991), a phenomenon which will be

discussed in the next section.

A further possible mechanism to explain the localisation of mRNA within cells is that of active, directed transport. Such a mechanism should include two critical features - a *cis*-acting signal, intrinsic to the mRNA itself, that determines its subcellular localisation, and the *trans*-acting cellular machinery that interacts with this signal to direct and maintain localisation.

1.4.3.1 *cis*-acting localisation signals - the 3'UTR

In all cases where mRNA localisation signals have been identified, they have been found to reside within the 3' untranslated region (UTR) of the transcript. This phenomenon was first demonstrated in 1988 when Macdonald and Struhl showed that a 625 base region of the *bicoid* 3'UTR was necessary for localisation of the *bicoid* transcript to the anterior cortex of the oocyte, and was also sufficient to cause anterior localisation of heterologous transcripts, such as *oskar* mRNA. 3'UTR localisation signals have subsequently been identified in several *Drosophila* maternal transcripts including *nanos* (Gavis and Lehmann, 1992), *cyclin B* (Dalby and Glover, 1992), *fs(1)K10* (Cheung *et al*, 1992), *oskar* (Kim-Ha *et al*, 1993), *orb* (Lantz and Schedl, 1994) and *adducin-like* (H. Lipshitz, personal communication). 3'UTR localisation signals are not exclusive to *Drosophila* maternal genes as they have also been shown to be required for the apical localisation of zygotic pair-rule transcripts in the blastoderm embryo (Davis and Ish-Horowicz, 1991), for the vegetal localisation of maternal transcripts in the *Xenopus* oocyte (Mowry and Melton, 1992) and for the peripheral localisation of actin mRNA in cultured fibroblasts (Kislauskis and Singer, 1992).

Subsequent research has concentrated on identifying functional elements within the 3'UTR responsible for directing transcript localisation. Macdonald *et al* (1993) constructed a series of *bicoid* transgenes encoding wild-type Bicoid protein but

carrying small deletions in their 3'UTRs. These were then tested for their ability to rescue anterior development in *bicoid* mutant embryos, with the degree of rescue providing a measure of mRNA localisation. In this way they identified a small region of the 3'UTR essential for transcript localisation, which they termed BLE1 (*bicoid* localisation element 1). In subsequent experiments, *bicoid* 3'UTR transgenes were tagged with *lacZ* to allow transcript localisation to be followed by *in situ* hybridisation to *lacZ*. The results confirmed that the 53 base BLE1 was necessary for anterior localisation and furthermore, that two copies of BLE1 were sufficient to direct the early, *exuperantia* dependent, stage of *bicoid* transcript localisation. As previously mentioned (1.3.5.1), localisation of *bicoid* mRNA involves at least three steps, each with different genetic requirements (St Johnson *et al*, 1989). Further analysis of the *bicoid* 3'UTR identified other elements which were specifically required for later stages of transcript localisation, indicating that different elements mediate discrete steps of the localisation pathway (Macdonald *et al*, 1993).

Multiple *cis*-acting targeting elements in the 3'UTR have also been shown to be required for the stepwise localisation of the *oskar* and *orb* transcripts during oogenesis (Kim-Ha *et al*, 1993; Lantz and Schedl, 1994). Like *bicoid* mRNA, localisation of *oskar* and *orb* mRNA involves a number of discrete steps with different genetic requirements. *oskar* mRNA is synthesised in the nurse cells then rapidly transported to the oocyte where it transiently accumulates at the anterior before transport across the oocyte and subsequent anchoring to the posterior pole (Ephrussi *et al*, 1991). A systematic deletion analysis of the *oskar* 3'UTR identified overlapping elements required for different steps of this localisation process (Kim-Ha *et al*, 1993). The *orb* transcript displays a complex localisation pattern during oogenesis where it first accumulates within the presumptive oocyte of the 16 cell cyst, then localises preferentially to the oocyte posterior between stages 2 and 7 and to the oocyte anterior between stages 8 and 10, before becoming diffuse throughout the oocyte for the remainder of oogenesis (Lantz and Schedl, 1994). A 280 base sequence of the *orb* 3'UTR was found to be necessary and sufficient to direct this transcript localisation pattern and furthermore, elements within this sequence were shown to be

required for discrete steps in the localisation pathway (Lantz and Schedl, 1994). The use of multiple, *cis*-acting, elements to direct distinct steps of localisation suggests that transcripts may interact with several different RNA-binding proteins at discrete steps in the localisation pathway and introduces the possibility that transcripts with different ultimate destinations may utilise the same mechanisms for shared intermediate steps.

Precise characterisation of *cis*-acting localisation elements has proved to be difficult as they generally involve large regions of sequence and are often complex, appearing to have overlapping or redundant functions. This may be attributed to the fact that single stranded mRNA is capable of folding into complex secondary structure and it appears to be this structure, rather than precise nucleotide sequence, that determines localisation. Macdonald (1990) demonstrated that the 3'UTRs from the *bicoid* transcript of three other *Drosophila* species could mediate the correct localisation of *bicoid* mRNA in *D. melanogaster*. Analysis of the 3'UTR sequences showed short stretches of homology at the nucleotide level but predicted that they could fold up into a stereotypical secondary structure conserved among the diverged *Drosophila* species. The importance of secondary structure might explain why two tandem copies of BLE1 are required to mediate the early stages of *bicoid* transcript localisation, when the wild type 3'UTR only contains one copy - if BLE1 is only active when it is folded correctly then the presence of two copies might substantially increase the probability of achieving this state (Macdonald *et al*, 1993).

Although secondary structure has been shown to be important for localisation, the importance of nucleotide sequence was demonstrated in that a nine nucleotide motif was found to be conserved in the 3'UTRs of transcripts from different organisms. The nonamer YUGUUYCUG, was identified within the 3'UTRs of the *Drosophila bicoid* and *nanos* transcripts, and the *Xenopus* maternal transcripts *An2* and *Vg1* (Gottlieb, 1992). Deletion of this nonamer from *bicoid* mRNA results in the partial mislocalisation of the transcript without any detrimental effect on transcript stability. This sequence cannot be sufficient for localisation as it resides in transcripts which

localise to opposite poles of the same egg, however, its importance is emphasised by the fact that it is conserved in the *bicoid* mRNA of eight *Drosophila* species which diverged up to 60 million years ago. It seems likely that a combination of both primary nucleotide sequence and folded secondary structure will be important in determining the interaction of the 3'UTR with the *trans*-acting RNA-binding proteins that mediate localisation.

1.4.3.2 *trans*-acting localisation factors - binding proteins

Despite the discovery and characterisation of numerous *cis*-acting localisation signals, little is known about the *trans*-acting binding proteins which presumably interact with these signals to bring about localisation. The best candidates for *trans*-acting binding proteins are the products of those genes which have been shown to be specifically required for mRNA localisation, thus the candidate *trans*-acting factors for *bicoid* mRNA localisation are the products of the *exuperantia*, *swallow* and *staufen* genes.

The product of the *exuperantia* gene is required for the localisation of *bicoid* to the anterior of the oocyte at stages 8-9 and to the apical regions of the nurse cells at stages 9-11, but not for the earliest stage of *bicoid* localisation to the oocyte at stage 5 (St Johnston *et al*, 1989). Mutations in *exuperantia* lead to a uniform distribution of *bicoid* mRNA throughout the egg, resulting in a *bicoid*-like phenotype (Berleth *et al*, 1988; Frohnhofer and Nusslein-Volhard, 1987). *exuperantia* encodes a novel, basic protein which has been shown to colocalise with *bicoid* mRNA in the nurse cells and at the anterior cortex (Marcey *et al*, 1991). Function of the *exuperantia* gene has been demonstrated to be required for some, but not all of the localisation steps performed by two copies of the BLE1 element (Macdonald *et al*, 1993). These results suggest a direct role for the Exuperantia protein in the localisation of *bicoid* mRNA, however specific binding of the protein to *bicoid* mRNA has not yet been demonstrated. More recently, Macdonald *et al* (1995) identified an ovarian protein, Exl, which does specifically bind to BLE1 *in vitro*. A mutational analysis of BLE1

revealed a correlation between *in vitro* Exl binding and a phase of *in vivo* localisation directed by BLE1. The defects in BLE1 directed localisation caused by mutations that prevent Exl binding are strikingly similar to those caused by lack of *exuperantia* function, hence the protein was named Exl for exu-like. These results suggest that the Exl and Exuperantia proteins interact to mediate *bicoid* mRNA localisation, with Exl binding directly to the *bicoid* 3'UTR. It therefore appears that Exl is an example of the predicted class of *trans*-acting localisation factors involved in the specific recognition of *cis*-acting localisation elements in mRNAs.

The product of the *swallow* gene is required for maintenance of *bicoid* mRNA at the anterior cortex of the stage 10 oocyte, suggesting a role for *swallow* in the anchoring of *bicoid* mRNA to the cortex (St Johnston *et al*, 1989; Hegde and Stephenson, 1993). *swallow* mutant embryos have defects in addition to the anterior defects expected from mislocalisation of *bicoid* mRNA, including defects in nuclear migration and cellularisation, leading to suggestions that *swallow* encodes a component of the cytoskeleton (Frohnhofer and Nusslein-Volhard, 1987; Stephenson *et al*, 1988). Sequence analysis of *swallow* predicts a protein with an RNA-binding region as well as an amphipathic α-helical domain capable of protein-protein interactions (Chao *et al*, 1991). Mutations in *swallow* also affect the localisation of the *adducin-like* transcript (Ding *et al*, 1993a). *adducin-like* mRNA also localises to the anterior of the oocyte, but in a different spatial and temporal pattern to that of *bicoid* mRNA. This common requirement for *swallow* indicates that mRNAs with different localisation patterns may use the same *trans*-acting factors to mediate shared intermediate steps.

The final stage of *bicoid* mRNA localisation - release from the anterior cortex of the stage 12 oocyte to maintenance in the anterio-dorsal cytoplasm of the freshly-laid egg - requires the product of the *staufen* gene (St Johnston *et al*, 1989). *staufen* function is also required earlier in oogenesis for the transport of *oskar* mRNA to the posterior of the oocyte from its site of transient accumulation at the oocyte anterior (Ephrussi *et al*, 1991; Kim-Ha *et al*, 1991). Consequently, *staufen* mutant embryos show mild

anterior defects in addition to abdominal defects and lack of pole cells (Schupbach and Wieschaus, 1986). Staufen protein colocalises with *oskar* mRNA during its microtubule dependent transport to the posterior pole (St Johnston *et al*, 1991; Clark *et al*, 1994). Furthermore the posterior localisation of Staufen depends on its association with *oskar* mRNA as increasing the *oskar* gene dosage, and hence the amount of *oskar* mRNA, increases the amount of Staufen transported to the posterior pole (Ferrandon *et al*, 1994). Staufen protein contains five copies of a double-stranded RNA (dsRNA) binding motif and a peptide containing this domain has been shown to bind to dsRNA *in vitro* (St Johnston *et al*, 1992). Taken together these observations suggest that Staufen interacts directly with the dsRNA of the folded *oskar* 3'UTR to mediate its localisation.

In mature eggs, Staufen is no longer localised to the posterior of the oocyte but instead accumulates at the anterior pole where it is required to anchor *bicoid* mRNA in the dorsal anterior cytoplasm (St Johnston *et al*, 1989; Ferrandon *et al*, 1994). Again, the amount of localised Staufen is proportional to the number of copies of *bicoid*, strongly suggesting that the protein and the mRNA interact (Ferrandon *et al*, 1994). When the *bicoid* 3'UTR is injected into the egg, it recruits Staufen protein to form large particles which move in a microtubule-dependent manner (Ferrandon *et al*, 1994). This injection assay was used to map the sequences required for the Staufen-*bicoid* 3'UTR interaction to three stable stem loop structures within the *bicoid* 3'UTR. Interestingly, one of these stem loops includes the BLE1 element, previously shown to be involved in the early phase of *bicoid* mRNA localisation (*Macdonald et al*, 1993). It may be that the binding of other *trans*-acting factors to the BLE1 during early oogenesis prevents the association of the *bicoid* 3'UTR and Staufen at this stage (Ferrandon *et al*, 1994).

The above results strongly suggest that the dsRNA-binding domains of Staufen protein directly interact with the secondary structure of the *bicoid* and *oskar cis*-acting localisation signals to mediate transcript localisation via the microtubules. However, direct binding of Staufen to the *bicoid* or *oskar* 3'UTR remains to be

demonstrated, as does a direct association with the microtubules.

1.4.3.3 *trans*-acting localisation factors - the cytoskeleton

The cytoskeletal network is likely to be part of the *trans*-acting cellular machinery required for active transport of mRNAs. Studies in *Drosophila*, *Xenopus* and also in cultured fibroblasts and neurons have implicated microtubules, microfilaments and intermediate filaments in the subcellular transport and anchoring of mRNAs. In *Xenopus*, the use of cytoskeletal inhibitors revealed that transport of the initially uniform *Vg1* mRNA to the vegetal cortex is dependent on microtubules, while its subsequent maintenance at the cortex is microfilament dependent (Yisraeli *et al*, 1990). A 69kDa specific *Vg1* RNA binding protein has been identified that appears to mediate the association of *Vg1* mRNA with the microtubules (Elisha *et al*, 1995). Additionally, the *Xenopus Vg1*, *Xcat-2* and *Xcat-3* transcripts all co-purify with an intermediate filament fraction indicating that intermediate filaments are also involved in the anchoring of mRNAs to the vegetal cortex (Pondel *et al*, 1988). In chick embryonic fibroblasts, the transport and subsequent anchoring of actin mRNA to the lamellipodia has been shown to be dependent on microfilaments, but not on microtubules or intermediate filaments (Sundell and Singer, 1991). Similarly, apical localisation of the transcript of the *Drosophila* pair-rule gene *fushi-tarazu* also requires the integrity of the microfilaments (Edgar *et al*, 1987). In contrast, localisation of *tau* mRNA to the axons and MAP2 mRNA to the dendrites of cultured neurons is dependent on intact microtubules but does not require microfilaments (Litman *et al*, 1994).

In the *Drosophila* oocyte, microtubules have been implicated in the asymmetric localisation of maternal mRNAs. During oogenesis, the microtubule network undergoes a series of rearrangements which correlate well with mRNA localisation (Theurkauf *et al*, 1992). Early in oogenesis, shortly after the formation of the 16 cell cyst, a prominent microtubule organising centre (MTOC) is established in the cell

destined to become the oocyte. During stages 1-6 of oogenesis a single microtubule network extends from this MTOC and through the ring canals so that the plus ends of these microtubules lie within the nurse cells (Theurkauf *et al*, 1992). Around this time, a number of mRNAs are synthesised in the nurse cells and transported to the developing oocyte, including the mRNAs of *Bicaudal-D*, *oskar*, *orb*, *cyclin B* and *gurken* (Suter and Steward, 1991; Ephrussi *et al*, 1991; Lantz *et al*, 1992; Dalby and Glover, 1992; Neuman-Silberberg and Schupbach, 1993). It is therefore possible that the early localisation of these mRNAs to the oocyte is mediated by the microtubules, via association with minus-end directed microtubule motors (Theurkauf *et al*, 1992). During stages 7 and 8 of oogenesis the MTOC degenerates and microtubules begin to associate with the anterior cortex of the oocyte (Theurkauf *et al*, 1992). At this time, several mRNAs, including *oskar*, *adducin-like* and *gurken*, show transient localisation at the oocyte anterior (Ephrussi *et al*, 1991; Ding *et al*, 1992; Neuman-Silberberg and Schupbach, 1993). From stages 7-10, microtubules originate at the anterior cortex of the oocyte and extend their plus ends towards the posterior pole. The machinery is therefore in place for the localisation of mRNAs to the oocyte anterior via association with minus-end directed motors and to the posterior via plus-end directed motors (Theurkauf *et al*, 1992, Theurkauf, 1994a).

Inhibitor studies support the role of microtubules in the localisation of *Drosophila* maternal mRNAs. An intact microtubule network has been shown to be required for all stages of *bicoid* mRNA localisation (Pokrywka and Stephenson, 1991). The localisation of *bicoid* mRNA to the anterior cortex of the oocyte was initially proposed to occur by trapping of the mRNA as it enters the anterior oocyte from its site of synthesis in the nurse cells (Berleth *et al*, 1988). Treatment of oocytes with the microtubule depolymerising drug, nocodazole, causes the release of *bicoid* mRNA from the anterior cortex, however, Pokrywka and Stephenson (1991) demonstrated that the mRNA could relocalise once the drug was washed out. This relocalisation of *bicoid* mRNA makes the simple anterior trapping model unlikely. Furthermore, in mutants such as $Notch^{ts}$ and *gurken* where the microtubule network is symmetrical and the oocyte develops as if it has two anterior ends, *bicoid* mRNA localises to both

the anterior and posterior poles (Ruohola *et al*, 1991; Gonzalez-Reyes *et al*, 1995). It therefore appears that *bicoid* mRNA is not merely trapped as it enters the oocyte but instead is localised by active transport towards the minus ends of microtubules.

There is also strong evidence to support the theory that *oskar* mRNA and Staufen protein are localised to the posterior of the oocyte by active transport along the microtubules. Transport of *oskar* mRNA and Staufen protein to the posterior from their site of transient accumulation at the anterior cortex, correlates perfectly with the reorganisation of the microtubules to form a polarised array (Theurkauf *et al*, 1992). The completion of *oskar* and Staufen localisation to the posterior at stage 10 also coincides with the further major reorganisation of the cytoskeleton that results in the onset of cytoplasmic streaming (Theurkauf *et al*, 1992). Further support for active transport along the microtubules comes from the work of Clark *et al* (1994) who used a chimeric protein consisting of the plus-end directed motor protein kinesin, fused to β-galactosidase, to act as a reporter for microtubule polarity. The kin:β-gal fusion protein localises to the posterior of the oocyte at the same time as *oskar* mRNA and Staufen protein, confirming that the plus-ends of the microtubules lie at the posterior at this time. Localisation of the fusion protein is dependent on the activity of the kinesin motor domain and, like localisation of *oskar* and Staufen, is disrupted by the microtubule-depolymerising drug colchicine (Clark *et al*, 1994). Again like *oskar* and Staufen, the kin:β-gal fusion protein fails to localise in *cappuccino* and *spire* mutants, where a premature rearrangement of the microtubule network results in early onset of cytoplasmic streaming (Clark *et al*, 1994; Theurkauf, 1994b). Furthermore, in temperature sensitive mutants of the neurogenic genes *Notch* or *Delta*, where the microtubule network develops symmetrically such that the minus-ends are at both poles and the plus-ends in the centre, *oskar* mRNA, Staufen protein and the kin:β-gal fusion protein all mislocalise to the centre of the oocyte (Ruohola *et al*, 1991; Clark *et al*, 1994). The sensitivity to colchicine and the common genetic requirements for the correct localisation of *oskar* mRNA, Staufen protein and the kin:β-gal fusion protein, strongly suggest that *oskar* and Staufen are transported to the posterior along the microtubules via an association with a kinesin-like plus-end directed microtubule

motor protein.

One problem with the above model of mRNA localisation by active transport along polarised microtubules is the discovery that the endogenous *Drosophila* minus-end directed motor protein dynein, also localises to the oocyte posterior at the same time as *oskar* mRNA and Staufen protein (Hays *et al*, 1994). Like the kin:β-gal fusion protein, dynein co-mislocalises with *oskar* and Staufen in *Notch* and *Delta* temperature sensitive mutants (Li *et al*, 1994). It is therefore possible that at least some of the microtubules are oriented with their minus-ends at the posterior. However, as it has not been demonstrated that dynein needs an active motor domain to be localised, it is also possible that it is transported to the posterior in an inactive state, perhaps by associating with a plus-end directed microtubule motor.

Although the microtubules and other components of the cytoskeleton are clearly implicated in the subcellular localisation of mRNAs, it is difficult to conclusively prove that localisation actually occurs by active transport of mRNA along the cytoskeleton. The most convincing way to demonstrate the occurrence of active transport is the visualisation of directed movement of mRNA in living cells. This has been possible in the case of transport of myelin basic protein (MBP) mRNA from the cell body to the myelinating processes of cultured oligodendrocytes (Ainger *et al*, 1993). On injection of fluorescently labelled MBP mRNA into these cells, the mRNA accumulates in particles of ~0.3μm diameter which then migrate anterograde from the perinuclear region into the cell processes at a speed of 0.2μm/sec. Although no direct cytoskeletal binding has been demonstrated, the particles are closely associated with microtubule bundles, making it reasonable to postulate that they are transported along the microtubules by a kinesin-like plus-end directed motor protein (Ainger *et al*, 1993).

The accumulation of MBP mRNA into large particles is very similar to the behaviour of the *bicoid* mRNA 3'UTR when injected into *Drosophila* embryos. The *bicoid* 3'UTR recruits Staufen protein to form large particles which move in a microtubule

dependent manner (Ferrandon *et al*, 1994). *Xenopus Vg1* mRNA also shows a particulate distribution as it localises to the vegetal pole (Forristall *et al*, 1995), suggesting that packaging into particles may be a common feature of mRNA localisation by active transport. This allows the possibility of packaging many mRNAs into the same particle for transport by a single motor, thereby increasing the efficiency of intracellular transport.

The subcellular localisation of mRNAs occurs in a diverse range of organisms and cell types and is clearly an important method for the targeting of proteins to their correct positions within the cell. The molecular mechanisms of mRNA localisation have begun to be elucidated, revealing a number of conserved features including localisation signals in the 3'UTR of transcripts and the accumulation of mRNAs to be localised into large particles. The cytoskeleton also appears to be universally important for mRNA localisation. Further understanding of the molecular interactions required to bring about mRNA localisation will require the identification and characterisation of the *cis*-acting signals, *trans*-acting factors and cytoskeletal components involved. The amenable genetics and cytology of *Drosophila* make it an ideal organism in which to continue these investigations.

1.5 Unconventional Myosins

1.5.1 Introduction

At the outset of this work a cDNA had been identified which corresponded to transcripts localised in a spatially and temporally specific pattern during *Drosophila* oogenesis. Sequence analysis of the cDNA revealed some homology to the C-terminal region of a class of unconventional myosins. The initial focus of this thesis was to investigate aspects of transcript localisation during oogenesis while concurrent work in the lab focused on the complete cloning and sequence analysis of the gene

(Bryce MacIver, Thesis). This work led to confirmation that the gene did indeed encode a class V unconventional myosin and the *Drosophila* gene was therefore termed *myosinV*.

Myosins are molecular motors which interact with filamentous actin and utilise ATP to generate mechanical force. The myosins were originally divided into two classes with the myosin II class including the conventional, dimeric, filament forming myosin found in smooth muscle, skeletal muscle and almost all non-muscle cells. Class I myosin originally refered to the monomeric, membrane associated myosins of *Acanthamoeba* but eventually the term was adopted for all single-headed myosins. As more non-muscle myosin types were identified it became more useful to categorise myosins as conventional, i.e. myosin II, or unconventional (Cheney and Mooseker, 1992). Currently, 10 classes of unconventional myosins have been identified based on phylogenetic sequence comparisons of their conserved head domains (Cheney *et al*, 1993a ; Mooseker and Cheney, 1995).

All members of the myosin superfamily are based on the myosin heavy chain which consists of a conserved actin-binding, ATP-hydrolising, head domain attached to a regulatory neck domain and a functionally specialised tail domain. Although largely conserved, myosin head domains have a number of class specific features which influence function. The neck domain contains one to six repeats of a unit known as an IQ motif - a basic, hydrophobic ~23 amino acid sequence with the core consensus IQxxxRGxxxRK (Mercer *et al*, 1991). These IQ motifs are the site of light chain or calmodulin binding. Sequences in the tail domain dictate whether a myosin will form dimers and may also determine sub-cellular localisation. Tail domains tend to be class specific and validate the classification of myosins by phylogenetic analysis of the head domains.

Unconventional myosins have been reviewed in detail by Mooseker and Cheney (1995). Here, a summary of each class of myosin will be given, followed by a more detailed description of the class V unconventional myosins, to which the product of

the *Drosophila myosinV* gene belongs.

1.5.2 Class I myosins

The Class I myosins include *Acanthamoeba* myosin I - the prototype unconventional myosin discovered by Pollard and Korn (1973). Unlike conventional class II myosins which have large, coiled-coil α-helix tail domains, class I myosins have short tail domains which cannot form coiled-coil domains capable of dimerisation. Class I myosins have remained the focus of intensive research and a diverse range of members have been identified and characterised. Consequently, the class has been further divided into four subclasses based on phylogenetic sequence comparisons of their head domains.

Myosin I subclass I or the amoeboid myosins, consists primarily of the class I myosins of *Acanthamoeba* and *Dictyostelium* but also includes examples from yeast and vertebrates. Five myosins of this subclass have been identified in *Acanthamoeba* which have either short tails rich in basic residues (myoA and myoE) or longer tails with three distinct tail homology (TH) domains (myoB, myoC and myoD) (Hammer, 1994). The TH1 domain is closest to the head domain and is rich in basic residues which mediate membrane binding via acidic phospholipids (Pollard *et al*, 1991). The TH2 domain is rich in glycine, proline and either alanine or glutamine and has been demonstrated to be an ATP-independent actin-binding site (Jung and Hammer, 1994). The TH3 domain is equivalent to a src homology domain, a domain which is known to mediate protein-protein interactions in signal transduction and membrane-cytoskeleton interactions (Pollard *et al*, 1991).

Gene knockout studies in *Dictyostelium* and *Acanthamoeba* indicate that these myosins are involved in cell motility phenomena, such as lamellapodial extension and phagocytosis. Deletion of individual myosin I genes in *Dictyostelium* result in very mild phenotypes, indicating that there is considerable functional overlap among the

numerous myosins I of this organism (Peterson *et al*, 1995). The additional ATP-independent actin-binding site in the TH2 domain also allows the formation of crosslinked arrays of actin filaments, however, the ability of the tail domain to bind actin is blocked in membrane-bound myosin I (Miyata *et al*, 1989). Maximal actin activated motility requires phosphorylation of a conserved serine or threonine residue in the head domain, whereas almost all myosins of other classes have acidic residues at this site and therefore would not be regulatable by phosphorylation (Bement and Mooseker, 1995).

Myosin I, subclass 2 is characterised by chicken intestinal brush border myosin I (BBMI) (Pollard *et al*, 1991). Homologues have also been identified in cow and human enterocytes where the protein appears to link the plasma membrane of the intestinal microvillus to the underlying bundle of actin filaments. Myosins of this subclass contain multiple calmodulin light chains and have 3-6 calmodulin binding IQ motifs in their neck region. The tail domain of BBMI is a substrate for protein kinase C and is also rich in basic residues which effect binding to acidic phospholipids (Hayden *et al*, 1990). The importance of BBMI binding to phospholipids in the microvillar membrane is unknown, as is the function of a molecular motor in what appears to be the simple structural role of linking actin to membrane.

Members of myosin I, subclass 3 have been identified in rat, cow, bullfrog and *Drosophila* (Mooseker and Cheney, 1995). These proteins are similar to brush border myosins but are characterised by a neck domain with three IQ motifs which bind calmodulin. In vertebrates, this subclass of myosin I is expressed in a broad range of organs and tissues, however, expression of *Drosophila* myosin-Ib is restricted to the gut and the ovarian follicle cells (Morgan *et al*, 1995). *Drosophila* myosin-Ib first appears in the polarised enterocytes of the gut during late embryogenesis. The protein moves from a basolateral position to an apical position co-incident with the formation of the microvilli of the brush border. However, during oogenesis, myosin-Ib is present on both the basolateral and apical domains of the follicle cells.

Myosin I, subclass 4 contains three members - *Drosophila* myosin-Ia, rat myr4 and *C.elegans* myosin Ia (Morgan *et al*, 1994; Bahler *et al*, 1994). These proteins have neck regions containing two IQ motifs and tail regions rich in basic residues. The expression profiles of *Drosophila* myosin-Ia and rat myr4 are markedly different with highest levels of myr4 found in the brain (Bahler *et al*, 1994) while myosin-Ia is exclusively localised to the gut (Morgan *et al*, 1995). Myosin-Ia is expressed in enterocytes in a similar, but temporally distinct pattern from that of myosin-Ib. *Drosophila* myosin-Ia differs from virtually all other myosins at a conserved residue of the actin contact site and so potentially has different actin binding and mechanochemical properties from other myosins.

1.5.3 Class II myosins

Class II myosins are the conventional, two-headed myosins which have been well characterised in muscle cells, and which are also ubiquitous in almost all nonmuscle cells. One such conventional, nonmuscle myosin is *Drosophila* nonmuscle myosin II which has been shown to be required for a diverse range of processes throughout development (Edwards and Kiehart, 1996). Mutations in the myosin heavy chain gene *zipper* cause defects in the cell sheet movements of embryogenesis, such as dorsal closure failure (Young *et al*, 1993). The regulatory light chain of nonmuscle myosin II is encoded by the *spaghetti squash* gene and has been shown to be required for nuclear migration, cellularisation and correct imaginal disc development during embryogenesis (Edwards and Kiehart, 1996). Maternally encoded *spaghetti squash* has also been demonstrated to be required for follicle cell migration and cytoplasmic transfer during oogenesis (Wheatley *et al*, 1995).

1.5.4 Class III myosins

To date, the only identified class III myosins are the ninaC myosins of *Drosophila*.

Alternative splicing of the *ninaC* gene produces two unconventional myosins, p174 and p132, which differ only in their tail domains (Montell and Rubin, 1988). The ninaC myosins are the most highly diverged of all classes of myosins and are unique in that they have a putative kinase domain N-terminal to the myosin head domain.

The ninaC myosins are exclusively expressed in the photoreceptor cells of the *Drosophila* eye. p174 is predominantly localised to the phototransducing organelle known as the rhabdomere - a microvillus-like extension of the plasma membrane. p132 is localised to the cell body cytoplasm which would suggest that the tail domain of p174 is responsible for targeting to the rhabdomere (Porter *et al*, 1992). *ninaC* null mutants have abnormal electroretinograms and show retinal degeneration over time and with exposure to light. Mutational analysis indicates that the kinase domain of p174 is required for phototransduction but is not required for subcellular targeting or maintenance of retinal structure (Porter and Montell, 1993). The ninaC myosins also appear to be required for the proper localisation of calmodulin to the rhabdomere, where it may be involved in the phototransduction process.

1.5.5 Class IV myosins

Class IV consists of the 178kD 'high molecular weight myosin I' discovered in *Acanthamoeba* by Horowitz and Hammer (1990). This protein has a myosin head domain, a single IQ motif, and a large tail domain which shares no homology to the amoeboid myosins except for a C-terminal TH-3 domain. Furthermore, the tail domain contains no membrane binding domain and is not predicted to form coiled-coil α-helix, so is presumed not to dimerise. Further study of this myosin will be required to define its function and to determine whether homologues are present in other organisms.

1.5.6 Class VI myosins

Class VI myosins include the well characterised *Drosophila* 95F myosin (Kellerman and Miller, 1992) and pig myosin-VI (Hasson and Mooseker, 1994). These two myosins consist of conserved head domains which share an ~25aa insertion, neck domains with a single IQ motif, and tail domains comprising a segment of coiled-coil followed by a globular domain. Interestingly, these globular tail domains share more homology than do the myosin head domains, indicating that they are critical for function.

Antibodies to pig myosin-VI indicate that it is widely expressed, with highest levels in kidney, brain lung and intestine (Hasson and Mooseker, 1994). The protein has been reported to have a sub-microvillar localisation in the brush borders of kidney tubules and enterocytes. *Drosophila* 95F myosin has also been reported in the larval intestinal brush border, however 95F has been most extensively studied during embryogenesis, where it is required for the proper organisation of the nuclei of the syncytial blastoderm (Mermall and Miller, 1995). 95F myosin associates with cytoplasmic particles which surround the interphase nuclei and undergo cell-cycle dependent redistribution (Mermall *et al*, 1994). Injection of antibodies to 95F disrupts the movement of these particles and results in abnormal furrow formation and aberrant nuclear morphology. This indicates that 95F myosin is not only required for the formation of actin-based transient membrane furrows, but also for the cell-cycle dependent movement of organelles (Mermall and Miller, 1995). Work performed in this laboratory indicates an additional role for the 95F myosin in epithelial morphogenesis, both during imaginal disc evagination and during oogenesis (Deng and Bownes, paper in preparation).

1.5.7 Class VII myosins

Class VII myosins include *Drosophila* 35BC myosin (Chen *et al*, 1991) and class VII myosins from human and pig (Bement *et al*, 1994). Sequence analysis of partial cDNAs reveals a neck domain with five IQ motifs and a region of tail domain

predicted to form coiled-coil α-helix, while Northern analysis indicates a transcript of >9kb (Mooseker and Cheney, 1995).

Mutations in class VII myosins have been associated with deafness in both mice and humans. Partial cloning of the mouse deafness gene *shaker-1* revealed a high level of homology to the head domain of human and porcine myosin-VIIa. Several *shaker-1* mutant alleles were subsequently discovered to have small deletions or missense mutations within the head domain of mouse myosin-VIIa (Gibson *et al*, 1995). The *shaker-1* gene was thought to be the orthologue of the gene defective in Usher Syndrome 1B, an inherited human deaf-blindness disease (Steel and Brown, 1994). Familial analysis confirmed that Usher Syndrome 1B was also associated with mutations in the head domain of human myosin-VIIa (Weil *et al*, 1995).

1.5.8 Class VIII myosins

Class VIII myosins have been exclusively described in plants and include the ATM1 and ATM2 myosins of *Arabidopsis thaliana* (Knight and Kendrick-Jones, 1993; Kinkema *et al*, 1994). ATM1 and ATM2 have head domains with N-terminal extensions, four and three IQ motifs respectively, and tail domains which share extensive regions of homology. These two class VIII myosins of *Arabidopsis* have been shown to have different expression patterns, with ATM1 expressed in leaf and root tissue and ATM2 predominantly expressed in flower and root tissue (Kinkema *et al*, 1994).

1.5.9 Class IX myosins

Members of this class of myosins include myr5 in rat (Reinhard *et al*, 1995) and myosin-IXa and -IXb in human and pig (Bement *et al*, 1994). Northern analysis indicates that these proteins are widely expressed with the highest levels of human

myosin-IXb found in leukocytes (Wirth *et al*, 199X). Sequence analysis of human myosin-IXb and rat myr5 has revealed several features which make this class of myosin unique (Wirth *et al*, 199X). Firstly, these two proteins have N-terminal extensions which are 80% identical to each other but otherwise novel. Secondly, both myosins have large insertions of ~140 amino acids at the presumed actin contact site which could potentially affect their mechanochemical properties. Both myosins have a neck domain with four IQ motifs followed by a tail domain with four distinct subdomains, none of which are predicted to form coiled-coils. The proximal subdomain is rich in proline while the second is a cysteine-rich subdomain capable of binding zinc. The third domain is remarkable in that it is homologous to the GTPase-activating proteins (GAP), which regulate the rho family of G-proteins (Lamarche and Hall, 1994). The forth domain is divergent, possibly as a consequence of alternative splicing. The discovery of the rho GAP domain in class IX myosins is important as a potential link between signal transduction pathways and rearrangements of the actin based cytoskeleton.

1.5.10 Class X myosins

Class X myosins have been identified in the cow and the bullfrog (Solc *et al*, 1994). These myosin are not well characterised but their main distinguishing feature is the presence of three pleckstrin homology (PH) domains within the tail domain (Oliver *et al,* 1996). The function of PH domains is unclear but they have been identified in many proteins associated with signal transduction or the membrane cytoskeleton.

1.5.11 Class XI myosins

Class XI myosins are again exclusively plant myosins, comprising of MYA1-6 from *Arabidopsis* and a partial sequence identified in the fern *Anemia* (Kinkema and Schiefelbein, 1994; Kinkema *et al*, 1994; Moepps *et al*, 1993). MYA1 and MYA2

have neck domains with six IQ motifs followed by a region of tail domain predicted to form coiled-coil α-helix. The structures of MYA1 and MYA2 were sufficiently similar to class V myosins that they were originally assigned to this class, however the discovery of other MYA1-like sequences led to their re-classification (Kinkema *et al*, 1994; Mooseker and Cheney, 1995). Northern analysis has revealed different expression patterns of MYA1-3 in the flowers, root, leaves and stem of *Arabidopsis*, however the function of these myosins in not yet understood (Kinkema *et al*, 1994).

1.5.12 Class V myosins

Despite their relatively recent discovery, the class V myosins are among the best characterised of the unconventional myosins, second only to the class I myosins. Examples of class V myosins include the product of the mouse *dilute* gene (Mercer *et al*, 1991), MYO2 and MYO4 in yeast (Johnston *et al*, 1992; Haarer *et al*, 1994), chicken p190 - a calmodulin binding protein from brain now known as myosin-V (Espreafico *et al*, 1992) and the product of the rat *myr6* gene (Zhao *et al*, 1996). Studies in this lab also indicate that a mouse sequence originally reported to encode a glutamate decarboxylase (Huang *et al*, 1990), in fact encodes a second class V myosin in the mouse (MacIver, Wilke, Loke and Bownes, unpublished).

Sequence analysis of the class V myosins has indicated that all members share certain structural features, including myosin head domains which are more similar to each other than to any other class of myosin, long neck regions consisting of six IQ motifs which are presumed to be the site of calmodulin binding, and tail domains with a region predicted to form coiled coil α-helix, followed by a C-terminal globular domain. These myosins are predicted to form two headed dimers but not myosin II-like filaments (fig 1.5).

The first class V myosin to be described was the product of the mouse *dilute* gene. The *dilute* mutation was so named because it causes a dilution or lightening of coat

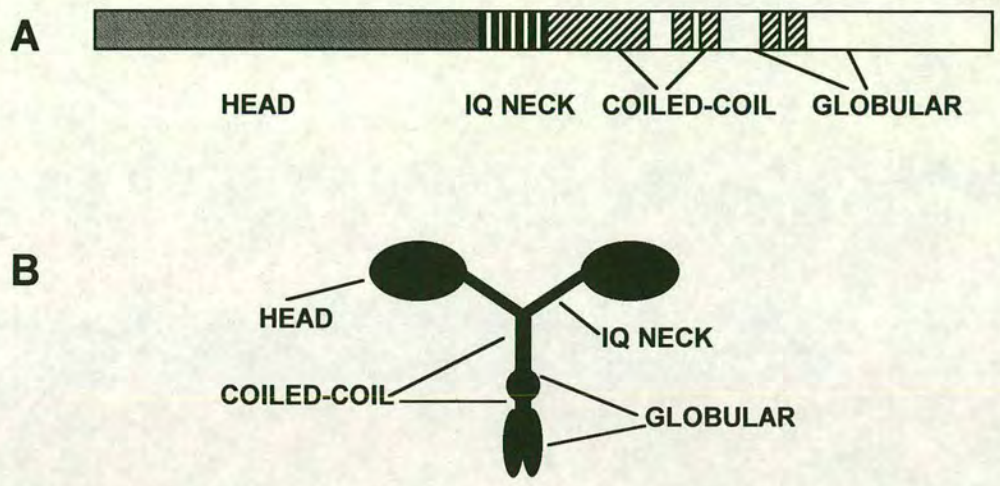

Figure 1.5 A) Schematic diagram of class V myosin showing the head, neck, coiled-coil and globular domains. B) Schematic diagram of class V myosin dimer.

colour. This dilution of coat colour is the result of a failure to transfer the pigment-containing melanosomes from their site of synthesis in the melanocytes to the keratinocytes of growing hair (Silvers, 1979). The *dilute* phenotype was originally thought to be the result of abnormal melanocyte morphology, however, recent studies indicate that *dilute* melanocyte morphology is normal, but the melanosomes are wrongly distributed (Wei *et al*, 1997). Immunolocalisation studies have shown that the *dilute* myosin V is associated with these melanosomes (Wu *et al*, 1997), consistent with the idea that *dilute* myosin V acts as a motor protein for the movement of melanosomes. More severe alleles of *dilute* cause neurological defects, whereby homozygous animals suffer seizures and usually die within a few weeks of birth (Searle, 1952). This would indicate that *dilute* is an essential gene, however, the brains of these mice show no obvious defects and as yet, the cause of lethality is unknown.

Two examples of class V unconventional myosins, MYO2 and MYO4, have been

discovered in the budding yeast *Saccharomyces cerevisiae* (Johnston *et al*, 1991). The yeast *MYO2* gene is an essential gene first discovered in a screen for temperature sensitive cell-division cycle mutations. At the restrictive temperature, *MYO2* mutants fail to bud and arrest as large cells filled with vesicles. This phenotype is consistent with an inability to target or transport secretory vesicles to areas of cell growth. Intracellular vesicle transport was previously thought to be mediated exclusively by the microtubules and their associated motors, however, the discovery that the *MYO2* phenotype can be suppressed by overexpression of SYM1, a kinesin-like protein, suggests some interaction between microtubule-based and actomyosin-based vesicle transport (Lillie and Brown, 1992).

MYO4, a second yeast class V myosin gene, was isolated by random cloning and sequence comparison (Haarer *et al*, 1994). The head domain of MYO4 is 73% identical to that of MYO2, however this second myosin is not essential. The *MYO4* gene has been discovered to correspond to *SHE1*, one of five genes involved in yeast mating type switching (Jansen *et al*, 1996). Mating type switching is brought about by the action of the *HO* endonuclease in the mother cell during cell division. In the daughter cell, mating type switching is prevented by the accumulation of the yeast transcriptional regulator Ash1p, which represses the transcription of the *HO* gene. Bobola *et al* (1996) demonstrated that the asymmetric distribution of the Ash1p protein depends on proteins of the actin cytoskeleton, including MYO4. They postulate that Ash1p, or a factor that controls its synthesis, is transported to the daughter cell by the myosin V motor protein.

Biochemical characterisation of the class V unconventional myosins has come from studies on chicken myosin-V. Chick myosin-V was first identified as a 190kDa, calmodulin-binding protein present in brain actomyosin preparations (Larson *et al*, 1988, 1990). Molecular cloning of the gene encoding the p190 protein revealed 91% homology to the mouse dilute gene and p190 was thus named chick myosin-V (Espreafico *et al*, 1992; Sanders *et al*, 1992). Purified myosin-V was found to have the unusual property of binding to calmodulin in the absence of calcium (Larson *et al*,

1990), and the site of calmodulin binding was revealed to be the six IQ motifs in the neck domain (Esprefico *et al*, 1992). The myosin-V protein was found to be present in most tissues but especially in the brain where immunolocalisation studies revealed a punctate staining pattern most intense at the cell periphery and co-localising with intracellular membranes in the perinuclear region (Espreafico *et al*, 1992).

Purification of chick myosin-V has allowed its visualisation by electron microscopy (Cheney *et al*, 1993). As predicted, myosin-V forms a two-headed dimer but does not form myosin II-like filaments. The head regions have extended neck domains attached to a stalk which terminates in a globular domain. The extended neck domain is presumably due to the six IQ motifs and appears to confer great mobility to the head region. Studies on the motor properties of chick myosin-V demonstrate it to be an actin-activated Mg-ATPase (Espindola *et al*, 1992), which can be switched on by physiologically relevant concentrations of calcium (Cheney *et al*, 1993). Paradoxically, several different motility assays show that myosin-V can translocate towards the barbed end of actin filaments in the absence of calcium, and the addition of calcium, in fact, slows movement (Cheney *et al*, 1993; Wolenski *et al*, 1995). This uncoupling of ATPase activity and motility is also observed in avian brush border myosin I (Wolenski *et al*, 1993) and is postulated to be due to the calcium induced loss of calmodulin light chains.

The phenotypes of the *dilute* and *MYO2* mutations, together with the localisation patterns of chick myosin-V and the *dilute* gene product, strongly suggest that the class V unconventional myosins are involved in intracellular vesicle transport. These myosins potentially function as molecular motors which transport vesicles or organelles via the actin cytoskeleton.

This thesis presents the characterisation of a class V unconventional myosin in *Drosophila melanogaster*. *Drosophila myosinV* was identified as a result of a reverse genetics approach to identify genes with interesting transcript localisation patterns during oogenesis. This current study concerns the expression pattern, localisation and

genetic analysis of *Drosophila myosinV*. It will be interesting to relate the findings on this new class V myosin to what is already known from studies on other members of this class and to explore the role of a potential molecular motor in *Drosophila* oogenesis.

Chapter 2

Materials and Methods

2.1 Materials

2.1.1 Chemicals and radiochemicals

All chemicals were of analytical grade and were obtained from Sigma, Fison or BDH Chemicals Ltd. Radiochemicals 5'[α-^{32}P] dCTP and 5'[α-^{35}S] dATP were obtained from Amersham.

2.1.2 Restriction and modifying enzymes

Restriction endonucleases were obtained from Gibco BRL, Promega or Northumbria Biological Laboratories (NBL). Modifying enzymes were obtained from Boehringer Mannheim, Gibco BRL or Promega. Restriction endonucleases and modifying enzymes came supplied with the appropriate buffer and were used as recommended by the manufacturer.

2.1.3 Buffers and Solutions

All buffers and solutions were prepared using double distilled water and, if necessary, were sterilised by autoclaving (15psi for 15 minutes) or by sterile filtering. All buffers were pH adjusted and used at room temperature unless otherwise stated. Common buffers and solutions are described below:

100X Denhardt's: 2% bovine serum albumin, 2% Ficoll, 2% polyvinylpyrolidone
MOPS Buffer: 20mM Na-MOPS, 5mM Na-acetate, 1mM EDTA, pH 7.0
PBS: 137mM NaCl, 2.7mM KCl, 4.3mM Na_2HPO_4, 1.4mM KH_2PO_4, pH 7.4
Ringer's saline: for 1 litre - 6.5g NaCl, 0.14g KCl, 0.2g $NaHCO_3$, 0.12g $CaCl_2$, 0.01g NaH_2PO_4

SM (phage buffer): 100mM NaCl, 8.1mM $MgSO_4$, 50mM Tris pH 7.5, 0.5% gelatin

20X SSC: 3M NaCl, 0.3M tri-sodium citrate

20X SSPE: 3.6M NaCl, 0.2M $NaPO_4$, 0.02M EDTA, pH 7.7

TAE: 40mM Tris-acetate, 1mM EDTA pH 7.8

TBE: 89mM Tris-HCl, 89mM boric acid, 2.5mM EDTA, pH 8.3

TE: 10mM Tris-HCl, 1mM EDTA, pH 8.0

2.1.4 Bacterial strains

The bacterial strains used are shown in table 2.1.

Table 2.1 Bacterial strains and markers

***E.coli* strain**	**Markers**	**Comments**
XL1 Blue	*A1, gyrA96, thi, hsdR17, supE44,* (F', *proAB, lacI^{q}ZΔM15)*	used to propagate pBluescript plasmids and to plate λZAP cDNA library
NM422	F', *lacI^{q}Δ(lacZ)M15 proA$^+$B$^+$/supE thi Δ(lac$^-$ proAB)/ Δ(hsdMS$^-$ mcrB)5* ($r_K^-m_K^-$ McrBC$^-$)	used to plate λFIX genomic DNA library

2.1.5 Plasmids

The plasmids used are shown in table 2.2

Table 2.2 Plasmids

Plasmid	Description	Features	Source
pBluescript	general cloning vector	contains D15 region of *lacZ*, ampicillin resistance	Stratagene
pGEM	general cloning vector	contains D15 region of *lacZ*, ampicillin resistance	Promega
pAdd3'UTR	germline trans-formation vector	contains P-element ends, *white* gene, ampicillin resistance	gift from Kellie Whittaker

2.1.5.1 pBluescript cloning vectors

The pBluescript series of vectors have a number of useful features which are worth describing here. They contain the *lacZ* α-peptide which includes a multiple cloning region. pBluescript vectors produce functional β-galactosidase when complemented in an *E.coli* strain containing the *lacZ*ΔM15 gene and therefore results in blue colonies when plated on media containing 5-bromo-4-chloro-3-indolyl-β-galactopyranoside (BCIG or X-Gal). However, disruption of the *lacZ* α-peptide by insertion into the multiple cloning region results in white colonies on media containing X-Gal. Induction of the *lac* promoter is facilitated by the inclusion of the lactose analog isopropyl-β-D-thio-galactopyranoside (IPTG) in the agar plates. The pBluescript vectors contain the origin of replication of the filamentous bacteriophage f1, which allows production of single stranded DNA for sequencing. In addition, the universal M13 sequencing primers can be used to sequence DNA cloned in the multiple cloning region and transcripts can be produced from inserts using T3 and T7 polymerase sites.

2.1.6 Libraries

2.1.6.1 λFIX genomic library

The λFIX genomic DNA library was obtained from Stratagene Inc. It uses the λFIX-II bacteriophage vector which contains *XhoI* endonuclease sites in the multiple cloning site. The library was constructed by ligating a size fractioned partial *Sau3AI* digestion of *Drosophila* CantonS genomic DNA to partially filled *XhoI* sites in the vector. Insert sizes vary from 9-23kb and each end is flanked by a T3 or T7 promoter.

2.1.6.2 Ovarian and testes λZAP cDNA libraries

These libraries were constructed by Stratagene Inc. in the λZAP-II bacteriophage vector. cDNA was prepared by both oligo dT and random primed first strand synthesis from polyA$^+$ RNA extracted from adult *Drosophila* ovaries or testes. The λZAP-II vector permits the excision of a pBluescript plasmid containing the cDNA insert by co-infection with a helper phage (see 2.8.5.2).

2.1.7 Media

All media was prepared by ICMB media services and sterilised by autoclaving.

Luria Broth (LB): 1% bacto-tryptone, 0.5% yeast extract, 1% NaCl, pH 7.0 (Luria and Burrows, 1957)

YT: 1.6% bacto-tryptone, 1% yeast extract, 0.5% NaCl, pH 7.0

LB agar: LB supplemented with 1.5% agar

Top agarose: LB supplemented with 0.7% agarose

Selective media: LB broth or agar supplemented with ampicillin, X-Gal and IPTG

ampicillin: 100mg/ml stock solution in H_20, used at final concentration of 100μg/ml

X-gal: 2% stock solution in dimethylformamide, used at final concentration of 2ml/l

IPTG: 100mM stock solution in H_20, used at final concentration of 0.3mM

2.2 *Drosophila*

2.2.1 Life cycle of *Drosophila melanogaster*

The wild type *Drosophila* strain used throughout this work was OregonR (Lindsay and Zimm, 1992). Other strains of flies used in this work are detailed in the relevant chapter. The developmental stages of OregonR development at 25°C are shown in table 2.3

Table 2.3 Stages of *Drosophila* development (Bownes and Dale, 1982)

Hours	Days	Developmental Stage
0	0	Fertilisation and fusion of pronuclei
1.5	0	Preblastoderm stage. Migration of cleavage nuclei and pole cell formation
3	0	Blastoderm stage. Migrated nuclei form cells
3.5	0	Gastrulation begins
6 - 8	0	Segmentation begins
18	0	Larval differentiation nears completion
24	1	Hatching from egg. Onset of first larval instar
48	2	First moult. Second larval instar begins
72	3	Second moult. Third larval instar begins
120	5	Puparium formation with white puparium
122	5	Puparium darkens
124	5	Puparium moult
132	5	Pupation. Evagination of imaginal discs
216 - 240	9 -10	Eclosion of adult from pupal case

2.2.2 Maintenance of *Drosophila* stocks

Stocks were maintained at 18°C or 25°C on Staffan cornmeal food consisting of cornflour (250g), sugar (500g), yeast pellets (175g) and agar (100g) dissolved in distilled water to a final volume of 10 litres. The food was boiled and allowed to cool

to approximately 60°C before being poured into bottles or vials. A fungicide, Nipagin, was added to a final concentration of 4.5 μg/L. Strips of Whatman 3M paper soaked in 3% benzyl benzoate in ethanol then air dried, were placed on top of the cornmeal food periodically to prevent mite contamination.

Adh food was used to prepare plates for the collection of embryos and first and second instar larvae. It consisted of 100g dried flake yeast, 100g brown sugar, 16g agar and 4.5 μg/ml Nipagin in a final volume of 1 litre.

During egg collections and prior to ovary dissection fly food was supplemented with yeast paste - either fresh bakers yeast or dried yeast made to a paste with 20% glucose solution.

2.2.3 Collection of staged embryos

2.2.3.1 0-4 hour embryos (eggs)

Young, well fed flies were transferred to an egg collection cage and allowed to lay on Adh plates supplemented with yeast paste for four hours at 25°C. The eggs were harvested by washing the collection plate with water and using a paintbrush to transfer the eggs to a sieve where remaining food was removed by rinsing with water. The 0-4 hour embryos were dechorionated using 50% bleach (2.2.8.1) then transferred to an eppendorf tube with a paintbrush and used immediately or frozen in liquid nitrogen and stored at -70°C.

2.2.3.2 4-16 hour embryos

Eggs were collected, as above, for a period of 12 hours and then allowed to develop a further four hours at 25°C before harvesting and dechorionation.

2.2.3.3 16-24 hour embryos

Eggs were collected, as above, for a period of eight hours and then allowed to develop a further 16 hours at 25°C before harvesting and dechorionation.

2.2.4 Collection of staged larvae

2.2.4.1 First instar larvae

Eggs were collected as above for a period of four hours and then allowed to develop a further ~28 hours at 25°C. First instar larvae were picked from the plate with a paintbrush and transferred to sieve then washed with water. Larvae were then transferred to an eppendorf tube with a paintbrush and frozen in liquid nitrogen.

2.2.4.2 Second instar larvae

Eggs were collected as above for a period of four hours and then allowed to develop a further ~52 hours at 25°C before washing and freezing.

2.2.4.3 Collection of sexed third instar larvae

Young, well fed flies were transferred to a bottle of fresh food supplemented with yeast paste and allowed to lay for four hours before being removed. The bottle was then incubated a further ~96 hours at 25°C. Late third instar larvae were picked with a paintbrush as they crawled up the sides of the bottle. Larvae were then transferred to a drop of Ringer's solution on a slide and examined under a dissecting microscope. Larvae were sexed according to the appearance of the male larval gonads then transferred to separate eppendorf tubes and frozen in liquid nitrogen.

2.2.5 Collection of pupae

Eggs were collected as for third instar larvae and incubated a further ~130 hours at 25°C. The pupae were picked off the sides of the bottle with a paintbrush, then washed and frozen.

2.2.6 Collection of sexed adult flies

Adult flies of various ages were anaesthetised with diethyl ether, examined under a dissecting microscope and sexed according to external morphology i.e. size, abdominal pigmentation or presence of sex combs on the male forelegs.

2.2.7 Collection of Virgin Females

All existing adult flies were tipped from the bottle which was then returned to the 25°C incubator. Newly eclosed flies were examined and sexed early in the morning and late in the day and placed into separate vials.

2.2.8 Dechorionation of embryos

2.2.8.1 Dechorionation with bleach

Embryos for RNA extraction and *in situ* hybridisation were dechorionated with 50% bleach. Embryos in a sieve were immersed in 50% bleach and observed under a dissecting microscope until they lost their opaque coat, became shiny and started to clump together. Embryos were then washed thoroughly in water.

2.2.8.2 Dechorionation by hand

Embryos for germline transformation and phenotypic analysis were dechorionated by hand. Embryos were transferred by paintbrush to a slide with a strip of double-sided sticky tape. Using fine forceps, the embryos were rolled gently on the sticky tape until the chorion stuck and ripped and the embryo popped out.

2.2.9 Clearing of embryos and larvae

Dechorionated embryos and larvae were fixed in glycerol:acetic acid (1:4) for 1 hour at 60°C then mounted in clearing medium consisting of lactic acid:ethanol (9:1) and dried on slide drier overnight at 50°C.

2.2.10 *in situ* detection of β-galactosidase expression patterns

Ovaries were dissected out in Ringer's saline then transferred to the well of a microtitre dish containing 100µl staining buffer - 10mM Na_2HPO_4 pH 7.0, 150mM NaCl, 1mM $MgCl_2$, 7mM $K_4Fe(CN)_6.3H_2O$, 7mM $K_3Fe(CN)_4.3H_2O$, 0.2% X-gal. Staining patterns were observed under a dissecting microscope after overnight incubation in the dark.

2.3 *in situ* hybridisation

2.3.1 *in situ* hybridisation to whole mount ovaries

A method modified from that of Tautz and Pfeifle (1989) was used. All incubations were carried out on a rotating wheel unless otherwise stated. Ovaries were dissected

from adult female flies which had been tipped to fresh food supplemented with dried yeast the day before. Dissected tissue was placed in a microfuge tube and maintained at a low temperature in dry ice. When sufficient tissue was collected it was fixed in 1ml of a freshly prepared fixative (4% paraformaldehyde, 6mM NaOH, 50mM PIPES pH 7.0, 1mM EGTA pH 8.0, 2mM $MgSO_4$) for one hour at room temperature on a rotating wheel. The fixative was removed and the ovaries washed in 3 changes of PBT (PBS + 0.1%Tween-20) with 5 minute incubations between changes. Ovaries were incubated in 50µg/ml Proteinase K for 30 minutes then washed in 2 changes of PBT then fixed for a further 20 minutes and washed 3 x 10 minutes in PBT.

To prepare the ovaries for hybridisation, they were washed in a 1:1 solution of PBT:HS for 20 minutes (HS: 50% formamide, 5xSSC, 50µg/ml heparin, 0.1% Tween-20, 100µg/ml sonicated salmon sperm DNA). Prehybridisation was carried out in HS for a minimum of 1 hour at 48°C in a heating block. Hybridisation was carried out at 48°C overnight by replacing the HS with ~50µl of denatured digoxigenin labelled DNA probe in HS (section 2.3.6).

The probe was removed by 20 minute washes, first in HS, then in HS:PBT washes at ratios of 4:1, 3:2, 2:3, 1:4 and finally in 2 washes of PBT. Signal was detected by incubation at room temperature with anti-digoxigenin-AP antibody (Boehringer Mannheim) at a dilution of 1:1000 for 1 hour. The antibody solution was pre-absorbed with fixed ovaries for at least 1 hour to reduce background signal. Excess antibody was removed with 4 washes of PBT at 20 minute intervals followed by three 5 minute washes in NMTLT buffer (100mM NaCl, 50mM $MgCl_2$, 100mM Tris-HCl pH 9.5, 1mM freshly prepared levamisole, 0.1% Tween-20).

Colour detection buffer was prepared with 1ml NMTLT buffer plus 4.5µl NBT (75mg/ml nitro-blue-tetrazolium salt in dimethylformamide) and 3.5µl X-phosphate (50mg/ml 5-bromo-4-chloro-3-indolyl phosphate toluidinium salt in dimethyl-formamide). Ovaries were incubated in colour detection buffer on a cavity slide in the dark and checked periodically for colour development. Development took between 1

and 3 hours and the reaction was stopped with three rinses in PBT. The ovaries were then mounted in PBT and observed by microscope.

2.3.2 *in situ* hybridisation to whole mount ovaries with digoxigenin RNA probes

in situ hybridisation with digoxigenein labelled RNA probes was performed essentially as for DNA probes (2.3.1) except that solutions were prepared with DEPC treated water to destroy RNases. The fixative used was 10% formaldehyde, 10% DMSO, 50mM EGTA, 1X PBS, and prehybridisation, hybridisation and washing were performed at 55°C. Digoxigenin labelling of RNA is described in section 2.3.7.

2.3.3 *in situ* hybridisation to whole mount testes

in situ hybridisation to whole mount testes was performed essentially as for whole mount ovaries (2.3.1) except that testes were only incubated in 50μg/ml Proteinase K for 5 minutes.

2.3.4 *in situ* hybridisation to whole mount embryos

Embryos were dechorionated with bleach (2.2.8.1) then fixed in 1:1 fixative:heptane for 1 hour. After removal of fixative:heptane, embryos were devitellinised by the addition of 9:1 methanol:EGTA (0.5M, pH 8.0) followed by vigorous shaking for 5 minutes. Embryos were rinsed in three changes of 9:1 methanol:EGTA then rehydrated by 5 minute incubations in methanol/EGTA:fixative at ratios of 7:3, 5:5 and 3:7, followed by a rinse and a 20 minute incubation in fixative. Embryos were washed in 3 changes of PBT, incubated in 50μg/ml proteinase K for 3.5 minutes, washed in 2 changes of PBT then fixed for a further 20 minutes followed by 2 washes in PBT. Prehybridisation, hybridisation, antibody incubation and colour detection

were then performed as described for whole mount ovaries (section 2.3.1).

2.3.5 *in situ* hybridisation to polytene chromosomes

2.3.5.1 Preparation of chromosomes

Third instar larvae were collected from the sides of vials or bottles with a moist paintbrush and transferred to a cavity slide. The salivary glands were dissected out in Ringer's saline under the dissecting microscope. The salivary glands were then transferred to a drop of 1:2:3 fixative (1 part lactic acid, 2 parts water, 3 parts acetic acid) on a clean microscope slide, then a clean siliconised coverslip was carefully placed on top. The salivary gland cells were disrupted by tapping the coverslip with the back end of the paintbrush in a circular motion and spread by gently streaking across the coverslip. An edge of the coverslip should be held during tapping and streaking to prevent it sliding and damaging the chromosomes.. The slide was then sandwiched between layers of blotting paper and the chromosomes squashed by applying considerable thumb pressure. The chromosomes were examined for quality at 250X or 400X magnification using phase contrast.

The slides were marked to show which side the chromosomes were on. Coverslips were removed by dipping the slide into liquid N_2 then quickly flicking the coverslip from the slide with a scalpel blade. The chromosomes were dehydrated in 70% ethanol for 5 minutes at room temperature followed by 95% ethanol for 5 minutes then air dried.

2.3.5.2 Denaturation

Prior to denaturation the chromosomes were treated in 2X SSC at 65°C for 30 minutes followed by treatment in 2X SSC at room temperature for 10 minutes. Chromosomes were denatured by treating in 70mM freshly prepared NaOH for 2-3

minutes followed by rinsing in 2X SSC. Dehydration through an ethanol series was then performed as above.

2.3.5.3 Hybridisation

A digoxigenin labelled DNA probe, prepared as described in section 2.3.6, was denatured by boiling in a water bath then plunging into ice. 40µl of probe was added to each slide and a covered carefully with a coverslip. The slides were then placed into a plastic box on a platform of Pasteur pipettes which rested on a wad of damp paper tissue to prevent dehydration. The box was sealed and incubated overnight at 55°C. The coverslips were removed by placing the slides in 2X SSC and allowing them to float off.

2.3.5.4 Washing and Detection

The slides were washed twice in 2X SSC at 55°C for 20 minutes and once at room temperature. Slides were then washed for 2 minutes in NTT buffer (150mM NaCl, 100mM Tris pH 7.2, 0.05% Tween-20) then blocked for 1 hour in blocking buffer (0.5% powdered milk in NTT). After a further 2 minute wash in NTT the slides were covered with ~0.5ml anti-digoxigenein-HRP antibody (1:100 in NTT) and incubated 1-2 hours at room temperature.

The slides were washed twice in NTT for five minutes and twice in PBS. Diaminobenzidine (DAB) was used for colour detection. A DAB pellet and a H_2O_2/urea pellet (Sigma) were dissolved in 1ml of PBS then ~0.3ml was applied to each slide for 15-20 minutes. Excess DAB solution was washed away by rinsing in PBS, then the slides were examined under phase contrast for appearance of signal (dark brown/black bands). The slides were then counterstained with Giemsa (BDH) 1:100 in water, to aid identification of chromosomes.

2.3.6 Digoxigenein labelling of DNA

DNA was labelled with digoxigenein by random priming using Boehringer Mannheim reagents. 200ng of linearised, purified DNA in a total volume of 19µl was denatured by heating to 95°C for 5 minutes then chilling on ice. To this was added 2.5µl of hexanucleotide mix, 2.5µl of DIG dNTP mix (dATP, dCTP, dGTP, dTTP + DIG-dUTP) and 2 units of Klenow enzyme. The reaction was incubated at 37°C overnight resulting in the synthesis of ~500ng DIG-labelled DNA. The reaction was stopped by the addition of 1µl 0.5M EDTA pH 8.0 and unincorporated nucleotides were removed by precipitation of the labelled DNA with 1.5µl 10M LiCl and 2.5 volumes of ethanol for 30 minutes at -70°C. The DNA was pelleted by centrifugation, washed in 75% cold ethanol and dried under vacuum. For *in situ* hybridisation to whole mount ovaries, testes and embryos the labelled DNA was resuspended in 200µl HS (HS: 50% formamide, 5xSSC, 50µg/ml heparin, 0.1% Tween-20, 100µg/ml sonicated salmon sperm DNA). For *in situ* hybridisation to polytene chromosomes the labelled DNA was resuspended in 100µl of 600mM NaCl, 1mM $MgCl_2$, 50mM phosphate buffer pH 7.2, 2X Denhardt's. Before use, probes were denatured by boiling and chilling on ice.

2.3.7 Digoxigenin labelling of RNA

Digoxigenein labelled *lacZ* RNA probes were transcribed from pGEM-lacZ using reagents from Boehringer Mannheim. Both antisense and sense (negative control) probes were transcribed from pGEM-lacZ using SP6 polymerase and T7 polymerase respectively. pGEM-lacZ was first linearised with *SmaI* or *HindIII* to prevent transcriptional run-on. A tenth of each digest was run out on an agarose gel to estimate concentration while the remainder was phenol chloroform extracted and ethanol precipitated. The digests were then resuspended in RNase free TE at 1µg/µl. An antisense probe was transcribed from 3µg of the pGEM-lacZ *SmaI* digest with 40

units of SP6 polymerase in a 20µl reaction which included 2µl DIG RNA labelling mix and 10 units RNase inhibitor. A sense probe was similarly transcribed from the *HindIII* digest with T7 polymerase. A tenth of each digest was run out to estimate concentration and the remainder was precipitated with 0.1 volume ammonium acetate and 2.5 volumes RNase free ethanol. The probes were resuspended at 100µg/ml in HYB (HYB: 50% formamide, 4X SSC, 250µg/ml tRNA, 50µg/ml heparin, 250µg/ml sonicated salmon sperm DNA, 1% Tween-20). Before use, probes were diluted to 5µg/ml in HYB and denatured by heating to 85°C for 5 minutes and chilling on ice.

2.4 Microscopy and Photography

Flies were examined and dissected under a dissecting microscope. Arrested embryos, β-gal expression patterns and *in situ* hybridisations to whole mounts were examined using a Leitz microscope with a 10X, 25X or 40X objective lens. Polytene chromosome were observed using a 100X oil immersion lens. Photographs were taken with a Wild photoautomat system using Kodak 35mm film. Photoprocessing was by Kodak.

2.5 P-element mediated germline transformation

2.5.1 Preparation of injection cocktail

The P-element transformation vector pmyoV3'UTR and the helper plasmid Δ2-3 'wings-clipped' were prepared by Wizard miniprep (Promega). 8µg of pmyoV3'UTR and 2µg of Δ2-3 were co-precipitated with ethanol and resuspended in 20µl injection buffer (5mM KCl, 0.1mM $NaPO_4$, pH 6.8). The injection mix was then backloaded into the injection needle.

2.5.2 Collection of embryos for microinjection

Embryo collection plates were prepared with grape juice agar and were supplemented with a smear of fresh yeast before use. Several hundred 4-5 day old white eyed *Wr* flies were transferred to embryo collection cages and allowed to settle overnight at 25°C. The plates were changed and flies were allowed to lay at 25°C, preferably in the sunlight. Plates were changed at 30 minute intervals and embryos were collected and dechorionated by hand (2.2.8.2). Dechorionation was performed at 18°C to slow down embryonic development as it is essential to inject embryos prior to blastoderm formation.

2.5.3 Establishment of transgenic lines by P-element transformation

Dechorionated embryos were lined up in the same orientation on a strip of double-sided sticky tape, on a coverslip stuck to a slide and desiccated in a petri dish containing silica gel for approximately 10 minutes. Embryos were then covered in halocarbon oil and DNA was injected into the posterior pole of pre-blastoderm embryos under a microscope, using a micromanipulator and an Eppendorf Transjector 5246. Embryos which had reached blastoderm stage were destroyed by running the needle through them. Injected embryos were transferred on the coverslip to tomato juice agar plates and allowed to develop a further 36-60 hours at 18°C. Hatched larvae were collected twice daily and transferred individually to vials of Staffan food and allowed to develop to adulthood at 25°C. Adults were backcrossed to *Wr* virgins and their progeny examined for red eyed flies. Transformants were crossed again with *Wr* flies to create males and females with the same insertions. Homozygous lines were then established by sibling matings.

2.6 DNA methods

2.6.1 Preparation of DNA

2.6.1.1 Preparation of *Drosophila* genomic DNA

Adult flies were etherised and sorted as required. The flies were then transferred to a microfuge tube and immersed briefly in liquid nitrogen before homogenising in Flybuffer (5% sucrose, 80mM NaCl, 100mM Tris-HCl pH 8.0, 50mM EDTA pH 8.0, 0.1% SDS) added at a ratio of 0.5ml per 50 flies. The homogeniser rod was rinsed with an equal volume of Flybuffer, then the homogenate was frozen for 15 minutes at -70°C. The homogenate was thawed on ice and RNase added to a final concentration of 10μg/ml, then transferred to a 70°C waterbath and incubated for 30 minutes. Potassium acetate (3M stock) was added to a final concentration of 160mM with incubation on ice for 30 minutes. Debris and insoluble material was separated by centrifugation in a microfuge for 5-10 minutes and the supernatant then transferred to a fresh microfuge tube. The solution was phenol/chloroform extracted twice and chloroform extracted once, then precipitated with 0.75 volumes of isopropanol. The precipitate was collected by centrifugation for 15 minutes in a microfuge and washed with 70% ethanol then air dried. The pellet was dissolved in a suitable volume (dependent on the number of flies used) of TE overnight at 4°C.

2.6.1.2 Minipreparation of plasmid DNA

The method of Birnboim and Doly (1979) was used to prepare 2-5μg of plasmid DNA from *E.coli*. A single bacterial colony was selected and inoculated into 5ml L-broth plus ampicillin then incubated overnight at 37°C with shaking. 1.5ml of culture was centrifuged in a microfuge for 30 seconds and the cell pellet was resuspended in 100μl of Solution I (40mM Tris-HCl pH 8.0, 10mM EDTA pH 8.0, 50mM glucose) followed by incubation at room temperature for 5 minutes. This step was followed by

the addition of 200µl of Solution II (1% SDS, 200mM NaOH) with mixing by gentle rolling of the tube to prevent shearing of genomic DNA. After incubation on ice for 10 minutes 150µl of Solution III (3M Sodium acetate pH 4.8) was added with gentle mixing and a further incubation on ice for 10 minutes. Cell debris was pelleted by centrifugation in a microfuge for 5 minutes with the supernatant being transferred to a fresh tube. The DNA was precipitated by the addition of 1ml ethanol at room temperature, mixed, then centrifuged in a microfuge for at least 5 minutes. The supernatant was removed and the pellet washed with 80% ethanol, re-centrifuged, then dried in a Speedvac desiccator. The DNA was then resuspended in 50µl of TE buffer.

2.6.1.3 Midipreparation of plasmid DNA

This procedure was used for preparation of 50-200µg of plasmid DNA from 100-200 ml of culture. The method was developed from a small-scale procedure as described by Ausubel *et al* (1989). 100-200ml of culture was grown overnight in L-broth plus antibiotic. The cells were pelleted by centrifugation at 5000 rpm for 10 minutes, then resuspended in 3ml Solution I (as for miniprep procedure), and left to stand at room temperature for 5 minutes. The cells were lysed by the addition of 6ml of Solution II (as for miniprep), mixed gently and allowed to stand at room temperature for 10 minutes. This was followed by the addition of 4.5ml of 3M sodium acetate pH 4.8 with gentle mixing and incubation on ice for 45 minutes. Cell debris was separated by centrifugation at 8000 rpm for 10 minutes. The supernatant was transferred to a fresh tube and centrifuged at 15 000 rpm for 30 minutes to pellet the last traces of cell debris. The supernatant was precipitated by the addition of 1 volume of isopropanol at room temperature for at least 10 minutes. The precipitate was collected by centrifugation at 15 000 rpm for 30 minutes, dried, then resuspended in 0.5ml TE and transferred to a microfuge tube. 20µl of 10mg/ml DNase-free RNase was added and the tube was incubated at 60°C for 15 minutes. Next, 375µl of 7M LiCl was added, incubated on ice for 20 minutes, then microfuged for 15 minutes. The supernatant was transferred to a fresh tube then phenol-chloroform extracted (section 2.6.3) followed by a chloroform extraction. The DNA was precipitated by the addition of 1

volume of isopropanol for 30 minutes at room temperature or overnight at -20°C. The DNA was pelleted by microfuging for 15 minutes, washed with 75% ethanol, air-dried then resuspended in 200-500µl TE.

2.6.1.4 Commercial kits for plasmid preparation

In some instances plasmid DNA was prepared using commercially available kits. The Qiagen Plasmid Midi Kit was used for midipreps and the Promega Wizard kit was used for minipreps. Both systems begun with an alkaline lysis procedure as described above, then utilised the manufacturer's proprietary matrix systems to preferentially bind DNA. Impurities were removed with supplied wash buffers and the DNA eluted with a low salt (TE) solution or water.

2.6.2 Estimation of DNA (and RNA) concentration by UV spectrophotometry

UV spectrophotometry was used for the quantification of nucleic acids and as a check on their purity. Typically, a sample of nucleic acid was diluted 1:10 or 1:20 in dH_2O and absorbance was measured at 260nm and 280nm in a quartz micro-cuvette with a minimum volume of 50µl. The nucleic acid concentration in µg/ml was calculated using the following formula:

DNA concentration = Absorbtion at 260nm (A_{260}) X 50 X dilution factor.
RNA concentration = Absorbtion at 260nm (A_{260}) X 40 X dilution factor

The purity of the nucleic acid sample, with respect to protein contamination, was estimated by the ratio A_{260}/A_{280}. A value greater than 1.8 for DNA, and 2.0 for RNA, indicates that the sample is free from protein contamination.

2.6.3 Phenol-chloroform extraction

Phenol-chloroform extraction is a common procedure for the removal of

proteinacious material from DNA solutions. Phenol was equilibrated with Tris-HCl pH 8, then mixed with chloroform and iso-amyl alcohol at a ratio of 25:24:1 and stored at 4°C in the dark. An equal volume of this mixture was added to DNA solutions and mixed by vortexing, or if shearing of DNA was to be avoided by repeated gentle inversions. The phases were separated by centrifugation and the upper aqueous phase was removed to a fresh tube. A second extraction was performed if necessary. A final extraction with an equal volume of 24:1 chloroform: iso-amyl alcohol was usually performed to ensure complete removal of phenol.

2.6.4 Precipitation with ethanol or isopropanol

DNA solutions were precipitated by adding 0.1 volume 3M sodium acetate pH 5.2 with either 2 volumes of ice-cold ethanol or 1 volume isopropanol Ethanol precipitation was at -20°C for at least one hour or in a dry ice and ethanol bath for 10 minutes, while isopropanol precipitation was at room temperature. RNA solutions required the addition of 2.5 volumes of ethanol. Nucleic acid was pelleted by centrifugation in a microfuge for 20 minutes. Additional salts were removed by rinsing the pellet with 75% ice-cold ethanol followed by a brief centrifugation and careful removal of as much liquid as possible. The pellet was air dried 10 minutes or dried under vacuum for 2-3 minutes and then resuspended in TE or the solution of choice for further manipulation.

2.6.5 Enzymatic reactions

2.6.5.1 Endonuclease restriction

Digestion of DNA with restriction endonucleases was performed according to the manufacturers instructions and using the recommended buffer supplied at 10X concentration. Typically, 5 units of enzyme was used to restrict 1μg of DNA in a

total volume of 20µl for a minimum of 1 hour. For larger quantities of DNA the reaction components were scaled up accordingly. When more than one restriction endonuclease was required and the buffers were incompatible, then digestion was performed first by the enzyme with lowest ionic strength buffer and the enzyme subsequently denatured by heat inactivation or phenol-chloroform extraction. The correct conditions for the second enzyme were then achieved by the addition of the appropriate components. Alternatively, the DNA was precipitated and resuspended in the appropriate buffer for the second enzyme.

2.6.5.2 Dephosphorylation of Plasmid Vectors

Dephosphorylation of cut vector ends with calf intestinal alkaline phosphatase (CIAP) was performed to facilitate the cloning of DNA fragments into vectors by prevention of vector religation. The plasmid was restricted with the desired restriction endonuclease then CIAP and CIAP buffer was added. Incubation was continued at 37°C for a further 30 minutes then at 55°C for 30 minutes. The plasmid DNA was extracted 2 or 3 times with phenol chloroform then precipitated with ethanol and resuspended in TE at a concentration of around 100ng/µl.

2.6.5.3 Ligation

The plasmid vector and DNA fragment to be inserted were restricted so as to have compatible ends for ligation. Typically, ~50ng of vector DNA was ligated to insert DNA at a molar ratio of between 1:1 and 1:3 vector:insert. Vector and insert DNA were ligated in 1X ligation buffer (50mM Tris-HCl pH 7.5, 10mM $MgCl_2$, 10mM DTT, 1mM ATP) with 1 unit of T4 DNA ligase in a 10-20µl reaction incubated overnight at 18°C. The ligation plasmid was then transformed into *E.coli.*

2.6.6 Transformation of plasmid DNA into *Escherichia coli*

2.6.6.1 Preparation of competent cells

E.coli were made competent for transformation by the Cold $CaCl_2$ method of Lederberg and Cohen (1974). A mid-log phase cultures was pelleted by centrifugation at 3000rpm, 10 minutes 4°C, then resuspended in 1/2 volume of cold, sterile 0.1M $MgCl_2$ and left on ice for 15 minutes. The cells were pelleted by centrifugation, then resuspended in 1/2 volume of cold sterile 0.1M $CaCl_2$ and incubated on ice for 30 minutes. The cells were again pelleted by centrifugation. The cells were then either resuspended in 1/20th volume 0.1M cold, sterile $CaCl_2$ and used immediately, or resuspended in 1/20th volume 0.05M cold, sterile $CaCl_2$ and 15% glycerol stored in 100µl aliquots at -70°C.

2.6.6.2 Transformation

Approximately 50ng of plasmid DNA was added to 100µl of competent cells, mixed gently and incubated on ice for 30 minutes. The cells were then heat shocked at 42°C for 90 seconds in a water bath. 900µl of LB was added and the cells allowed to grow at 37°C for 1-1.5 hours on a shaker. 100-500µl of the culture was then spread onto LB-amp plates and incubated overnight at 37°C to select for transformants.

2.6.7 Electrophoresis of DNA

2.6.7.1 Preparation and running of agarose gels

Horizontal slab gels were prepared using agarose from Boehringer Mannheim. Typically gels were prepared at a concentration of 1% in 1X TAE or 1X TBE buffer. Agarose concentration could be increased to 1.2% for the separation of DNA

fragment of less than 1kb or reduced to 0.6% for the separation of DNA fragments greater than 5kb. TAE buffer was used preferentially when DNA fragment were to be recovered from the gel. Agarose was added to the buffer and heated until completely dissolved. Ethidium bromide at a stock concentration of 10mg/ml was added to the gel at a final concentration of 0.5μg/ml. The molten gel was allowed to cool to ~60°C then poured into the appropriate casting tray and allowed to set at room temperature. The gel was submerged in 1X TAE or 1X TBE in an electrophoresis tank. DNA samples were mixed with 0.1 volume of 10X loading dye (0.25% bromophenol blue, 0.25% xylene cyanol, 30% glycerol) and loaded into the wells. The gel was then run at ~10 volts/cm until the desired separation of DNA was achieved.

2.6.7.2 Molecular weight markers

Molecular weight markers were run out on each agarose gel to allow estimation of the size of DNA fragments. The marker commonly used was a λ 1kb ladder from Gibco BRL. 500ng of this ladder in 1X loading dye was loaded the gel.

2.6.7.3 Visualisation and imaging

The DNA in the gel was visualised by its fluorescence under UV light in the presence of ethidium bromide. An image of the gel was captured using a gel documentation system and printed out on heat sensitive paper.

2.6.7.4 Recovery of DNA fragments

DNA fragments were extracted from agarose-TAE gels using either the Qiaex II kit or Qiaquick kit from Qiagen. In both cases the DNA fragment of interest was cut from the gel in the minimum amount of agarose using a clean scalpel blade and dissolved in 3 volumes of solubilisation buffer (QX1) by heating to 55°C. With the Qiaex II system, Qiaex II silica based particles were added to the solution to bind the DNA. The particles were then pelleted by centrifugation, the supernatant discarded

and the particles washed by resuspending in QX1. Impurities were removed by similar washes in QX2 and the ethanol based wash buffer PE. The silica particles were then dried briefly and resuspended in 50µl TE to elute the DNA. The DNA was recovered by pelleting of the Qiaex II particles and careful removal of the supernatant to a fresh tube. The Qiaquick system worked by a similar principle but used silica particles in a microfuge column instead of the loose particles in the Qiaex II kit. Qiaquick columns prevented contamination of the DNA with traces of silica which could inhibit downstream enzymatic reactions.

2.6.8 DNA sequencing and analysis

2.6.8.1 Manual sequencing

DNA sequencing was by the dideoxy chain termination method of Sanger *et al* (1977) using the commercially available Sequenase^{R} version 2.0 kit (United States Biochemical Corporation). Oligonucleotide primers were obtained from Oswel. 5µg of double stranded DNA was denatured by the addition of 5µl denaturing solution (2M NaOH, 10mM EDTA) and incubation at 37°C for 30 minutes. The template was ethanol precipitated and resuspended in 2µl Sequenase^{R} buffer (200mM Tris-HCl pH 7.5, 100mM $MgCl_2$, 250mM NaCl). 20ng of oligonucleotide primer was added and the reaction made up to 10µl with dH_2O. The DNA and oligo were annealed by incubation at 37°C for 30 minutes then transferred to ice. To this was added 2µl of labelling mix (1.5µM dGTP, dCTP and dTTP), 1µl 100mM DTT, 0.5µl [α-^{35}S]dATP (10µCi/µl) and 2µl Sequenase^{R} DNA polymerase (1.6 units/µl). This labelling reaction was incubated at room temperature for 5 minutes before 3.5µl aliquots were removed and added to 2.5µl of each termination mix (ddA, ddC, ddG and ddT) which were prewarmed to 37°C. Each termination mix consisted of the following: 80µM dATP, dCTP, dGTP and dTTP, 50mM NaCl and 8µM of the appropriate dideoxynucleotide (ddATP, ddCTP, ddGTP, ddTTP). The termination reactions

were incubated at 37°C for 5 minutes then stopped by the addition of 4µl ice cold loading buffer (95% formamide, 20mM EDTA, 0.05% bromophenol blue, 0.05% xylene cyanol). The reactions could be stored at -20°C until use.

2.6.8.2 Sequencing gel electrophoresis

Sequencing reactions were separated on a 6% polyacrylamide gel (20:1 acrylamide: bisacrylamide) containing 7M urea in 1X TBE. Commercially available LongRanger acrylamide solution was used and 40ml of the gel mix was polymerised by the addition of 200µl 10% ammonium persulphate and 20µl TEMED. The gel was cast between a pair of glass plates separated by 0.3mm spacers. 4µl of each sequencing reaction was denatured at 95°C for 5 minutes then loaded onto the pre-run gel using a sharks-tooth comb. Gels were electrophoresed at a constant power of 40 Watts in 1X TBE. The run was monitored by the migration of the loading dyes - bromophenol blue co-migrates with 106 base fragments while xylene cyanol co-migrates with 8 base fragments. After the appropriate length of run the gel was transferred onto Whatman 3MM blotting paper and dried under vacuum for 1 hour at 80°C. The dried gel was exposed to X-ray film overnight at room temperature.

2.6.8.3 Automated sequencing

A departmental automated sequencing service became available towards the end of this project whereby sequencing reactions were handed over to the service for electrophoresis on the Applied Biosystems 377A automated sequencer. The sequencing reactions were based on the dideoxy chain termination method of Sanger *et al* (1977) however DNA band were detected by fluorescent dyes incorporated into the dideoxynucleotides. The Perkin-Elmer Prism™ Ready Reaction DyeDeoxy™ Terminator system was used with a cycle sequencing protocol. 250-500ng of double stranded plasmid DNA or 60-90ng of purified PCR product was added to 8µl of terminator mix and 3.2pmoles of oligonucleotide primer in a total volume of 20µl. The reaction mixture was overlaid with mineral oil and cycle sequencing was

performed by 25 cycles of 96°C for 30 seconds, 50°C for 15 seconds, 60°C for 4 minutes. The sequenced DNA was recovered by adding the reaction mix to 2µl of sodium acetate pH 5.2 and 50µl ethanol followed by incubation on ice for at least 10 minutes. The DNA was collected by centrifugation for 20 minutes and the pellet washed with 250µl of 75% ethanol then dried under vacuum. The sequencing reaction was then handed over to the automated sequencer operator. The sequencing results were provided in the form of a computer file.

2.6.8.4 Sequence analysis

Sequence analysis was carried out using the University of Wisconsin Genetics Computer Group (GCG) sequence analysis software package (Devereux *et al*, 1984) using VMS VAX and Unix operating systems. Sequence editing was performed using the SEQED program, and sequence alignment was performed using the GELSTART set of programs. Manual sequences were input by hand while sequences generated by the automated sequencer were edited with GeneJockey II (Oxford) or Factura (Applied Biosystems Inc) software before being transferred to GCG readable files.

2.6.9 Polymerase chain reaction

The polymerase chain reaction (PCR) was performed using a Hybaid thermal cycler. Oligonucleotide primers were obtained from Oswel, deoxynucleotides were obtained from Pharmacia and Taq polymerase and 10X thermophilic buffer were obtained from Promega. The standard reaction mix was as follows:

~1ng	template DNA
1µl	primer #1 (25pmol/µl)
1µl	primer #2 (25pmol/µl)
2µl	dNTP mix (10mM each of dATP, dCTP, dGTP and dTTP)
3µl	$MgCl_2$ (25mM)
5µl	10X buffer (500mM KCl, 200mM Tris-HCl pH 8.3, 0.01% gelatin)
0.4µl	Taq polymerase (5units/µl)
to 50µl	H_20

The reactions were set up in sterile, thin-walled, 0.5ml tubes and were overlaid with light mineral oil (Sigma) to prevent evaporation. The cycles of denaturing, annealing and extending were performed as described in the relevant chapters. The PCR reactions were often hot started i.e. the Taq polymerase was not added until after template denaturation to prevent the polymerisation of non-specific products at low temperatures. PCR products were analysed by agarose gel electrophoresis (section 2.6.7).

2.7 RNA methods

2.7.1 Precautions for working with RNA

RNA is very susceptible to degradation by ribonucleases (RNases) which are very stable enzymes that are difficult to inactivate. Great care was therefore be taken to eliminate possible RNase contamination. Gloves were worn and changed frequently to prevent RNase contamination from the skin. Manipulations were performed quickly, keeping the RNA on ice as much as possible. Before use, plasticware was soaked in a 0.1% solution of the RNase inhibitor DEPC (diethyl pyrocarbonate) then autoclaved. Glassware was baked for at least 4 hours at >240°C. Reagents were of molecular biology grade and solutions were prepared using molecular biology grade chemicals and water which had been incubated with 0.1% DEPC overnight at 37°C, and then autoclaved. Gel apparatus was soaked in 0.1% NaOH and 0.1% SDS then rinsed in DEPC treated water before use.

2.7.2 Preparation of RNA

2.7.2.1 Preparation of total RNA

Total RNA was prepared from whole flies or tissues using either RNeasy kit from Qiagen or Trizol reagent from Gibco BRL. With the RNeasy kit, up to 30mg of tissue was homogenised in RLT lysis buffer, which contains guanidinium isothiocyanate and β-mercaptoethanol. This lysate was centrifuged to remove insoluble material, 1 volume of ethanol was added then the sample was applied to an RNeasy spin column. The column consists of a silica gel-based membrane which selectively binds RNA under high salt conditions while impurities are efficiently washed away with a series of wash buffers. The RNA was then eluted in with two applications of 50µl DEPC treated water heated to 65°C.

The Trizol system, a solution of phenol and guanidinium isothiocyanate, is based on the method of Chomczynski and Sacchi (1987). 50-100mg of tissue was homogenised in 0.5ml Trizol solution with a further 0.5ml of Trizol then added. The homogenate was incubated at room temperature for 5 minutes, 200µl of chloroform was added and the solution shaken vigorously then incubated at room temp for 3 minutes. The aqueous and organic phases were then separated by centrifugation at 12000g at 4°C. The aqueous phase, which contains the RNA, was removed and the RNA precipitated by the addition of 0.7 volumes of isopropanol at room temperature for 10 minutes followed by centrifugation at 12000g for 15 minutes at 4°C. The supernatant was removed and the RNA pellet washed with 1ml of 75% ethanol with centrifugation at 7500g for 5 minutes. The ethanol wash was removed and the pellet air dried then resuspended in the desired volume of DEPC treated water. RNA preps were stored at -20°C

2.7.2.2 Preparation of polyA$^+$ mRNA

PolyA$^+$ mRNA was prepared from total RNA using the Dynabeads mRNA Direct kit from Dynal. Dynabeads are uniform, superparamagnetic, monodispersed polymer beads covalently linked to oligo dT_{25} residues. Their use relies on the base pairing between the polyA residues at the 3' end of most messenger RNA and the oligo dT residues coupled to the Dynabeads. Placing a microfuge tube containing Dynabeads

into a magnetic stand causes the beads to collect at the side of the tube, allowing easy removal of supernatant. The beads can be reconditioned up to four times with the solutions provided. The Dynabeads mRNA Direct kit can be used to isolate polyA$^+$ RNA direct from tissue, however here 200µl of Dynabeads oligo dT was used to extract polyA$^+$ mRNA from ~30µg of total mRNA. Samples were eluted in 15µl of low salt buffer.

2.7.3 Electrophoresis of RNA

RNA was separated by electrophoresis through a denaturing agarose-formaldehyde gel in 1X MOPS buffer. 150ml of a 1% agarose gel was prepared as follows: 1.5g of agarose was added to 15ml of 10X MOPS buffer and 108ml of DEPC treated water and heated to dissolve; when the gel solution had cooled to around 60°C, 27ml of 37% formaldehyde was added and the gel cast in a fume hood. Typically, 10µg of RNA or 5µg of RNA markers (Gibco BRL) were denatured in 50% formamide, 6% formaldehyde and 1X MOPS at 70°C for 5 minutes, then chilled on ice. 2µl of RNase free ethidium bromide and 0.1 volume of 10X loading dye (section 2.6.7.1) were added before loading onto the gel. The gel was run at ~10 volts/cm in 1X MOPS using a Buffer-Puffer gel tank (Hybaid) which recirculates the MOPS buffer. Visualisation and imaging of RNA gels was as for DNA gels (section 2.6.7.3).

2.7.4 Reverse transcription and RT-PCR

2.7.4.1 Reverse transcription of total RNA

First strand cDNA was reverse transcribed from total RNA using Superscript II reverse transcriptase (Gibco BRL). Gene specific oligonucleotide primers and oligo dT were obtained from Oswel. Around 5µg of total RNA was added to 2µg of oligonucleotide primer in a total volume of 10µl and incubated at 70°C for 5 minutes

then chilled on ice. To this was added 4µl of 5X first strand buffer (Gibco BRL), 2µl 0.1M DTT, 2µl dNTP mix (10mM each of dATP, dCTP, dGTP and dTTP), 1µl of RNase inhibitor (40 units/µl, Promega) and 1µl of Superscript II reverse transcriptase (200 units/µl). The reaction mix was incubated at 42°C for 45 minutes then 55°C for 5 minutes then chilled on ice. The first strand cDNA could then be visualised by running out on an agarose gel (section 2.6.7). For RT-PCR, 1µl of first strand cDNA was generally used as a template for PCR as described in section 2.6.9. As a control for the presence of contaminating genomic DNA in the RNA preps, two reverse transcription reactions were set up for each RNA prep - a genuine reaction and a control reaction which contains no reverse transcriptase and which will therefore not produce any first strand cDNA. Amplification of PCR products from the control reaction indicates the presence of contaminating genomic DNA so that the results from the genuine reaction must be disregarded.

2.7.4.2 Removal of contaminating genomic DNA from RNA preps

Genomic DNA can act as a template for PCR and must therefore be eliminated from total RNA preps to prevent the generation of false RT-PCR results. RNase-free DNaseI (Boehringer Mannheim) was added to RNA preps at 1 unit per µg RNA and $MgCl_2$ was added to a final concentration of 1mM. The reaction was incubated for 45 minutes at 37°C then phenol-chloroform extracted and precipitated with isopropanol. The RNA was resuspended at the desired concentration in DEPC treated water.

2.8 Screening of recombinant bacteriophage libraries

2.8.1 Preparation of plating cells

A single colony of the appropriate *E.coli* strain was used to inoculate 5ml of LB medium which was then incubated overnight at 37°C with shaking. The following

day, 2ml of the culture was used to inoculate 100ml of LB containing 10mM $MgSO_4$ and 0.2% maltose. The culture was grown at 37°C with shaking for a further 2-4 hours, until it had reached an OD_{650} of approximately 1. The cells were collected by centrifugation at 4000rpm for 10 minutes at 4°C then resuspended in 1/2 volume of ice-cold, sterile 0.1M $MgSO_4$ and incubated on ice for 30 minutes. The cells were again collected by centrifugation and resuspended in 1/4 volume 0.1M $MgSO_4$. The cells were then stored at 4°C for up to 2 weeks.

2.8.2 Plating out a recombinant bacteriophage library

The bacteriophage library was diluted in SM phage buffer to a titre of 10^6 pfu/ml. 100µl of this dilution was then used to plate out 100 000 phage on a 25cm x 25cm plate. 100 000 phage was thought to be sufficient to represent all the recombinants in the library. LB agar was poured onto the 25cm x 25cm plate, allowed to set, dried and kept warm at 42°C. 100µl of the diluted phage was added to 1ml of plating cells and incubated 15 minutes at room temperature, then 15 minutes at 37°C. 50ml of molten top agarose (0.7% agarose in LB), cooled to 42-50°C was then added to the cells, mixed and poured immediately onto the warmed agar plate. Once set, the plate was inverted and incubated overnight at 37°C.

2.8.3 Plaque lifts

After overnight incubation at 37°C the phage plates were placed in the fridge to harden. The phage DNA was transferred to Hybond-N nylon membrane (Amersham) by laying a sheet of the membrane, cut to size, onto the surface of the plate for 1-2 minutes. The orientation of the membrane to the plate was marked by making holes with a sterile needle. The membrane was then lifted off and placed, DNA side up, on a sheet of blotting paper soaked in denaturing solution (1.5M NaCl, 0,5M NaOH) for 7 minutes. The membrane was then transferred to a sheet of blotting paper soaked in

neutralising solution (1.5M NaCl, 0.5M Tris-HCl pH 7.2, 1mM EDTA) for 5 minutes. This neutralisation step was repeated, then the membrane was washed in 2X SSC to remove any remaining agarose and air dried on blotting paper, DNA side up. A replica plaque lift was taken from the plate in the same way. The DNA was then fixed to the membranes by a 10 minute exposure to UV light. The membranes were then ready for prehybridisation and hybridisation with the appropriate probe (2.9.2).

2.8.4 Secondary and tertiary screens

Positive plaques (i.e. ones whose DNA hybridised to the probe) were identified by aligning the autorad of the hybridised membranes to the original phage plate. Replica membranes were used to facilitate the identification of true positives. Positive plaques were picked in a plug of agarose using the wide end of a Pasteur pipette. The plug was placed into 1ml of SM phage buffer and incubated at least 1 hour at 4°C to allow the phage to diffuse out into the buffer. A drop of chloroform was added to the buffer to prevent the growth of phage resistant bacteria. As the plug was unlikely to represent a single phage at the high plating density used, the screening process had to be repeated until a single positive phage could be easily identified. For the secondary screen, the phage from the plug were diluted 1 in 10 in phage buffer. 5-50µl of diluted phage was added to 150µl of plating cells and 3.5ml of top agarose and replated onto 9cm LB-agar plates. It was aimed to replate ~100 phage so that positive plaques could be easily identified and picked. Plaque lifts were taken as before onto precut circles of Hybond-N. If, after hybridisation, positive plaques could still not be identified and picked with certainty, a tertiary screen was undertaken. 150µl of plating cells was added to 3.5ml of top agarose, poured onto a 9cm LB-agar plate and allowed to set. A grid was drawn onto the bottom of the plate then a toothpick was inserted into possible positive plaques from the secondary screen and streaked out onto the surface of the plate. The bacteria and phage were allowed to grow overnight at 37°C and a plaque lift taken as before. Hybridisation to the streaked out phage should allow unequivocal identification of positive plaques. A

plug from the positive plaque was then taken with the narrow end of a Pasteur pipette and allowed to diffuse in 1ml SM phage buffer plus chloroform at 4°C.

2.8.5 Preparation of DNA from recombinant bacteriophage

2.8.5.1 Preparation of DNA from λFIX bacteriophage

10-100µl of diffused positive phage was added to 2ml of an overnight culture of the appropriate *E.coli* strain grown in LB supplemented with 10mM $MgSO_4$ and 0.2% maltose. The infected bacterial culture was then added to 20ml L-broth also containing 10mM $MgSO_4$ and 0.2% maltose. Incubation was carried out at 37°C with vigorous shaking for 5 to 7 hours until lysis of the bacteria was observed. The bacteria were then completely lysed by the addition of 300µl of chloroform with shaking continued for a further 10 minutes. The cell debris was removed by centrifugation for 10 minutes at 7000rpm. 50µl of 10mg/ml DNase and 50µl of 20mg/ml RNase were added to the clarified supernatant and incubated at 37°C for 1 hour to digest the bacterial nucleic acids. Next, 4ml of TES buffer (250mM Tris-HCl pH 7.5, 25mM EDTA, 2.5% SDS) was added and the mixture was incubated at 70°C for 30 minutes then allowed to cool to room temperature for 10 minutes. 5ml of 5M potassium acetate was then added and the mixture incubated on ice for 15 minutes. The potassium-SDS precipitate was removed by centrifugation for 15 minutes at 12000rpm, 4°C. The supernatant was added to 0.7 volumes isopropanol, precipitated at room temperature for 10 minutes then pelleted by centrifugation at 15000rpm for 30 minutes. The pellet was resuspended in 500µl of 0.3M sodium acetate and then extracted twice with phenol-chloroform and once with chloroform. The phage DNA was then precipitated with 0.7 volumes isopropanol, washed in 75% ethanol, air dried and resuspended in 100-200µl of TE.

2.8.5.2 Preparation of DNA from λZAP bacteriophage

The λZAP bacteriophage has the useful feature of allowing the cDNA to be excised in the form of a pBluescript recombinant plasmid, eliminating the need for subcloning. A culture of XL1 Blue *E.coli* was grown to an OD_{650} of 1 in LB plus 10mM $MgSO_4$ and 0.2% maltose. 200µl of this culture was added to 100µl of diffused positive λZAP phage in SM buffer and 1µl of VCMS13 helper phage. The mix was incubated at room temperature for 15 minutes and 37°C for 10 minutes to allow adsorption and penetration of phage DNA. 2ml of YT media was then added and incubated at 37°C for 2-3 hours with shaking. The culture was then heated to 70°C for 20 minutes to kill the bacteria and the debris was removed by centrifugation at 4000rpm for 15 minutes. The supernatant was collected as a phagemid stock, with 20µl chloroform added to prevent bacterial growth. 1µl and 10µl of this phagemid stock was used to inoculate 200µl of XL1 Blue cells with incubation at 37°C for 15 minutes. The culture was then plated onto LB-amp plates and incubated overnight at 37°C to select for bacteria carrying the pBluescript recombinant plasmid. Plasmid DNA was then prepared by miniprep (section 2.6.1.2).

2.9 Hybridisation techniques

2.9.1 Transfer of nucleic acids to nylon membranes

2.9.1.1 Southern transfer

DNA was transferred to nylon membranes based on the method of Southern (1975). DNA was electrophoresed in agarose gels as previously described (section 2.6.7) then blotted onto Hybond-N or Hybond-N^+ in either 20X SSC or 0.4M NaOH. For transfer in 20X SSC, the gel was soaked in a 0.25M HCl solution for approximately 30 minutes to depurinate and improve transfer of large fragments. The gel was rinsed

with water then soaked in denaturing solution (1.5M NaCl, 0.5M NaOH) until the running dyes had returned to their original colours. The gel was then soaked in 2 changes of neutralising solution (1.5M NaCl, 0.5M Tris-HCl pH 7.2, 1mM EDTA) for 15 minutes each. A capillary blot was then set up whereby a platform was placed in a tray of 20X SSC then covered with a wick made from 3 sheets of blotting paper soaked in 20X SSC. The gel was placed on top of the platform and covered with Hybond membrane cut to size, ensuring that no air bubbles were trapped. The membrane was covered with 3 layers of blotting paper, cut to size and soaked in 20X SSC. A stack of absorbent towels, approximately 10cm high was placed on top of the blotting paper, followed by a plastic tray with a 300-500g weight on top. The DNA was transferred to the membrane overnight by capillary action. After blotting, the membrane was washed in 2X SSC, air dried then fixed by 10 minutes exposure to UV light. For alkali transfer in 0.4M NaOH, the gel was depurinated as above then a capillary blot set up in 0.4M NaOH for a minimum of 2 hours. The membrane was again washed in 2X SSC but did not require UV fixing before prehybridisation and hybridisation.

2.9.1.2 Northern transfer

RNA was transferred to nylon membrane by Northern transfer. RNA was electrophoresed through denaturing agarose-formaldehyde as described in section 2.7.3. Immediately after electrophoresis, the RNA was blotted onto Hybond-N^+ membranes by a capillary blot in 20X SSC as described above, except that the SSC was prepared using DEPC treated water. The membrane was then UV fixed without washing.

2.9.2 Hybridisation with ^{32}P labelled probes

Southern blots, Northern blots and plaque lifts were prehybridised and hybridised according to the Amersham Hybond protocol in a Hybaid hybridisation oven.

Membranes were prehybridised at 65°C for at least 1 hour in 25ml or 50ml (depending on size and number of membranes) of prehybridisation solution (5x SSPE, 5x Denhardt's, 0.5% SDS plus 40μg/ml of heterologous sonicated salmon sperm DNA). The ^{32}P probe, prepared as described in section 2.9.3, was denatured in a heating block at 110°C for 5 minutes, then plunged into ice. The probe was then added directly to the prehybridisation solution or, if the probe was being reused, the prehybridisation solution was removed and stored and the probe solution added. Hybridisation was then performed at 65°C for at least 12 hours. After hybridisation, the probe was carefully removed and stored. Approximately 100ml of a 2X SSC, 0.1% SDS wash solution was added and gently shaken for 10 minutes at room temperature. A second, identical wash was then performed. The membranes were then washed twice in 100ml of 0.1X SSC, 0.1% SDS at 65°C for 15 minutes. The membranes were monitored with a Geiger counter and washed further if necessary. Membranes were then wrapped in Saranwrap and exposed to X-ray film at -70°C, in cassettes containing one or two intensifying screens, for times varying from a few hours to several days. The film was developed using an X-OGRAPH X1 automatic X-ray developer (IBI Ltd).

Alternatively, Northern blots were prehybridised and hybridised at 42°C in formamide prehybridisation solution (50% formamide, 5x SSPE, 5x Denhardt's, 0.5% SDS, plus 40μg/ml of heterologous sonicated salmon sperm DNA) or dextran sulphate prehybridisation solution (20% dextran sulphate, 50% formamide, 5x SSPE, 5x Denhardt's, 0.5% SDS, plus 40μg/ml of heterologous sonicated salmon sperm DNA). Washing of the membranes was also performed at 42°C.

2.9.3 Labelling of ^{32}P probes

2.9.3.1 Random primed labelling

DNA was labelled with ^{32}P using the random priming method of Feinberg and

Vogelstein (1983). Approximately 50-200ng of DNA was denatured first by boiling then immediately plunged into ice. The DNA was labelled in a reaction mix containing, 10µl OLB buffer, 5µl of [α-^{32}P] dCTP (10µCi/µl), 1µl of 20mg/ml BSA and 5 units of Klenow enzyme in a final volume of 50µl. The reaction was incubated at 37°C for 30 minutes. OLB (oligo labelling buffer) consists of a ratio of 2:5:3 of solutions A, B and C. (Solution A: 950µl of solution O [125mM $MgCl_2$, 1.25M Tris-HCl pH 8], 18µl of β-mercaptoethanol, 25µl each of 20mM dATP, dGTP and dTTP. Solution B: 2M HEPES pH 6.6. Solution C: Hexanucleotides [Pharmacia] resuspended in TE buffer at 90 OD units/ml).

Later stages of the project used the Pharmacia Ready-To-Go kit which provides hexanucleotides, dATP, dGTP, dTTP, Klenow polymerase and buffer salts as a lyophilised mix that was reconstituted in 20µl of sterile distilled water. 25-50ng of DNA in a volume of 25µl was denatured, as above, and added to the reaction mix along with 5µl of [α-^{32}P] dCTP (10µCi/µl), and incubated at 37°C for 15-30 minutes.

The Ready-To-Go kit was also used to label large DNA fragments in low melting point agarose as follows. Sufficient DNA was digested and run out in a low melting point agarose gel such that the band of interest contained at least 250ng of DNA. The band was excised in the minimum of agarose, weighed, added to 3 volumes of dH_2O and dissolved at 65°C for 2 minutes. 25µl of this DNA-agarose mixture was heated to 95°C for 7 minutes, incubated at 37°C for 10 minutes then added to the reconstituted Ready-To-Go mix and 5µl of [α-^{32}P] dCTP and incubated as above.

2.9.3.2 End labelling of λ 1kb ladder

For Southern blots it is useful to have ^{32}P labelled DNA markers which will show up on the autorad. This is most easily accomplished by end filling the 'sticky ends' of the standard λ 1kb ladder (Gibco BRL). Approximately 200ng of λ 1kb ladder was labelled in a 40µl reaction mix with 1µl of [α-^{32}P] dCTP (10µCi/µl), 50mM each of

dATP, dGTP and dTTP, and 1 unit of Klenow enzyme (Boehringer Mannheim). The reaction mix was then incubated at 37°C for 30 minutes. Unincorporated nucleotides were removed using a Pharmacia Nick column which elutes the labelled DNA in a volume of 400µl. 1µl of this was added to 500ng of unlabelled ladder in 1X loading dye and run out on the gel as normal (section 2.6.7.2).

2.9.3.3 Removal of unincorporated nucleotides

Unincorporated radiolabel was removed using a Pharmacia Nick Column. These columns use Sephadex G-50 for gel filtration allowing the larger labelled DNA molecules to pass through the column while retaining the unincorporated nucleotides. The column was prepared by tipping off the storage solution, rinsing with one column volume of TE followed by one column volume of TE run through the column. The labelling reaction was pipetteted directly on to the top support surface of the gel bed and washed in with 400µl of TE. The material collected at this stage contained very little labelled DNA and was discarded, while a second application of 400µl TE eluted the bulk of the labelled DNA. Efficiency of incorporation was not determined other than by rough estimation from the hand held monitors. The probe was then denatured at 110°C in a heating block, chilled on ice and added to the prehybridisation solution.

2.9.4 Stripping of membranes

To remove a probe from a membrane to allow use of a fresh probe, the membrane was boiled in a solution of 0.1% SDS for 5 minutes. If the membrane still sounded hot, this process was repeated. Membranes were checked for removal of probe by overnight exposure to X-ray film.

2.9.5 Non-radioactive hybridisation and detection

2.9.5.1 Preparation of digoxigenin labelled probes for membrane hybridisation

200ng of linearised, purified DNA was labelled with digoxigenin to give around 500ng of DIG-labelled DNA as described in section 2.3.6. The precipitated DNA was then resuspended in 50µl TE to give a concentration of around 10ng/µl DIG-labelled DNA. Before use, the DIG-labelled probe was denatured at 95°C, chilled on ice and added to high SDS prehybridisation solution at 10-20ng/ml DIG-labelled DNA. 5ml of this hybridisation solution was used per membrane. The hybridisation solution could be reused by heating to 65°C before use. High SDS prehybridisation solution consisted of 7% SDS, 50% formamide, 5X SSC, 2% powdered milk, 50mM sodium phosphate and 0.1% N-lauroylsarcosine.

2.9.5.2 Hybridisation with digoxigenin labelled probes

Membranes were prehybridised with 50ml per membrane of high SDS pre-hybridisation solution (as above) at 42°C for at least 1 hour. The prehybridisation solution was replaced with 5ml per membrane of hybridisation solution containing 10-20ng/ml DIG-labelled probe and hybridised overnight at 42°C. The membranes were washed twice in 100ml of 2X SSC, 0.1% SDS for 5 minutes at 42°C, then twice in 100ml of 0.1X SSC, 0.1% SDS for 15 minutes at 42°C. The membranes were then used directly for detection or air dried and stored at 4°C.

2.9.5.3 Chemiluminescent detection

The membranes were washed for 2-5 minutes in 50ml per membrane washing buffer (0.1M maleic acid, 0.15M NaCl pH 7.5, 0.3% Tween-20). The membranes were then blocked for 30 minutes in 100ml per membrane blocking solution (1% powdered milk in 0.1M maleic acid, 0.15M NaCl pH 7.5), then incubated for 30 minutes in 50ml per membrane antibody solution (anti-DIG-AP conjugate [Boehringer Mannheim] diluted

1:10000 in blocking solution). The membranes were washed twice for 15 minutes in 100ml per membrane washing buffer then equilibrated for 2-5 minutes in 20ml per membrane of detection buffer (0.1M Tris-HCl pH 9.5, 0.1M NaCl, 0.05M $MgCl_2$). A 10mg/ml stock solution of the chemiluminescent substrate, Lumigen PPD (Boehringer Mannheim) was diluted 1:100 in detection buffer and used to incubate the membranes for 5 minutes at 10ml per membrane. Excess liquid was blotted off, then the membranes were sealed in a hybridisation bag, pre-incubated at 37°C for 5-15 minutes, then exposed to X-ray film for 15-25 minutes at room temperature. Multiple exposures could be taken as the signal lasted for at least 24 hours. The membranes could be stripped for reprobing by washing briefly in water, then twice in 0.2M NaOH, 0.1% SDS for 15 minutes at 37°C, then washing briefly in 2X SSC.

Chapter 3

Expression of the *myosinV* Gene

3.1 Introduction

3.1.1 Results obtained by Roger Slee prior to commencement of this work

The *myosinV* gene was discovered in the course of an enhancer trap screen to identify genes with interesting expression patterns during oogenesis. One of the lines produced by the screen was the H14 line, a line shown by Southern analysis to contain two P-elements. Flies of this line produce a β-gal staining pattern in the polar follicle cells and migrating border cells. In an attempt to isolate the gene responsible for the H14 pattern, a genomic library was constructed and screened to isolate the DNA flanking the P-elements. A 5.2kb *Eco*RI fragment was isolated and used to screen a whole body cDNA library. Three cDNAs were isolated, NMC1, NMC4 and NMC7 of 1kb, 1.5kb and 1.6kb respectively. *in situ* hybridisation to whole mount ovaries showed that NMC1 and NMC4 corresponded to transcripts localised mainly to the nurse cells and so these cDNAs were not studied any further. However NMC7 identified transcripts localised to the oocyte from very early in oogenesis and later localised within the oocyte as a band at the anterior margin. This localisation pattern was unrelated to the H14 pattern but nonetheless suggested an interesting role in oogenesis. Localised transcripts are known to play a very important role in oogenesis and embryogenesis, e.g. localisation of the *gurken* transcript is required for axis specification during oogenesis while anterior embryonic patterning requires the localisation of the *bicoid* transcript (Gonzalez-Reyes *et al*, 1995, Berleth *et al*, 1988). It is not possible to screen directly for such localised transcripts so it was very fortunate that this transcript was discovered. It was therefore decided to focus attention on further study of this transcript and its corresponding gene. Meanwhile, the gene responsible for the H14 pattern has remained elusive.

3.1.2 Results obtained by Bryce MacIver concurrent with this work

NMC7 was subcloned into pBluescript as two fragments, NMC7a and NMC7b each of approximately 800bp by means of a central *Eco*RI site (fig 3.1). These subclones

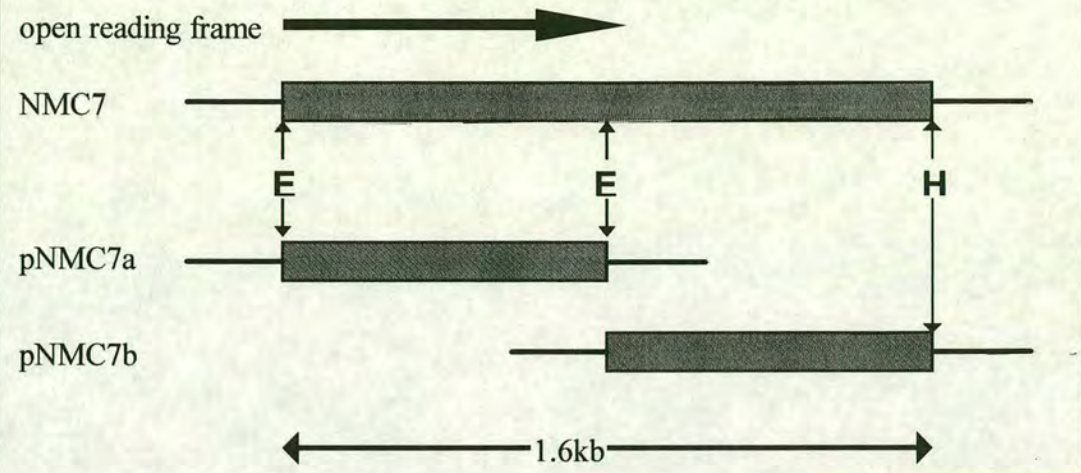

Figure 3.1 Schematic representation of cDNA NMC7, and the two subcloned plasmids pNMC7a and pNMC7b. E: *Eco*RI, H: *Hind*III

were sequenced to reveal a partial open reading frame of 315 amino acids and a 3' untranslated region (3'UTR) of ~700bp. An initial database comparison with the predicted protein sequence showed significant homology to a mouse L-glutamic acid decarboxylase (GAD) reported by Huang *et al* (1990). NMC7a was then used to screen a λZAP ovarian cDNA library and a 2.2kb ovarian cDNA was isolated, representing a further 1.4kb of sequence 5' to NMC7a (fig 3.2). Subsequent database comparisons indicated that the protein products of the Huang GAD sequence and the 2.2kb cDNA sequence both showed significant homology to the C-terminal region of a class of unconventional myosins.

The mouse gene identified by Huang *et al* (1990) shows little similarity to other cloned glutamic acid decarboxylases and the evidence that it encodes a GAD was questionable, leading to speculation that the gene in fact encodes an unconventional myosin from which the N-terminal half is missing (Bu *et al*, 1992; Espreafico *et al*, 1992). As no Northern blot data was included in the original mouse GAD paper (Huang *et al*, 1990) this possibility could not be ruled out. Northern analysis of the

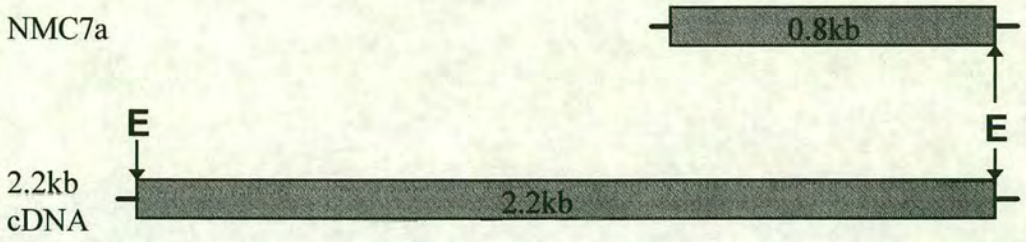

Figure 3.2 Schematic diagram showing relationship between NMC7a and the 2.2kb cDNA from the λ ZAP ovarian library. E: *Eco*RI

new *Drosophila* gene showed a large ovarian transcript of around 6kb indicating that it could encode a full length unconventional myosin. Due to problems with cDNA libraries it was not possible to isolate any further cDNAs for the *Drosophila* gene so the gene was eventually cloned by a combination of genomic library screening and 5'RACE (Rapid Amplification of cDNA Ends). The predicted protein has been shown to include all the features of a class V unconventional myosin - a myosin head domain with ATP-binding and actin-binding domains, a series of IQ repeats and a tail domain predicted to form coiled-coil α-helices. The new gene was therefore confirmed to encode a class V or *dilute* class unconventional myosin and was thus termed *myosinV*. Class V unconventional myosins are molecular motors, thought to play a role in vesicular transport and are discussed in chapter 1 (section 1.5.12). Other members of this lab have since been able to prove that the mouse 'GAD' gene also encodes a protein belonging to this class (MacIver, Wilke, Loke and Bownes, unpublished).

3.2 Results

3.2.1 Localisation of the *myosinV* transcript during oogenesis

In order to examine the localisation pattern of the *myosinV* transcript in greater detail, *in situ* hybridisation to wild type ovaries was performed using the NMC7a cDNA to make digoxigenin labelled DNA probes. The 800bp NMC7a fragment was excised from pBluescript SK$^-$ by an *Eco*RI digest (fig 3.1) and was separated from plasmid DNA by electrophoreses through a 0.8% agarose TAE gel (2.6.7). The 800bp band was then cut from the gel and the DNA recovered using Qiaex II gel purification kit (2.6.7.4). Recovered DNA was quantified by running out 10% of total yield on an agarose gel alongside 1kb λ DNA ladder (2.6.7.2). 200ng of purified NMC7a DNA was then digoxigenin labelled by random priming using Boehringer DIG DNA labelling system (2.3.6). *in situ* hybridisation of the NMC7a probe to whole mount ovaries was performed as described in the materials and methods (2.3.1). The resulting localisation pattern is shown in figure 3.3.

myosinV mRNA was found to be localised to the oocyte, the most posterior germ-line cell in each egg chamber, from stage 1 of oogenesis as the egg chamber buds off from the germarium (fig 3.3). In these early stages only low levels of the transcript are detectable in the nurse cells. At stages 6-7 the transcript seems to be predominantly localised to the posterior of the oocyte, along with the oocyte nucleus. Between stages 8 and 10 the *myosinV* transcript accumulates as a band at the anterior margin of the oocyte (fig 3.3). From stage 10 the transcript is expressed strongly in all the nurse cells (fig 3.3). Localisation at the anterior cortex persists until the degenerating nurse cells transfer their cytoplasmic contents to the oocyte and beyond stage 11 *myosinV* mRNA is uniformly distributed throughout the oocyte.

An identical localisation pattern to that described above was obtained using a probe made from the 800bp *Eco*RI-*Hind*III fragment of pNMC7b (fig 3.1), which consists

Figure 3.3 Localisation of the *myosinV* transcript in wild type ovaries. The *myosinV* transcript is localised to the oocyte - the most posterior germ-line cell of the egg chamber - from stage 1 of oogenesis as the egg chamber buds off from the germarium. At stage 6/7 the *myosinV* transcript is predominantly localised to the posterior of the oocyte (arrowhead), then between stages 8 and 10 it accumulates at the oocyte's anterior margin (arrows). From stage 10 the transcript is strongly expressed in the nurse cells. Anterior localisation is lost as the degenerating nurse cells dump their contents into the maturing oocyte. Anterior is to the left and developmental stages are indicated.

Figure 3.4 *in situ* hybridisation - background staining levels. *in situ* hybridisation to wild type ovaries with a linearised pBluescript probe reveals that background staining levels are weak and easily distinguishable from genuine staining patterns.

Figure 3.3

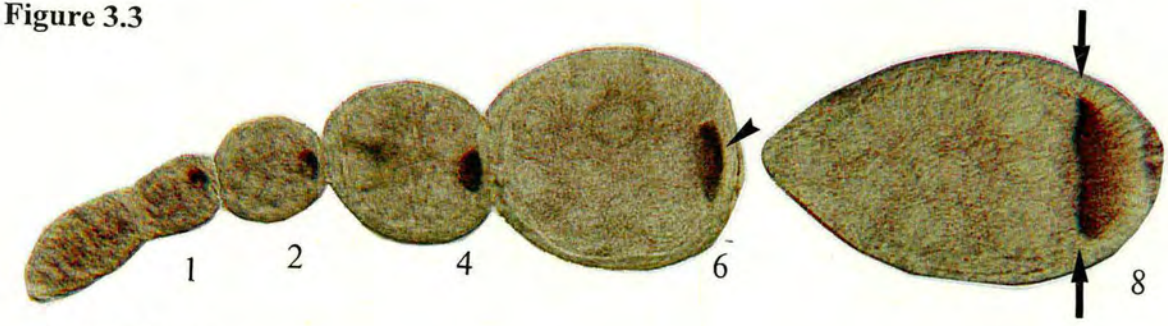

germarium

Figure 3.4

almost entirely of 3'UTR sequence. A probe made from digoxigenin labelled, linearised pBluescript SK$^-$ was used as a control for background staining levels. Background staining was found to be faint throughout the egg chamber and easily distinguishable from the genuine staining pattern (fig 3.4).

The early localisation and transient anterior accumulation of the *myosinV* transcript is similar to that of the *orb*, *fs(1)K10* and *Adducin-like* transcripts, which suggests that *myosinV* might play an important role in oogenesis, as these genes do (Lantz and Schedl, 1994; Cheung *et al*, 1992; Ding *et al*, 1993). The late expression of the *myosinV* transcript in the nurse cells and subsequent transferal into the maturing oocyte suggests that the *myosinV* product is being laid down for use during embryogenesis. The biphasic expression pattern therefore suggests that *myosinV* is involved in both oogenesis and embryogenesis.

3.2.2 Northern Analysis of *myosinV*

The *myosinV* gene was known to be expressed in the ovaries of wild type flies. In order to determine if the transcript was also present in testes or carcass tissue a Northern blot was performed. Around 60 female and male OregonR flies were dissected into ovaries, testes, female carcass and male carcass. The RNA was extracted using Qiagen RNeasy columns and resuspended in 60µl DEPC-H_20 with standard precautions for the preparation and handling of RNA (2.7.2.1). A 5µl sample of each RNA prep was used for spectrophotometry to determine the concentration and purity of the RNA (2.6.2). 10µg of each RNA prep was denatured then electrophoresed through a denaturing agarose-formaldehyde gel (2.7.3) alongside 5µg of Gibco RNA ladder. Ethidium bromide was added to the RNA samples so that the RNA could be visualised when the gel was viewed under ultraviolet light. The ribosomal RNA is the most abundant RNA species present and can be clearly seen running at around 2kb (fig 3.5A). The RNA was then Northern blotted onto Hybond-N$^+$ membrane (2.9.1.2). A *myosinV* probe was prepared by

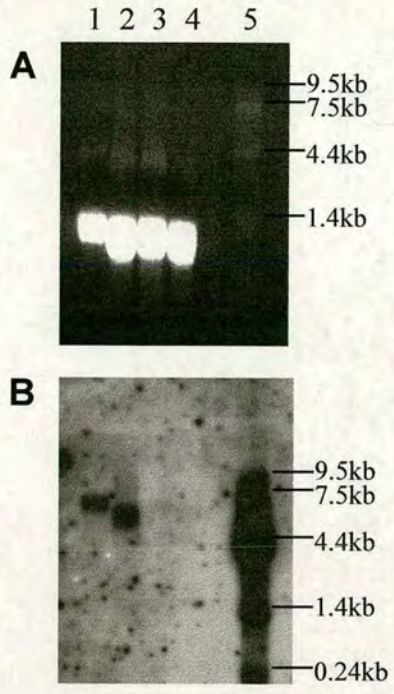

lane

1 ovary
2 testes
3 female carcass
4 male carcass
5 RNA ladder

Figure 3.5 Northern analysis of *myosinV*. A) Ethidium bromide stained agarose gel. B) Northern blot probed with 2.2kb ovarian cDNA indicating that the *myosinV* transcript is expressed in ovary and testes but not in carcass tissue. The testes transcript is around 500bp smaller than the ovarian transcript.

random primed labelling of the 2.2kb ovarian cDNA with ^{32}P, using Pharmacia Ready-To-Go labelling kit (2.9.3.1). The membrane was prehybridised, hybridised with the 2.2kb cDNA probe, then washed all according to standard protocols (2.9.2). The membrane was then exposed to X-ray film for four days and the resulting autoradiograph is shown in figure 3.5B. The *myosinV* transcript is detectable in ovary and testes RNA but not in carcass RNA. Even after 14 days exposure no transcript is detectable in carcass tissue. The testes transcript appears to be considerably smaller than the ovarian transcript. Subsequent hybridisation of the membrane with a λ DNA probe failed to detect the λ RNA size markers, however comparison of the autorad with the agarose gel puts the ovarian transcript at around 6kb. This is in agreement with previous studies. The testes transcript, at 5.5kb, is approximately 500bp smaller than the ovarian transcript. So it appears that the *myosinV* gene is expressed only in the gonads and produces an ovary specific transcript and a testes specific transcript.

3.2.3 Localisation of *myosinV* transcript in testes

The discovery that the *myosinV* gene encoded a testes specific transcript made it necessary to examine the localisation of the transcript within the testes. *in situ* hybridisation to whole mount testes were performed using the same digoxigenin labelled, 0.8kb NMC7a probe used for the ovary *in situs*. Again labelled, linearised pBluescript was used as a control for background staining. The protocol for *in situ* hybridisation to testes is identical to that for ovaries except that proteinase K treatment is cut from 30 minutes to five minutes (2.3.3) as extended proteinase K treatment causes the testes to split, allowing the long sperm tails to escape and become tangled. *myosinV* mRNA was found to be localised to the germ line derived regions of the testis as opposed to the somatically derived accessory glands, seminal vesicle and ejaculatory bulb (fig 3.6A). On closer inspection, it is apparent that the *myosinV* transcript is localised to the inner surface of the coiled testes (fig 3.6B), corresponding to the position of the developing sperm heads. The restriction of the transcript to the germ line derived cells of the testes is similar to the situation in ovaries, where the transcript is present in the oocyte and nurse cells but not in the somatically derived follicle cells. Together these localisation patterns suggest that *myosinV* gene expression is germ line specific.

3.2.4 Size difference in ovarian and testes transcripts

It is possible that the 0.5kb difference in size between the *myosinV* ovary and testes transcripts could be due to differences in the 3'UTR of each transcript. Several other transcripts localised during oogenesis e.g. *bicoid* and *nanos*, have been shown to contain a localisation signal within the 3'UTR of the transcript (Macdonald and Struhl, 1988; Gavis and Lehmann, 1992). If this is the case for the *myosinV* transcript then the signal required for localisation within the ovaries is unlikely to be the same as the signal required for localisation within the testes. The *myosinV* cDNA, NMC7, was found to encode a relatively long 3'UTR of ~700bp, however as this cDNA was

Figure 3.6 Localisation of the *myosinV* transcript in the testis and reproductive tract. A) The *myosinV* transcript is localised to the germ-line derived testis (t) but is absent from the somatically derived accessory gland (ag), seminal vesicle and ejaculatory bulb (eb). The enlargement of the testis in B) shows that the *myosinV* transcript is localised to the inner surface of the testis (arrowheads), in the region of developing sperm heads.

Figure 3.11 Localisation of the *myosinV* transcript in early embryos. A) The *myosinV* transcript is ubiquitous throughout the newly laid eggs on the right. The embryo on the left is undergoing ventral furrow formation and the *myosinV* transcript appears to concentrated in the invaginating folds of the ventral furrow (vf). B) In the embryo undergoing gastrulation, the *myosinV* transcript is concentrated in the folds of the gastrula. y: yolk, eg: extended germband, A: anterior, P: posterior, D: dorsal, V: ventral.

FIG 3.6A

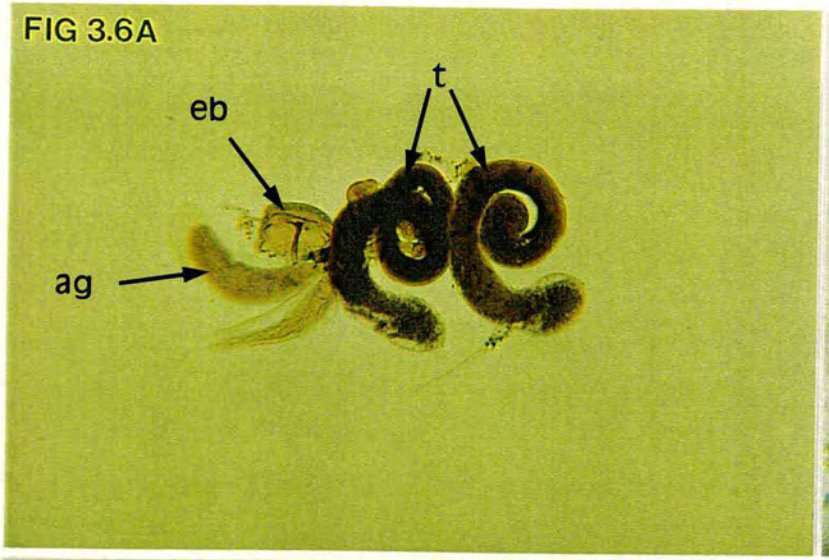

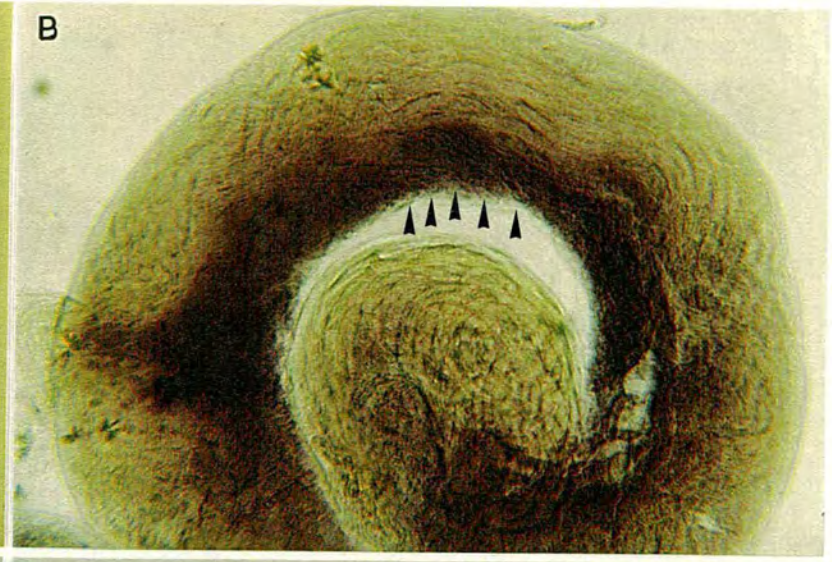

FIG 3.11A

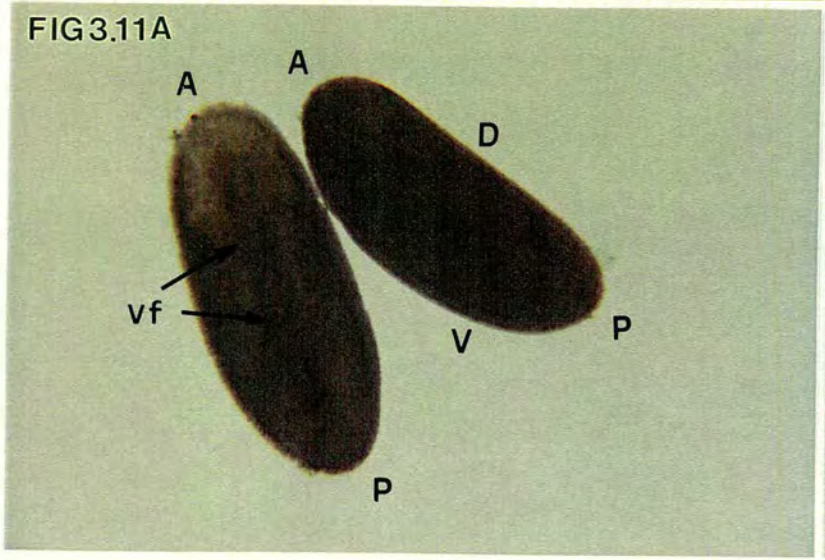

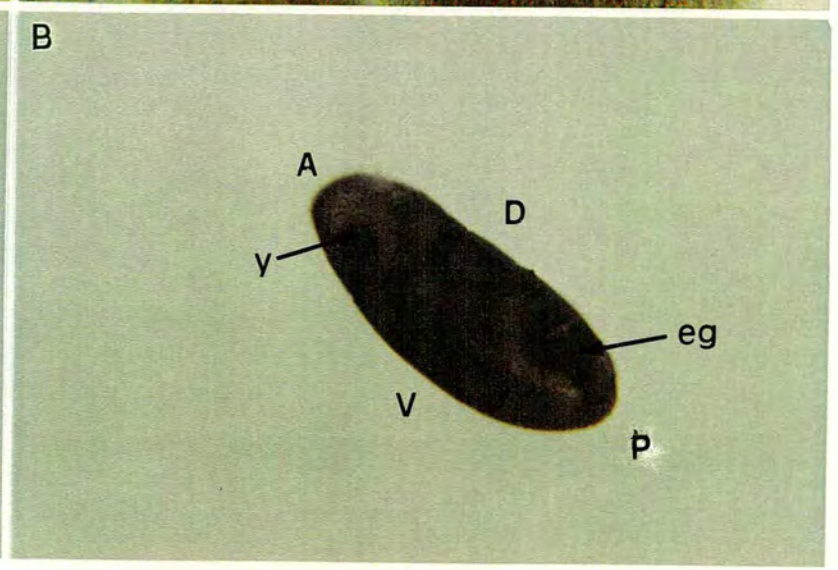

isolated from a whole body cDNA library it was unclear as to whether this represented the ovarian or the testes transcript. To determine which transcript corresponds to NMC7, further screens of ovarian and testes cDNA libraries were undertaken.

A λZAP ovarian cDNA library (2.6.1.2) was screened with a probe made from a 5kb *Eco*RI genomic subclone derived from a genomic library screen (see 6.2.3). The genomic subclone overlaps the most 3' region of the NMC7 cDNA, with the 5' *Eco*RI site corresponding to the site used to subclone NMC7 into two fragments (fig 3.7). The 5kb genomic fragment was labelled with ^{32}P to make a probe (2.9.3.1) and used to screen the λZAP library for homologous sequences as detailed in section 2.8. Positive phage were followed through to the tertiary screen then the cDNAs were excised out of phage λ into pBluescript (2.8.5.2) and sequenced from the T3 and T7 sites (2.6.8). Two cDNAs were found to contain 3'UTR sequence. One of these possessed an identical 3' end to that found in NMC7 although it was truncated at the 5' end where it was co-ligated to an unrelated sequence, presumably a cloning artifact. The second cDNA was identical to NMC7 except for an extra seven base pairs at the 3' end. These extra seven base pairs match the sequence of the genomic DNA (Bryce MacIver, personal communication) and so would appear to be genuine, rather than merely a cloning artifact. These extra base pairs are likely to be a consequence of the fact that there is no clear polyadenylation consensus signal in the *myosinV* gene, so that polyadenylation can occur at a number of sites. Apart from these extra bases, the ovarian cDNA corresponds to NMC7.

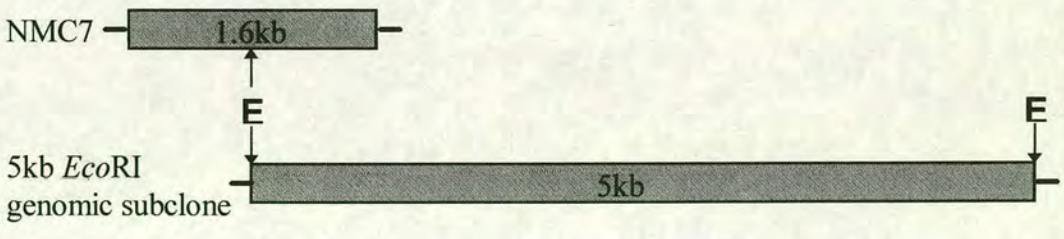

Figure 3.7 Schematic diagram showing the relationship between the 5kb *Eco*RI genomic subclone and the original cDNA, NMC7. E: *Eco*RI

A λZAP testes cDNA library was also screened with the 5kb genomic probe but no positives plaques were obtained. The testes library was subsequently screened using the 2.2kb ovarian cDNA as a probe, but again without success. The 2.2kb cDNA probe failed to detect any homologous transcripts in the testes cDNA library, although it is clear from the Northern blot data and from *in situ* hybridisation to the testes, that such transcripts exist.

3.2.5 RT-PCR to detect differences in ovary and testes 3'UTR

With the failure to isolate a *myosinV* testes specific cDNA, the 3'UTRs of the ovarian and testes transcripts were compared by RT-PCR. RT-PCR involves the reverse transcription of RNA into first strand cDNA (2.7.4), followed by PCR with gene specific primers (2.6.9). RNA was prepared from ovary and testes tissue using the Trizol method (2.7.2.1). 5μg of each RNA prep was then reverse transcribed using the oligo dT primer G7202, which consists of 17 Ts plus an inbuilt *Eco*RI site to facilitate the cloning of RT-PCR products (Colin MacDougall, personal communication). This oligo dT primer should allow the reverse transcription of all polyA$^+$ RNA. PCR was performed on the first strand cDNA using primer pairs G7202 & 1806 and N1659 & 1806. N1659 is a primer to the most 3' end of the

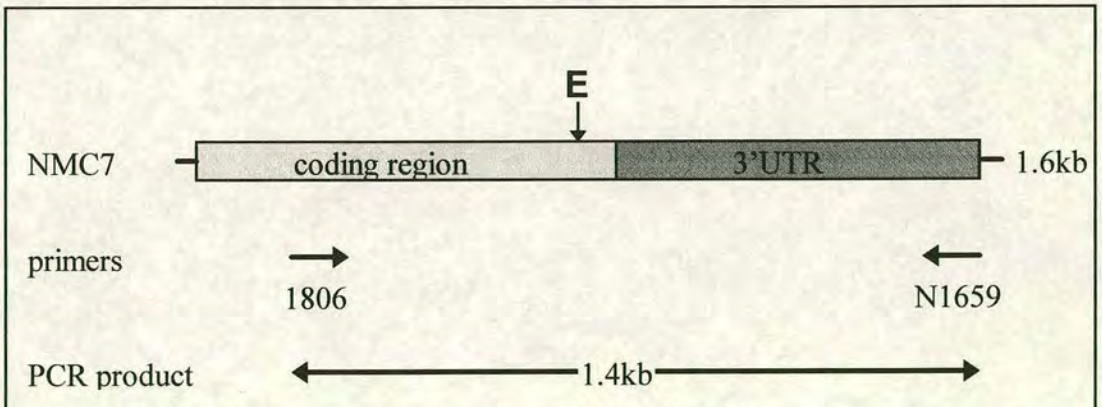

Figure 3.8 Schematic diagram showing the position of RT-PCR primers 1806 and N1659 in relation to the original cDNA, NMC7. These primers should amplify a product of 1.4kb from ovarian cDNA. E: *Eco*RI

ovarian 3'UTR and includes a *Eag*I site designed for the PCR cloning of the UTR (see 5.2.1). 1806 is a primer to the coding region of the ovarian transcript and should give a product of 1.4kb when used in conjunction with both G7202 and N1659 (fig 3.8). The PCR was hot started followed by 35 cycles of 94°C, 15sec; 50°C, 15sec; 72°C, 1min, followed by a 10 minute extension at 72°C.

Figure 3.9 shows the reaction products run out on a 0.8% agarose gel. Lanes one and two are the ovary and testes cDNA with primers G7202 & 1806. There are many small spurious bands, probably due to the promiscuous priming of 1806 at the low annealing temperature required for G7202. Lanes three and four show a single product using the primers N1659 & 1806. The ovary and the testes products look to be the same size, around 1.4kb. Lane 5 shows a slightly larger product of around 1.5kb obtained using genomic DNA as a template for N1659 & 1806. This is due to the existence of two small introns of 40bp and 60bp in the genomic DNA (Bryce MacIver, personal communication). Lane 6 shows a faint 1.5kb product obtained using primers N1659 & 1806 on testes RNA which has not been reverse transcribed, indicating there is slight genomic DNA contamination of the RNA preps. This is not a problem as the product from first strand cDNA is clearly smaller and more abundant. Lane 7 contained no template. These preliminary results indicate that the ovary and testes 3'UTR are of the same length.

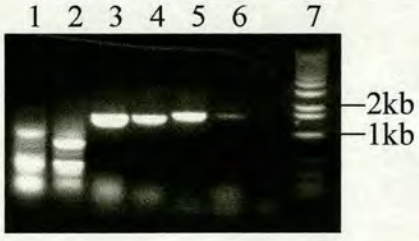

lane	template	primer pair
1	ovary cDNA	G7202 & 1806
2	testes cDNA	G7202 & 1806
3	ovary cDNA	N1659 & 1806
4	testes cDNA	N1659 & 1806
5	genomic DNA	N1659 & 1806
6	testes RNA	N1659 & 1806
7	Gibco 1kb ladder	

Figure 3.9 RT-PCR to detect difference in ovary and testes 3'UTR. Lanes 1 and 2 show spurious bands due to promiscuous priming. Lanes 3 and 4 show that these primersamplify a 1.4kb product from both ovary and testes cDNA templates. Lane 5 shows a slightly larger product using a genomic DNA template. The presence of a faint band in lane 6 indicates genomic DNA contamination of the RNA prep.

3.2.6 Direct sequencing of RT-PCR products

The RT-PCR products from ovary and testes appear to be the same size, but to determine if they are identical they were directly sequenced using automated sequencing technology. The above PCR on ovary and testes first strand cDNA with N1659 & 1806 primers, was repeated to generate sufficient product for sequencing. The 1.4kb ovary and testes products were gel purified using Qiaquick columns (2.6.7.4) and quantified by running out samples on an agarose gel alongside a known concentration of 1kb ladder. Purified PCR products were sequenced with primers N1659 and 1806, with around 60-90ng of PCR product required as a template for each primer (2.6.8.3). Around 450-500 bases of good sequence was obtained from each primer by direct sequencing of RT-PCR products. The sequences of the ovary and testes RT-PCR products were found to be identical. There was a central region which remained unsequenced, however it seems unlikely that there is a difference between the 3'UTRs of the *myosinV* ovary and testes transcripts. Certainly the 0.5kb size difference between the ovary and testes transcripts cannot be accounted for by a difference in their 3'UTRs. This size difference may be due instead to alternate splicing or differences in the 5'UTR of ovarian and testes transcripts.

3.2.7 Developmental profile of *myosinV* expression

The *myosinV* gene is now known to be expressed during oogenesis and spermatogenesis. In order to determine if the gene is expressed at any other stage during development it was decided to construct a developmental profile. This is a Northern blot with RNA from various stages of the *Drosophila* life cycle to detect at which stages the *myosinV* gene is being expressed. RNA was extracted from the following stages: adult ovary; adult testes; 0-4 hour embryos; 4-16 hour embryos; 16-24 hour embryos; first instar larvae; second instar larvae; female third instar larvae; male third instar larvae; pupae; adult female carcass and adult male carcass (see 2.2 for details of staged collections). RNA was prepared using Qiagen RNeasy columns

(2.7.2.1) and quantified by spectrophotometry (2.6.2)). 10μg of each sample plus 5μg of λ RNA ladder was electrophoresed through a denaturing agarose-formaldehyde gel in 1X MOPS (2.7.3). An ethidium bromide stain of the agarose gel indicates that the first and second instar larvae and the male carcass lanes were underloaded (fig 3.10A). The separated RNA was Northern blotted onto Hybond-N^+ membrane (2.9.1.2) then incubated with prehybridisation solution at 42°C. A *myosinV* probe was prepared by random primed labelling of the 2.2kb ovarian cDNA with ^{32}P, using Pharmacia Ready-To-Go labelling kit (2.9.3.1). Hybridisation with the 2.2kb cDNA probe and subsequent washing of the membrane were performed according to standard protocols (2.9.2). The membrane was exposed to X-ray film for three days and the resulting autorad is shown in figure 3.10B.

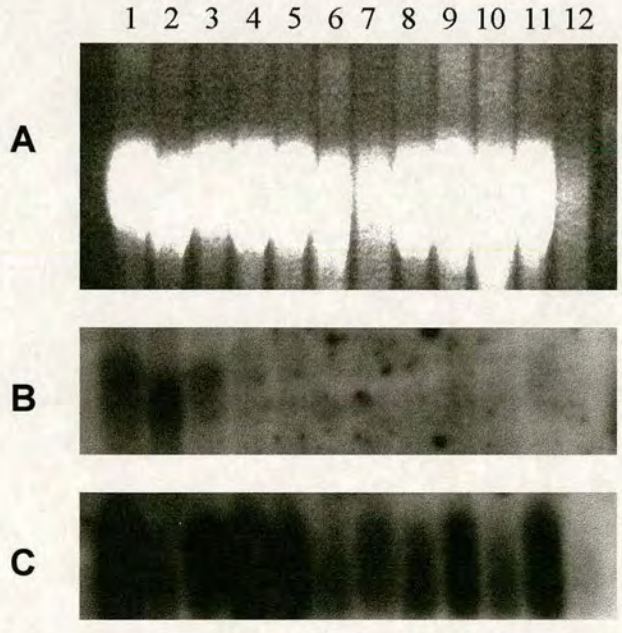

lane

1 ovary
2 testes
3 0-4 hr embryos
4 4-16 hr embryos
5 16-24 hr embryos
6 1st instar larvae
7 2nd instar larvae
8 female 3rd instar
9 male 3rd instar
10 pupae
11 female carcass
12 male carcass

Figure 3.10 Developmental profile of *myosinV* transcript expression. A) Ethidium bromide stained agarose gel. B) Northern blot probed with 2.2kb ovarian cDNA indicating transcript present only in ovary, testes and 0-4 hr embryos. C) Northern blot reprobed with RP49 as a loading control.

The *myosinV* transcript is only clearly detectable in ovaries, testes and 0-4 hour embryos. No transcript was detected in any other stage, even after a prolonged exposure time. The ovary and early embryo transcripts are around 6kb while the testes transcript is 5.5kb. It is unsurprising that the transcript should be present in early embryos as *in situ* hybridisation to the ovaries shows that the transcript is present in the oocyte at the final stages of oogenesis. In agreement with earlier results the *myosinV* transcript is not detected in carcass tissue, suggesting that it is specific to the gonads. However, it is not present at detectable levels in the gonadal tissue of larvae or pupae.

To ensure that the RNA from each sample was present at comparable levels a loading check was performed. This involves re-probing the Northern membrane with a probe made from the ubiquitous ribosomal protein RP49. The intensity of signal obtained with this probe should be directly proportional to the amount of RNA present in each lane. A 0.6kb fragment of RP49 was excised from pRP49 by an *Eco*RI/*Hind*III digest, and gel purified using Qiaquick columns (2.6.7.4). The fragment was labelled with ^{32}P and used to re-probe the membrane. The resulting autorad would suggests that the testes lane is underloaded (3.10C), although the *myosinV* transcript seems to be abundant in this lane (fig 3.10B). It has since been reported that testes tissue is not as rich in RP49 as other tissues (Flybase). The autorad also shows that the first instar larvae, second instar larvae and the male carcass lanes were underloaded, as was indicated by ethidium bromide staining. It is however known from the previous Northern that the *myosinV* transcript is not detectable in male carcass. The results of the developmental profile therefore suggest that the *myosinV* gene is only expressed in ovaries, testes and early embryos.

3.2.8 Localisation of the *myosinV* transcript in early embryos

The *myosinV* transcript was detected in early embryos and so *in situ* hybridisation to whole mount embryos was performed to determine if the transcript is localised within

the embryo. The protocol for *in situ* hybridisation to embryos is similar to that for ovaries, except that a few extra steps are required to remove the chorion and vitelline membrane which would otherwise prevent the probe from penetrating (2.3.4). The embryos were probed with the same digoxigenin labelled, 0.8kb NMC7a probe used for the ovary *in situs*. Linearised pBluescript was again used as a control probe. *myosinV* mRNA was detected throughout the embryos but was found to be enriched in the folds of the ventral furrow and the folds of gastrulation (fig 3.11). The transcript is found most abundantly in the earliest embryos then gradually fades away as the embryos age. It is likely that the *myosinV* transcript present in the embryos is the maternal transcript produced in the nurse cells late in oogenesis, transferred into the maturing oocyte and carried over to the early embryo. The transcript then degrades after four hours of embryogenesis. It is not clear whether the MyosinV protein is being translated in ovaries and embryos, or if it is localised in a similar pattern to its transcript. A MyosinV-GST fusion protein has been expressed in bacterial cells and production of an antibody is underway (Bryce MacIver, personal communication). This will allow the question of whether the protein is present and localised in ovaries and early embryos to be addressed.

3.2.9 Is the *myosinV* transcript germ line specific?

The developmental profile indicates that the *myosinV* transcript is restricted to the gonads and furthermore, *in situ* hybridisation to ovaries and testes show that the transcript is found only in the germ line cells of the gonads. The *myosinV* gene has recently been proposed to correspond to *l(2)43Cc*, a locus identified by Heitzler *et al* (1990) in a screen of the 43 region of the *Drosophila* second chromosome (see chapter 7). However, the *43Cc* gene was found to have lethal alleles, whereas mutations in a gene required exclusively during oogenesis would be expected to have a female sterile or maternal effect lethal phenotype. The fact that a mutation in the *43Cc* gene is lethal does not fit well with expression only during oogenesis and spermatogenesis. It may be that *myosinV* gene expression is required at other stages

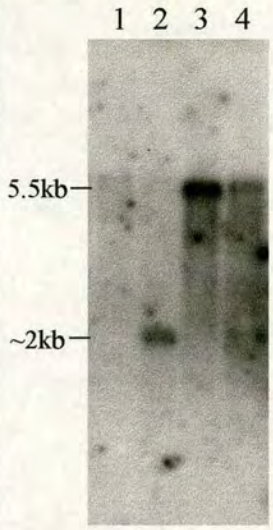

lane
1 male carcass
2 female carcass
3 testes
4 ovaries

Figure 3.12 PolyA$^+$ Northern. The 2kb band in the female carcass lane indicates the presence of a smaller, female carcass specific transcript

throughout development, but at levels so low as to be undetectable by a conventional Northern blot. To address this problem it was decided to attempt a polyA$^+$ RNA Northern. PolyA$^+$ RNA represents only a small proportion of the total RNA present in a tissue. As there is a limit to the amount of RNA which can successfully be loaded onto a gel, removing all the ribosomal RNA and transfer RNA increases the relative concentration of the target mRNA.

A polyA$^+$ Northern membrane already existed in the lab. It contained polyA$^+$ RNA from ovaries, testes, female carcass and male carcass which had been prepared using the Dynabeads PolyA$^+$ Direct system (Colin MacDougall, personal communication). This membrane was stripped and reprobed with the 2.2kb ovarian cDNA according to standard procedures. The resulting autorad shows a clear signal in the testes lane representing the testes transcript (fig 3.12). The reduced signal in the ovary lane can be accounted for by the underloading of ovary RNA on the original gel (Colin MacDougall, personal communication). But confusingly, on this Northern the ovary and testes transcripts appear to be of the same size. There appears to be a very faint signal at 5.5/6kb in the male and female carcass lanes, however there is also a stronger signal at around 2kb in the female carcass lane (fig 3.12). This firstly suggests that

expression of *myosinV* is not germ-line specific and also suggests the existence of a 2kb, alternately spliced, female carcass specific transcript. These carcass signals were not evident in either of the previous total RNA Northerns, despite heavy loading and extended exposure. The 5.5/6kb carcass signals are very faint compared to the testes signal although the original loadings were comparable, indicating that these transcripts are rare. However, the 2kb female carcass specific signal is quite strong and would have been expected to show up on previous Northerns. Due to the confusing nature of this result, it was decided to repeat the polyA$^+$ Northern to confirm the existence of the 2kb female carcass specific transcript.

3.2.10 PolyA$^+$ Northern to detect *myosinV* transcripts

To ascertain whether the 2kb signal on the polyA$^+$ Northern represents a genuine female carcass specific transcript, an attempt was made to repeat the result. In addition to probing gonadal and carcass tissue, it was decided to look for the existence of *myosinV* mRNA in the progeny of *tudor* homozygotes. *tudor* homozygotes fail to produce pole cells, resulting in offspring which are lacking in germ line cells and so should be entirely devoid of a germ line specific transcript. Two mutant alleles of *tudor*, $tud^{2.5}$ and $tud^{2.6}$ were used in a cross to generate flies with no germ line as described in figure 3.13. Total RNA was prepared from ovaries, female carcass, female *tudor* flies and male *tudor* flies using the Trizol method (2.7.2.1). PolyA$^+$ RNA was then extracted from these preps using the Dynabeads PolyA$^+$ Direct system (2.7.2.2). Around 30µg of each total RNA prep was used in the preparation of polyA$^+$ RNA. The ovary and female carcass preps were prepared using new Dynabeads, whereas the *tudor* preps were prepared using reconditioned Dynabeads which may have had an adverse affect on the recovery of polyA$^+$ RNA. The polyA$^+$ RNA was electrophoresed through a denaturing agarose-formaldehyde gel (2.7.3). The removal of the ribosomal RNA means that the RNA cannot be easily visualised by ethidium bromide staining under UV light, however faint bands of RNA could be detected, at least in the ovary and female carcass lanes. The polyA$^+$ RNA

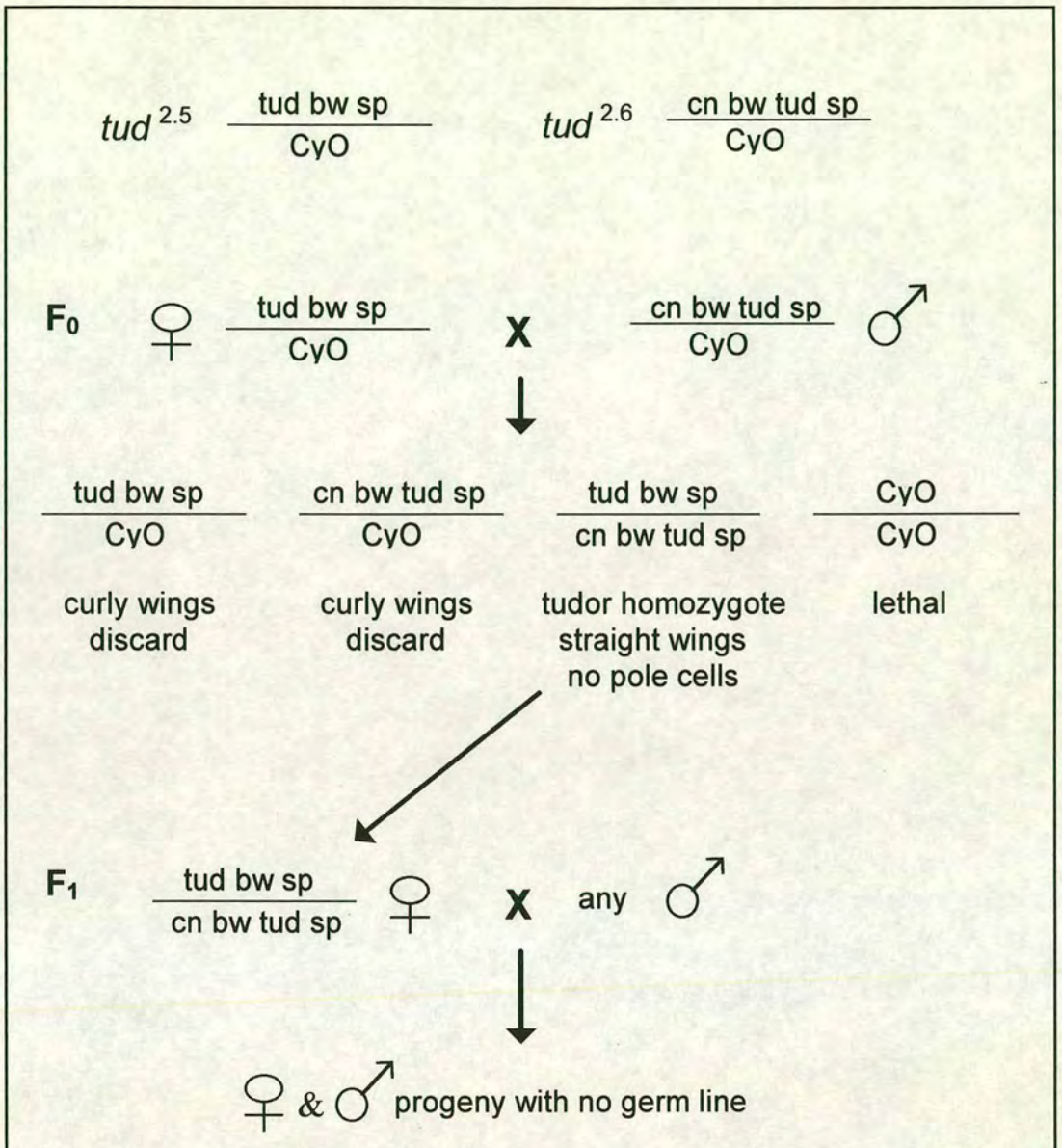

Figure 3.13 Cross of two *tudor* alleles, *tud* $^{2.5}$ and *tud* $^{2.6}$ to generate flies with no germ line. bw: *brown*, sp: *speck*, cn: *cinnabar*, CyO: *Curly of Oster* balancer.

was Northern blotted onto Hybond-N membrane and probed with the ^{32}P labelled 2.2kb ovarian cDNA according to standard protocols. The membrane was exposed to X-ray film for up to seven days but no signal was evident apart from some hybridisation to the λ RNA ladder. This hybridisation to the markers is probably due to some contamination of the 2.2kb fragment with vector DNA and serves to indicate that transfer from the gel to the membrane was successful. The polyA$^+$ Northern was

re-screened with a new batch of the 2.2kb probe, then the entire Northern was repeated from scratch, all without success. A subsequent reversion to total RNA Northerns was also unsuccessful, despite them being performed in a seemingly identical manner to previous Northerns. No attempt at trouble-shooting could resolve this problem which turned out to be a general one throughout the lab. It was therefore not possible to confirm the existence of a 2kb female carcass specific transcript by means of a Northern blot.

3.2.11 RT-PCR to determine if the *myosinV* transcript is germ line specific

In the absence of convincing Northern blot evidence, an RT-PCR approach was adopted to determine whether the *myosinV* transcript exists outwith the germ line. The RNA from specific tissues was first reverse transcribed into first strand cDNA. If a PCR product can be amplified from this first strand cDNA using *myosinV* specific primers then a *myosinV* transcript must have been present in the original RNA prep. RNA was prepared from ovary, female carcass and female *tudor* flies using the Trizol method, then reverse transcribed using primer N1659, a primer to the most 3' end of the ovarian transcript (2.7.4). It is a previous experience that RNA preps can be contaminated with genomic DNA which is carried through to the first strand cDNA prep and acts as a template for the primers, giving false results (see 3.2.5). To overcome this problem the primers chosen for PCR spanned an intron in the *myosinV* gene such that they gave a product of 1kb when priming from genomic DNA and a product of 0.3kb when priming from cDNA (Bryce MacIver, personal communication). This could be considered a somewhat risky strategy, as the primers cover such a small region of the gene that it might not be present in an alternately spliced transcript. However, these primers, DID3 & DID4, were designed for the sequencing of the 5' region of the gene and are known to prime in the region of the myosin head domain (Bryce MacIver, personal communication). The head domain is the most functionally significant domain of any myosin and would be expected to be included in any transcript.

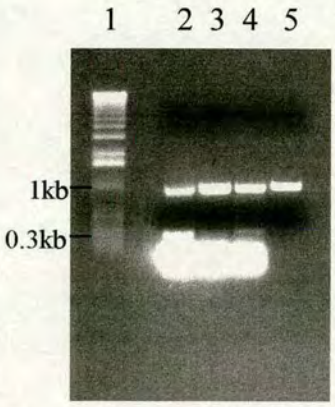

lane

1 Gibco 1kb ladder
2 ovary cDNA
3 female carcass cDNA
4 *tudor* female cDNA
5 genomic DNA

Figure 3.14 RT-PCR with DID3 and DID4 primers. The amplification of a 0.3kb product from female carcass and *tudor* female cDNA indicates that the *myosinV* transcript is not germ line specific. The 1kb band indicates genomic contamination.

The cDNA preps and a genomic DNA control were amplified with DID3 & DID4 by hot start PCR with 35 cycles of 94°C, 15sec; 50°C, 15sec; 72°C, 1min, followed by a 5 minute extension at 72°C. Figure 3.14 shows the PCR products run out on a 0.8% agarose gel. It can be seen that all the cDNA preps are contaminated with genomic DNA as all give the same 1kb product as the genomic DNA template. The first strand cDNA preps must contain an excess of RNA which was not reverse transcribed, as this can be seen as a large diffuse band running at below 0.25kb, in all but the genomic DNA reaction. However just above this RNA band a 0.3kb band is visible. This band is clear in the ovary cDNA lane but very faint in the female carcass and female *tudor* cDNA lanes. This 0.3kb band indicates that the *myosinV* transcript is indeed present in female carcass and female *tudor* flies although the faintness of the bands suggests a rare transcript. It can nonetheless be concluded that the *myosinV* transcript is not germ line specific.

3.3 Summary

Analysis of cDNAs related to an enhancer trap screen led to the discovery of a 1.6kb cDNA which corresponded to a transcript which was localised during oogenesis but

which was unrelated to any enhancer trap pattern. The transcript was localised to the developing oocyte from very early in oogenesis then later seen as a band at the anterior cortex of the oocyte. This pattern was similar to the localisation patterns of the *orb*, *gurken*, and *Adducin-like* transcripts, which suggested that the localisation of the *myosinV* transcript might have an important bearing on its function, as is thought to be the case for the transcripts mentioned above. The *myosinV* transcript is also strongly expressed in the nurse cells late in oogenesis and subsequently transferred into the oocyte, suggesting that *myosinV* might also be required during early embryogenesis.

A further 1.4kb of cDNA was obtained but Northern blot data indicated that the full length ovarian transcript was around 6kb. Database comparison of the predicted protein sequence indicated homology to the C-terminal domain of a class of unconventional myosins thought to be involved in vesicle transport. Subsequent cloning and sequencing of the 5' region of the gene revealed that the gene encoded a protein with all the features of a class V unconventional myosin - a myosin head domain with ATP-binding and actin-binding domains, a series of IQ repeats and a tail domain predicted to form coiled-coil α-helices.

The *myosinV* transcript was found to be also present in testes and early embryos. The embryo transcript is thought to be maternally encoded transcript, laid down during oogenesis. The transcript is present throughout the early embryo but appears to be concentrated in the folds of ventral furrow formation and gastrulation. The testes transcript is around 5.5kb and appears to be localised to the developing sperm heads. The 0.5kb size difference between the ovarian and testes transcripts was shown not to be due to differences in the 3'UTRs of the transcripts. The difference may be due instead to differences in the 5'UTR or due to alternate splicing of the transcripts.

The localisation of the *myosinV* transcript to the germ-line derived cells of the ovary and testes suggested that the transcript was germ-line specific, however a polyA$^+$ Northern provided some evidence for the existence of a 5.5/6kb transcript in male and

female carcass and a 2kb female carcass specific transcript. Although the existence of these transcripts was not verified by Northern analysis, RT-PCR confirmed that the gene was being transcribed at low levels in other tissues.

Chapter 4

myosinV Transcript Localisation in Mutant Backgrounds

4.1 Introduction

The asymmetric localisation of maternally inherited transcripts plays an important role during *Drosophila* development. For example, the localisation of *egalitarian* and *Bicaudal-D* transcripts is required for oocyte determination, the localisation of *gurken* mRNA is essential for the establishment of egg chamber polarity and the localisation of *bicoid* and *nanos* mRNAs to opposite poles of the egg is essential for pattern formation in the developing embryo. Localisation of these transcripts is, in turn, dependent on the function of other genes. By studying the genetic requirements of transcript localisation during oogenesis it has been possible to establish a number of overlapping genetic pathways. The genetic interactions required for the localisation of certain maternal transcripts are discussed in more detail in chapter one (1.3 & 1.4).

The *myosinV* gene was originally selected for further study because its transcript is localised early to the oocyte then asymmetrically localised within the oocyte (fig 4.1). From stage 1 of oogenesis, within the germarium, the *myosinV* transcript is localised to the oocyte. In stage 6 and 7 egg chambers the transcript appears to be predominantly localised to the posterior of the oocyte, then from stages 8-10 the transcript is localised as a discrete band at the anterior cortex of the oocyte. This anterior localisation persists through to stage 10 while much transcript is also seen building up in the nurse cells. At stage 10b the nurse cells transfer almost their entire contents into the oocyte and with the onset of cytoplasmic streaming the *myosinV* transcript becomes diffuse throughout the oocyte.

The early oocyte localisation and transient anterior accumulation of the *myosinV* transcript would suggest that the *myosinV* product is required during oogenesis as opposed to embryogenesis. The localisation of the *myosinV* transcript is similar to that of the *orb*, *fs(1)K10* and *Adducin-like* transcripts, which all have functions during oogenesis. The late expression of *myosinV* transcript in the nurse cells and its subsequent transferal into the late stage oocyte suggests that *myosinV* might play a

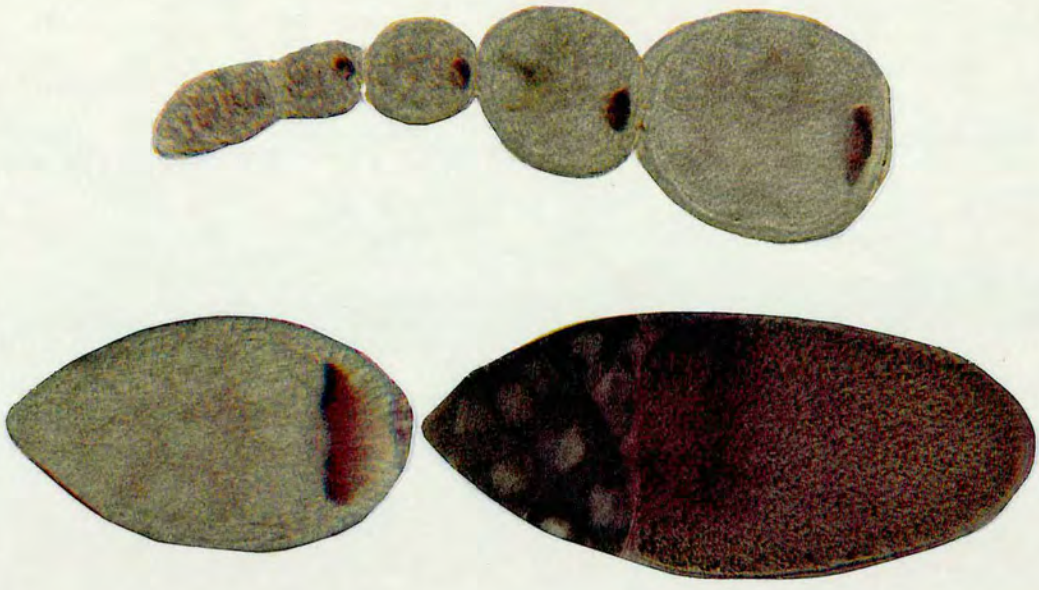

Figure 4.1 Localisation pattern of the *myosinV* transcript in *OregonR* wild type ovaries. See text for details.

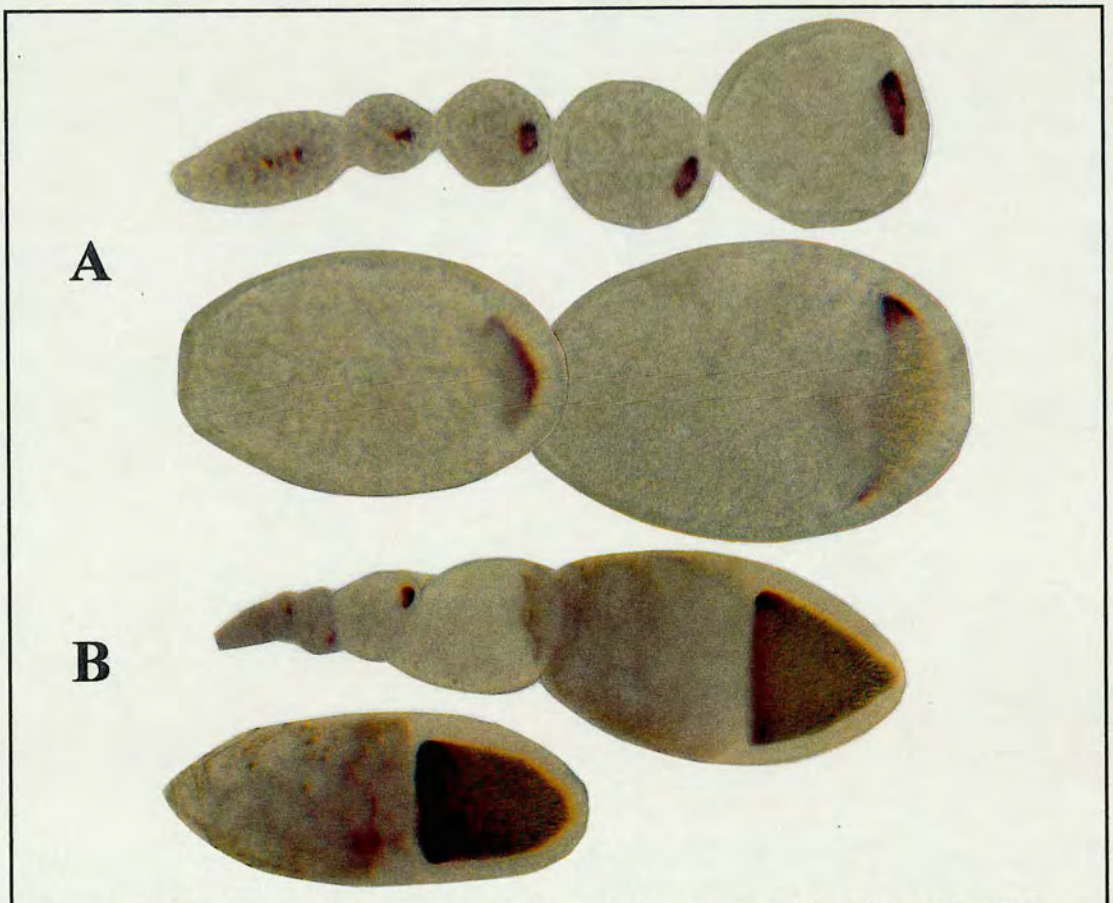

Figure 4.3 A) Localisation pattern of the *gurken* transcript in *OregonR* wild type ovaries. B) Localisation pattern of the *fs(1)K10* transcript in *OregonR* wild type ovaries. See text for details.

role in embryogenesis, but one which does not require a localised transcript. This is a common expression pattern for those genes whose products are required early in embryogenesis before there is any significant transcription from the zygotic genome, and therefore must be supplied maternally. The complex localisation pattern of the *myosinV* transcript therefore suggests that the *myosinV* product may have two roles - one during oogenesis which may be related to the anterior accumulation of its transcript and a second role in early embryogenesis.

In an attempt to elucidate the role of the *myosinV* gene it was decided to establish the position of the gene within the genetic pathways which govern transcript localisation during oogenesis. This was achieved by looking at the localisation of the *myosinV* transcript in the ovaries of flies carrying mutations for genes involved in oogenesis - in particular, mutations in those genes known to be required for the correct localisation of the *bicoid*, *gurken*, *oskar* and *nanos* transcripts. Failure of the *myosinV* transcript to localise when a particular gene is mutant indicates a dependence on that wild type gene product for normal localisation. However, mutations in some genes cause major disruption to oogenesis and/or prevent the function of downstream genes, so failure of the *myosinV* transcript to localise in a particular mutant background does not necessarily indicate a direct interaction between the wild type gene product and the *myosinV* transcript. Instead, it can only be concluded that *myosinV* may be involved in the same genetic pathway.

4.1.1 Fly stocks

The flies used in this study were mutant for the following genes: *egalitarian, Bicaudal-D, chickadee, exuperantia, swallow, staufen, orb, gurken, fs(1)K10, cappuccino, spire, oskar, vasa, tudor, valois, Notch* and *Delta*. The functions of these genes are discussed in chapter one (1.3 and 1.4) and the fly stocks are described in Table 4.1. Flies used for *in situ* hybridisation were homozygous for the particular mutation, unless otherwise described in the text.

Table 4.1 Fly stocks used in this study.

Mutant	Markers & Balancers	Source
egl^{WU}	*cn bw egl*^{WU} *sp / CyO*	Umea
Bic-D ^{7134R}	*dp b Bic-D* $^{7134\text{-}R26}$ */ CyO*	Tubingen
chi^{11}	*P{ry* $^{+t7.2}$ *=A92} chi*^{11} */ CyO; ry*^{506}	Bloomington
exu^{QR}	*cn exu*^{QR} *bw / CyO*	Tubingen
sww^{99}	*y cv sww*^{99} *v t / FM3*	Tubingen
stau^{D3}	*cn stau*^{D3} */ CyO*	Umea
orb^{MEL}	*orb*^{MEL} *st / TM3 sb ry e*	D McKearin, Texas
orb^{F343}	*BsY orb*^{F343} *ru st e ca / TM3 sb p*^{p} *ri e*	D McKearin, Texas
grk^{WG}	*grk*^{WG} *b bw sp / CyO*	Bloomington
grk^{HK}	*grk*^{HK} *cn bw sp / CyO*	Bloomington
fs(1)K10	*fs(1)K10 w f mal / ClB*	Tubingen
capu^{HK}	*capu*^{HK} *cn bw sp / CyO l(2) DTS100*	Umea
spir^{339}	*spir*^{339} *cn sca / CyO*	Umea
osk^{54}	*st osk*^{54} *e / TM3 Ser*	Umea
vasa^{PD23}	*vas*^{PD23} *cn bw / CyO*	Umea
tud^{WC8}	*tud*^{WC8} *bw sp / CyO*	Bloomington
vls^{1}	*vls*^{1} *cn bw / CyO-513*	Bloomington
Notch^{ts1}	*N*^{ts1} *y g*^{2} *f*	Bloomington
Delta^{6B}	*st Dl*^{6B} *e / TM3 sb*	Tubingen

4.2 Results

4.2.1 *in situ* hybridisation - probes and controls

in situ hybridisations to determine the localisation of the *myosinV* transcript in mutant ovaries were performed according to the protocol detailed in 2.3.1 using digoxigenin labelled *myosinV* DNA probes made from the 0.8kb *Eco*RI fragment of pNMC7a or

the 0.8kb *Eco*RI/*Hind*III fragment of pNMC7b (see fig 3.1). These probes were found to give identical staining patterns. Digoxigenin labelled, linearised pBluescript was used as a probe to control for background staining. As a control for the quality of staining pattern obtainable with the hybridisation and detection system used, *in situ* hybridisations were performed on wild type flies using *gurken* and *fs(1)K10* probes. The *gurken* probe was a 1.7kb *Xho*I/*Not*I fragment of pGRK (fig 4.2A) and the *fs(1)K10* probe was a 1kb *Xho*I/*Eco*RI fragment of pKKS (fig 4.2B), both kindly provided by D. St. Johnstone. The *gurken* transcript was found to be localised to the oocyte from stage 1, transiently to the oocyte posterior at stages 6-7, to the anterior cortex at stage 8 and then to the anterio-dorsal corner of the oocyte from stage 9-10b (fig 4.3A). The *fs(1)K10* transcript was found to localise to the oocyte from stage 2, then to the anterior cortex at stages 8-10b (fig 4.3B). The transcripts of both *gurken* and *fs(1)K10* are less abundant in the nurse cells and oocyte than the *myosinV* transcript. In addition the *fs(1)K10* transcript appears to be more tightly localised to the oocytes anterior margin at stages 8-10b than does the *myosinV* transcript. These *in situ* results are in exact agreement with the reported localisation patterns of *gurken* and *fs(1)K10* transcripts (Neuman-Silberberg and Schupbach, 1993; Cheung *et al*, 1992) and indicate that the detection of stage specific localisation patterns is well within the limits of the hybridisation/detection system used.

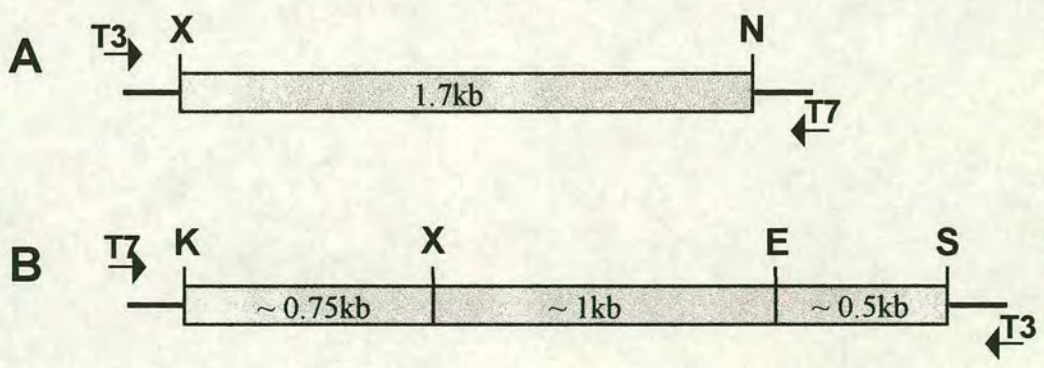

Figure 4.2 A) pGRK - *gurken* cDNA cloned into pBluescript KS. The 1.7kb *Xho*I/*Not*I fragment was used as a template for *in situ* hybridisation probes. B) pKKS - coding region of *fs(1)K10* cloned into pBluescript SK⁻. The 1kb *Xho*I/*Eco*RI fragment was used as a probe template. X: *Xho*I, N: *Not*I, K: *Kpn*I, E: *Eco*RI, S: *Sal*I.

4.2.2 Localisation of *myosinV* transcript in *egalitarian* mutants

egalitarian is a gene required for oocyte determination, the process by which one cell of the germarial 16 cell cluster becomes an oocyte while the remaining 15 cells become polyploid nurse cells. In egl^{WU} mutants oocyte determination fails, resulting in the formation of a 16 cell cyst which degenerates around what would be stage 7. *in situ* hybridisation with the *myosinV* probe shows that the transcript is present throughout the 16 cell cyst but not localised (fig 4.4A). The presence of the transcript in the absence of an oocyte indicates that *myosinV* transcription occurs in the nurse cells rather than exclusively in the oocyte. It is therefore likely that in wild type ovaries the transcript is produced in the nurse cells and rapidly transported to the oocyte.

4.2.3 Localisation of *myosinV* transcript in *Bicaudal-D* mutants

Bicaudal-D is required for oocyte determination and abdominal pattern formation, with a variety of alleles giving rise to different defects. Here the $Bic\text{-}D^{7134R}$ allele was used, which like egl^{WU} results in the formation of 16 cell cysts which later degenerate. Again the *myosinV* transcript is present but not localised within these cysts suggesting that *myosinV* transcription occurs mainly in the nurse cells. The transcript is expressed strongly in some of these cysts, perhaps at the same stage it would normally be strongly expressed in the nurse cells of wild type ovaries (fig 4.4B).

4.2.4 Localisation of *myosinV* transcript in *chickadee* mutants

The *chickadee* gene encodes a homologue of mammalian profilin, a protein involved in the assembly of actin into microfilaments (Cooley *et al*, 1992). In *chickadee* mutants, the bulk transfer of nurse cell contents to the oocyte at stage 10b is disrupted because the ring canals become blocked with nurse cell nuclei. This suggests that the

Figure 4.4 Localisation of the *myosinV* transcript in mutant backgrounds. A) egl^{WU} - the *myosinV* transcript is ubiquitous throughout all 16 nurse cells. B) $Bic\text{-}D^{7134R}$ - again the *myosinV* transcript is ubiquitous throughout all 16 nurse cells. C) chi^{11} - the *myosinV* transcript localises normally in stage 8/9 egg chambers (arrowhead) but at stage 10 cytoplasmic transfer fails and the transcript becomes backed up in the nurse cells (arrows). D) exu^{QR} - the *myosinV* transcript localises normally until stage 8 when it fails to become tightly localised to the oocyte's anterior margin and instead forms a very broad band in the anterior two thirds of the oocyte (arrowheads).

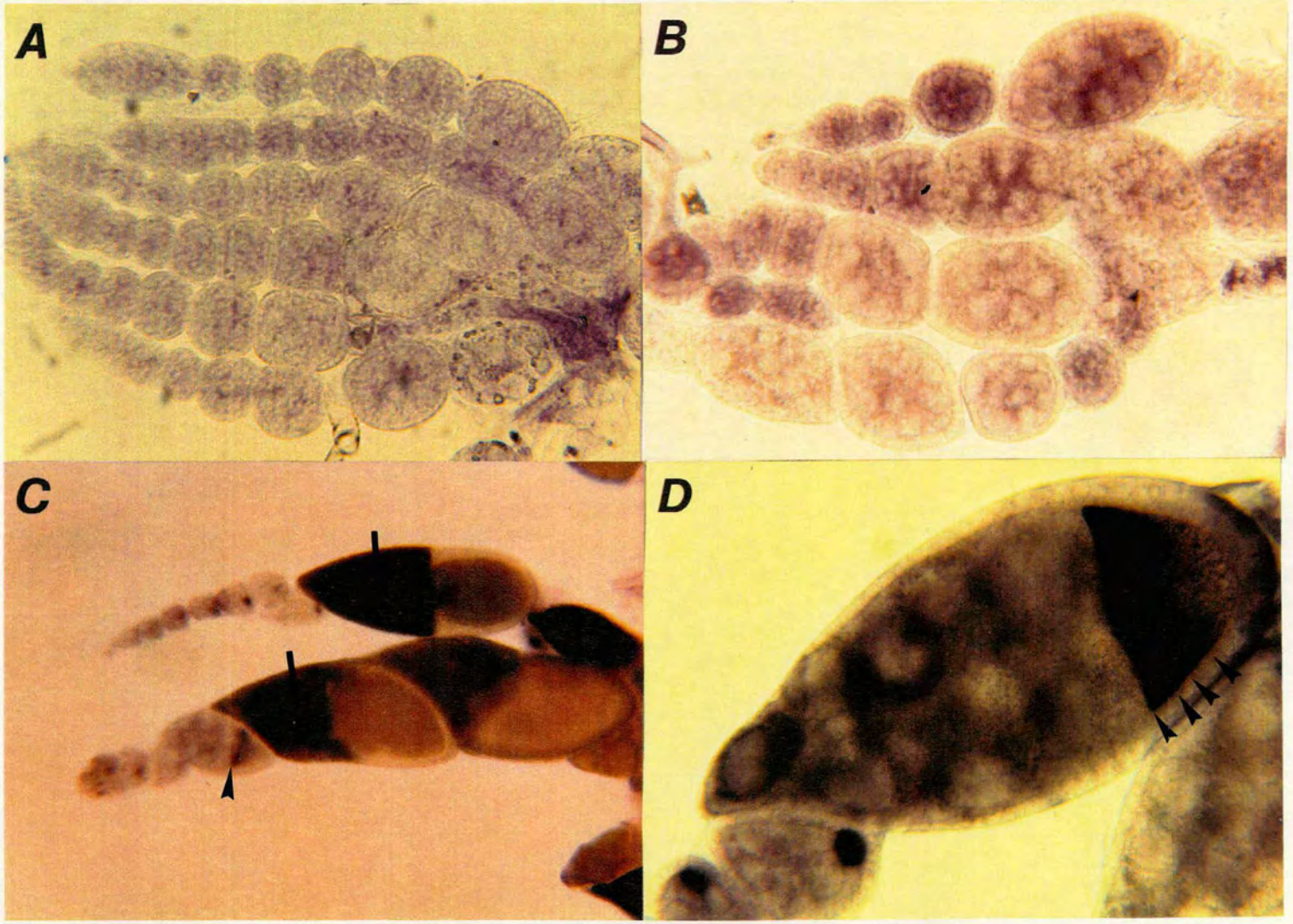
A
B
C
D

role of the Chickadee protein is to anchor the nurse cell nuclei to the microfilaments. Failure of cytoplasmic transfer results in oocytes which are greatly reduced in size and volume. Localisation of the *myosinV* transcript in the ovaries of *chi*^{11} mutants appears to be normal up to the point where the ring canals become blocked. The transcript localises to the oocyte from stage 1 and then to the anterior of the oocyte at stage 8 as in wild type flies, but then becomes backed up in the nurse cells (fig 4.4C). However, it would appear that *chickadee* is not actually required for the correct localisation of the *myosinV* transcript within the oocyte, but only for the transfer of transcript from the nurse cells.

4.2.5 Localisation of *myosinV* transcript in *exuperantia* mutants

The product of the *exuperantia* gene is involved in the correct localisation of the anterior determinant *bicoid*. *exuperantia* is required for the localisation of the *bicoid* transcript to the anterior margin of the oocyte at stages 8-9 and to the apical regions of the nurse cells at stages 9-11. Mutant alleles such as *exu*^{QR} give rise to embryos with anterior region defects as a consequence of failure to correctly localise *bicoid* mRNA. In *exu*^{QR} ovaries the *myosinV* transcript localises early to the oocyte as it does in wild type ovaries. However, at stage 8 the transcript fails to become tightly localised to the anterior cortex and appears instead as a very wide band in the anterior half of the oocyte (fig 4.4D). The transcript is then produced in the nurse cells and transferred into the oocyte as in wild type ovaries. It is only the transient anterior localisation of the *myosinV* transcript which seems to be affected in *exu*^{QR} ovaries, suggesting that *exuperantia* is required for this step of the localisation pattern.

4.2.6 Localisation of *myosinV* transcript in *swallow* mutants

The *swallow* gene is required for the second step of *bicoid* transcript localisation which is accumulation and maintenance of *bicoid* mRNA at the anterior cortex of the

oocyte at stage 10b. Mutations in the *swallow* gene again result in embryos with anterior defects. *swallow* is also required for the correct anterior localisation of the *Adducin-like* transcript. Localisation of the *myosinV* transcript was studied in sww^{99} homozygotes. The pattern of transcript localisation was found to be entirely normal in the ovaries of sww^{99} flies (data not shown). From this result, it would appear that *swallow* is not involved in the localisation of the *myosinV* transcript.

4.2.7 Localisation of *myosinV* transcript in *staufen* mutants

The product of the *staufen* gene is required for the localisation of *bicoid* and *oskar* transcripts to opposite poles of the same egg. Staufen protein is first required at stage 8 for the transport of *oskar* mRNA from its site of transient accumulation at the oocyte anterior, to the oocyte posterior where it defines the position of the pole plasm. Staufen protein is subsequently required for the final step of *bicoid* transcript localisation - its maintenance in the anterior cytoplasm of the mature egg. Defects in the *staufen* gene result in embryos with mild anterior defects, abdominal defects and no pole cells. Localisation of the *myosinV* transcript was found to be entirely normal in the ovaries of $stau^{D3}$ flies indicating that Staufen protein is not required for localisation of the *myosinV* transcript (data not shown).

4.2.8 Localisation of *myosinV* transcript in *orb* mutants

The *orb* gene is required for several different processes during oogenesis. It is first required for oocyte determination, then for the localisation of *gurken* mRNA to the anterio-dorsal corner of the oocyte at stage 9 and subsequently for the localisation of *oskar* mRNA to the oocyte posterior at stage 10. Different alleles of *orb* give rise to different phenotypes, e.g. orb^{F343} is a female sterile allele and orb^{MEL} is maternal effect lethal. *myosinV* transcript localisation was assessed in the ovaries of orb^{MEL} homozygotes and also in orb^{F343}/orb^{MEL} heterozygotes, which are viable but have a

more severe phenotype than *orb*^{MEL} homozygotes. In *orb*^{MEL} homozygotes the early localisation of the *myosinV* transcript to the oocyte is abolished and the transcript does not accumulate in the oocyte until around stages 5-6. At stage 8 the transcript is abundant in the oocyte but is diffuse throughout the oocyte rather than localised to the anterior margin (fig 4.5A). In the ovaries of *orb*^{F343}/*orb*^{MEL} heterozygotes a large number of the egg chambers are only 1/2 - 3/4 of the normal length. This has been previously reported by Christerson and McKearin (1994) and is thought to be due to the incomplete transfer of nurse cell contents into the oocytes. In *orb*^{F343}/*orb*^{MEL} oocytes the *myosinV* transcript localises to the oocyte from around stages 3-4, i.e. earlier than in *orb*^{MEL} homozygotes but later than in wild type. From stage 8 onwards, the *myosinV* transcript is seen as a spot at the posterior end of the egg chamber (fig 4.5B), presumably as a consequence of the failure in oocyte growth. The lack of anterior oocyte localisation in *orb*^{MEL} homozygotes and the failure of early oocyte localisation in both *orb*^{F343}/*orb*^{MEL} heterozygotes and *orb*^{MEL} homozygotes indicates that the *orb* product is normally involved in the correct localisation of the *myosinV* product both to, and within the oocyte.

4.2.9 Localisation of *myosinV* transcript in *gurken* mutants

The *gurken* gene is essential for the establishment of the antero-posterior and dorsoventral axes of the oocyte. *gurken* transcript is localised to the posterior of the oocyte at stages 6-7 where it is translated into protein which signals to the neighbouring follicle cells to become posterior follicle cells. Anterior follicle cells become so by default. By localising to the anterio-dorsal corner at stage 9, *gurken* similarly determines the dorsal follicle cells. Mutations in the *gurken* gene result in ventralised embryos which often have duplicated anteriors. Localisation of the *myosinV* transcript was assessed in the ovaries of *grk*^{WG} and *grk*^{HK} homozygotes and was found to be identical to that of wild type (data not shown). *myosinV* transcript localisation therefore does not appear to require the product of the *gurken* gene.

Figure 4.5 Localisation of the *myosinV* transcript in mutant backgrounds. A) orb^{MEL} - the *myosinV* transcript fails to localise in early egg chambers (arrowheads), does not localise to the oocyte until stage 5/6 and then fails to become localised to the oocyte anterior at stage 8 but instead remains diffuse throughout the oocyte (arrow). B) orb^{F343}/orb^{MEL} - the *myosinV* transcript fails to localise in stage 1-3 oocytes (arrowheads), does not localise to the oocyte until stage 4/5 and then appears as a spot at the posterior of later stage egg chambers (arrows), presumably due to the failure in oocyte growth as a consequence of cytoplasmic transfer failure. C) $capu^{HK}$ - in some ovarioles the *myosinV* transcript appears as a spot at the posterior of the egg chamber (arrow) while other ovarioles appear normal. D) $capu^{HK}$ - the *myosinV* transcript mislocalises to the lateral cortex (arrowheads). E) $capu^{HK}$ - the *myosinV* transcript mislocalises to the posterior cortex (arrowhead).

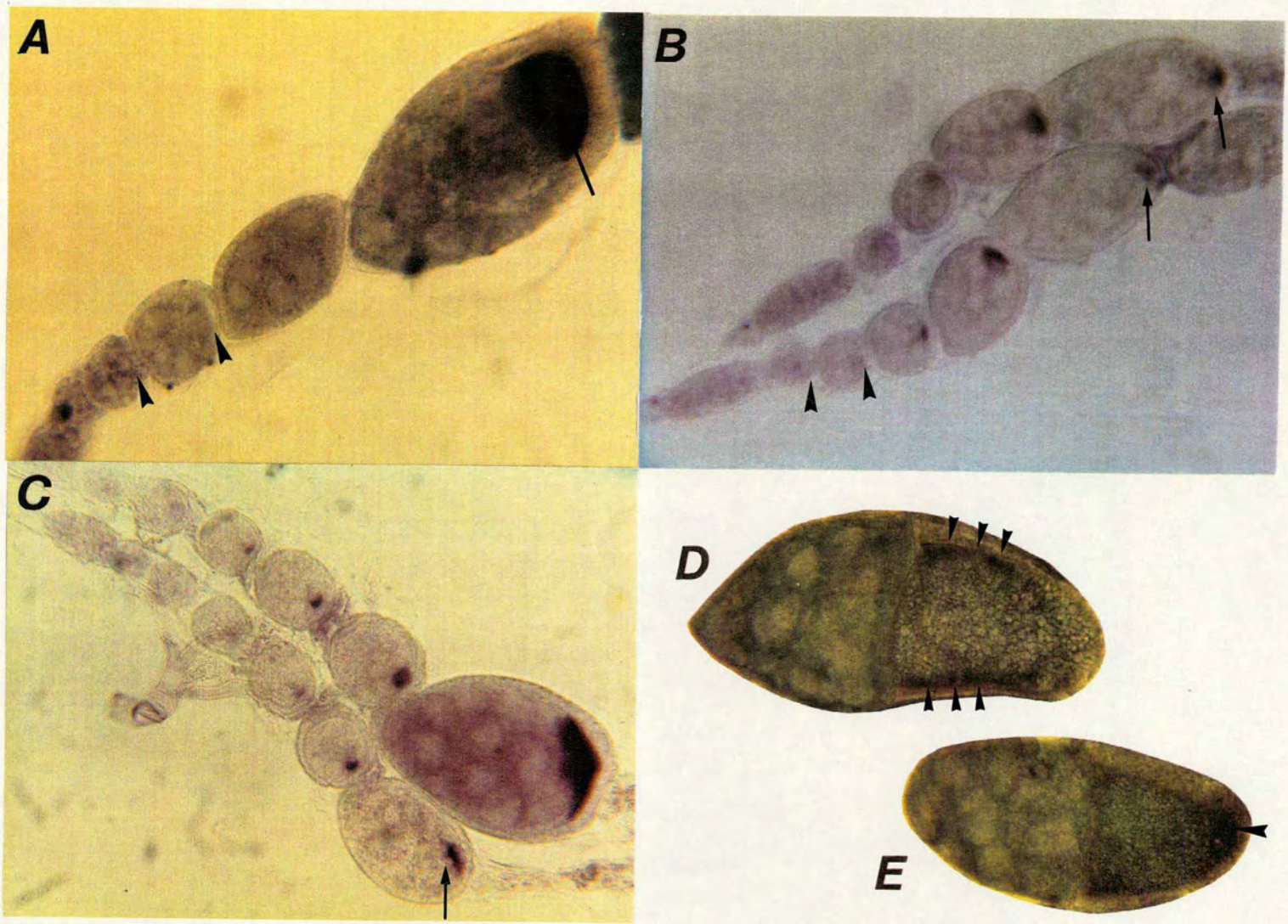
A
B
C
D
E

4.2.10 Localisation of *myosinV* transcript in *fs(1)K10* mutants

The product of the *fs(1)K10* gene is required for the correct localisation of *gurken* mRNA to the anterio-dorsal corner of the oocyte at stage 9. Mutations in *fs(1)K10* result in dorsalisation as a consequence of failure to correctly restrict Gurken activity. Localisation of the *myosinV* transcript to the oocyte was found to be normal throughout all stages of oogenesis in *fs(1)K10* flies (data not shown). It can therefore be concluded that *fs(1)K10* function is not required for the correct localisation of the *myosinV* transcript during oogenesis.

4.2.11 Localisation of *myosinV* transcript in *cappuccino* mutants

The *cappuccino* gene is required for the correct localisation of *gurken* mRNA to the anterio-dorsal corner of the oocyte at stage 9 and the localisation of *oskar* mRNA to the oocyte posterior at stage 10. Embryos from *cappuccino* mutant mothers therefore display abdominal defects and lack pole cells in addition to being dorsalised. Localisation of the *myosinV* transcript was examined in $capu^{HK}$ mutants. A range of transcript localisation patterns was observed in the ovaries of these flies. Early localisation to the oocyte appears to be normal in most cases, however, in a number of mid stage egg chambers the *myosinV* transcript is restricted to a small spot at the posterior of the egg chamber (fig 4.5C). This may reflect a failure in oocyte development but such a phenotype has not previously been described for an allele of *cappuccino*. In some stage 8-10 egg chambers the *myosinV* transcript is localised to the anterior of the oocyte as in wild type, however, in others it is mislocalised along the lateral cortex of the oocyte (fig 4.5D) or to the posterior tip of the oocyte (fig 4.5E). From these results it can be concluded that *cappuccino* function is required for the correct localisation of the *myosinV* transcript, particularly its localisation to the oocyte anterior at stages 8-10.

4.2.12 Localisation of *myosinV* transcript in *spire* mutants

The *spire* gene is also required for the correct localisation of *gurken* and *oskar* transcripts, and mutations give rise to similar phenotypes as those seen in *cappuccino* mutants. *myosinV* transcript localisation was examined in the ovaries of $spir^{339}$ homozygotes. Again, early localisation to the oocyte appears normal, however, at stage 8 the transcript fails to become localised to the anterior cortex but instead is distributed throughout the oocyte (fig 4.6A). It therefore appears that function of the *spire* gene is required for the correct localisation of the *myosinV* transcript within the oocyte.

4.2.13 Localisation of *myosinV* transcript in *oskar* mutants

The product of the *oskar* gene is localised to the posterior of the oocyte where it is required for the correct localisation of the posterior determinant *nanos* and to define the position of pole plasm formation. When *oskar* is absent or defective, flies produce embryos which lack pole cells and have abdominal patterning defects. In the ovaries of osk^{54} flies, localisation of the *myosinV* transcript was found to be identical to that seen in wild type ovaries indicating that *oskar* is not required for *myosinV* transcript localisation (data not shown).

4.2.14 Localisation of *myosinV* transcript in *vasa* mutants

The *vasa* gene is one of several posterior group genes whose function is required for pole cell determination and the localisation of *nanos* mRNA to the posterior of the oocyte. *vasa* mutant mothers produce embryos which have abdominal defects and no pole cells. In the ovaries of $vasa^{PD23}$ homozygous flies, the localisation pattern of the *myosinV* transcript appears to be identical to that of wild type ovaries (data not shown). The product of the *vasa* gene is therefore not required for the correct

localisation of the *myosinV* transcript.

4.2.15 Localisation of *myosinV* transcript in *tudor* mutants

The *tudor* gene is another posterior group gene required for pole cell formation and abdominal patterning. *in situ* hybridisation to the ovaries of tud^{WC8} flies reveals that the *myosinV* transcript localises early to the oocyte, then to the anterior of the oocyte at stage 8-10 as it does in wild type (data not shown). The *tudor* gene therefore appears not to be involved in the localisation pathway of the *myosinV* transcript.

4.2.16 Localisation of *myosinV* transcript in *valois* mutants

valois is another posterior group gene required for both pole cell formation and localisation of *nanos* mRNA. Mutations in *valois* cause similar posterior defects to those seen in *vasa* and *tudor* mutants. The *myosinV* transcript was again found to localise normally in the oocytes of vls^{1} homozygotes (data not shown), indicating that product of the *valois* gene is not involved in the localisation of the *myosinV* transcript.

4.2.17 Localisation of *myosinV* transcript in *Notch* mutants

Notch is a neurogenic gene involved in the determination of primary neuroblast cell fate during neurogenesis. During oogenesis, the *Notch* - *Delta* signal transduction pathway interacts with the *gurken* - *torpedo* signalling pathway which defines the axes of the oocyte. *Notch* is required in the somatic follicle cells for the cell-cell signalling to specify posterior and dorsal follicle cell fate. Loss of *Notch* function in the follicle cells prevents the cell-cell interactions necessary to specify posterior follicle cell fate and results in failure of the follicle cells to signal back to the oocyte to polarise its cytoskeleton. The resulting mirror-symmetric cytoskeleton prevents the localisation

Figure 4.6 Localisation of the *myosinV* transcript in mutant backgrounds. A) *spir*^{399} - the *myosinV* transcript fails to become localised to the anterior cortex at stage 8 but remains diffuse throughout the oocyte as in the stage 9 egg chamber shown (arrow). B) *Notch*^{ts1} - localisation of the *myosinV* transcript is variable but in many cases it mislocalises to one anterior corner of the stage 8/9 oocyte (arrow). C) & D) *Delta*^{6B} - again localisation of the *myosinV* transcript is variable but in many cases the transcript fails to localise to the anterior at stage 8 (arrowheads) and often persists at the oocyte posterior until stage 9/10 (arrows).

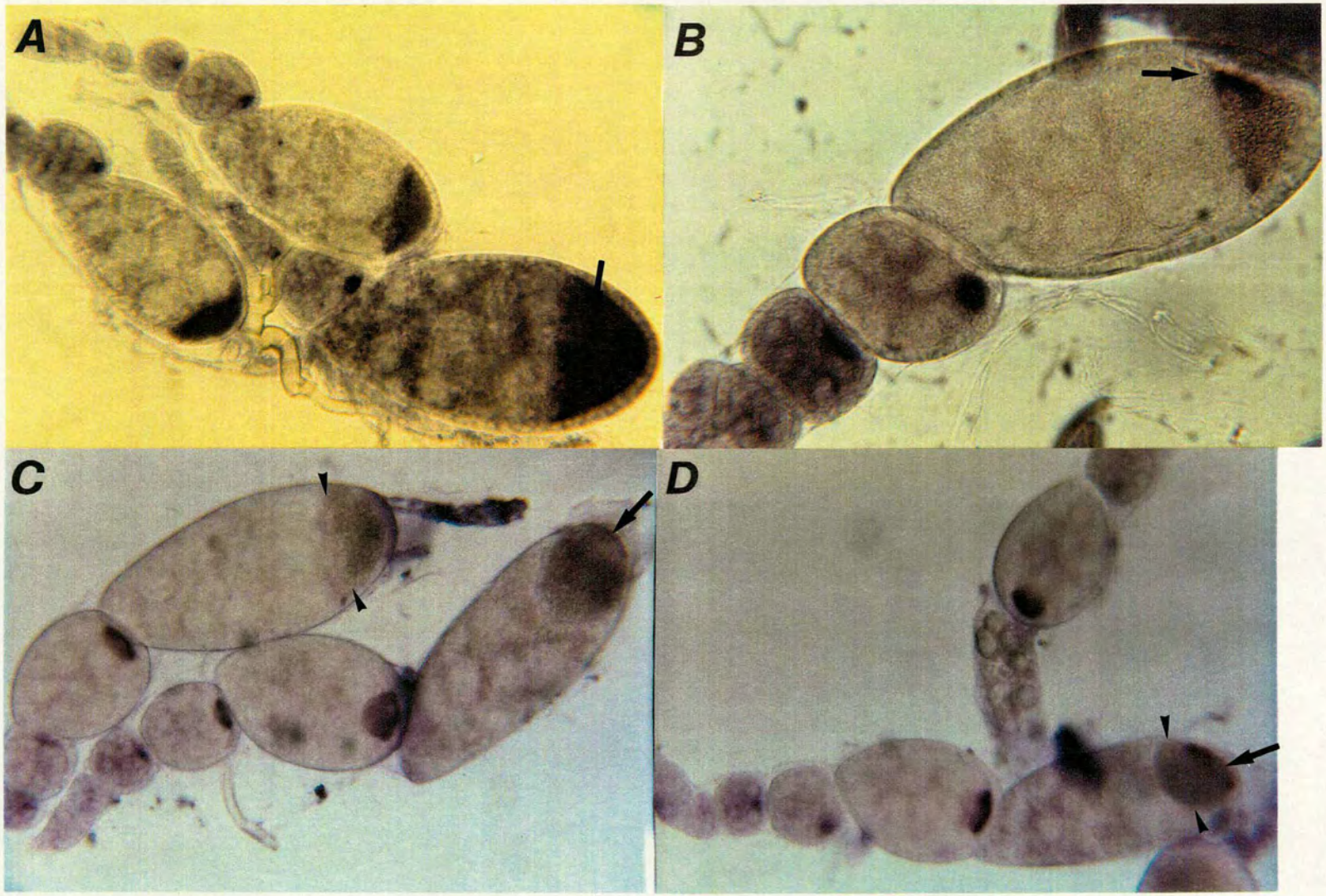
A
B
C
D

of gurken mRNA and the specification of dorsal follicle cell fate. The requirement for *Notch* in the development of the nervous system means that mutations in the gene are lethal so in order to see the maternal effect of loss of *Notch* on oogenesis it is necessary to use a temperature sensitive allele. Such an allele results in a range of defects in oocyte polarity dependent on the length of time spent at the restrictive temperature. Here, N^{ts1} flies were maintained at 25°C then shifted to 31°C for the 24 hours prior to sacrifice for *in situ* hybridisation. The early localisation of the *myosinV* transcript to the oocyte appears to be normal in the ovaries of these flies and in many cases the anterior localisation of the transcript at stage 8 also appears to occur as normal. However, in a significant number of egg chambers the *myosinV* transcript is not localised to the anterior at stage 8 but instead is mislocalised to one anterior corner of the oocyte (fig 4.6B). From this evidence it can be concluded that function of the *Notch* gene is required during oogenesis for the correct localisation of the *myosinV* transcript.

4.2.18 Localisation of *myosinV* transcript in *Delta* mutants

Delta is another neurogenic gene which is also required in the somatic follicle cells during oogenesis where it is involved in the same cell-cell signalling pathway as *Notch*. Again it is necessary to use a temperature sensitive allele to view the effect of loss of *Delta* on oogenesis and the resulting oocyte polarity defects are identical to those seen in *Notch* mutants. *in situ* hybridisation to the *myosinV* transcript was performed on the ovaries of Dl^{6B} flies which had been incubated at 31°C for 24 hours. Again the early stages of localisation to the oocyte appear to be normal in these ovaries. However, at stages 7/8 the *myosinV* transcript appears to be more predominantly localised to the posterior of the oocyte than is the case in wild type flies. Furthermore, the transcript often persists at the posterior until stage 9/10 and fails to localise to the anterior margin of the oocyte (fig 4.6C&D). These results indicate that *Delta* function is required in the follicle cells for the correct localisation of the *myosinV* transcript during oogenesis.

4.3 Summary

The asymmetric localisation of certain maternal transcripts is essential for pattern formation during *Drosophila* development. The localisation of these transcripts often requires the function of several other maternal genes. For example, localisation of the anterior determinant *bicoid* is known to require the function of the *exuperantia*, *swallow* and *staufen* genes, which act in a stepwise fashion to bring about the correct anterior localisation of the *bicoid* transcript (St Johnston *et al*, 1989). Here, an attempt has been made to determine those genes necessary for the correct localisation of the *myosinV* transcript by studying localisation of the transcript in a number of mutant backgrounds. The results indicate that localisation of the *myosinV* transcript requires the function of the *egalitarian, Bicaudal-D, chickadee, exuperantia, orb, cappuccino, spire, Notch* and *Delta* genes, but does not require the functions of the *swallow, staufen, gurken, fs(1)K10, oskar, vasa, tudor*, or *valois* genes. These results are summarised in table 4.2.

The localisation of the *myosinV* transcript was unsurprisingly found to depend upon the oocyte determination genes *egalitarian* and *Bicaudal-D*. When these genes are defective no oocyte is formed, resulting in the formation of 16 cell cysts. The accumulation of *myosinV* transcripts within these cysts serves to indicate that the transcript is normally produced in the nurse cells then transported to the oocyte, as opposed to being uniquely produced in the oocyte itself.

The *chickadee* gene was demonstrated to be required for the bulk transfer of the nurse cell contents, including the *myosinV* transcript, through the ring canals to the oocyte at stage 10b. However, the early localisation of the *myosinV* transcript to the oocyte and anterior localisation at stages 8-10 were found to occur normally in *chickadee* mutant ovaries, indicating that the profilin homologue Chickadee is not required for the specific localisation of the *myosinV* transcript.

Table 4.2 Summary of *myosinV* transcript localisation in mutant backgrounds.

Genotype	Phenotype	Localisation of *myosinV* transcript
OrR	wild type	transcript localises early to the oocyte, then to the oocyte anterior from stages 8-10, then comes on strongly in the nurse cells before being transferred into the oocyte
egl^{WU}	no oocyte/ 16 nurse cells	transcript ubiquitous throughout all 16 nurse cells
$Bic\text{-}D^{7134R}$	no oocyte/ 16 nurse cells	transcript ubiquitous throughout all 16 nurse cells
chi^{11}	failure of cytoplasmic transfer	transcript localises as in wild type until stage 10 when it becomes backed up in nurse cells
exu^{QR}	anterior defects	transcript fails to become tightly localised to the oocyte anterior at stage 8-10 and instead appears as a very broad band in anterior 2/3 of oocyte
sww^{99}	anterior defects	transcript localises as in wild type
$stau^{D3}$	mild anterior defects abdominal defects no pole cells	transcript localises as in wild type
orb^{MEL}	ventralised eggshell abdominal defects	transcript does not localise to the oocyte until stage 5/6 then fails to become localised at the oocyte anterior at stage 8-10 but instead remains diffuse throughout oocyte
grk^{WG} and grk^{HK}	ventralised eggshell AP polarity defects	transcript localises as in wild type
fs(1)K10	dorsalised eggshell	transcript localises as in wild type
$capu^{HK}$	dorsalised eggshell abdominal defects no pole cells	transcript localises early to oocyte then either localises normally to the anterior at stage 8 or mislocalises to the lateral cortex or posterior
$spir^{339}$	dorsalised eggshell abdominal defects no pole cells	transcript localises early to the oocyte then fails to become localised at the anterior at stage 8 but remains diffuse throughout oocyte
osk^{54}	abdominal defects no pole cells	transcript localises as in wild type
$vasa^{PD23}$	abdominal defects no pole cells	transcript localises as in wild type
tud^{WC8}	abdominal defects no pole cells	transcript localises as in wild type
vls^{1}	abdominal defects no pole cells	transcript localises as in wild type
$Notch^{ts1}$	oocyte polarity defects	transcript localises early to oocyte then either localises normally to the anterior at stage 8 or mislocalises to one anterior corner
$Delta^{6B}$	oocyte polarity defects	transcript localises early to the oocyte but fails to become localised at the anterior and often persists at the posterior until stage 9/10

Of the three genes required for anterior localisation of the *bicoid* transcript, only one - *exuperantia* - was found to be also required for the anterior localisation of the *myosinV* transcript. This indicates that although anterior localisation is not brought about by one generalised mechanism, the same genes can be employed for the localisation of different transcripts. Similarly, localisation of the *Adducin-like* transcript to the anterior of the oocyte is known to require *swallow* function but not *exuperantia* function (Ding *et al*, 1993). The failure of the *myosinV* transcript to become tightly localised to the anterior cortex at stage 8-10 in *exuperantia* ovaries is similar to the reported mislocalisation of the *bicoid* transcript as a diffuse anterior band (St Johnstone *et al*, 1989). Exuperantia protein is concentrated at the anterior cortex of the oocyte between stages 8-10 (Wang and Hazelrigg, 1994) and appears to be involved in maintaining the boundaries of both *bicoid* and *myosinV* transcript localisation.

Function of the *orb* gene was found to be required for the correct localisation of the *myosinV* transcript, both to the pre-vitellogenic oocyte and to the anterior cortex of the stage 8-10 oocyte. The *orb* gene encodes a germ-line specific RNA binding protein which is known to be required for mRNA localisation events throughout oogenesis including the localisation of several mRNAs to the pro-oocyte, the localisation of *gurken* mRNA to the anterio-dorsal corner of the oocyte at stage 9 and the localisation of *oskar* mRNA to the posterior at stage 10. The Orb protein has been proposed to be part of a multiprotein complex required for the subcellular localisation of mRNAs and it is therefore unsurprising that it is required for the localisation of the *myosinV* transcript both to and within the oocyte.

Localisation of the *myosinV* transcript was found to depend on the function of the *cappuccino* and *spire* genes. Both these genes are also known to be required for the correct localisation of the *gurken* transcript to the anterio-dorsal corner of the oocyte at stage 9 and for localisation of the *oskar* transcript to the oocyte posterior at stage 10. The mislocalisation of *myosinV* as small spots in *cappuccino* egg chambers seems likely to reflect an arrest in oocyte development rather than mislocalisation within the

oocyte. Failure of the *myosinV* transcript to localise to the oocyte anterior at stages 8-10 in *cappuccino* and *spire* egg chambers may be due to the early onset of cytoplasmic streaming which occurs in these mutants as a consequence of a premature rearrangement of the microtubule cytoskeleton (Theurkauf *et al*, 1994b). The mislocalisation of the *myosinV* transcript to the lateral and posterior cortex in *cappuccino* mutants may be due to the attachment of the *myosinV* transcript to some component of the cortex as it is transported round the egg by cytoplasmic streaming. This lateral and posterior mislocalisation does not appear to occur in *spire* mutant egg chambers but at present the reason for this difference is not clear.

The *myosinV* transcript is mislocalised in *Notch* and *Delta* temperature sensitive mutants which have been kept at the restrictive temperature for 24 hours, indicating that the functions of *Notch* and *Delta* are required for the correct localisation of the *myosinV* transcript. *Notch* and *Delta* are required in the follicle cells for the oocyte-follicle cell signalling which defines the polarity of the oocyte. When Notch or Delta are absent or defective then the follicle cells do not signal back to the oocyte to reorganise its microtubule cytoskeleton. This results in the development of a mirror-symmetric cytoskeleton in which the microtubule plus-ends are in the centre and the minus-ends extend towards both poles. A consequence of this microtubule polarity defect is that transcripts such as *bicoid, orb, fs(1)K10* and *Adducin-like*, which are normally localised to the anterior of the oocyte via an association with minus-end directed microtubule motor proteins, are instead mislocalised to both poles of *Notch* and *Delta* mutants. The *myosinV* transcript, however, is not mislocalised to both poles of *Notch* and *Delta* mutants but is instead mislocalised to one anterior corner of *Notch* mutants and is retained at the posterior pole of *Delta* mutants. It should be noted that *Notch* and *Delta* temperature sensitive mutations are incompletely penetrant and can give rise to a wide range of phenotypes, depending on the time and temperature of incubation. However, in this instance there were no examples at all of *myosinV* transcript mis-localisation to both poles of the oocyte, suggesting that *myosinV* mRNA is not transported along the microtubules like the *bicoid, orb, fs(1)K10* and *Adducin-like* transcripts. This result concurs with the normal

localisation of the *myosinV* transcript in two different *gurken* mutants, because if *myosinV* mRNA was transported along the microtubules then it would be expected to be disrupted in *gurken* mutants which have the same microtubule polarity defects as *Notch* and *Delta* mutants.

The results of *myosinV* transcript localisation in *gurken*, *Notch* and *Delta* mutant backgrounds somewhat contradict the results of chapter 5, where the mis-localisation of the *myosinV* transcript upon exposure to the microtubule depolymerising drug colchicine indicates that intact microtubules are required for *myosinV* transcript localisation. It may be that an intact microtubule cytoskeleton is required for *myosinV* transcript localisation but that the mechanism of localisation is not transport along the microtubules via a minus-end directed microtubule motor protein.

The correct localisation of the *myosinV* transcript requires the functions of the *egalitarian, Bicaudal-D, chickadee, exuperantia, orb, cappuccino, spire, Notch* and *Delta* genes. Of these, the anterior group gene *exuperantia* and the *orb* gene seem to be specifically required for *myosinV* transcript localisation while the other genes would appear to disrupt localisation as a consequence of their affect on egg chamber organisation and polarity. One interesting aspect of the results is that the *myosinV* transcript localises normally in *gurken* mutants and does not behave like the *bicoid, orb, fs(1)K10* and *Adducin-like* transcripts in *Notch* and *Delta* mutants. This would suggest that the localisation of the *myosinV* transcript is not achieved by directed transport along the microtubules. A future possibility to advance the understanding of the role of the *myosinV* gene in oogenesis would be to perform the reciprocal experiments and look at the localisation of e.g. the *bicoid, orb* and *gurken* transcripts in the ovaries of a *myosinV* mutant when one becomes available.

Chapter 5

Mechanisms of Transcript Localisation

5.1 Introduction

It has long been understood that early pattern formation within the *Drosophila* embryo is determined by the asymmetric distribution of maternal transcripts such as *bicoid*, *nanos*, and *gurken*, which are laid down during oogenesis. However, it is only relatively recently that the mechanisms behind mRNA localisation have begun to be elucidated. Any model attempting to explain the mechanisms of transcript localisation should include two features, a signal intrinsic to the mRNA molecule, and the cellular machinery to interact with this signal to direct and maintain localisation. In all cases where the localisation signal has been identified, it has been found to reside in the 3'UTR of the localised transcript. Well characterised examples of 3'UTR localisation signals such as those found in *bicoid*, *nanos* and *oskar* transcripts, are discussed in chapter one (section 1.4).

As the transcript of the *myosinV* gene has a long 3'UTR and is specifically localised during oogenesis, it seems reasonable to postulate that there may be a localisation signal contained within the 3'UTR of the *myosinV* transcript. Indeed, as it appears that localisation signals have a modular basis (Macdonald *et al*, 1993; Kim-Ha *et al*, 1993), there may be several localisation signals within the *myosinV* 3'UTR, e.g. one for early localisation to the oocyte and one for subsequent localisation at the oocyte anterior. In this chapter an attempt is made to determine if the *myosinV* 3'UTR is capable of directing localisation, by fusing it to *lacZ* in a transformation vector and looking at the localisation of the *lacZ/myoV3'UTR* fusion transcript within the ovaries of transformed flies. If the 3'UTR turns out to be responsible for localisation then it may be possible to determine which regions of UTR are important for steps of the localisation pattern, by making deletions of the transformation vector. It may ultimately be possible to identify binding factors necessary to bring about localisation.

The cellular machinery required for transcript localisation would be expected to include cytoskeletal elements such as the microtubules. The microtubules are

important for oocyte determination and establishment of egg chamber polarity, and have been implicated in the localisation of a number of transcripts such as *bicoid* and *oskar* (Theurkauf *et al*, 1992; Clark *et al*, 1994). Here, the importance of the microtubules is tested by looking at the effect of the microtubule depolymerising drug, colchicine, on *myosinV* transcript localisation.

5.2 Results

5.2.1 Construction of Transformation Vector

In order to determine whether the 3'UTR of the *myosinV* transcript directs localisation during oogenesis, it was decided to fuse the 780bp *myosinV* 3'UTR to *lacZ* within a transformation vector and observe whether the *lacZ/myoV3'UTR* transcript is localised in the ovaries of transformed flies. A suitable transformation vector - pAdd3'UTR - was obtained from Kellie Whittaker. This vector had been successfully used to show that the 3'UTR of the *Adducin-like* transcript is responsible for its transcript localisation during oogenesis (K. Whittaker, personal communication). pAdd3'UTR consists of a hsp26-Sgs3 promoter-enhancer fused to 600bp of *lacZ* sequence, followed by the 341bp *Adducin-like* 3'UTR in pCaSpeR-4, a P-element vector with the *white* gene included (fig 5.1). The hsp26-Sgs3 cassette drives expression in the nurse cells (Serano *et al*, 1994), while the *white* gene allows for selection of transformed lines on the basis of eye colour.

The *Adducin-like* transcript is first detectable in the germarium and from stages 2 through 5 of oogenesis the transcript is localised to the oocyte. From stage 6 through 12 the transcript is localised to the anterior margin of the oocyte and becomes more concentrated anterodorsally (Ding *et al*, 1993). In the ovaries of pAdd3'UTR transformed flies, the *lacZ/Add3'UTR* fusion transcript localises to the oocyte in an identical pattern to that of the *Adducin-like* transcript, indicating that the *Adducin-like*

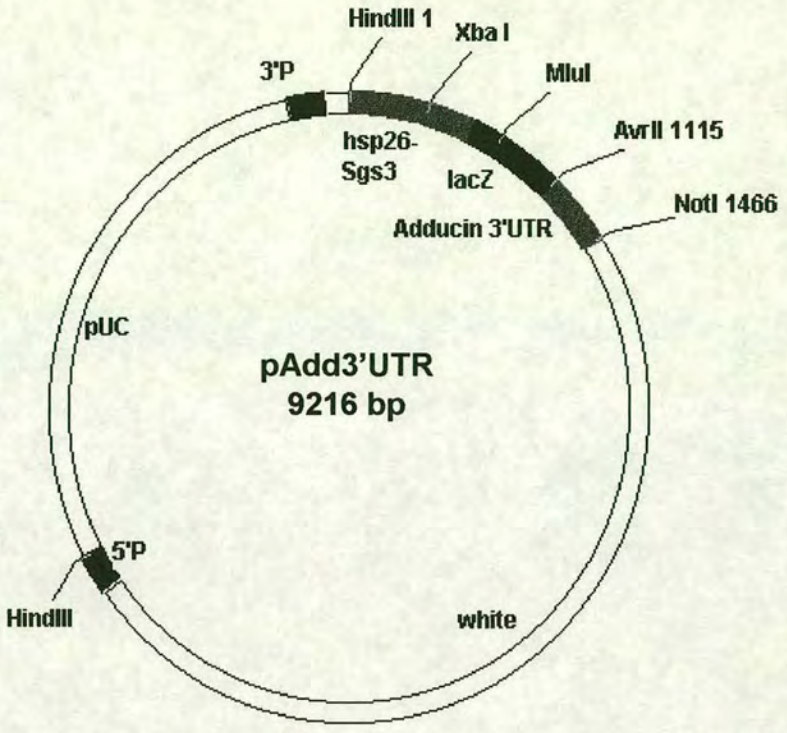

Figure 5.1 P-element transformation vector pAdd3'UTR. The 345bp *Adducin-like* 3'UTR is cloned in at the *Avr*II and *Not*I sites. The vector DNA integrates into the genome via the 5' and 3' P-element ends. The hsp26-Sgs3 promoter-enhancer drives expression in the nurse cells and the *white* gene allows for the selection of transformants on the basis of eye colour.

3'UTR is necessary and sufficient to direct transcript localisation (K. Whittaker, personal communication). By manipulating pAdd3'UTR such that the *Adducin-like* 3'UTR is replaced by the 3'UTR of the *myosinV* transcript, it should be possible to determine whether the *myosinV* 3'UTR is also capable of directing transcript localisation.

The *Adducin-like* 3'UTR was cloned into pAdd3'UTR at unique *Avr*II and *Not*I sites and an initial attempt was made to clone the *myosinV* 3'UTR into these sites by blunt ended ligation, however this proved unsuccessful. A PCR approach was subsequently adopted whereby the *myosinV* 3'UTR was amplified from linearised pNMC7b using primer pair M1706 and N1659. M7106 is a 5' primer designed to incorporate an

*Avr*II site while N1659 is a 3' primer designed to incorporate an *Eag*I site. An *Eag*I digest produces sticky ends compatible with those of a *Not*I digest but is a more desirable site for primer incorporation because it is shorter and requires fewer adjacent bases for successful digestion, significantly reducing the Tm and cost of the primer. The PCR was carried out using high integrity Deep Vent *Taq* polymerase (New England BioLabs), to minimise introduction of errors into the PCR product. The conditions for PCR were 95°C for 3min followed by 30 cycles of 94°C 1min; 48°C 1min; 72°C 1min, followed by a 10 minute extension at 72°C. The purified PCR product was then directionally cloned into pBluescript SK⁻ at the *Sma*I and *Eag*I sites and sequenced to check for PCR introduced errors. Sequencing by the Sanger dideoxy method (2.6.8.1) using the primers shown in fig 5.2 revealed that there were no errors in the PCR product. The *myosinV* 3'UTR PCR product was then subcloned into pAdd3'UTR at the *Avr*II and *Not*I sites, replacing the *Adducin-like* 3'UTR. The resulting transformation vector was named pmyoV3'UTR (fig 5.3). The organisation and orientation of pmyoV3'UTR was shown to be correct by sequencing across the cloning sites using LZ19, a primer for *lacZ* and M4549, a primer for the *white* gene (fig 5.3).

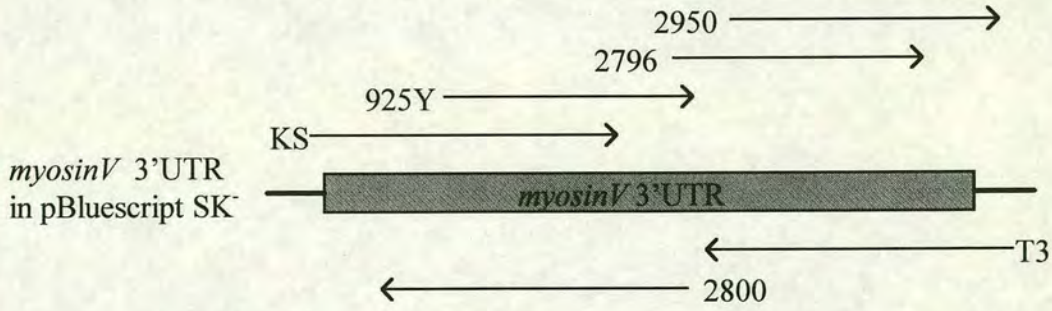

Figure 5.2 Primers used to sequence the *myosinV* 3'UTR cloned into pBluescript. Primer sites KS and T3 are within pBluescript. The primer sites within the *myosinV* 3'UTR are numbered according to an early cDNA clone.

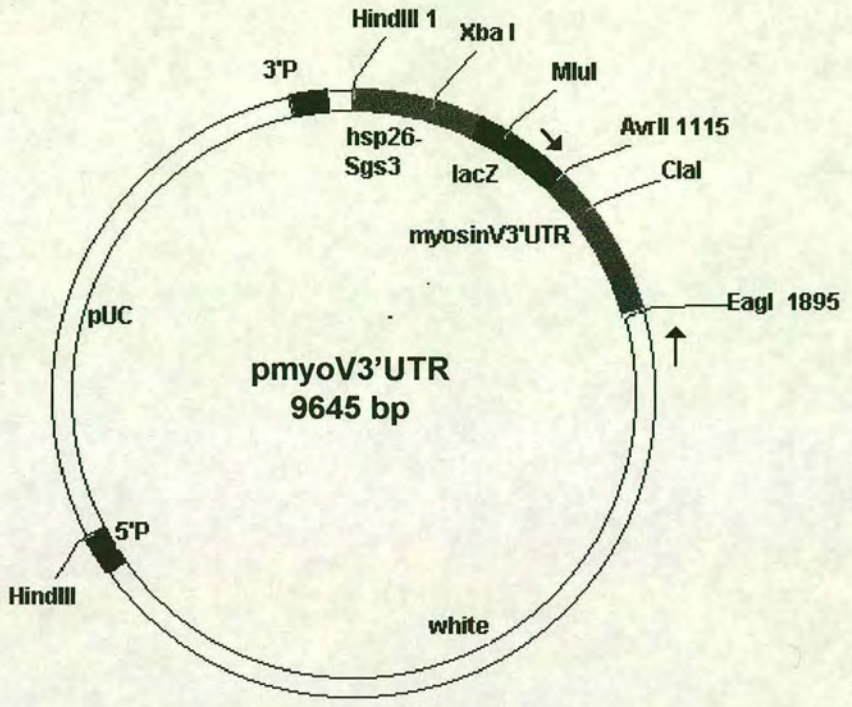

Figure 5.3 P-element transformation pmyoV3'UTR, derived from pAdd3'UTR by replacing the *Adducin-like* 3'UTR with the 780bp *myosinV* 3'UTR. Arrows represent primer sites LZ19 within the *lacZ* sequence and M4549 within the *white* gene. These primers were used to verify the correct insertion of the *myosinV* 3'UTR.

5.2.2 Germline Transformation

The details of germline transformation are described in the materials and methods (2.5). An injection cocktail was prepared by co-precipitating transformation vector pmyoV3'UTR and helper plasmid pΔ2-3 (wings-clipped), then resuspending in injection buffer (2.5.1). pΔ2-3 is a P-element vector which encodes transposase, the enzyme essential for transposition, but has defective P-element ends, so cannot itself transpose. The cocktail was injected into *Wr* embryos. These *Wr* flies lack the *white* gene so have white eyes. Flies developing from injected embryos are crossed to *Wr*, and those flies successfully transformed with pmyoV3'UTR will produce red eyed progeny.

The survival rates and transformation rates obtained using this system of germline transformation were disappointing. Typically, from around 600 injected embryos only 60-90 would survive to adult flies, a survival rate of only 10-15% which is considerably lower than the expected survival rate of 50-80%. On the first two attempts at microinjection no transformants were found among the surviving flies compared to the expected rate of 5% of survivors transformed. However on the third attempt one transformed line was recovered and was named mV0. It has subsequently been discovered in the lab that using caesium chloride to prepare the DNA for injection dramatically increases both survival and transformation frequencies (Debiao Zhao, personal communication).

5.2.3 DNA *in situ* hybridisation to *lacZ/myoV3'UTR* transcript

To determine whether the *lacZ/myoV3'UTR* transcript was localised in the ovaries of transformed mV0 flies, *in situ* hybridisation was performed using a digoxigenin labelled *lacZ* DNA probe (2.3.1). Two different fragments of *lacZ* were used to make probes, a 335bp *Mlu*I/*Avr*II fragment from pAdd3'UTR (fig 5.1) and a 2kb *Sac*I fragment from pGEM-lacZ (fig 5.4). Both these fragments include part of the *lacZ* sequence found in pmyoV3'UTR. No localised transcript was detectable using either of the *lacZ* probes, however it was difficult to determine whether the transcript was absent from the ovaries of transformed flies, or if it was indeed present but not localised within the ovaries.

5.2.4 Creation of new transformants by P-hopping

Failure to see a localised *lacZ/myoV3'UTR* transcript in mV0 flies could be due to failure of transcription from the inserted P-element pmyoV3'UTR. This could happen if the P-element has inserted into an area of the genome which is not transcribed i.e. heterochromatin, in a phenomenon known as position effect. This would seem

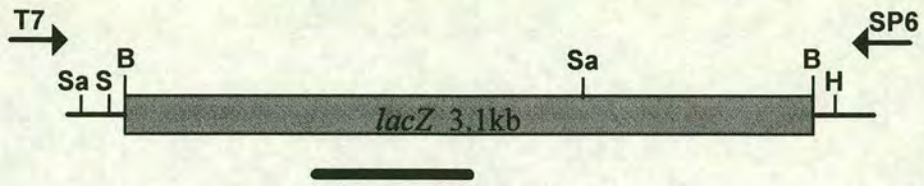

Figure 5.4 pGEM-lacZ. *lacZ* cloned into pGEM-1 as a 3.1kb *Bam*HI fragment. The 2kb *Sac*I fragment was used to make DNA probes. The T7 and SP6 polymerase sites were used for the transcription of *lacZ* RNA probes. The bar represents the fragment of *lacZ* cloned into pAdd3'UTR and pmyoV3'UTR. Sa: *Sac*I, S: *Sma*I, B: *Bam*HI, H: *Hind*III.

unlikely in the case of mV0 flies as their red eye colour indicates that the *white* gene is being transcribed. However, in order to overcome this problem with germline transformation, it is usual to look at several transformed lines which presumably have P-element insertions at different points in the genome. As only one transformed line had been created by germline transformation, and as transformation efficiency was too low to consider making more transformants in this way, it was decided to create more transformed lines by hopping the P-element around the genome. This was achieved by crossing the original transformed line mV0 to Δ2-3 flies, a line of flies which carries the Δ2-3 (wings-clipped) P-element. The transposase provided by the Δ2-3 flies allows the pmyoV3'UTR element to hop around the genome for one generation only and then the transformation is stable. The details of the cross are described in figure 5.5. Around 50 lines were generated in this way.

5.2.5 Screening for new lines

The P-hop lines generated by the mV0 X Δ2-3 cross were screened for new P-element insertion sites by digesting the genomic DNA with *Cla*I and hybridising the Southern blots with a *lacZ* probe. *Cla*I cuts the inserted P-element within the *myosinV* 3'UTR (fig 5.3) and so the size of the *Cla*I fragment containing the *lacZ*

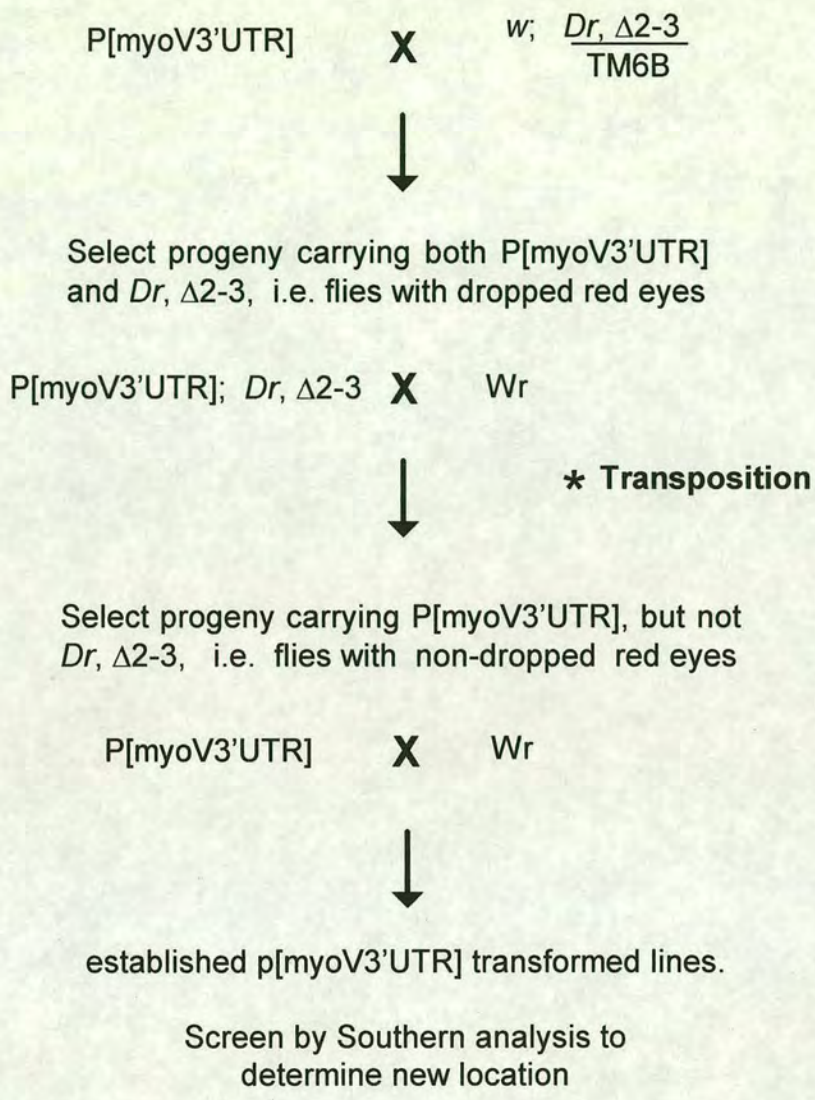

Figure 5.5 Strategy for the generation of new transformed lines by local hopping of the P-element P[myoV3'UTR]. Red eyed flies carrying P[myoV3'UTR] are crossed to white eyed flies carrying Δ2-3. The Δ2-3 P-element encodes the transposase enzyme but has defective P-element ends, so cannot itself transpose. Transposition can occur when a genome carrying both P-elements undergoes meiosis, i.e. when the P[myoV3'UTR]; Dr, Δ2-3 flies are crossed to Wr flies. Wr flies are used so that the progress of P[myoV3'UTR] can be followed by scoring for red eyed flies in a white eyed background. Following transposition, flies carrying *Dr*, Δ2-3 (i.e. flies with dropped eyes) are discarded so that no further transpositions can take place and P-elements are stable in their new location. Single flies carrying P[myoV3'UTR] are then crossed to Wr flies to generate transformed lines. To maintain transformed lines, red eyed progeny must be selected for in subsequent generations. *w*: *white*, Dr: *Drop*, TM6B: balancer.

sequence will depend on where the next upstream *Cla*I site is in the flanking genomic DNA. Different insertion sites should therefore result in different sized *Cla*I fragments hybridising to the *lacZ* probe. Genomic DNA was prepared from the first 18 lines (2.6.1.1) and digested to completion with *Cla*I. The genomic DNA digests were run out on 0.8% agarose gels in 1X TAE buffer then Southern blotted onto Hybond-N^+ membranes (2.9.1.1). The membranes were hybridised with a ^{32}P labelled *lacZ* probe made from the 2kb *Sac*I fragment of pGEM-lacZ (2.9.3). The resulting autoradiographs are shown in figure 5.6.

The autorads reveal that the original transformed line mV0, actually contains two P-element insertions. This can be seen as *Cla*I fragments of 3kb and 3.4kb hybridising to the *lacZ* probe. The large band at ~10kb band is probably due to incomplete digestion of the genomic DNA and appears to be associated with the P-element insertion site which gives rise to the 3kb *Cla*I fragment. Incomplete digestion is a typical feature of *Cla*I digests. In the course of the P-hop cross, the two P-elements in the original transformed line have recombined apart giving several lines containing only one P-element, e.g. mV9 has only the 3.4kb *lacZ* containing fragment whereas mV11 has only the 3kb *lacZ* containing fragment (fig 5.6).

The autorads also reveal that several of the P-hop lines have new, different sized *Cla*I fragments hybridising to the *lacZ* probe, e.g. line mV4 has the 3kb band plus a new 1.6kb band, while line mV8 has the 3.4kb band plus a new 5.5kb band (fig 5.6). These new *Cla*I fragments indicate that the P-elements have successfully hopped to new sites in the genome within these lines.

5.2.6 DNA *in situ* hybridisation on new transformed lines

DNA *in situ* hybridisations were performed on ovaries from lines mV0, mV4, mV8, mV9 and mV11 using a digoxigenin labelled *lacZ* DNA probe made from the 2kb *Sac*I fragment of pGEM-lacZ. Again, neither the presence nor the localisation of

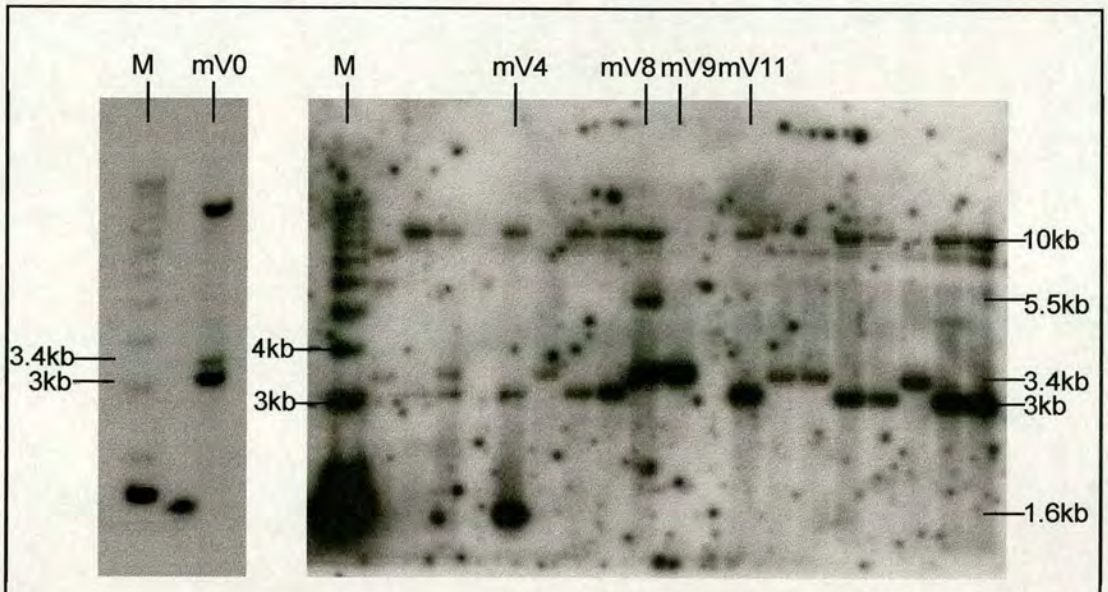

Figure 5.6 Southern blots of *Cla*I digested genomic DNA from transformed line mV0 and P-hop lines mV1-mV18. Blots were probed with 2kb *Sac*I fragment of pGEM-lacZ. Line mV0 has two inserted P-elements with the *lacZ* probe hybridising to *Cla*I fragments of 3kb and 3.4kb. The two P-elements have recombined apart in the course of the P-hop cross e.g. line mV9 has lost the 3kb band and retains the 3.4kb band while line mV11 has lost the 3.4kb band and retains the 3kb band. In several lines a P-element has hopped to a new position e.g. line mV4 has the 3kb band plus a new 1.6kb band while line mV8 has the 3.4kb band plus a new 5.5kb band. The 10kb band appears to be due to un-digested genomic DNA associated with the P-element insert which gives rise to the 3kb *Cla*I fragment. M: DNA markers.

the *lacZ/myoV3'UTR* transcript was evident. This was despite a longer period of prehybridisation of the ovaries before addition of the probe, and longer pre-absorption of the anti-DIG antibody

Consideration of the lines mV0, mV4, mV8, mV9 and mV11, which have P-element insertions at four different sites, should normally be sufficient to cover the possibility of position effect. However, in the absence of a positive *in situ* hybridisation result, it was necessary to show that the pmyoV3'UTR DNA is actually being transcribed within the transformed flies by means of RT-PCR.

5.2.7 RT-PCR to detect the *lacZ/myoV3'UTR* transcript

With the failure to detect the *lacZ/myoV3'UTR* transcript by *in situ* hybridisation, it was decided to adopt an RT-PCR approach. RT-PCR involves the reverse transcription of RNA into first strand cDNA, followed by PCR with gene specific primers. If a gene specific product can be amplified from the first strand cDNA, then the gene transcript must have been present in the RNA pool. Total RNA was prepared from the ovaries of mV0, mV9 and OrR flies using the Trizol method (2.7.2.1). The RNA was then reverse transcribed using primer N1659, a primer to the most 3' end of the *myosinV* 3'UTR, designed for the PCR cloning of the 3'UTR. PCR was then performed on the first strand cDNA using primers N1659 and LZ19, a primer for *lacZ* (see fig 5.3). These two primers should amplify a ~800bp product specific to the *lacZ/myoV3'UTR* first strand cDNA. Controls used in this experiment included using primer pair N1659 & 1806, which should amplify a product of 1.4kb from the first strand cDNA reverse transcribed from the intrinsic *myosinV* transcript. The PCR was hot started, followed by 30 cycles of 94°C 15sec; 50°C 15sec; 72°C 1min, followed by a 10 minute extension at 72°C. An additional control was included to check for genomic DNA contamination of the RNA preps. If there is genomic DNA present in the RNA prep then the primers could prime from genomic DNA rather than from the first strand cDNA, potentially giving a false positive result. The PCR product from genomic DNA will be the same size as the product from the first strand cDNA because there are of course no introns in the integrated P-element pmyoV3'UTR. To address this problem, two reverse transcription reactions were set up for each RNA prep but one contained no reverse transcriptase enzyme. If the primers can prime from this control reaction mix, which contains no first strand cDNA, then the prep must be contaminated with genomic DNA and the results from the genuine enzyme containing reaction mix must be disregarded.

Initial PCR reactions on mV0 genuine and control first strand cDNA preps indicated that there was indeed a problem with genomic DNA contamination. Figure 5.7 shows that it was possible to obtain products from both genuine and control first strand

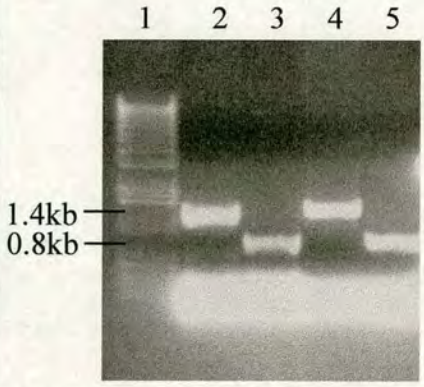

lane

1	markers
2	mV0 cDNA + N1659 & 1806
3	mV0 cDNA + N1659 & LZ19
4	mV0 control + N1659 & 1806
5	mV0 control + N1659 & LZ19

Figure 5.7 RT-PCR on genuine and control mV0 first strand cDNA. Control reactions were prepared from RNA without reverse transcriptase enzyme and therefore contain no cDNA. Primers N1659 & LZ19 amplify a 0.8kb product from both the genuine and the control prep. Primers N1659 & 1806 amplify a 1.4kb product from both the genuine and the control prep. Amplification from the control prep indicates the presence of contaminating genomic DNA and the results from the genuine prep must therefore be disregarded. The large smear at the bottom of the gel is due to RNA which has not been reverse transcribed.

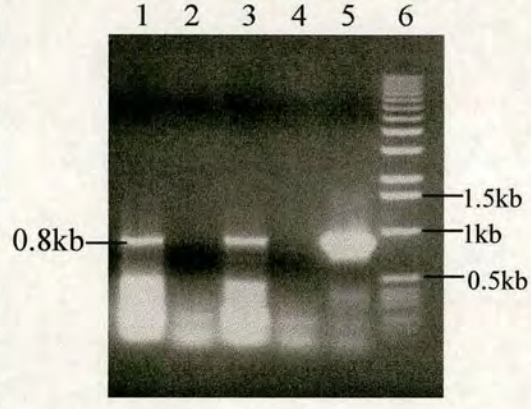

lane

1	mV0 cDNA + N1659 & LZ19
2	mV0 control + N1659 & LZ19
3	mV9 cDNA + N1659 & LZ19
4	mV9 control + N1659 & LZ19
5	pmyoV3'UTR + N1659 & LZ19
6	markers

Figure 5.8 RT-PCR to confirm transcription of *lacZ/myoV3'UTR* in transformed lines mV0 and mV9. All RNA preps were treated with RNase-free DNaseI prior to reverse transcription to remove genomic DNA contamination. Control reactions were prepared from RNA without reverse transcriptase enzyme and therefore contain no cDNA. The 0.8kb *lacZ/myoV3'UTR* specific PCR product can be amplified from mV0 and mV9 first strand cDNA but not from control reactions, indicating that amplification is from cDNA and not from contaminating genomic DNA. This result confirms that *lacZ/myoV3'UTR* is being transcribed in mV0 and mV9 transformed lines. The pmyoV3'UTR vector template was included as a positive control.

cDNA preps using two different sets of primers, N1659 & LZ19 and N1659 & 1806. N1659 & 1806 amplify the expected product of 1.4kb and N1659 & LZ19 amplify the expected 0.8kb product. However, the ability of both sets of primers to also amplify products from the control reactions indicates the presence of contaminating genomic DNA which renders the results from the genuine preps invalid. It was therefore necessary to remove genomic DNA contamination from subsequent RT-PCR reactions. This was achieved by treating the RNA preps with RNase-free DNaseI (Boehringer Mannheim) prior to reverse transcription (2.7.4.2).

Further PCR reaction were carried out on mV0 and mV9 first strand cDNA preps which were free from genomic contamination. Again primers N1659 and LZ19 were used with genuine and control first strand cDNA reactions as templates. Figure 5.8 show that, while there is no longer any PCR product from the mV0 and mV9 control templates, the genuine mV0 and mV9 templates still give the *lacZ/myoV3'UTR* specific ~0.8kb product. This indicates that integrated pmyoV3'UTR is transcribed and so the *lacZ/myoV3'UTR* transcript is indeed present in transformed flies.

5.2.8 RNA *in situ* hybridisation to *lacZ/myoV3'UTR* transcript

It was now clear that pmyoV3'UTR is being transcribed in transformed flies but localisation of the *lacZ/myoV3'UTR* transcript was yet to be demonstrated. In order to claim that the transcript is not localised during oogenesis it is necessary to show that the *in situ* hybridisation technique is capable of detecting *lacZ* fusion transcripts during oogenesis. As previously mentioned, the pmyoV3'UTR vector was based on transformation vector pAdd3'UTR which had successfully been used to show that the 3'UTR of the *Adducin-like* transcript is responsible for transcript localisation during oogenesis (K. Whittaker, personal communication). Advice was sought from K. Whittaker on *in situ* hybridisation techniques, and pAdd3'UTR transformed flies were obtained to use as positive controls for *lacZ* fusion transcript localisation. It was advised that, in order to demonstrate the localisation of the *lacZ/Add3'UTR* transcript,

it had been necessary to perform *in situ* hybridisation using RNA probes. RNA probes offer a number of advantages over DNA probes. Two single stranded RNA probes, a sense strand and an antisense strand, can be transcribed from plasmid DNA using suitable polymerase sites in the plasmid. The antisense strand will hybridise to the target transcript with a higher specific activity than a double stranded DNA probe and is therefore more sensitive. The sense strand will not hybridise to the transcript and can be used as a control probe.

A digoxigenin labelled antisense *lacZ* probes was transcribed from pGEM-lacZ using SP6 RNA polymerase and a control sense probe was transcribed using T7 polymerase (2.3.7) (see fig 5.4). The probes were then used for *in situ* hybridisation on ovaries from mV0, mV9, pAdd3'UTR and OrR flies as described in the materials and methods (2.3.2), with appropriate precautions taken for manipulations with RNA. Using the antisense *lacZ* probe, oocyte localisation of the *lacZ/Add3'UTR* transcript could be detected in pAdd3'UTR ovaries after only 30 minutes of staining in the detection buffer (fig 5.9). In contrast, no localisation could be seen in the ovaries of mV0 and mV9 flies, even after prolonged incubation in detection buffer. No localisation was detected in *OrR* ovaries using the antisense probe, or in any ovaries probed with the control sense probe. However, careful comparison of antisense probed mV0 and mV9 ovaries with background staining in control ovaries, revealed that the *lacZ/myoV3'UTR* transcript is present in mV0 and mV9 ovaries but remains diffuse throughout the nurse cells and oocyte, failing to become localised in the characteristic *myosinV* transcript localisation pattern. It would therefore appear that the *myosinV* 3'UTR is not capable of directing the localisation of the *lacZ/myoV3'UTR* fusion transcript.

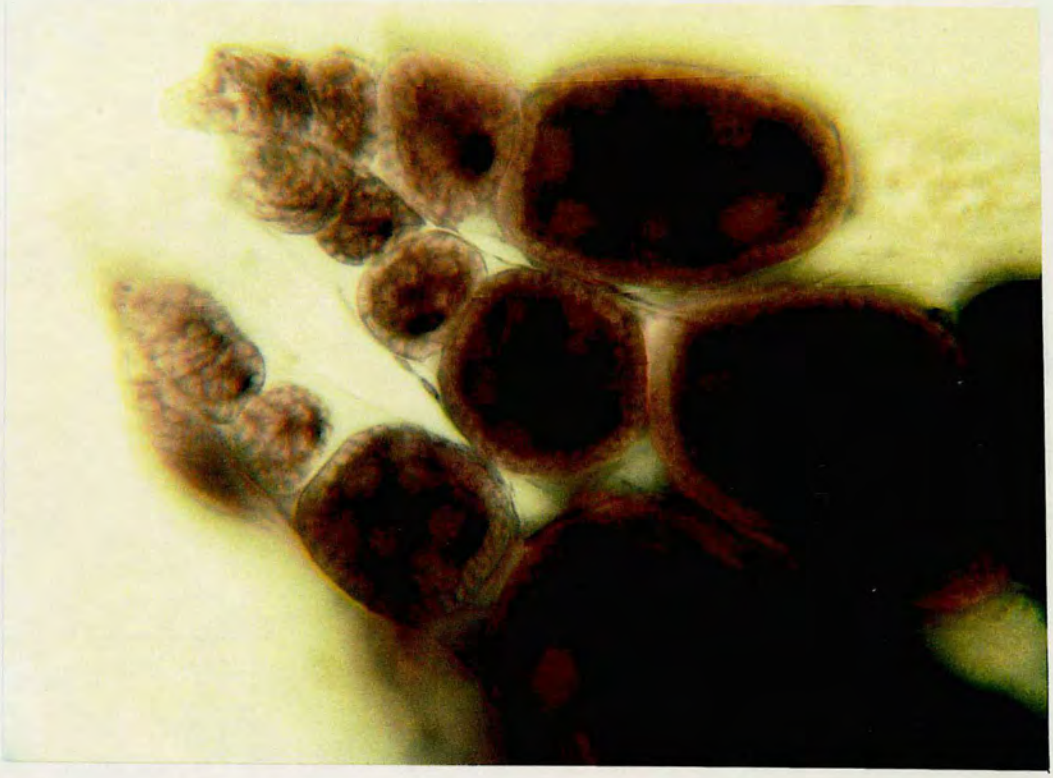

Figure 5.9 Localisation of the *lacZ/Add3'UTR* transcript in the ovaries of pAdd3'UTR flies. pAdd3'UTR ovaries were probed with an antisense *lacZ* RNA probe, transcribed from pGEM-lacZ using SP6 polymerase. *The lacZ/Add3'UTR* transcript is localised to the oocyte in an identical pattern to that of *the Adducin-like* transcript, indicating that the *Adducin-like* 3'UTR is capable of directing transcript localisation. In contrast, no localisation of the *lacZ/myoV3'UTR* transcript was detected when the ovaries of pmyoV3'UTR transformed flies were probed with the same *lacZ* RNA probe.

5.2.9 Role of the microtubules in *myosinV* transcript localisation

In order to establish whether the microtubules play a role in normal localisation of the *myosinV* transcript, it was decided to look at transcript localisation in ovaries treated with the microtubule depolymerising drug colchicine. This was achieved by feeding flies on yeast paste containing colchicine before removing their ovaries for *in situ* hybridisation with a digoxigenin labelled *myosinV* probe. The colchicine was prepared at 5mg/ml in ethanol, diluted to 100μg/ml in water, then used to prepare yeast paste. To examine the progressive effects of microtubule depolymerisation on different stage egg chambers, the flies were exposed to the colchicine for 0, 12, 18 and 24 hours. Prior to colchicine exposure, flies were starved overnight in agarose starvation vials so as to temporarily halt oogenesis and to ensure they would eat the colchicine laced yeast paste. Flies were transferred to the colchicine containing vials at time intervals such that the flies would all be ready for sacrifice at the same time.

Disruption to localisation of the *myosinV* transcript was assessed by *in situ* hybridisation with a 0.8kb *myosinV* probe (2.3.1). The results are shown in figure 5.10. In flies fed colchicine for zero hours, the normal, wild type localisation pattern of the *myosinV* transcript is observed. The transcript localises to the oocyte from within the germarium then, at stage eight, becomes localised as a band at the anterior of the oocyte. At stage 10 much transcript is produced in the nurse cells and subsequently transferred to the oocyte such that anterior localisation is lost. After 12 hours of colchicine exposure the transcript is no longer localised to the oocyte in stage 1 and 2 egg chambers, but is still localised in later stages. However, there is only a faint trace of transcript accumulation at the anterior of stage 8/9 oocytes. After 18 hours of colchicine treatment, the *myosinV* transcript appears to be diffuse throughout all stage egg chambers, with only a few spots of localised staining remaining. After 24 hours of colchicine treatment, it is clear that while the *myosinV* transcript is still being produced, it is completely failing to localise. It is also apparent from figure 5.10 that the general morphology of later stage egg chambers remains intact, even after 24 hours of colchicine treatment, although oocyte differentiation

Figure 5.10 Localisation of the *myosinV* transcript with increasing exposure to colchicine. At 0 hours colchicine treatment the *myosinV* transcript is localised to the oocyte from stage 1 (arrows), is localised to the anterior margin of the oocyte from stages 8-10 (arrowheads), then is expressed strongly in the nurse cells at stage 10 and is subsequently transferred in the oocyte. After 12 hours treatment the *myosinV* transcript is no longer localised to the oocyte in stage 1 and 2 egg chambers (arrows) and there is only a faint trace of transcript accumulation at the anterior of the stage 8/9 oocyte (arrowheads). After 18 hours the transcript is diffuse throughout all stage egg chambers with only a few spots of localised transcript in the later stages. After 24 hours of colchicine treatment, it is clear that the *myosinV* transcript is still being produced but is completely failing to localise, although the overall morphology of later stage egg chambers appears to remain intact. Anterior is to the left.

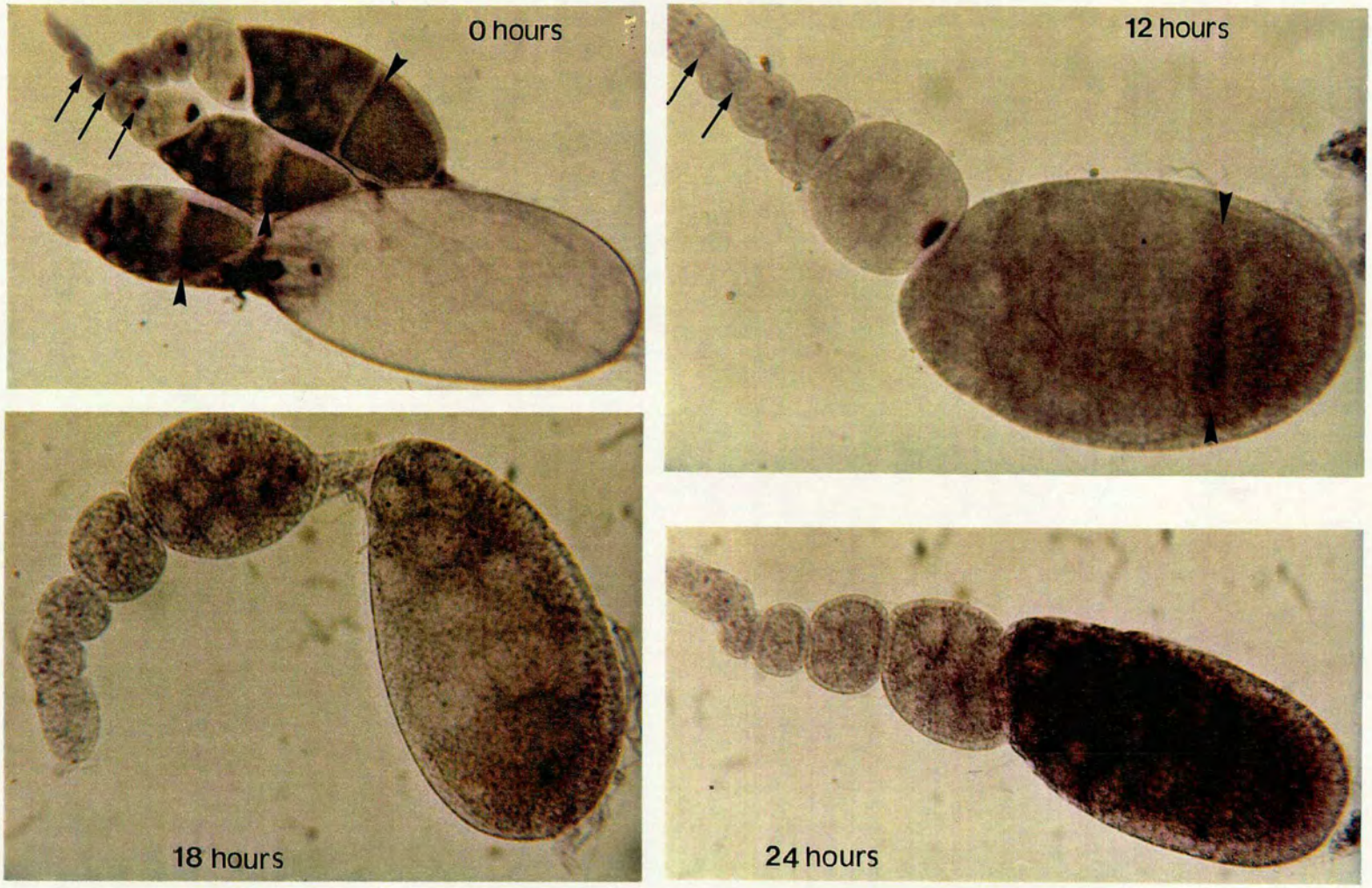
0 hours
12 hours
18 hours
24 hours

may have failed in egg chambers which have developed since the onset of colchicine treatment. The deterioration of *myosinV* transcript localisation, on increasing exposure to the microtubule depolymerising drug colchicine, strongly suggests that the microtubules are part of the cellular machinery required to localise the *myosinV* transcript during oogenesis.

5.3 Summary

Pattern formation in the *Drosophila* egg and embryo has been shown to depend on the asymmetric distribution of maternal transcripts laid down during oogenesis. Where the signal for transcript localisation has been identified, it has been found to reside within the 3'UTR of the transcript itself. Here, the 3'UTR of the *myosinV* transcript has been tested for its ability to direct transcript localisation. This was achieved by fusing the *myosinV* 3'UTR onto *lacZ* within the P-element transformation vector pmyoV3'UTR then assessing the localisation of fusion transcript *lacZ/myoV3'UTR* within the ovaries of transformed flies.

Repeated attempts at germline transformation resulted in the generation of only one line transformed with pmyoV3'UTR, however several independent lines were subsequently created by allowing the P-element to hop around the genome. Standard *in situ* hybridisation with a *lacZ* DNA probe failed to detect localisation of the *lacZ/myoV3'UTR* fusion transcript. RT-PCR was therefore employed to confirm that the transcript was actually present within the ovaries of transformed flies. *in situ* hybridisation with more sensitive RNA probes detected *lacZ* transcript localisation within the ovaries of control flies transformed with pAdd3'UTR, but not within the ovaries of flies transformed with pmyoV3'UTR. It therefore appears that the 3'UTR of the *myosinV* transcript is not capable of directing transcript localisation.

To determine whether the microtubules are involved in localisation of the *myosinV* transcript, localisation was assessed after exposure to the microtubule depolymerising drug colchicine. The results showed that *myosinV* transcript localisation deteriorated with increasing length of exposure to colchicine. This effect of colchicine suggests that the microtubules are an important part of the cellular machinery required to localise the *myosinV* transcript. It should be noted that these results somewhat contradict the results of Chapter 4, where the *myosinV* transcript was found to localise normally in flies carrying mutations known to disrupt the organisation of the microtubule cytoskeleton. The functions of the *gurken*, *Notch* and *Delta* genes are known to be required for the stage 7/8 reorganisation of the microtubules into a polarised array in which their minus ends are anchored at the oocyte's anterior and their plus ends extend towards the posterior pole. In *gurken*, *Notch* and *Delta* mutant ovaries, the microtubules instead form a mirror-symmetric cytoskeleton in which their plus ends are in the centre of the oocyte and their minus ends extend towards both poles. In these mutants, transcripts such as *bicoid* and *Adducin-like*, which are normally localised to the minus ends of microtubules at the oocytes anterior, are instead localised to both poles, and transcripts such as *oskar* which normally localise to the plus end of microtubules at the oocytes posterior, are instead localised to the centre of the oocyte. However, the *myosinV* transcript was found to localise normally in *gurken* mutants, and was not mislocalised to both poles of *Notch* and *Delta* mutants as would be expected if it was transported towards the minus ends of microtubules. It would therefore appear that intact microtubules are required for *myosinV* transcript localisation, but that the mechanism of localisation is not directed transport of *myosinV* towards the microtubule minus ends.

Chapter 6

Screens for the *myosinV* gene and other genes identified in the process

6.1 Introduction

The full length *myosinV* ovarian transcript has been shown by Northern analysis to be around 6kb, however at the outset of this project only a total of 3kb of *myosinV* cDNA had been isolated. This comprised NMC7, the original 1.6kb cDNA isolated from a whole body library by Roger Slee, and a 2.2kb cDNA from a λZAP ovarian library isolated by Bryce MacIver. These two cDNAs contain the 3' region of the gene and their relationship is shown in figure 6.1. The efforts to isolate the 5' region of the *myosinV* gene encountered considerable technical problems and several different libraries were screened in the process. In the course of these screens, two previously uncharacterised *Drosophila* genes were identified. These two new genes and the screening strategy that led to their isolation are the subject of this chapter. Some of the work in this chapter was performed in collaboration with Bryce MacIver as indicated in the text.

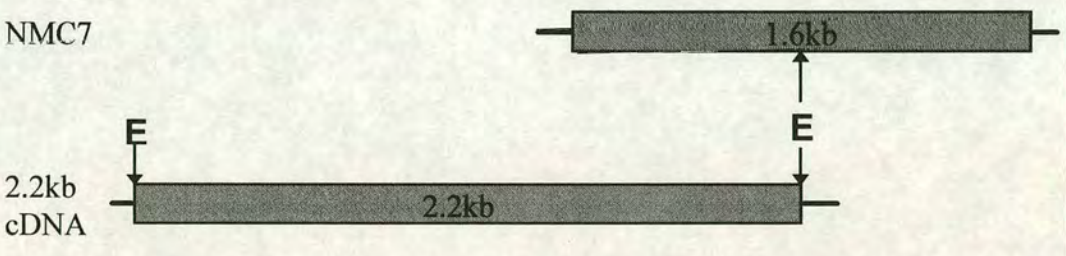

Figure 6.1 Schematic diagram showing relationship between NMC7 and the 2.2kb cDNA from the λZAP ovarian library. E: *Eco*RI

6.2 Results

6.2.1 Re-screening of the λZAP ovarian cDNA library

The λZAP ovarian cDNA library which had yielded the 2.2kb cDNA, was re-screened

in an attempt to recover upstream sequences. The screening of recombinant phage libraries is described in detail in materials and methods (2.8). The λZAP library was plated out onto a 25 x 25cm plate with *E.coli* XL1 Blue plating cells at a dilution such that around 100 000 phage grew on the plate (2..8.2). Replica lifts were taken onto Hybond-N membrane and denatured, neutralised and fixed as described in 2.8.3. The library was screened with a probe made by random primed ^{32}P labelling of the 2.2kb cDNA using Pharmacia Ready-To-Go labelling kit. Pre-hybridisation, hybridisation and washing of the membranes were all performed according to standard protocols (2.9.2). At the end of the tertiary screen, four positive recombinant phage had been identified. The positive cDNAs were excised from phage λ as pBluescript plasmids with the aid of helper phage (2.8.5.2). Plasmid DNA was propagated in XL1 Blue cells then recovered by miniprep (2.6.1.2). The cDNAs were released from pBluescript by an *Eco*RI digest and their size determined by electrophoresis through a 0.8% agarose gel. The results showed that the all four cDNAs isolated from the λZAP library were 2.2kb in length and were therefore almost certainly identical to the 2.2kb cDNA used as a probe. This was confirmed by restriction mapping. The fact that no upstream sequences were recovered in the screen indicates a problem with the construction of the library. The 3' *Eco*RI site of the 2.2kb cDNA is known to be a genuine site within the cDNA, rather than an *Eco*RI linker added during cloning, as it is also present in NMC7 (fig 6.1). It was speculated that the 5' *Eco*RI site of the 2.2kb cDNA may also be a genuine site in the *myosinV* cDNA and that these internal *Eco*RI sites were not properly protected during the preparation of the library. Subsequent isolation and sequencing of genomic DNA revealed that there is an *Eco*RI site in the *myosinV* gene at this position, confirming that the library had been poorly constructed. This explains why it was never possible to isolate upstream sequences from the λZAP ovarian library using the 2.2kb probe.

6.2.2 Screening of a λFIX genomic DNA library

With the failure to isolate *myosinV* upstream sequences from a cDNA library, a screen

of a genomic DNA library was undertaken. The library was in λFIX recombinant phage as described in 2.1.6.1. The library was plated out with NM422 plating cells and replica plaque lifts taken onto Hybond-N membrane. The membranes were hybridised with the same ^{32}P labelled 2.2kb cDNA used to probe the λZAP cDNA library. Only one positive recombinant phage carried through to the tertiary screen. A stock of this recombinant phage, termed FIX1A, was prepared in NM422 cells and phage DNA was prepared by means of a liquid lysate (2.8.5.1). The genomic DNA was released from the λ arms by a *Not*I digest, revealing a genomic DNA insert running at around 12kb, equivalent to the largest band in the 1kb ladder, and between the λ arms which are known to be 9kb and 20kb (fig 6.2). An initial attempt was made to map FIX1A genomic DNA by restriction digests with combinations of *Bam*HI, *Eco*RI, *Not*I and *Xba*I (Bryce MacIver, personal communication). *Not*I and *Xba*I restriction sites are built into the λFIX vector so that restriction with these enzymes releases the inserted genomic DNA from the λ arms. It proved difficult to obtain large amounts of good quality phage DNA for the restriction digests as lysis conditions were found to be inconsistent and large scale methods produced poor quality phage DNA which did not cut. Mapping gels were therefore difficult to interpret with small fragments being practically invisible and inconsistencies in band intensity suggesting partial digests. *Eco*RI fragments of around 7kb, 5kb, 3kb, 2kb and 1kb and *Xba*I fragments of 6kb, 3.5kb, 3kb, 2.8kb and 2.2kb were identified, but it was not possible to construct an accurate map of FIX1A from the available restriction mapping data.

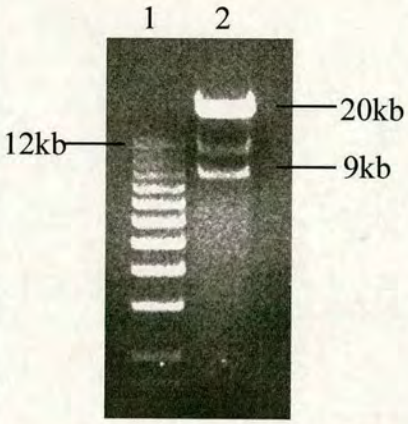

1 Gibco BRL 1kb ladder
2 *Not*I digest of FIX1A

Figure 6.2 *Not*I digest of FIX1A revealing a genomic DNA insert with an apparent size of 12kb running between the 9kb and 20kb λ arms.

6.2.3 Subcloning of FIX1A genomic DNA

To facilitate the mapping of FIX1A an attempt was made to subclone the *Eco*RI and *Xba*I fragments by a 'shotgun' approach. FIX1A recombinant phage DNA was digested with *Eco*RI or *Xba*I and the enzymes heat denatured at 65°C for 15 minutes. pBluescript plasmid DNA was also digested with either *Eco*RI or *Xba*I, then treated with phosphatase to prevent the religation of sticky ends (2.6.5.2). Aliquots of the phage DNA restriction reactions were then ligated to the cut plasmid DNA in the presence of T4 DNA ligase (2.6.5.3). The ligation mix was used to transform competent XL1 Blue cells which were then plated out onto LB-amp plates supplemented with X-gal and IPTG so that those colonies containing recombinant plasmids appeared white due to disruption of the β-gal gene of pBluescript (2.6.6 and 2.1.5.1). White colonies were used to inoculate overnight cultures from which plasmid DNA was recovered by miniprep. Recovered recombinant plasmid DNA was then digested with *Eco*RI or *Xba*I to determine the size of the inserted genomic DNA. In this way, four of the *Eco*RI fragments and two of the *Xba*I fragments were successfully subcloned. The resulting recombinant plasmids are listed in table 6.1.

Table 6.1 Recombinant plasmid subclones of FIX1A

Plasmid	Restriction Enzyme	Insert Size
pE1	*Eco*RI	~1kb
pE3	*Eco*RI	~3kb
pE5	*Eco*RI	~5kb
pE7	*Eco*RI	~7kb
pX2.8	*Xba*I	~2.8kb
pX3	*Xba*I	~3kb

6.2.4 Working map of FIX1A genomic DNA

The FIX1A genomic subclones were restriction mapped, sequenced from the T3 and T7 sites in pBluescript and hybridised back to a Southern blot of the FIX1A mapping gel (Bryce MacIver, personal communication). From this information a working map of FIX1A was constructed, however this map was not entirely satisfactory as it contained a central area which could not be pieced together (fig 6.3). In addition, the length of the assembled FIX1A fragments was over 20kb, whereas the entire genomic insert excised by *Not*I appears to run at around 12kb on an agarose gel. Hybridisation of the *myosinV* 2.2kb cDNA to the FIX1A Southern indicated that the gene was located at the most 3' end of the genomic insert (fig 6.3) but sequence comparison revealed that the genomic DNA did not extend any further 5' than the 2.2kb cDNA used a probe. FIX1A was therefore no help in terms of isolating the 5' region of the *myosinV* gene, however work on FIX1A did lead to the discovery of a new *Drosophila* gene downstream of the *myosinV* gene (Bryce MacIver, personal communication). This gene has been termed *c34* and its position and direction of transcription in relation to FIX1A is indicated in figure 6.3.

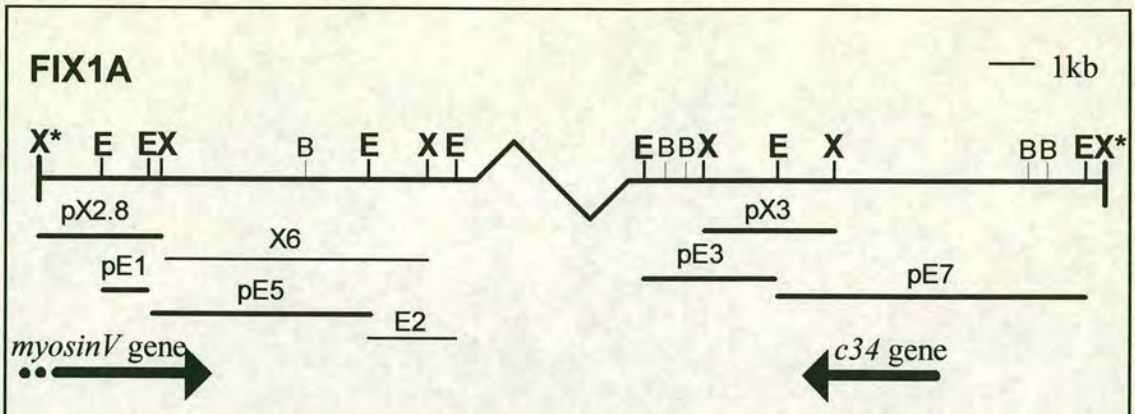

Figure 6.3 Working map of FIX1A genomic DNA with unresolved central area. Lines underneath FIX1A represent *Eco*RI and *Xba*I restriction fragments with the bold lines representing subcloned fragments. The position and direction of transcription of the *myosinV* and the *c34* genes are indicated. B: *Bam*HI, E: *Eco*RI, X: *Xba*I, X*: *Xba*I site in λFIX multiple cloning site.

6.2.5 Cloning of the *c34* gene

Before it became clear that the FIX1A genomic DNA did not contain any 5' sequence of the *myosinV* gene, a Reverse Northern approach was employed in an attempt to identify the sequence. In a Reverse Northern, RNA is used as a template to make a probe which can then be used to identify those fragments of DNA containing the relevant coding sequence. It was in the course of a Reverse Northern that the *c34* gene was discovered (Bryce MacIver, personal communication). A *myosinV* gene specific primer, designed to the 5' end of the 2.2kb cDNA, was used to reverse transcribe 5' sequence from total RNA. This was done in the presence of [α-^{32}P] dCTP so that the resulting first strand cDNA could be used to probe the FIX1A Southern to identify 5' exons. Several large fragments were identified as coding for 5' sequence and DNA from one of these fragments was used as a probe to screen the λZAP ovarian library for 5' cDNAs. One cDNA, termed cDNA 34, was recovered from the screen but the initial sequence data from this cDNA did not show any homology to the 2.2kb cDNA or to the mouse *dilute* class V myosin. It was therefore concluded that an entirely unrelated gene had been isolated (Bryce MacIver, personal communication). This new gene, termed *c34,* is related to the large fragments

identified in the Reverse Northern, but why these fragments were picked up by what was supposed to be a *myosinV* 5' probe, is not well understood.

cDNA 34 was entirely sequenced and was found to be a full length cDNA consisting of an open reading frame of 524 amino acids plus a 3'UTR of 654nt and a 5'UTR of 433nt (fig 6.4) (Bryce MacIver, personal communication). Database comparison identified sequence similarity to a rat sodium-dependent inorganic phosphate cotransporter (BNPI, Ni *et al* [1994]). The BNPI protein is a membrane spanning protein which transports inorganic phosphate driven by a sodium ion gradient. The regulation of cytosolic inorganic phosphate is important for both metabolic and signaling events. The predicted c34 protein was found to contain a putative sodium binding site and hydrophobic membrane spanning domains in common with the BNPI protein.

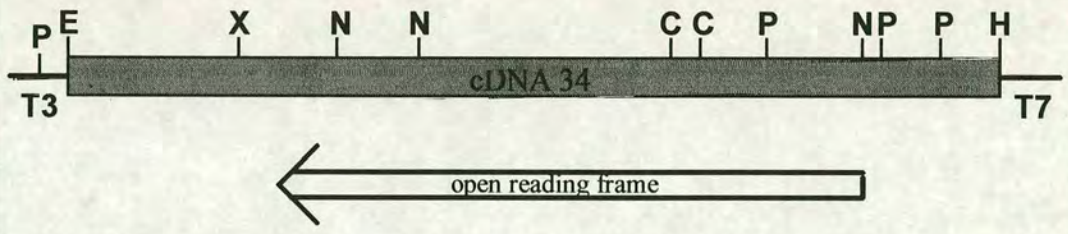

Figure 6.4 Schematic map of cDNA 34 in pBluescript, comprising an open reading frame of 524 amino acids plus a 3'UTR of 654nt and a 5'UTR of 433nt. C: *Cla*I, E: *Eco*RI, H: *Hind*III, N: *Nco*I, P: *Pst*I, X: *Xba*I. After Bryce MacIver, (Thesis, 1997).

6.2.6 Expression of the *c34* gene

cDNA 34 was isolated from an ovarian library so the *c34* gene is known to be expressed in ovaries. To gain further insights into the expression of the *c34* gene, the localisation of the *c34* transcript within the ovaries was determined by *in situ* hybridisation to whole mount OrR ovaries using a digoxigenin labelled 1.8kb *Pst*I fragment of cDNA 34 as a probe (fig 6.4). *in situ* hybridisation was performed

according to the protocol in the materials and methods (2.3.1). The *c34* transcript appears to be present throughout oogenesis and is particularly strongly expressed in very early stage and late stage egg chambers (fig 6.5). The strong germarial expression may reflect a requirement for the putative phosphate cotransporter protein in the membranes of the 16 cystocytes and the pre-follicle cells where the regulation of intracellular inorganic phosphate levels may be required for cell-cell signalling to specify cell fate.

6.2.7 Cloning of a second new gene adjacent to the *myosinV* gene

In the course of screening a λZAP ovarian cDNA library to find the 3'UTR of the ovarian *myosinV* transcript (see 3.2.4), a second new *Drosophila* gene was discovered. The λZAP library was screened with a probe made from the 5kb *Eco*RI genomic subclone. This fragment overlaps and extends 3' of the cloned *myosinV* 3'UTR (fig 6.6) and so should have identified any additional 3'UTR sequence which exists. cDNAs identified by the 5kb genomic DNA probe were excised from phage λ as pBluescript plasmids (2.8.5.2) then sequenced from the T3 and T7 sites. Two of the positive cDNAs identified by this screen contained 3'UTR sequence, however, partial sequencing of a third cDNA revealed a prominent polyA tail but otherwise no homology to the *myosinV* 3'UTR. It was originally thought that this cDNA might

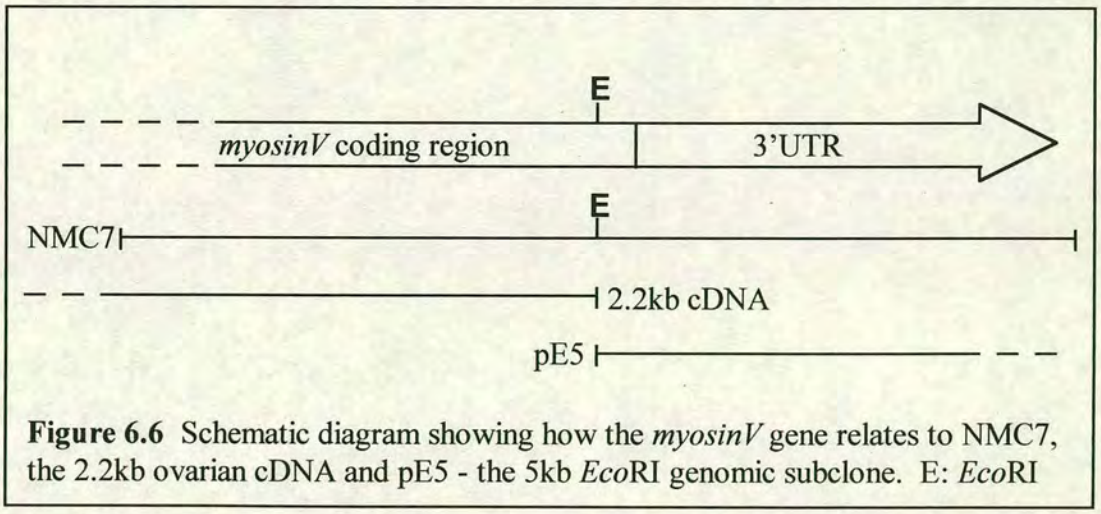

Figure 6.6 Schematic diagram showing how the *myosinV* gene relates to NMC7, the 2.2kb ovarian cDNA and pE5 - the 5kb *Eco*RI genomic subclone. E: *Eco*RI

Figure 6.5 *in situ* hybridisation to reveal the localisation of the *c34* transcript in wild type ovaries. The *c34* transcript is strongly expressed in the germarium and is present throughout the nurse cells and oocyte in stage 1-3 egg chambers. The transcript appears to be present at low levels in stage 4 - 8 egg chambers then comes on strongly again in the nurse cells at stage nine prior to transferal of the nurse cell contents to the oocyte. Anterior is to the top.

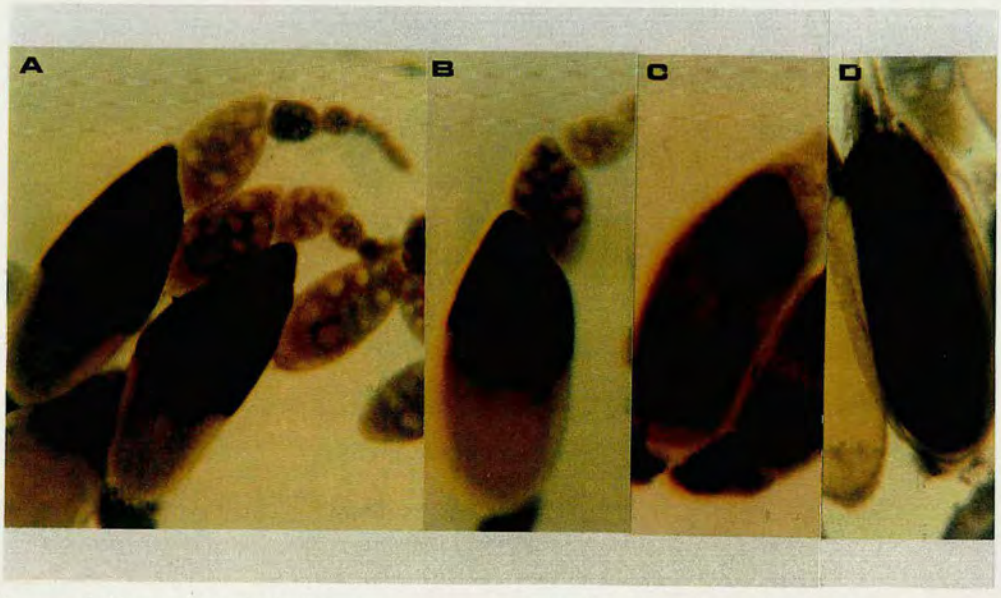

Figure 6.13 *in situ* hybridisation to reveal the localisation of the *az2* transcript in wild type ovaries. The transcript is present in the nurse cells and oocyte throughout oogenesis but becomes especially abundant in stage 10 nurse cells and is subsequently dumped into the oocyte. A) stages 1-10. B) stage 11. C) stage 12. D) stage 13. Anterior is to the top.

represent an alternative *myosinV* 3'UTR but further sequence analysis revealed an open reading frame being transcribed in the opposite direction to the *myosinV* gene. This third cDNA, given the title AZ2, was a 2.6kb *Eco*RI insert in pBluescript (fig 6.7A). It was sequence data from the T3 site which revealed the partial open reading frame and the polyA tail, but the plasmid failed to sequence from the T7 site. Attempts to sequence from the -20 and -40 primer sites also failed indicating that a region of the pBluescript multiple cloning site had been lost in the cloning process.

The AZ2 cDNA was partially mapped by digesting the plasmid with restriction enzymes which cut in the T3 region of the multiple cloning site and using those enzymes which resulted in a single restriction fragment to map the insert (fig 6.7A). The AZ2 cDNA then was subcloned into pBluescript SK$^-$ as two *Eco*RI-*Hind*III fragments of 0.9kb and 1.7kb (fig 6.7B). The 1.7kb fragment was subcloned again by excision of the *Bam*HI fragment followed by religation of the plasmid and subsequent ligation of the *Bam*HI fragment into *Bam*HI digested pBluescript. This resulted in a

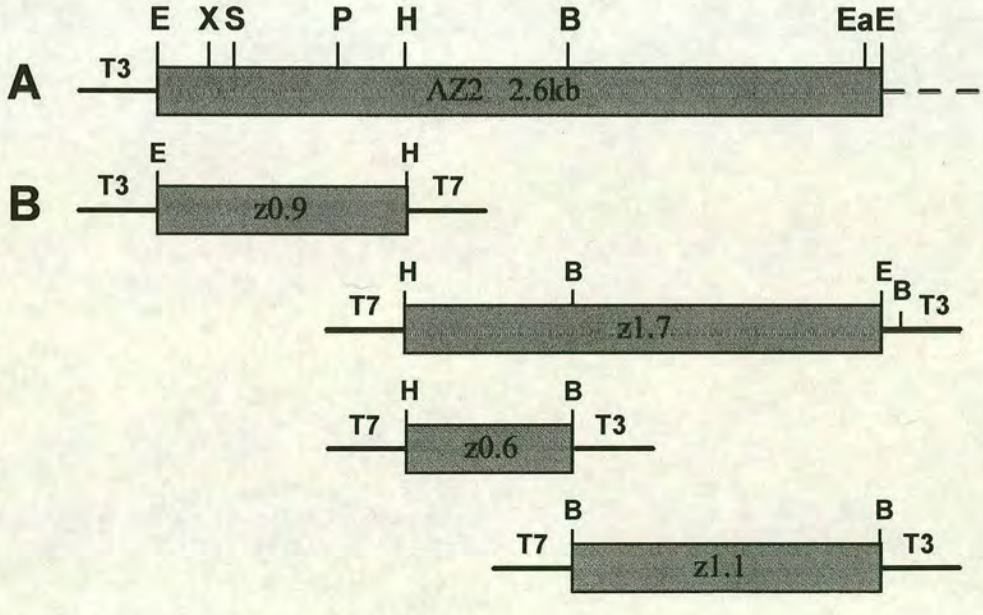

Figure 6.7 A) Restriction map of cDNA AZ2 in pBluescript. The region of pBluescript around the T7 primer site has been lost in the cloning process. B) Subclones of AZ2 in pBluescript named according to their size. E: *Eco*RI, X: *Xba*I, S: *Sac*I, P: *Pst*I, H: *Hind*III, B: *Bam*HI and Ea: *Eag*I.

0.6kb *Bam*HI-*Hind*III fragment and a 1.1kb *Bam*HI fragment (fig 6.7B). The subclones were sequenced using T3 and T7 primers and one gene specific primer AZ2A1, such that the entire cDNA was sequenced on at least one strand (figure 6.8).

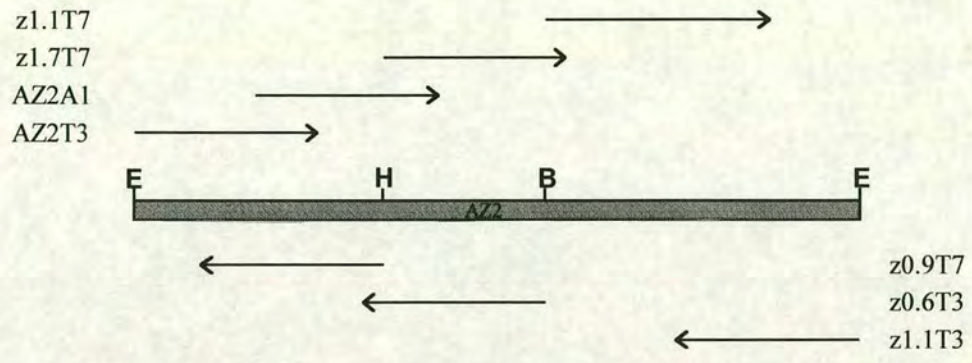

Figure 6.8 Schematic diagram showing sequenced regions of cDNA AZ2. Sequence was obtained using T3 and T7 sites in AZ2 subclones except for AZ2A1 which used a gene specific primer. The entire cDNA was sequenced on at least one strand. E: *Eco*RI, H: *Hind*III and B: *Bam*HI.

6.2.8 Sequence analysis of the *az2* gene

Sequence analysis of the AZ2 cDNA with GCG MAP and TFASTA programs, revealed that it actually consisted of two independent cDNAs which had become co-ligated during the cloning procedure. The cDNA of the *Drosophila* glyceraldehyde-3-phosphate dehydrogenase-2 (DmGADPH) gene (Tso *et al*, 1985) was co-ligated to a cDNA which matches no other in the database and therefore must represent a new gene (fig 6.9). This new gene was given the working name *az2*. The largest open reading frame of *az2* suggests a transcript of around 1.4 kb but it is possible that the cDNA has been truncated by co-ligation to the DmGADPH cDNA. Further restriction and hybridisation analysis of the *az2* gene indicated that it maps entirely within the 5kb *Eco*RI genomic fragment and is immediately downstream of the *myosinV* gene on the chromosome (fig 6.10).

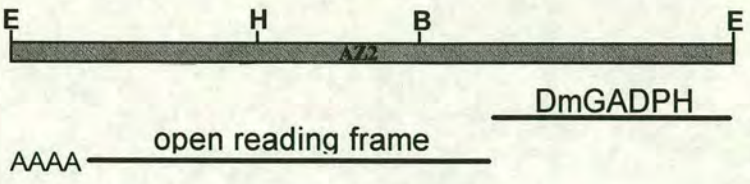

Figure 6.9 Sequence analysis of the AZ2 cDNA indicates that it consists of two independant cDNAs. An 835bp region of the cDNA for the *Drosophila* glyceraldehyde-3-phosphate dehydrogenase-2 gene (DmGADPH) is co-ligated to a second cDNA encoding a novel open reading frame. E: *Eco*RI, H: *Hind*III and B: *Bam*HI.

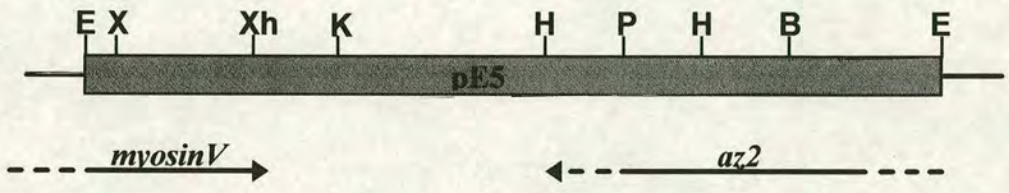

Figure 6.10 Schematic diagram showing position and direction of transcription of the *myosinV* and *az2* genes in relation to the 5kb *Eco*RI genomic subclone pE5. The *az2* gene is adjacent to the *myosinV* gene on the chromosome and appears to map entirely within pE5. E: *Eco*RI, X: *Xba*I, Xh: *Xho*I, K: *Kpn*I, H: *Hind*III and B: *Bam*HI.

Database comparisons with the az2 predicted protein indicate that the C-terminal region contains several zinc finger domains. Zinc finger domains are nucleic acid binding motifs first identified in the *Xenopus* transcription factor TFIIIA. A zinc finger domain consists of around 25 amino acid residues with two cysteine (C) or histidine (H) residues at either end which are involved in the tetrahedral co-ordination of a zinc atom. This structure then interacts directly with the DNA to mediate transcription. Classes of zinc fingers are characterised by the number and positions of the cysteine and histidine residues involved in zinc atom co-ordination, with the C2H2 type having the consensus C-X-X-C-X-X-X-[LIVMFYWC]-X-X-X-X-X-X-X-X-H-X-X-X-(X)-H. The C-terminal region of the *az2* gene contains four consecutive C2H2 type zinc finger domains in common with several other known zinc finger

proteins (fig 6.11). The N terminal region, however, shows no significant homology to any protein in the database suggesting that the *az2* gene may encode a novel type of transcriptional regulator.

```
hshkr1  GE.KPYVCRE CGRGFRQHSH LVRHK.RTHS .GEKP.YICR ECEQGFSQKS
hsznf8  GE.RHHKCSE CGKAFTQKST LRMHQ.RIHT .GERS.YICT QCGQAFIQKA
mmmkr5  GE.KPYECEI CRKAFSHHAS LTQHQ.RVHS .GEKP.FKCK ECGKAFRQNI
mm2nf3  GE.KPFECDH CGKAFPSSSY LNVH.LKIHT .GEKP.FRCT VCGKTFTCSS
dmglas  GEMKPNLCRL CGKTYARPST LKTH.LRTHS .GERP.YRCP DCNKSFSQAA
   az2  QKLK...CEV CEHSFSTDHA LQAHQFRDHK MGDGGWFRCT LCELNFDRKC

hshkr1  HLIRHL.RTH TGEKPYVCTE CGRHFSWKSN LKTHQRTHSG ...VKPYVCL
hsznf8  HLIAH.QRIH TGEKPYECSD CGKSFPSKSQ LQMHKRIHTG ...EKPYICT
mmmkr5  HLASH.WRIH TGEKPFECGE CGKSFSISSQ LATHQRIHTG ...EKPFECK
mm2nf3  YLPVHM.RTH TGGRPFRCII CGRSFLWSSY LRVHMRIHTG ...EKPYVCQ
dmglas  NLTAHV.RTH TGQKPFRCPI CDRRFSQSSS VTTHMRTHSG ...ERPYRCS
   az2  HLQQHSQRVH M.DKSFVCEI CSRSFAFGSQ LAIHKRTHDE KHVAKPFVCE

hshkr1  ECGQCFSLKS NLNKH.QRSH TGEKPFVC..  human Kruppel related[1]
hsznf8  ECGKAFTNRS NLNTH.QKSH TGEKSYICAE  human ZNF81[2]
mmmkr5  VCRKAFRQNI HLASH.WRIH TGEKPFECGE  mouse mkr5[3]
mm2nf3  YCGKAFTEHS GLNKHLRK.H TGEKPYEYKE  mouse mkr3[3]
dmglas  SCKKSFSDSS TLTKHLR.IH SGEKPYQCKL  Drosophila glass[4]
   az2  FCGKCFKQKI QMTTHVTAVH TKIRALQVRH  Drosophila az2
```

Figure 6.11 Alignment of zinc finger proteins from several species using the GCG PILEUP program. C2H2-type zinc finger domains consist of the consensus pattern C-X-X-C-X-X-X-[LIVMFYWC]-X-X-X-X-X-X-X-X-H-X-X-X-(X)-H where the two C's and the two H's are the zinc ligands. The C-terminal region of the az2 predicted protein contains four copies of this consensus in common with regions of the above five known zinc finger proteins. [1-4] Ruppert *et al*, (1988); Marino *et al*, (1993); Chowdhury *et al*, (1988); Moses *et al*, (1989).

6.2.9 Northern analysis of the *az2* gene

The *az2* cDNA was isolated from an ovarian library. In order to establish the size of the full length ovarian transcript, and to determine whether the gene is also expressed in carcass tissue, Northern analysis was performed. Total RNA was extracted from OrR ovary and female carcass tissue by the Trizol method (2.7.2.1). Around 20µg of

each prep was electrophoresed through a denaturing agarose-formaldehyde gel alongside 5μg of Gibco RNA ladder (2.7.3). An ethidium stain of the gel indicates that the gel is overloaded with RNA causing the ladder to be slightly distorted (fig 6.12A). The RNA was Northern blotted onto Hybond-N^+ membrane then prehybridised in a prehyb solution which included dextran sulphate (2.9.2). A probe was prepared by ^{32}P labelling of the 0.9kb *Eco*RI-*Hind*III fragment of the AZ2 cDNA, which contains only *az2* sequence (fig 6.9). The probe was added to the prehybridisation solution and hybridised to the membrane overnight at 42°C, before washing and exposure to X-ray film. After only four hours exposure a clear signal can be seen in both the ovary and female carcass lanes (fig 6.12B). The ovarian transcript and the female carcass transcript are both very abundant and appear to be the same size. Comparison of the autorad with the ethidium stained gel puts the transcript at around 1.3kb, running below the 1.4kb ribosomal band. This result suggests that the AZ2 cDNA contains the full length transcript of the *az2* gene.

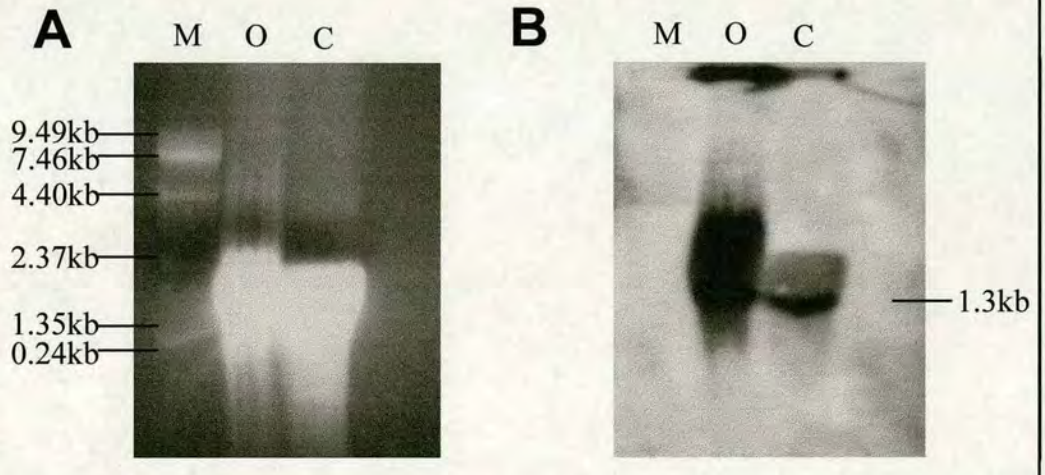

Figure 6.12 Northern analysis of the *az2* gene. A) ethidium stained gel showing RNA markers (M), ovary RNA (O) and female carcass RNA (C). Overloading of the ovary and carcass RNA has caused the markers to become distorted. B) Northern blot probed with the 0.9kb *Eco*RI-*Hind*III fragment of the AZ2 cDNA. The *az2* transcript appears to be 1.3kb, running below the abundant 1.4kb ribosomal RNA band.

6.2.10 *in situ* hybridisation to the ovarian *az2* transcript

The localisation of the *az2* transcript during oogenesis was determined by *in situ* hybridisation to whole mount ovaries. The 0.9kb *Eco*RI-*Hind*III fragment of the AZ2 cDNA was labelled with digoxigenin then used to probe OrR ovaries. Hybridisation, antibody incubation and signal detection were all carried out according to standard protocols (2.3.1). The results show that the *az2* transcript is present at low levels in the nurse cells from the early stages of oogenesis but becomes very abundant in the nurse cells around stages 9-10 (fig 6.13A, page 175). From stage 10b the transcript is transferred to the oocyte as the degenerating nurse cells transfer almost their entire contents into the developing oocyte (fig 6.13B). The *az2* transcript is then found unlocalised throughout the mature oocyte (fig 6.13D).

The stage 10b transfer to the oocyte is a pattern of localisation commonly seen for maternal transcripts which are not actually required during oogenesis but are laid down in the oocyte for use during embryogenesis. The *az2* gene is predicted to encode a zinc-finger like protein and this fits well with the transcript localisation pattern, as a transcriptional regulator is more likely to be required in the transcriptionally active early embryo rather than in the mature oocyte which is almost transcriptionally inert. It can therefore be speculated that the product of the *az2* gene is a transcriptional regulator involved in pattern formation during early embryogenesis.

6.2.11 Cloning of the 5' half of the *myosinV* gene using recombinant P1s

In a further attempt to find the elusive 5' region of the *myosinV* gene, P1 recombinant bacteriophage were employed. P1s are recombinant bacteriophage which carry around 80-90kb of cloned genomic DNA and are available from *Drosophila* resource centres. The *myosinV* gene had been located to the right arm of the second chromosome at position 43BC by *in situ* hybridisation to polytene chromosomes

(Bryce MacIver, personal communication), so several P1s containing genomic DNA from the 43BC region were obtained. Hybridisation of a *myosinV* probe to a dot blot of the P1 DNA revealed that the *myosinV* gene was contained within P1 DS00574. This P1 was shotgun subcloned and the resulting recombinant plasmids were screened with a probe made from a 5' fragment of the *myosinV* 2.2kb cDNA. A 7kb *Xba*I genomic fragment, termed pP1X7, was isolated and sequenced from the T3 and T7 primer sites in pBluescript. Sequence from the T3 end was found to match the 2.2kb cDNA while sequence from the T7 end showed similarity to the mouse *dilute* class V myosin, indicating that much of the remaining *myosinV* gene was contained within the 7kb *Xba*I fragment. Subsequent subcloning and sequencing of pP1X7 did indeed yield most of the 5' coding region of the *Drosophila* class V unconventional myosin with the remaining 5' sequence isolated by 5'RACE (Bryce MacIver, personal communication).

6.2.12 Updated map of FIX1A genomic DNA

As previously stated, the working map of FIX1A genomic DNA was never entirely satisfactory as there was a central region where the fragments could not be pieced together (fig 6.3). In addition, although the entire *Not*I insert of FIX1A appears to run at 12kb on an agarose gel, the combined length of the mapped fragments was over 20kb with some fragments not yet accounted for. This puts the size of the insert close to the maximum of 23kb which can be cloned into a λFIX vector (Sambrook *et al*, 1989). Further genomic subcloning was undertaken in an attempt to refine the FIX1A map. The P1 DS00574 subclone mini library was re-screened using the 5kb *Eco*RI genomic fragment as a probe and recombinant plasmids carrying a 6kb *Xba*I fragment (pP1X6) and an 8kb *Bam*HI fragment (pP1B8) were identified. These P1 subclones were used in conjunction with the genomic FIX1A subclones for cross hybridisations to resolve the central area of the FIX1A map, however, no area of overlap could be detected (Bryce MacIver, personal communication).

The lack of any overlap between the area of the map around the *myosinV* and *az2*

genes and the area around the *c34* gene, along with the observed size inconsistencies, indicated that FIX1A was in fact a mixture of two independent phage carrying two different fragments of genomic DNA. The *myosinV* gene and the *az2* gene are on one 12kb fragment while the *c34* gene is on another, entirely unrelated 12kb fragment. Failure of cDNA 34 to hybridise to P1 DS00574 on the P1 dot blot, was further evidence that the *myosinV* gene and the *c34* gene were not on a contiguous piece of genomic DNA. The genomic fragment containing the *myosinV* and the *az2* genes was renamed FIX1A-myosin while the fragment containing the *c34* gene was renamed FIX1A-c34. The updated maps of FIX1A-myosin and FIX1A-c34 are shown in figure 6.14.

The two different recombinant phage probably failed to be separated due to the fact that the tertiary screen involved picking and streaking out positive phage from the secondary screen rather than a further round of picking plugs and plating out at a lower density. Had this step been performed, FIX1A-myosin and FIX1A-c34 would almost certainly have been separated, however once a phage stock had been established it was impossible to distinguish the two genomic DNA fragments as they were both around 12kb. Several of the restriction fragments were also around the same size which only served to complicate the matter. In retrospect , it can be seen that the faint bands on the mapping gels which had been put down to partial digests, were in fact the fragments of the less abundant recombinant phage. It will be possible to separate the two species of phage by plating out the FIX1A phage stock at low density and screening independently with *myosinV* and *c34* probes.

The transitional nature of the FIX1A genomic DNA map is of direct relevance to the work of chapter 7 - genetic analysis of the *myosinV* gene. At the outset of this work it was presumed that the *myosinV* gene and the *c34* gene were adjacent on the right arm of the second chromosome at 43BC. The discovery of the *az2* gene between the other two genes and the subsequent revelation that the *c34* gene was actually on an unrelated piece of genomic DNA, all affect the interpretation of data. This will be discussed in more detail in chapter 7.

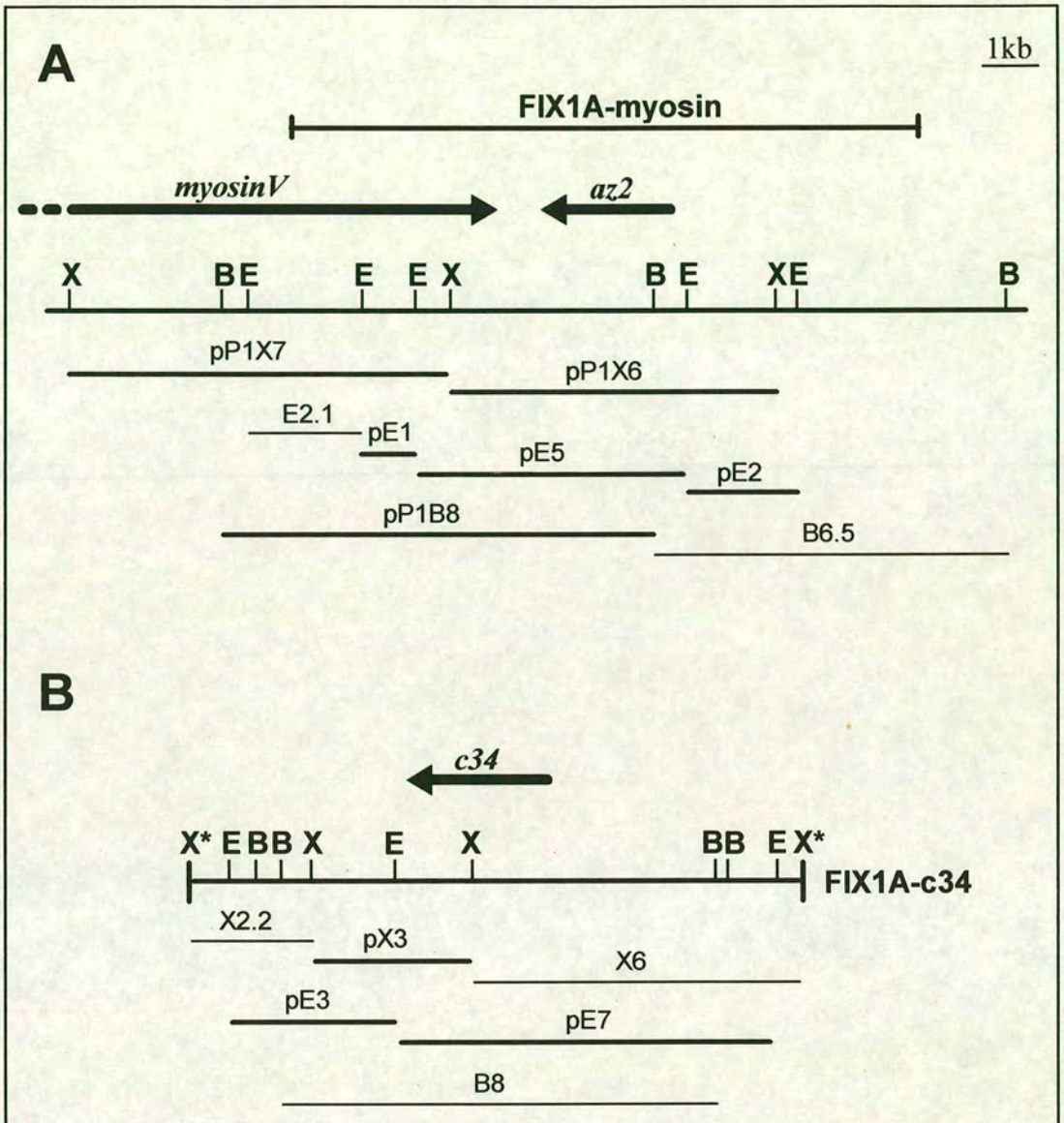

Figure 6.14 Updated maps of FIX1A-myosin and FIX1A-c34 genomic DNA. A) Map of genomic region around the *myosinV* and *az2* genes indicating the position and direction of transcription of both genes and their relationship to recombinant phage FIX1A-myosin. B) Map of FIX1A-c34 genomic DNA indicating the position and direction of transcription of the *c34* gene. Genomic and P1 restriction fragments are shown underneath both maps with those in bold representing subcloned fragments. B: *Bam*HI, E: *Eco*RI, X: *Xba*I, X*: *Xba*I site in λFIX multiple cloning site.

6.3 Summary

Screening of a λFIX genomic library to find the 5' region of the *myosinV* gene, led to the isolation of FIX1A recombinant phage. FIX1A was found to extend no further 5' than already cloned cDNAs and so did not help in the search for the remainder of the *myosinV* gene, however work on FIX1A did lead to the isolation of two previously uncharacterised *Drosophila* genes. FIX1A genomic DNA was found to include the *c34* gene which encodes a putative sodium-dependent inorganic phosphate cotransporter. The *c34* gene produces an ovarian transcript which is particularly strongly expressed in the germarium. The c34 protein is predicted to span the membrane and may function in follicle cell - cystocyte signalling pathways by regulating the intracellular levels of inorganic phosphate.

In the course of a screen to isolate the *myosinV* 3'UTR, the *az2* gene was discovered immediately downstream of the *myosinV* gene. The *az2* transcript is abundant in ovaries where it is made in the nurse cells then transported to the mature oocyte in the late stages of oogenesis. The transcript is also present in female carcass and is predicted to encode a zinc-finger like protein. It can be speculated that the *az2* gene encodes a transcriptional regulator which is required both in embryonic development and throughout adult life.

FIX1A was eventually mapped and found to consist of two independent recombinant phage. FIX1A-myosin genomic DNA contains the *myosinV* gene and the *az2* gene and is known to map to chromosome position 43BC. The putative phosphate cotransporter gene, *c34,* is contained in an entirely unrelated fragment of genomic DNA. The *myosinV* and *c34* genes were originally thought to be adjacent on the chromosome so the changes to the genomic DNA map have implications for the genetic analysis of the *myosinV* gene which are discussed in chapter 7.

Chapter 7

Genetic Analysis

7.1 Introduction

Much information has now been collated on the *myosinV* gene. The gene is known to encode a class V unconventional myosin, a class of myosins thought to be involved in vesicular transport. The *myosinV* transcript is abundant in testes, ovaries and early embryos and has also been shown to be present at low levels in other tissues. The ovarian *myosinV* transcript is localised during oogenesis in a pattern presumed to be important to its function. Localisation of the transcript is dependent on the products of several other genes and the integrity of the microtubules but does not appear to depend on a signal in its 3'UTR.

The *myosinV* gene was isolated serendipitously in the course of an enhancer trap screen to find genes with interesting expression patterns during oogenesis. Although the *myosinV* gene was not related to the original enhancer trap pattern, it was decided to continue to study the new gene as it had an interesting pattern of transcript localisation, suggesting it would function during oogenesis. Thus, the *myosinV* gene was originally identified by reverse genetics, an approach which involves isolation of a gene with no knowledge of its phenotype or function, and it was now essential to analyse the function of the *myosinV* product during development.

To fully characterise the function of *myosinV*, it is necessary to study the effect of mutations in the gene. This can involve creating mutations in the gene in order to study the resulting phenotype. Alternatively, the gene may correspond to a locus which has already been identified and genetically mapped by its mutant phenotype but has not been characterised any further, in which case the cloned gene has to be shown to correspond to the mapped gene. These approaches have been used in a genetic analysis of the *myosinV*, *az2* and *c34* genes in order to further characterise them. Some of the work in this chapter was performed in collaboration with Bryce MacIver, as indicated in the text.

7.2 Results

7.2.1 Separation of P-elements in the H14 line

The *myosinV* gene was mapped to position 43BC on the right arm of the second chromosome by *in situ* hybridisation to the polytene chromosomes of third instar larvae salivary glands (Bryce MacIver, personal communication). The original enhancer trap line H14, which although unrelated led to the dicovery of *myosinV*, was shown by Southern analysis to contain two P-element inserts. Polytene *in situ* hybridisation indicated that these P-elements map close to each other and close to the *myosinV* gene at around positions 41-43 (Roger Slee, personal communication). These P-elements were considered sufficiently close to the *myosinV* gene to attempt to create a mutant in the gene by local hopping of the P-elements. The P-elements can be mobilised by crossing a stock to flies carrying the Δ2-3 P-element, which encodes transposase but has defective P-element ends so cannot itself transpose. The mobilised P-elements can cause insertional mutations by re-inserting within the gene of interest or alternatively, if the P-element inserts close to the gene, a deletion mutation can then be generated by imprecise excision of the P-element.

As it would be very complicated to follow the progress of two identical P-elements in a P-hop cross, it was decided to first separate the two P-elements of the H14 by recombination, to generate two new, single P-element lines. The recombination cross is described in detail in figure 7.1. The P-elements contain the *rosy* gene and the cross was carried out in a *rosy* mutant background so that flies with P-element insertions have red eyes and can be easily selected.

Around 200 F1 crosses were set up and the F2 generation was screened for eye colour. Around 50 lines had all rosy eyed flies in the F2 generation so were discarded. The red eyed flies in the remaining lines were screened by Southern analysis to determine whether they contained one or other or both P-elements.

H14 = $\frac{P_{1.3}\,P_6}{+\ +}$; $\frac{rosy^{506}}{rosy^{506}}$

F_0

en masse

♀ $\frac{P_{1.3}\,P_6}{+\ +}$; $\frac{rosy^{506}}{rosy^{506}}$ **X** $\frac{+\ +}{+\ +}$; $\frac{rosy^{506}}{rosy^{506}}$ ♂

♀ $\frac{+\ +}{+\ +}$; $\frac{rosy^{506}}{rosy^{506}}$ **X** $\frac{P_{1.3}\,P_6}{+\ +}$; $\frac{rosy^{506}}{rosy^{506}}$ ♂

F_1 collect virgin females from both crosses and mate individually to $rosy^{506}$ males

F_2

$\frac{P_{1.3}\,P_6}{+\ +}$; $\frac{rosy^{506}}{rosy^{506}}$ red eyes, 1.3kb and 6kb bands on Southern

or

$\frac{P_{1.3}+}{+\ +}$; $\frac{rosy^{506}}{rosy^{506}}$ red eyes, 1.3kb band on Southern

or

$\frac{+\ P_6}{+\ +}$; $\frac{rosy^{506}}{rosy^{506}}$ red eyes, 6kb band on Southern

or

$\frac{+\ +}{+\ +}$; $\frac{rosy^{506}}{rosy^{506}}$ rosy eyes, Discard

Figure 7.1 Separation of the two P-elements in the H14 line by natural recombination. The cross was carried out in a *rosy*^{506} background so that the progress of the P-elements could be followed. *rosy*^{506} flies lack the *rosy* gene and therefore have rosy coloured eyes. The P-element includes the *rosy* gene such that flies with P-element insertions have red eyes. Of the 200 F1 crosses set up around 50 F2 lines were discarded for having all rosy eyes. The remaining 150 red eyed lines were screened for loss of one of the P-elements by Southern analysis.

Genomic DNA was extracted from 20 red eyed flies from each line (2.6.1.1). Half of each prep was digested with *Eco*RI then electrophoresed through a 0.8% agarose gel in 1X TBE (2.6.7). The DNA was Southern blotted onto Hybond-N^+ membrane in 20X SSC (2.9.1.1). The membranes were probed with a 0.6kb *Hind*III fragment of Carnegie 20, which contains P-element ends and so hybridises to those *Eco*RI genomic fragments which contain P-elements. Hybridisation and detection were performed by both radioactive and non-radioactive methods. The probe was either labelled with ^{32}P and hybridisation and detection were according to standard protocols (2.9.2), or the probe was labelled with digoxigenin then hybridisation and chemiluminescent detection were performed as described in materials and methods (2.9.5). Detection of the size markers was achieved by end labelling of the 1kb ladder with ^{32}P or digoxigenin using Klenow polymerase, prior to loading on the gel (2.9.3.2). Examples of the results obtained are shown in figure 7.2.

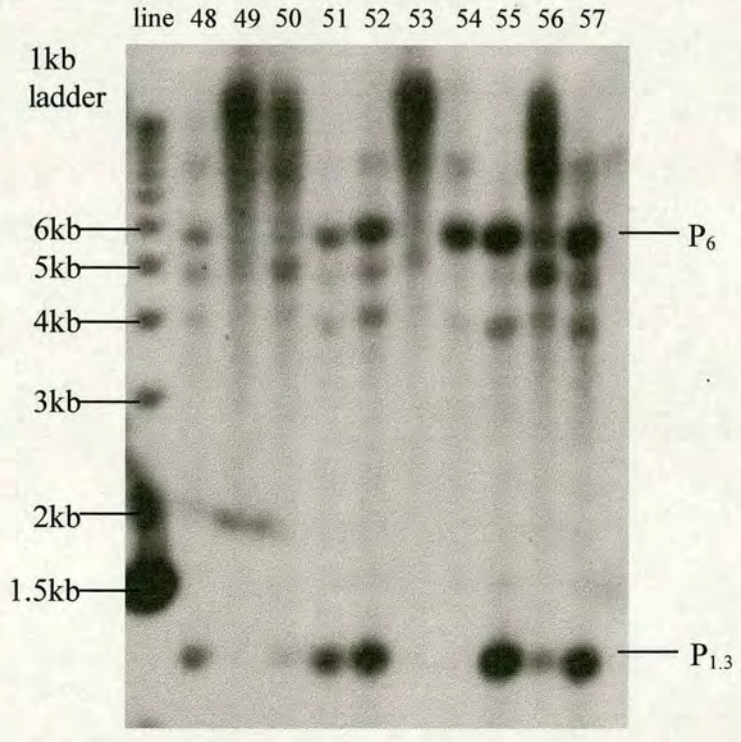

Figure 7.2 Southern analysis of the H14 P-element recombination cross. Genomic DNA from red eyed flies was digested with *Eco*RI and the resulting blot was probed with the 0.6kb *Hind*III fragment of Carnegie20 which hybridises to P-element ends. The two H14 P-elements are contained on *Eco*RI fragments of 1.3kb and 6kb and so are designated $P_{1.3}$ and P_6 respectively. Analysis of lines 48 to 57 is shown above. Despite the problems of partial digests and degradation in some lanes, it can be clearly seen that line 54 has lost $P_{1.3}$ but retains P_6.

The two P-elements in the H14 line were known to be contained within 1.3kb and 6kb *Eco*RI fragments, so the P-elements were termed $P_{1.3}$ and P_6 respectively. Of the 150 lines screened, 13 lines lost the $P_{1.3}$ P-element and retained the P_6 P-element. One such example is line 54 shown in figure 7.2. The remainder of the lines retained both P-elements. No lines were found which had lost the P_6 P-element and retained the $P_{1.3}$ P-element.

Several of lines which contained only the P_6 P-element were analysed for their β-gal expression pattern to determine whether the H14 expression pattern was associated with the P_6 P-element. Ovaries were dissected from red eyed flies and incubated in X-Gal staining buffer overnight in the dark (2.2.10). The ovaries were then teased apart and the β-gal staining pattern was examined. All the ovaries examined were found to show β-gal expression in the polar follicle cells and migrating border cells in an identical pattern to that detected in flies of the H14 line. It can therefore be concluded that the H14 expression pattern is associated with the P_6 P-element.

The $P_{1.3}$ and P_6 P-elements had not previously been matched to the chromosome positions of the two P-elements in the H14 line. In order to determine cytologically which P-element had been successfully separated, *in situ* hybridisation was performed on the polytene chromosomes of the new, one P-element lines. Chromosome squashes were prepared from the salivary glands of third instar larvae and *in situ* hybridisation was performed according to the protocol in materials and methods (2.3.5). A *lacZ* probe was prepared by digoxigenein labelling of the 2kb *Sac*II fragment of pGEM-lacZ (2.3.6). Polytene chromosome squashes from the H14 line were also probed as a control for staining and to refine the chromosome positions of both P-elements.

Figure 7.3 shows the results of *in situ* hybridisation to the H14 line and to line 99 which has lost the $P_{1.3}$ P-element. By the use of published cytological maps (Lindsay and Zimm, 1992) the chromosome positions of the P-elements in the H14 line were refined to 41F-42A and 42EF. These positions were confirmed by Debiao Zhao

Figure 7.3 *in situ* hybridisation to polytene chromosomes from the third instar larvae of the H14 line and recombination line 99. A and B show the H14 line which contains two P-elements. C and D show line 99 which was derived from the H14 line by the loss of one P-element. In the enlargements B and D, the P-element at 41F-42A is indicated by an arrow while the P-element at 42E-F is indicated by an arrowhead. Line 99 has lost the $P_{1.3}$ P-element at 41F-42A.

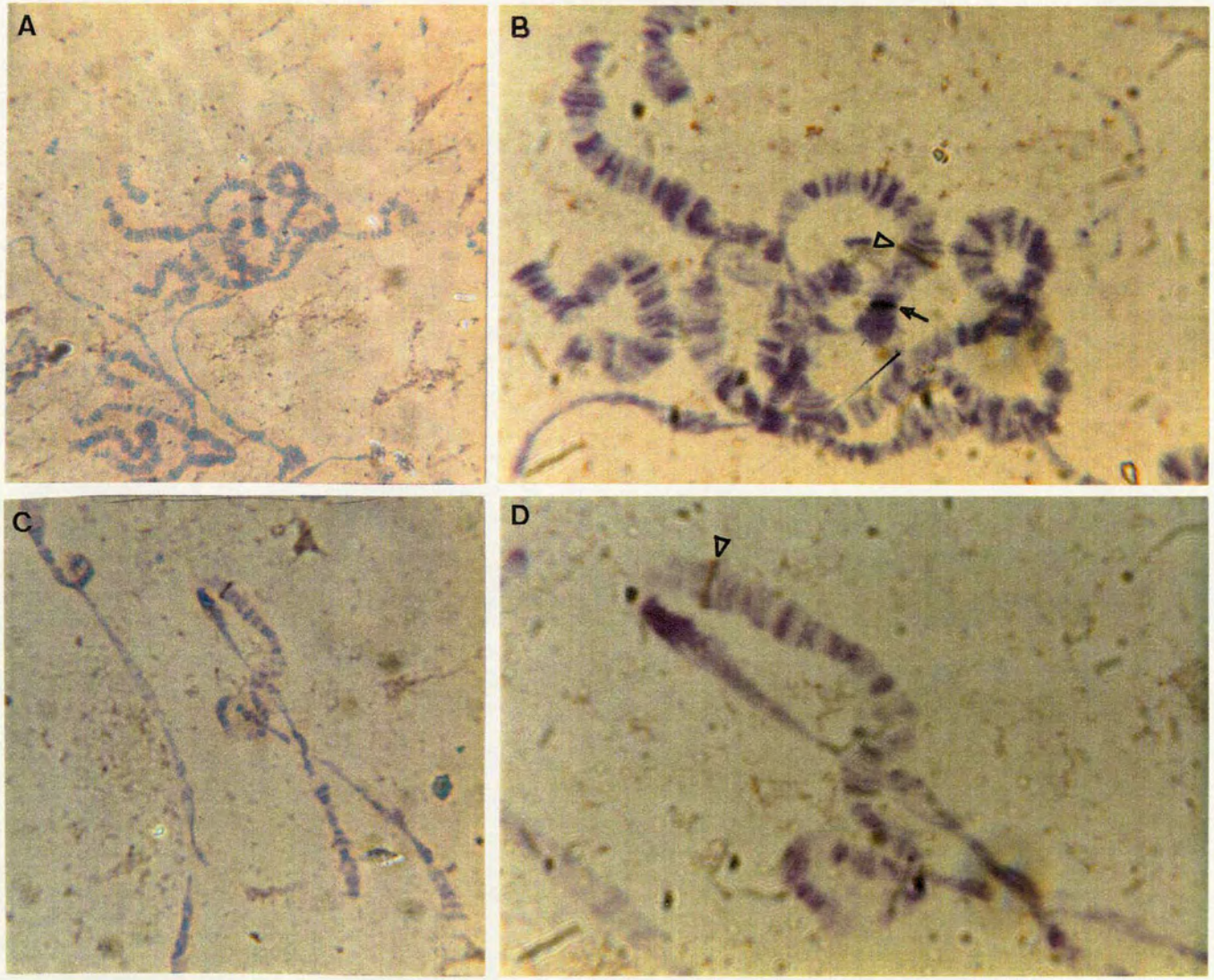
A
B
C
D

(personal communication). Figure 7.3A shows that line 99 has lost the proximal P-element at 41F-42A and retains the distal P-element at 42EF. $P_{1.3}$ therefore corresponds to the P-element at 41F-42A while P_6 corresponds to the P-element at 42EF.

It should now have been possible to attempt a mutagenesis of the *myosinV* gene by local hopping of the single P-element at 42EF into or near to the *myosinV* gene at 43BC. However, this P-element is too distant to be likely to generate mutants at a high frequency and it was therefore decided to first investigate whether the locus corresponding to the *myosinV* gene had already been identified. This seemed possible as Heitzler *et al* (1993) had undertaken a saturation mutagenesis of the 43 region.

7.2.2 The 43 region

The 43 region was extensively mapped by deficiency mapping and 27 complementation groups were identified (Heitzler *et al*, (1993). Some of these loci correspond to already cloned genes and are named accordingly, but others are uncharacterised and have been designated according to their position. A map of section 43 is shown in figure 7.4.

7.2.3 The *humilis* gene

The *myosinV* gene has been cytologically mapped to position 43BC and so should correspond to one of the uncharacterised loci in the 43 region. The *humilis (hum)* locus at 43B was a promising candidate to correspond to the *myosinV* gene. *humilis* is an uncharacterised gene and was the only gene with a female sterile phenotype to be identified in the mutagenesis. A female sterile phenotype would concur with the expression and localisation of the *myosinV* transcript during oogenesis. The complementation analysis of the *humilis* gene suggested that it was a large gene

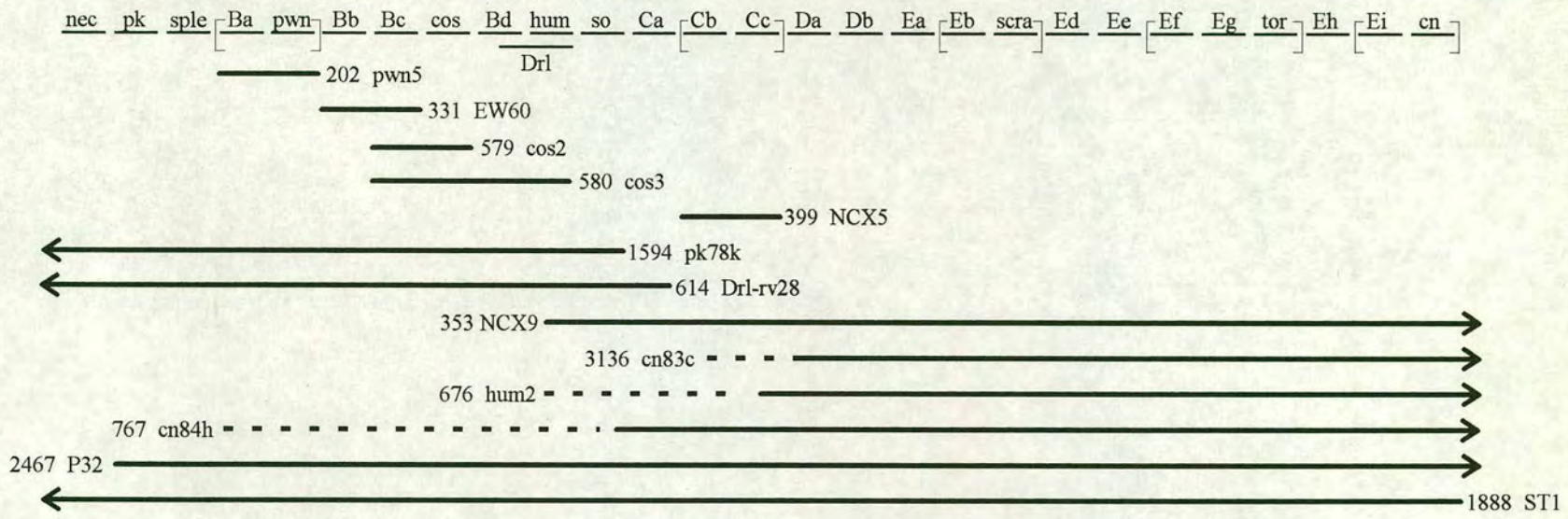

Figure 7.4 A complementation map of the 43A-E region modified from Heitzler *et al* (1993). Loci are shown relative to each other and to the chromosomal deficiencies used in the present study. Loci that have not been ordered with respect to each other are enclosed in square brackets. Chromosomal deficiencies are labelled with name and stock number - see also table 7.4. Dashed lines indicate that the deficiency breakpoint is not well defined. Arrows indicate that deficiency extends beyond the 43 region. *nec: necrotic, pk: prickle, sple: spiny-legs, pwn: l(2)pawn, cos: costa, hum: humilis, Drl: Droplet, so: sine oculis, scra: scraps, tor: torso* and *cn: cinnabar*.

(Pascal Heitzler, personal communication) and again this agrees with what is known about the *myosinV* gene. It was decided to study the *humilis* gene further in an attempt to establish if it matched the *myosinV* gene. In order to achieve this, two female sterile alleles of *humilis* were obtained along with two deficiency stocks - ST1 which uncovers the entire 43BC region and NCX9 which breaks in the middle of the *humilis* gene (table 7.1 and figure 7.4).

Table 7.1 Fly stocks used in *humilis* analysis.

Line	Name	Source	Comments
hum^1	$fs^2\ hum^1\ cn^1\ bw^1\ sp^1$ /CyO	Cambridge	homozygotes should have white eyes & straight wings
hum^5	$fs^2\ hum^5\ bw^D$ /CyO	Cambridge	homozygotes should have brown eyes & straight wings
353	*Df(2R)NCX9/CyO*	Cambridge	uncovers half of *hum* gene
1888	*Df(2R)ST1/CyO*	Cambridge	uncovers all of *hum* gene

No homozygotes were found in the two *humilis* female sterile lines, so in order to examine the female sterile phenotype, the two different alleles had to be crossed to generate hum^1/hum^5 flies. This cross is described in figure 7.5. These hum^1/hum^5 flies were then crossed to wild type OrR flies and to themselves to determine whether they were female or male sterile (table 7.2). The hum^1/hum^5 flies were found to be female sterile but not male sterile. The hum^1/hum^5 female sterile flies laid normal looking, mature eggs but these arrested during embryogenesis and so failed to hatch. Arrested embryos were dechorionated (2.2.8.2) and examined for defects. The embryos from a hum^1/hum^5 female x OrR male cross, showed several defects including failure of head involution, missing thoracic segments, dorsal closure failure and midgut failure (fig 7.6A). The arrested embryos from the hum^1/hum^5 female x hum^1/hum^5 male cross had a similar but slightly more severe phenotype (fig 7.6B) indicating that there is a zygotic component to the mutation. These results are summarised in table 7.2. The anterior defects such as missing thoracic segments and

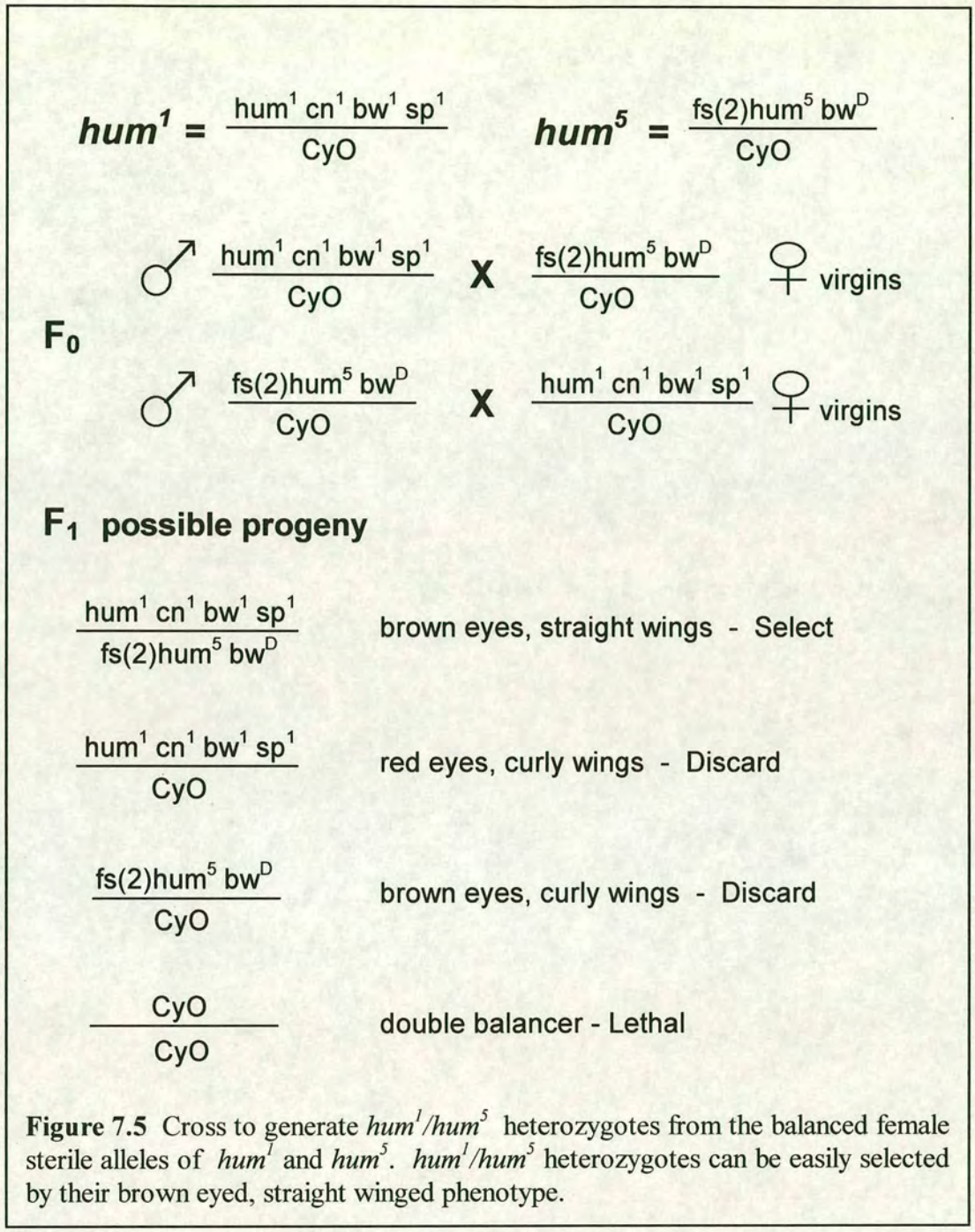

Figure 7.5 Cross to generate *hum*^{1}/*hum*^{5} heterozygotes from the balanced female sterile alleles of *hum*^{1} and *hum*^{5}. *hum*^{1}/*hum*^{5} heterozygotes can be easily selected by their brown eyed, straight winged phenotype.

failure of head involution are consistent with the idea that *humilis* corresponds to *myosinV* as the *myosinV* transcript is localised to the anterior of the oocyte.

Table 7.2 *hum^{1}/hum^{5}* sterility analysis.

cross	sterile?	embryonic defects
hum^{1}/hum^{5} female x OrR male	yes	missing thoracic segments, failure of head involution, dorsal closure failure, midgut failure
OrR female x *hum^{1}/hum^{5}* male	no	-
hum^{1}/hum^{5} female x *hum^{1}/hum^{5}* male	yes	severe segmentation defects, failure of head involution, dorsal closure failure, midgut failure

In an attempt to match the *humilis* mutation to the *myosinV* gene, *in situ* hybridisation was performed to examine the localisation pattern of the *myosinV* transcript in the ovaries of *hum^{1}/hum^{5}* flies. The ovaries were probed with the digoxigenin labelled, 0.8kb *Eco*RI fragment of pNMC7a (2.3.1). The localisation of the *myosinV* transcript in *hum^{1}/hum^{5}* flies appeared to be identical to that observed in wild type ovaries (fig 7.7A). The normal localisation of the *myosinV* transcript in *hum^{1}/hum^{5}* flies does not exclude the possibility that *humilis* and *myosinV* are the same gene. The *hum^{1}* and *hum^{5}* alleles were generated using EMS as a mutagen so are most likely to consist of single base changes which would not necessarily affect transcription and localisation.

To further characterise the *humilis* phenotype an attempt was made to determine whether the anterior pattern defects observed in the embryos of *hum^{1}/hum^{5}* mothers, are linked to the mislocalisation of the anterior determinant *bicoid*. *in situ* hybridisation was performed on the ovaries of *hum^{1}/hum^{5}* flies using a probe made from a 2.5kb *Eco*RI fragment of the *bicoid* cDNA. Localisation of the *bicoid* transcript was found to be entirely normal within the mutant ovaries (fig 7.7B). The *humilis* phenotype therfore appears to be unconnected to the localisation of the *bicoid* transcript.

Because the *hum^{1}* and *hum^{5}* alleles are probably point mutations, and because no homozygous flies were recovered from these lines, it was decided to look at the effect

Figure 7.6 The *humilis* female sterile phenotype. A) Arrested embryo from a hum^{1}/hum^{5} female x *OrR* male cross - defects include failure of head involution, abnormal mouth hooks (arrow), missing thoracic segments (arrowheads) and midgut failure. B) Arrested embryo from a hum^{1}/hum^{5} female x hum^{1}/hum^{5} male cross - defects are similar but more severe to those above, including drastically reduced mouth hooks (arrowhead) and yolk not confined to the gut (arrow). A: anterior, P: posterior.

Figure 7.7 Localisation of the *myosinV* and *bicoid* transcripts in hum^{1}/hum^{5} ovaries. A) In hum^{1}/hum^{5} mutant ovaries the *myosinV* transcript localises normally to the anterior margin of stage 9/10 oocytes (arrow). B) In hum^{1}/hum^{5} mutant ovaries the *bicoid* transcript localises normally to the oocyte's anterior margin (e.g. stage 10, arrow) and to the anterior cortex of stage 11/12 oocytes (arrowhead).

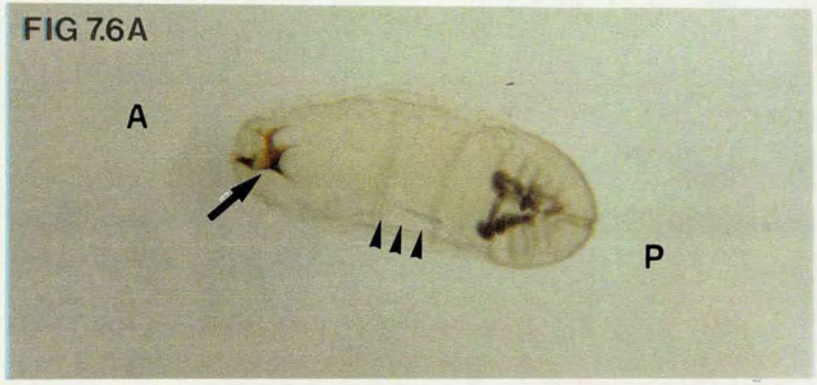
FIG 7.6A
A
P

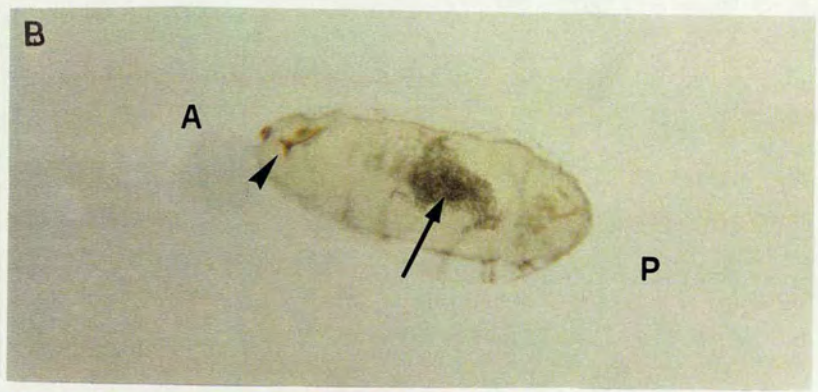
B
A
P


FIG 7.7A


B

of crossing *hum*^{1} and *hum*^{5} to flies carrying deficiencies in the 43 region. Both *hum*^{1} and *hum*^{5} flies were crossed to ST1 and NCX9 deficiency stocks. ST1 uncovers the entire 43BC region and NCX9 breaks in the middle of the *humilis* gene. These deficiency stocks are described in table 7.1 and figure 7.4. A schematic plan of the necessary crosses is given in figure 7.8.

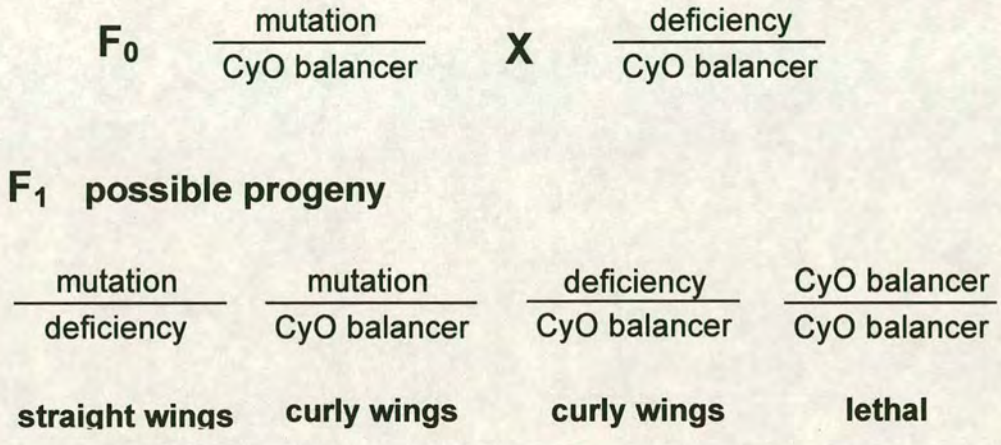

Figure 7.8 Strategy for the *humilis* x deficiency crosses. The F1 generation is screened for straight winged flies. If none are found it can be assumed that the combination of mutation plus deficiency is lethal.

hum^{1}/ST1 was found to be lethal and *hum*^{5}/ST1 resulted in reduced viability. *hum*^{1}/NCX9 and *hum*^{5}/NCX9 were found to be viable and so were tested for male and female sterility by crossing to OrR flies. These results are summarised in table 7.3.

Table 7.3 *humilis* x deficiency crosses

cross	lethal	female sterile	male sterile
hum^{1}/NCX9	no	no	no
hum^{5}/NCX9	no	yes	no
hum^{1}/ST1	yes	-	-
hum^{5}/ST1	reduced viability	yes	?

Arrested embryos arising from the above crosses were examined and again found to have anterior defects such as abnormal segmentation and failure of head involution along with dorsal closure failure and midgut failure. The localisation patterns of the *myosinV* and *bicoid* transcripts were again assessed by *in situ* hybridisation to the ovaries of viable flies. Transcript localisation was found to be unperturbed by the combination of mutation plus deficiency.

The above results suggest that the hum^{1} mutation occurs in an important functional or regulatory region so is lethal in combination with ST1 which uncovers the entire gene. However, in combination with NCX9 it is neither lethal nor female sterile, suggesting that the hum^{1} mutation occurs outwith the area uncovered by NCX9 deficiency so that the two can complement one another. hum^{5} may occur in the female regulatory region of the gene, within the region that is uncovered by NCX9, such that a combination of mutation and deficiency results in female sterility.

7.2.4 Deficiency mapping of the *myosinV* gene

Despite the wealth of information accumulated on the *humilis* gene, there was still no evidence that it corresponded to the *myosinV* gene. It was therefore decided to refine the position of the *myosinV* gene within the 43BC region by deficiency mapping. Deficiency breakpoints cause an alteration in the size of genomic restriction fragments which can be detected as additional bands on genomic Southern blots. A number of fly stocks carrying deficiencies with breakpoints in the 43BC region were therefore obtained for Southern analysis. These deficiency lines are depicted in figure 7.4 and described in table 7.4.

Table 7.4 Deficiency stocks.

Stock No	Deficiency/ Balancer	Breakpoints
202	*Df(2R)pwn5, bw^D/ In(2LR)O, Cy dp^{lvl} pr cn^2*	[43B]; [43B]
331	*Df(2R)Ew60, bw^D/ In(2LR)O, Cy dp^{lvl} pr cn^2*	[43B]; [43B]
353	*Df(2R)NCX9, cn^- bw^D/ In(2LR)O, Cy dp^{lvl} pr cn^2*	43C3-7; 43F2
579	*Df(2R)cos-2 cn bw sp/ In(2LR)O, Cy dp^{lvl} pr cn^2*	[43B]; [43B]
580	*Df(2R)cos-3 cn bw sp/ In(2LR)O, Cy dp^{lvl} pr cn^2*	43B1; 43B1
676	*hum^2 bw^D/ In(2LR)O + Df(2R)cnS6, Cy dp^{lvl} pr cn^-*	43C3-7; 43F2-8
767	*Df(2R)cn84h/ In(2LR)SM5, al^2 Cy lt^v cn^2 sp^2*	43B3-C1;44A6-B1
1594	*Dr(2R) pk78k/ CyO*	42E3; 43C3
2467	*Df(2R) P32/ CyO*	43A3; 43F6
3136	*Cn83c/ SM5*	43C5-D1;44B5-C1

Genomic DNA was prepared from the above ten deficiency lines (2.6.1.1) and around 2μg of each prep was digested separately with *Bam*HI, *Eco*RI and *Xba*I. The digests were electrophoresed through a 0.8% agarose gel in 1X TAE then Southern blotted onto Hybond-N^+ in 0.4M NaOH. The Southern blots were initially probed with FIX1A genomic DNA. It is important to note that at this time FIX1A was believed to be a large single genomic insert containing the 3' region of the *myosinV* gene with the *c34* gene adjacent (see 6.2.4). The FIX1A genomic DNA was released from the λ bacteriophage arms by a *Not*I digest. Due to the difficulty in gel purification of large DNA fragments, the digest was separated through a 0.6% low melting point agarose gel and the genomic insert was excised and ^{32}P labelled in low melting point agarose using Pharmacia Ready-To-Go labelling kit (2.9.3.1). The deficiency line Southern blots were prehybridised, hybridised and washed according to standard protocols

(2.9.2). The resulting autorads are shown in figure 7.9.

The FIX1A probe hybridised to *Bam*HI fragments of 8kb and 6.5kb, *Eco*RI fragments of 7kb, 5kb and 2kb and an *Xba*I fragment of 7kb. There were several inconsistencies in the autorads due to uneven loading and partial digests, particularly in the set of *XbaI* digests. However, two lines 579 (*cos-2*) and 580 (*cos-3*) can be clearly seen to have additional bands in both the *Bam*HI and *Eco*RI digests. These extra bands are indicated by arrows in figure 7.9. Lines 579 and 580 are known to share the same proximal breakpoint between genes *l(2)43Bb* and *l(2)43Bc* (John Roote, personal communication) and this is consistent with the additional bands being of the same size in both lines. This result suggested that the *myosinV* and *c34* genes corresponded to two adjacent genes out of *l(2)43Ba*, *l(2)43Bb* and *l(2)43Bc*. Other genes in the vicinity such as *pawn* and *costa* were eliminated as candidates because they had already been cloned and shown not to encode either a class V unconventional myosin or a phosphate cotransporter.

To further refine the deficiency map, the deficiency line Southern blots were reprobed with smaller cDNA probes specific to the *myosinV* gene or the *c34* gene. The membranes were initially reprobed with the *myosinV* 2.2kb ovarian cDNA. This probe failed to detect the same additional fragments identified by the FIX1A probe. The membranes were later reprobed with the combined 6kb and 7kb *Xba*I fragments which cover much of the *myosinV* gene (see figure 6.14A). The X6/X7 probe hybridised to the 8kb and 6.5kb *Bam*HI fragments, *Eco*RI fragments of ~12kb, 5kb, 2kb and 1kb and the 7kb and 6kb *Xba*I fragments, but again failed to hybridise to the same extra bands in lines 579 and 580 as observed with the FIX1A probe (fig 7.10). It was therefore concluded that 579 and 580 deficiencies do not have breakpoints within the *myosinV* gene.

The Southern blots were subsequently reprobed with a 1.8kb *Pst*I fragment of cDNA 34. This probe hybridised to an 8kb *Bam*HI fragment, a 7kb *Eco*RI fragment and a 6kb *Xba*I fragment and also to the extra bands in the *Bam*HI and *Eco*RI digests of

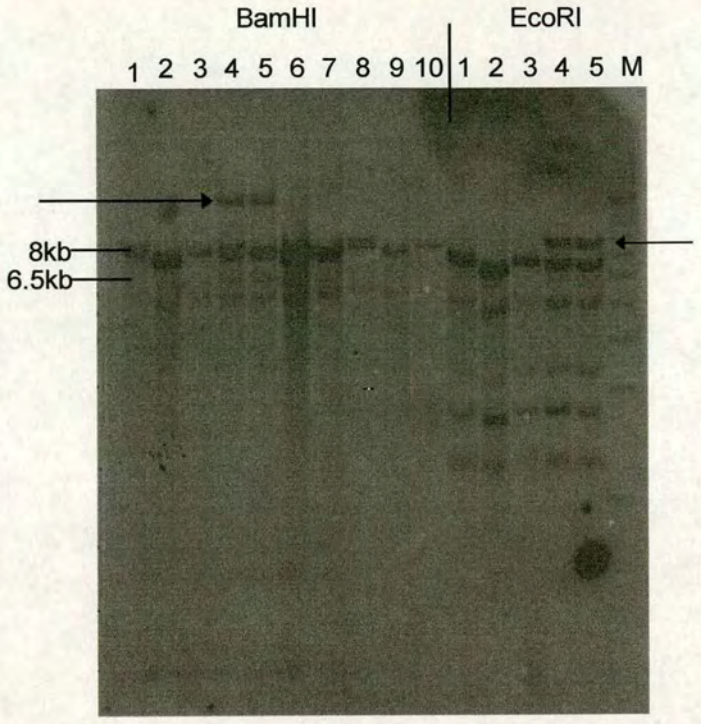

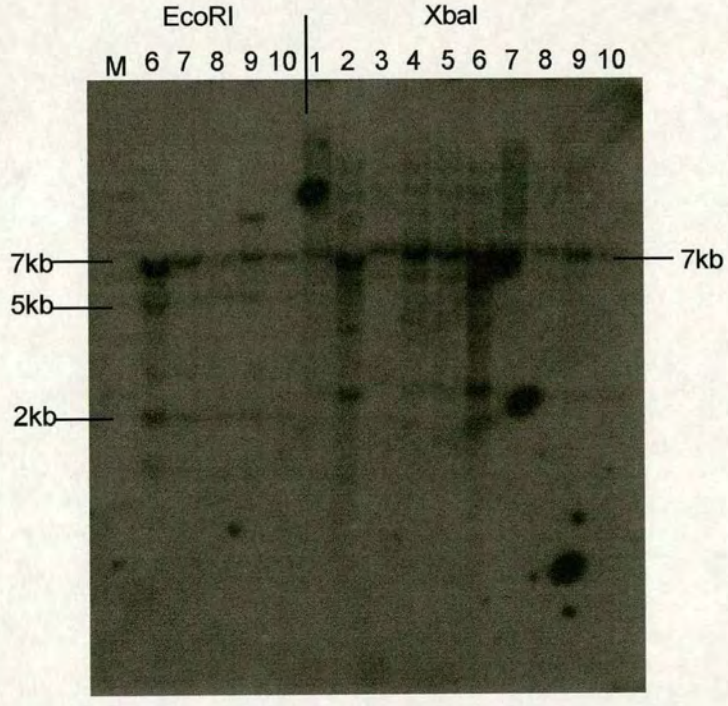

Figure 7.9 Southern blots of genomic DNA from ten deficiency lines, digested with *Bam*HI, *Eco*RI and *Xba*I and probed with FIX1A genomic DNA. The sizes of known restriction fragments are indicated, however some bands are due to partial digests. Two lines, 579 and 580, were found to have additional restriction fragments in both the *Bam*HI and *Eco*RI digests. These bands are marked with arrows. M: markers.

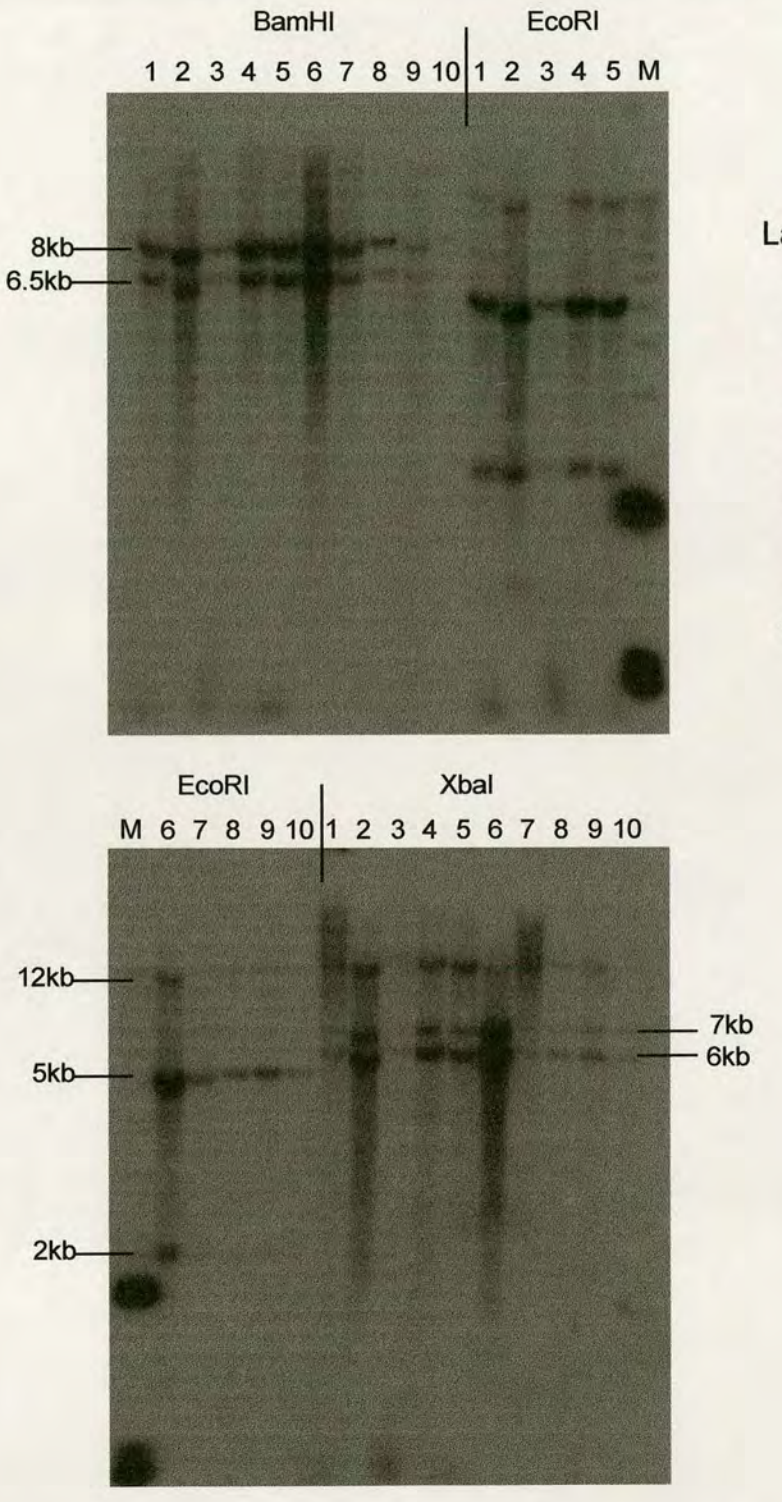

Figure 7.10 Southern blots of genomic DNA from ten deficiency lines, digested with *Bam*HI, *Eco*RI and *Xba*I and probed with the combined pP1X7 and pP1X6 genomic subclones, which include much of the *myosinV* gene. The sizes of known restriction fragments are indicated. No additional restriction fragments were detected in lines 579 and 580.

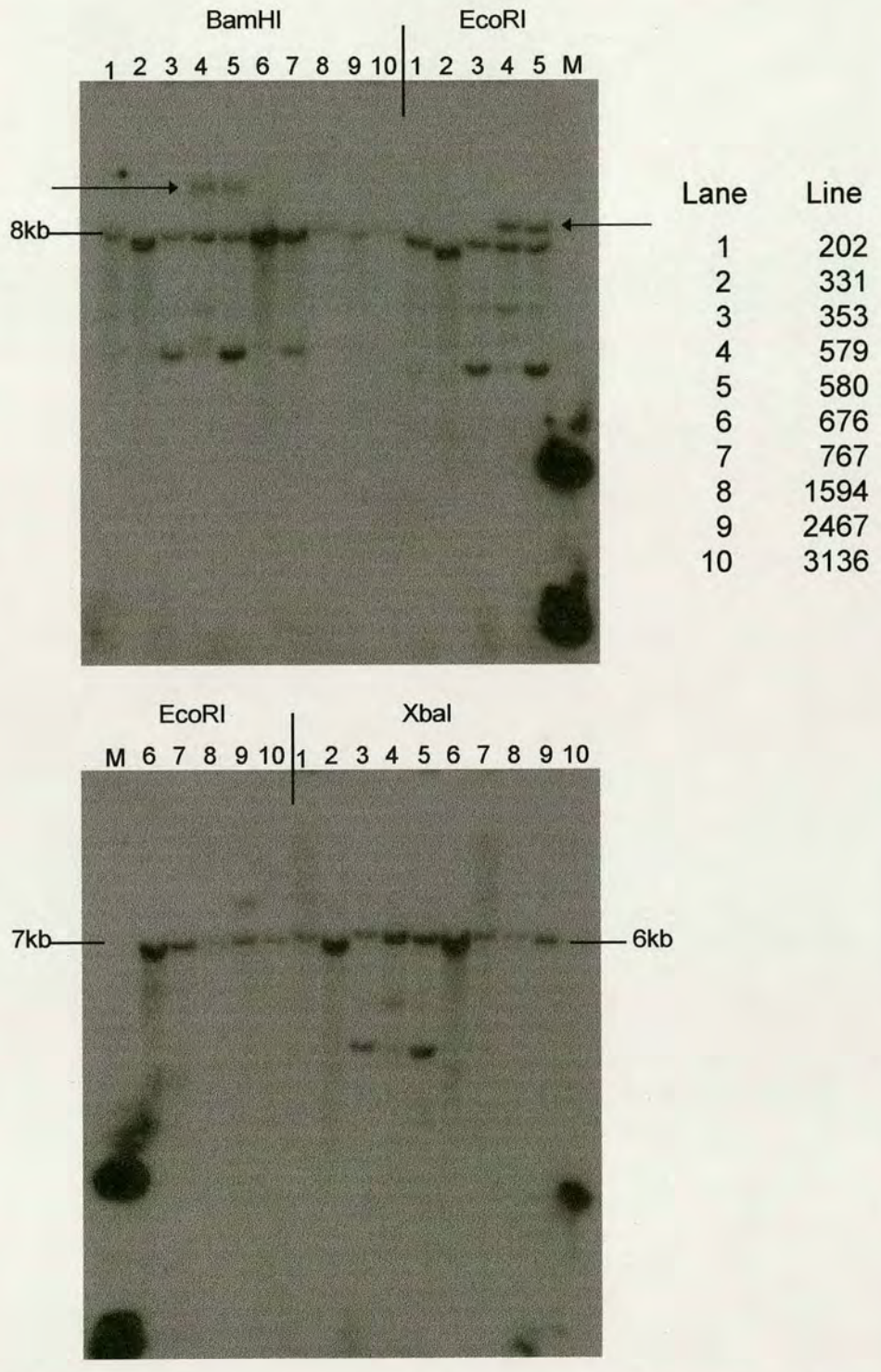

Figure 7.11 Southern blots of genomic DNA from ten deficiency lines, digested with *Bam*HI, *Eco*RI and *Xba*I and probed with a 1.8kb *Pst*I fragment of cDNA 34. The sizes of known restriction fragments are indicated. The cDNA 34 probe detected the same additional restriction fragments in the *Bam*HI and *Eco*RI digests of lines 579 and 580 as were detected by the FIX1A probe. These additional bands are marked with arrows.

lines 579 and 580 which had been detected by the FIX1A probe (fig 7.11). It therefore appeared that the *c34* gene was at least partially uncovered by the 579 and 580 deficiencies. On the basis of the above deficiency mapping result, and with the assumption that the *myosinV* and *c34* genes were adjacent on the chromosome, it was concluded that the *myosinV* gene corresponded to the *l(2)43Bb* gene and the *c34* gene corresponded to the *l(2)43Bc* gene. This is depicted in figure 7.12.

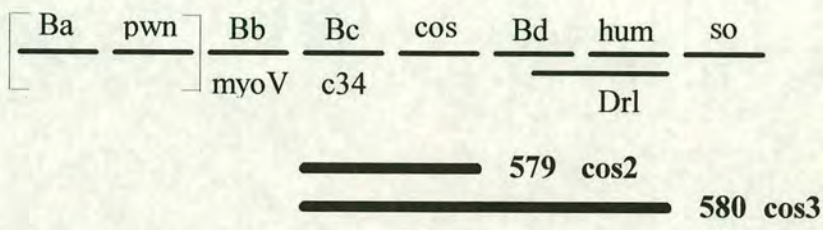

Figure 7.12 Proposed map locations of the *myosinV* and *c34* genes in the 43B region. Deficiency mapping indicated that deficiencies cos2 and cos3 uncover the *c34* gene but not the *myosinV* gene. With the assumption that the *myosinV* gene and the *c34* gene were adjacent on the chromosome, it was concluded that *myosinV* gene corresponds to locus *l(2)43Bb* while the *c34* gene corresponds to locus *l(2)43Bc*.

7.2.5 Genetic Analysis of the *l(2)43Bb* gene

l(2)43Bb was a locus identified in the genetic analysis of the 43 region by Heitzler *et al* (1993). Five mutant alleles of *l(2)43Bb* were recovered in Heitzler's study, on the basis of their failure to complement one another, however no further analysis of these alleles was reported. The five alleles were all homozygous lethal meaning that embryos homozygous for mutations in the *l(2)43Bb* gene arrest development before completing embryogenesis. In an attempt to relate the *l(2)43Bb* gene to the *myosinV* gene, several alleles of *l(2)43Bb* were obtained in order to study the phenotype of arrested embryos. These alleles are described in table 7.5.

Table 7.5 Alleles of *l(2)43Bb* used in genetic analysis.

Allele	Genetic Description	Source	Comments
$43Bb^1$	*l(2)43Bb*^{1} *bw*^{D} / *In(2LR)O, dp*^{lvl} *pr cn*^{2}	Cambridge	heterozygotes have brown eyes due to bw^D marker
$43Bb^2$	*l(2)43Bb[PZ04616]cn* / *In(2LR)O, Cy dp*^{lvl} *pr nec*^{JR} *cn*^{2}	Cambridge	P-element insertion allele
$43Bb^3$	*Tp(2;3) DX11 l(2)43Bb*^{3} *cn bw sp*/ *In(2LR)O, Cy dp*^{lvl} *pr Tp(2;2) pk-sple*^{26} *cn*^{2}	Cambridge	Transposition allele

To examine the homozygous lethal phenotype of the above *l(2)43Bb* alleles, it was first necessary to cross each *43Bb* stock to wild type OregonR flies to remove the balancer chromosome. This is because a cross of *43Bb*/balancer x *43Bb*/balancer would result in a quarter of the progeny being balancer/balancer for the second chromosome. Double balancer chromosomes are also embryonic lethal and would therefore be difficult to distinguish from the lethal *43Bb/43Bb* embryos. In a cross of *43Bb*/balancer x OrR/OrR the *43Bb*/OrR progeny have wild type straight wings and can therefore be easily separated from the curly winged OrR/balancer progeny. In the second cross, *43Bb*/OrR x *43Bb*/OrR, all possible progeny are viable except for *43Bb/43Bb,* so it can be assumed that those embryos which do not hatch into larvae after 24 hours are *43Bb/43Bb*. The strategy of these crosses is described in figure 7.13.

43Bb/OrR x *43Bb*/OrR crosses were set up in egg collection cages at 25°C. After a settling period, flies were allowed to lay for four hours on plates of Adh food supplemented with yeast paste. 100 eggs were then transferred to a fresh Adh/yeast plate and allowed to develop a further 24 hours at 25°C. After 24 hours, unhatched eggs were counted, dechorionated, mounted in Aquamount and examined under the microscope for defects. Some arrested embryos had their contents cleared (2.2.9) in order that the segmentation pattern of the cuticle could be examined under darkfield microscopy.

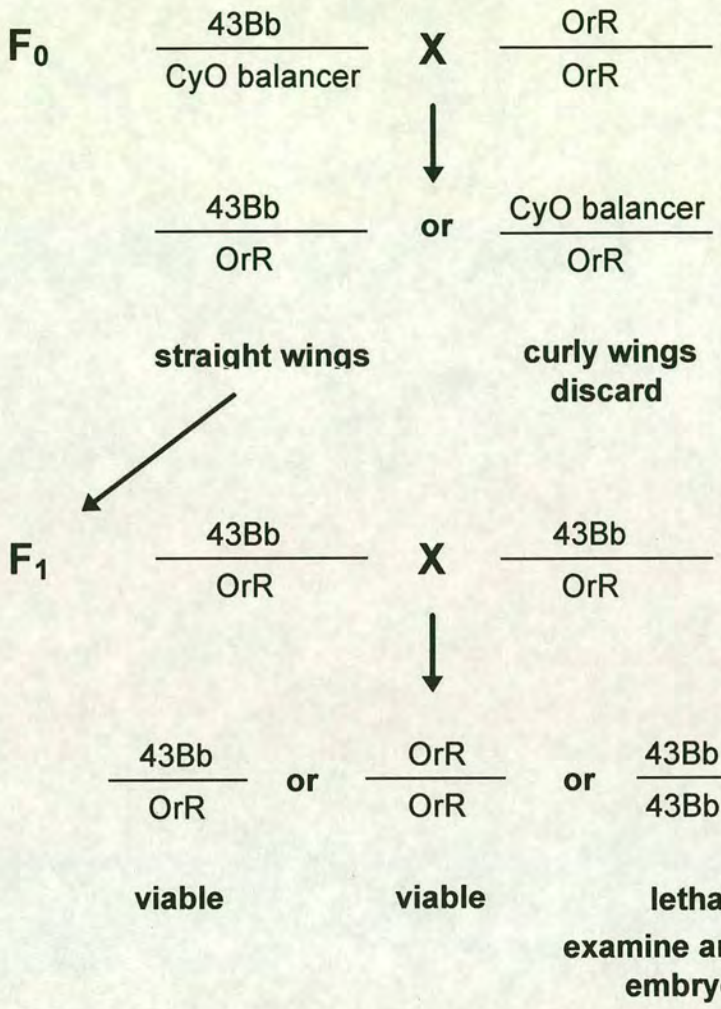

Figure 7.13 Strategy of crosses to examine the homozygous lethal phenotype of *l(2)43Bb* alleles. Each *l(2)43Bb* stock must first be crossed to *OrR* flies in order that the balancer chromosome be crossed out. This is to prevent confusion between the *l(2)43Bb* homozygous lethal embryos and lethal double balancer embryos.

In the cross of $43Bb^{1}$/OrR x $43Bb^{1}$/OrR an average of 24.5% of eggs failed to hatch. This is in agreement with a quarter of the progeny being predicted to be $43Bb^{1}/43Bb^{1}$. Many of the arrested embryos had reached a late stage of development and showed a range of defects including shortened length, failure of dorsal closure and failure of head involution. However the most striking feature of the arrested embryos was the defects in the tracheal system. The tracheal system is an intricately branched network

of respiratory tubes which supply oxygen to the interior tissues of the developing embryo. *43Bb^1/43Bb^1* embryos consistently showed defects in the tracheal system including many irregular breaks in the trachae, trachae not properly filled with air and trachae which are over curly and convoluted (fig 7.14A&B). To ensure that the observed defects in the tracheal system were not merely an artifact of mounting and drying, several embryos were dechorionated and mounted in Ringer's solution under a raised coverslip. Tracheal breaks could still be observed in these embryos, some of which were still living but had failed to hatch. Meanwhile, darkfield microscopy of late stage arrested embryos revealed a largely normal cuticle segmentation pattern (fig 7.14C).

To observe the effect the *43Bb^1* mutation in combination with the complete loss of one copy of the *43Bb* gene, flies carrying the *43Bb^1* allele were crossed to flies carrying the deficiency 1594 which uncovers the entire 43B region (figure 7.4 and table 7.4). Again, both stocks were first crossed to OrR flies to remove the balancer chromosomes. From the cross of *43Bb^1*/OrR x 1594/OrR an average 27.6% of embryos failed to hatch. These arrested embryos showed defects which were similar to, but more severe than the defects exhibited by *43Bb^1/43Bb^1* embryos. Overall the embryos had ceased development at an earlier stage than the *43Bb^1/43Bb^1* embryos and, in addition to more severe defects in the tracheal system, there were also defects in other tubule networks such as the gut and the malpighian tubules (fig 7.14D-E). In some embryos there was no evidence of a tracheal system while the yolk was clearly not confined to a gut (fig 7.14F).

The homozygous lethal phenotypes of the transposition allele *43Bb^2* and the P-element insertion allele *43Bb^3* were also studied, along with *43Bb^3* in combination with the deficiency 1594. *43Bb^2/43Bb^2* embryos showed similar defects to *43Bb^1/43Bb^1* embryos, while *43Bb^3/43Bb^3* and *43Bb^3/1594* embryos shared the more severe phenotype of the *43Bb^1*/1594 embryos. The results are summarised in table 7.6. The high hatch failure rates of crosses involving the *43Bb^3* allele suggest that embryos heterozygous for this allele have reduced viability.

Figure 7.14 Defects displayed by *l(2)43Bb* arrested embryos. A, B & C - Defects in Bb^{1}/Bb^{1} arrested embryos include A) over developed tracheal system and B) breaks in tracheal system (arrows), while C) darkfield photography reveals that the cuticle segmentation pattern is normal. D, E & F - Bb^{1}/1594 embryos arrest at an earlier stage and show more severe defects including D) failure of tubule networks such as gut and trachae, E) breaks in under-developed tracheal system (arrows) and F) failure of dorsal closure and head involution plus yolk not contained to a gut (arrow). Anterior is to the left.

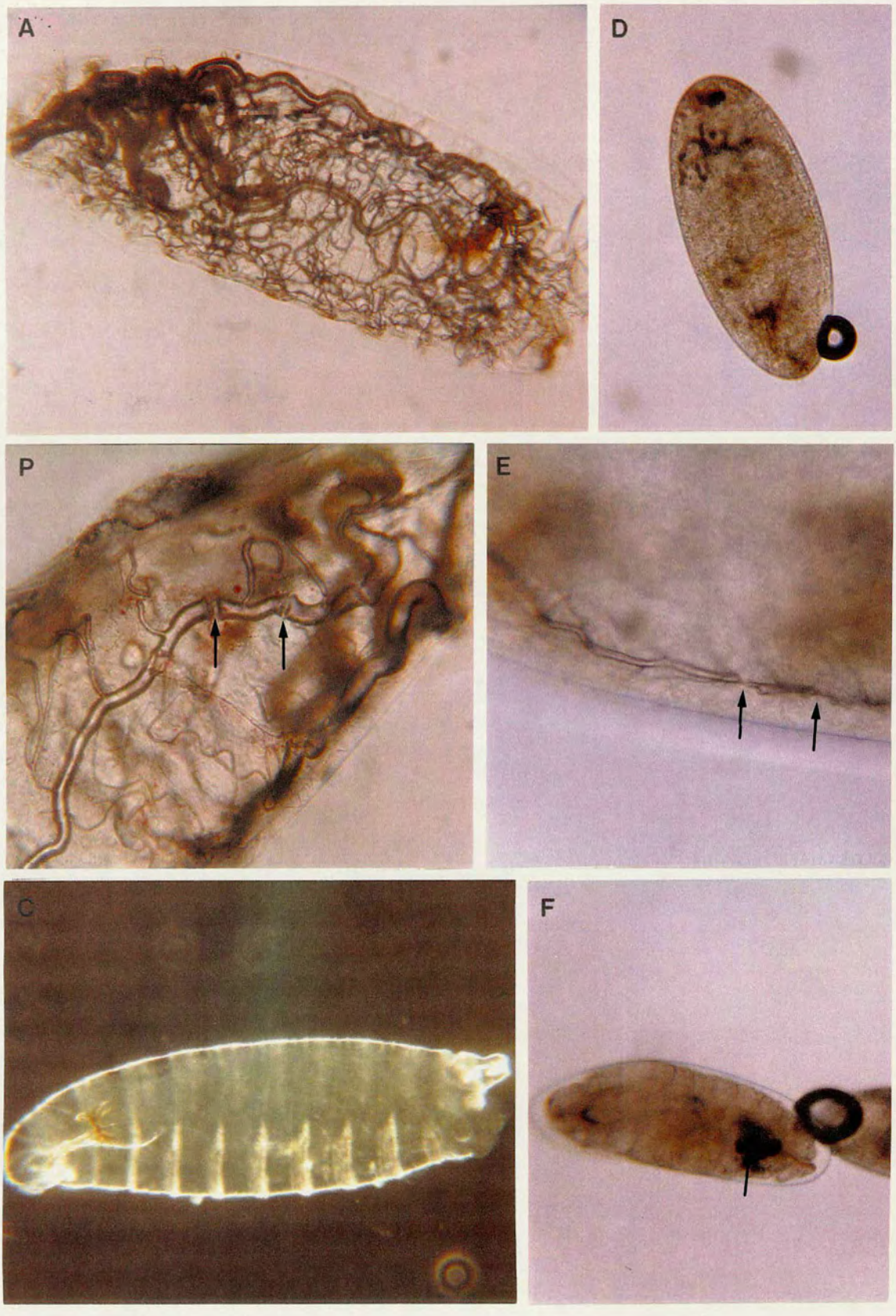
A
D
P
E
C
F

Table 7.6 Summary of results of *43Bb* crosses

cross	% hatch failure	defects observed in arrested embryos
43Bb^{1}/OrR x *43Bb*^{1}/OrR	24.5	embryos arrested at late stage, tracheal defects
43Bb^{1}/OrR x 1594/OrR	27.6	embryos arrested at mid stage, tracheal system defective or absent, defects in other tubule networks
43Bb^{2}/OrR x *43Bb*^{2}/OrR	27.2	embryos arrested at late stage, tracheal defects
43Bb^{3}/OrR x *43Bb*^{3}/OrR	76.0	embryos arrested at mid stage, tracheal system defective or absent, defects in other tubule networks
43Bb^{3}/OrR x 1594/OrR	41.3	embryos arrest at early stage, tracheal system defective or absent, severe defects in gut and malpighian tubules

The *43Bb* alleles all show phenotypes consistent with defects in the formation of tubule networks such as the gut, the malpighian tubules, and in particular, the tracheal system. This phenotype suggests a failure of the guidance system which controls the formation of tubules, with the *43Bb* gene perhaps encoding some sort of signpost protein. While this phenotypic analysis of the *43Bb* gene produced very interesting results, it provided no further indication that the *43Bb* gene corresponded to the *myosinV* gene. Additional molecular information was also becoming available which made it increasingly unlikely that the *43Bb* gene corresponded to the *myosinV* gene.

7.2.6 Problems with the mapping of the *myosinV* gene to *43Bb*

The *myosinV* gene was placed at *43Bb* on the basis of a deficiency mapping result which placed the adjacent *c34* gene at *43Bc*. However several pieces of data did not

concur with this result. Large and disruptive mutations such as P-element insertions and transpositions would be expected to give an altered banding pattern on Southern analysis. However, the *43Bb*^{2} P-element allele did not give an altered banding pattern when probed with a *myosinV* probe while the transposition allele *43Bb*^{3} gave an altered banding pattern when probed with a *c34* probe but not with a *myosinV* probe. The *43Bb*^{3} transposition allele was derived from the same progenitor chromosome as deficiency lines 579 and 580, suggesting that all three altered banding patterns could be due to a polymorphism in the progenitor chromosome rather than due to a genuine deficiency breakpoint.

Confirmation that the *l(2)43Bb* gene did not correspond to the *myosinV* gene came from the discovery of the *az2* gene adjacent to the *myosinV* gene (see 6.2.7) and the simultaneous realisation that FIX1A consisted of two independent recombinant phage, meaning that the *myosinV* gene and the *c34* gene were not adjacent on chromosome 2R and were not contained on the same fragment of cloned genomic DNA (see 6.2.12). The *myosinV* gene had been mapped to *43Bb* on the basis of being adjacent to the *c34* gene and now this was clearly not the case. A subsequent dot blot analysis of recombinant P1's from the 43BC region indicated that the *myosinV* gene hybridised to P1 DS00574 (Bryce MacIver, personal communication). This P1 had been shown by the *Drosophila* Genome Sequencing Project to map to the 43C region as opposed to the 43B region. Genetic analysis was therefore resumed in the attempt to link the adjacent *myosinV* and *az2* genes to identified loci in the 43C region.

The *c34* gene, meanwhile, failed to hybridise to any of the recombinant P1's from the 43BC region. A subsequent Southern analysis of several deficiency lines and mutant alleles with the same progenitor chromosome as lines 579 and 580 confirmed the suspicion that the altered banding pattern observed with the *c34* probe was in fact due to a polymorphism in the progenitor chromosome used to derive these lines (data not shown). This meant that there was now nothing to place the *c34* gene in the 43BC region. In order to confirm that the *c34* gene does not map to 43BC, *in situ* hybridisation to polytene chromosomes was performed using the pE7 genomic

subclone which covers the *c34* gene (see fig 6.14B) as a probe (2.3.5). The pE7 probe hybridised to several sites in the genome but not to 43BC. This multiple hybridisation was probably due to repeat sequences in the genomic DNA used as a probe. However, the probe did not hybridise anywhere in the 43BC region confirming that the *c34* gene is not adjacent to the *myosinV* gene.

7.2.7 Analysis of the 43C region

P1 dot blot analysis indicated that the *myosinV* gene mapped within the 43C region. According to Heitzler's map (fig 7.4), this means that the *myosinV* gene and the adjacent *az2* gene should correspond to two adjacent loci out of *43Ca*, *43Cb*, *43Cc* and *43Da*. Heitzler *et al* (1993) were unable to order loci *43Cb* and *43Cc* with respect to each other, indicating that they map close together physically. It was therefore speculated that loci *43Cb* and *43Cc* may correspond to the *myosinV* and *az2* genes as these genes are known to be approximately 1kb apart. In order to refine the position of the *myosinV* and *az2* genes within the 43C region, two deficiency lines which partially uncover the 43C region were obtained for Southern analysis to determine whether their breakpoints were associated with either gene. The *Drl-rv28* deficiency uncovers an area of the 43 region, proximal to, and including *43Ca* while deficiency *NCX5* uncovers *43Cb* and *43Cc* (fig 7.4 and table 7.7).

Table 7.7 Deficiency Stocks in 43C region

Stock No	Deficiency/Balancer	Breakpoints
614	*Df(2R)Drl-rv28 / In(2LR)O, Cy dp^{lvl} pr cn^{2}*	42D1; 43B3
399	*Df(2R)NCX5 cn bw sp / In(2lR)O Cy dp^{lvl} pr cn*	[43C]; [43C]

Genomic DNA was prepared from the above two deficiency lines and also from OrR and deficiency lines 579 and 580 (table 7.4). These two lines were derived from the same genetic background as line 399 (*NCX5*) and were included as controls for

polymorphisms in the progenitor chromosome. No lines with the same genetic background as line 614 (*Drl-rv28*) were available. Around 5µg of each prep was digested separately with *Bam*HI and *Eco*RI then electrophoresed through a 0.8% agarose gel in 1X TAE and Southern blotted onto Hybond-N^+ in 0.4M NaOH. The deficiency blots were initially probed with a combination of labelled genomic subclones pP1X7 and pP1X6, which include much of the *myosinV* gene and the entire *az2* gene (see fig 6.14). The deficiency blots were prehybridised, hybridised and washed according to standard protocols (2.9.2). The resulting autorad is shown in figure 7.15.

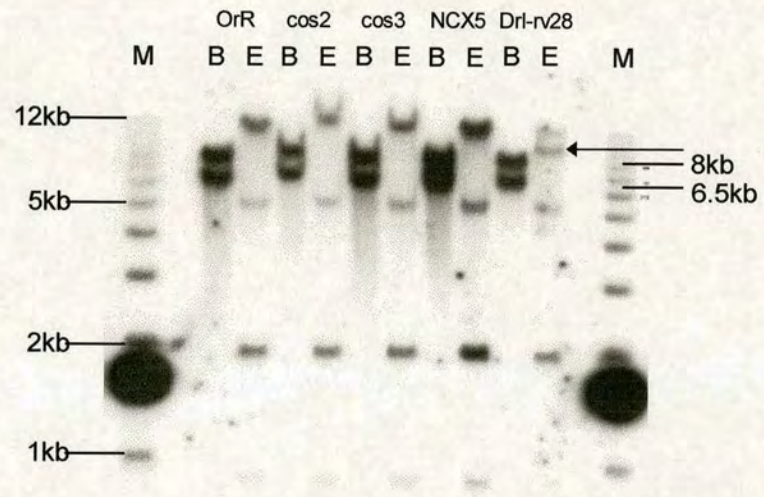

Figure 7.15 Southern blot of genomic DNA from OrR and deficiency lines *cos2*, *cos3*, *NCX5* and *Drl-rv28*, probed with the combined pP1X6 and pP1X7 probes. These probes hybridise to *Bam*HI fragments of 6.5kb and 8kb, and *Eco*RI fragments of around 1kb, 2kb, 5kb and 12kb. However in deficiency line *Drl-rv28* and additional *Eco*RI fragment of around 10kb was also detected. This band is marked with an arrow. M: markers, B: *Bam*HI, E: *Eco*RI.

The X6/X7 probe hybridised to *EcoRI* fragments of 1kb, 2kb, 5kb and 12kb in each line, indicating that the upstream *Eco*RI fragment in the unmapped region of the *myosinV* gene is 12kb. The X6/X7 probe hybridised to *Bam*HI fragments of 6.5kb and 8kb in each line, indicating that the upstream *Bam*HI fragment in the unmapped region of the *myosinV* gene must be either 6.5kb or 8kb because it is indistinguishable on the autorad from the already mapped fragments. However, in line 614 (*Drl-rv28*), the probe hybridised to an additional *Eco*RI fragment of around 10kb. The fact that deficiency *Drl-rv28* results in an extra *Eco*RI fragment but not an extra *Bam*HI fragment, suggested that the deficiency breakpoint is proximal to the *Bam*HI site but distal to the *Eco*RI site as depicted in figure 7.16. The *NCX5* deficiency, however, does not give rise to any additional restriction fragments, indicating that the deficiency breakpoints lie outwith the restriction fragments detectable by the X6/X7 probe. These data were interpreted to mean that the two deficiencies overlap rather than share a common breakpoint, as depicted in figure 7.16.

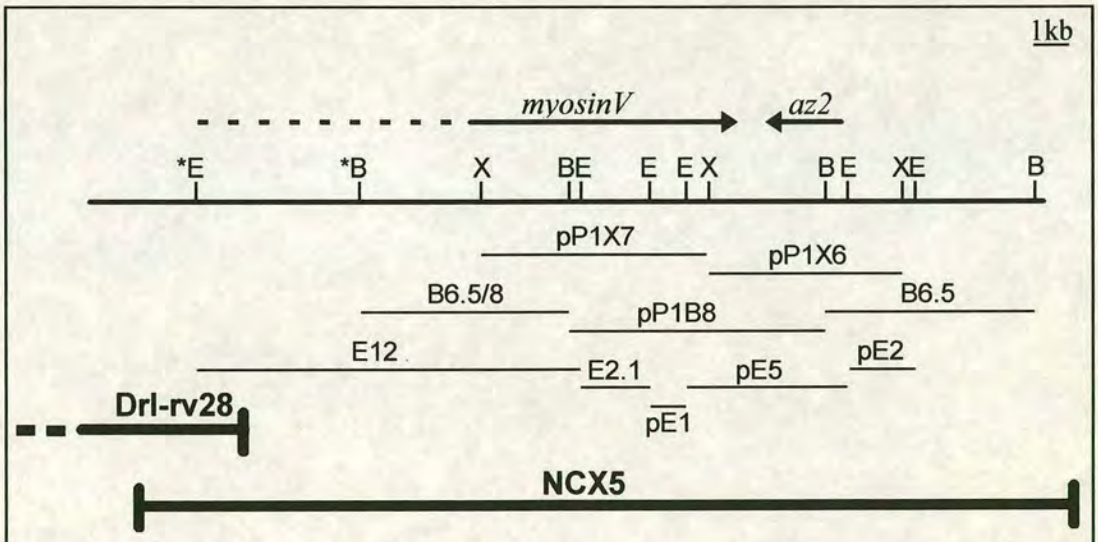

Figure 7.16 Schematic representation of deficiency mapping results. Deficiency line *Drl-rv28* genomic DNA gives an additional 10kb *Eco*RI restriction fragment when probed with the combined X6/X7 probes, but no additional *Bam*HI fragments. This indicates that the deficiency breakpoint is distal to the **Eco*RI site but proximal to the **Bam*HI site. Deficiency line *NCX5* genomic DNA does not give rise to any additional restriction fragments when probed with the combined X6/X7 probe, indicating that the deficiency breakpoints lie outwith the restriction fragments detectable by this probe. The two deficiencies, therefore, do not share a common breakpoint. B: *Bam*HI, E: *Eco*RI, X: *Xba*I.

The above deficiency mapping result suggested that the *myosinV* and the *az2* genes were distal to the *Drl-rv28* breakpoint, but were within the region uncovered by *NCX5*. Comparison with Heitzler's map of the 43 region (fig 7.4) would indicate that the *myosinV* and *az2* genes correspond to loci *43Cb* and *43Cc*. If this is indeed the case, the physical proximity of the *myosinV* and *az2* genes may explain why it was not possible to order loci *43Cb* and *43Cc* by deficiency mapping. However, in the absence of a control line with the same genetic background as *Drl-rv28*, it was not possible to eliminate the possibility that the result was due to a polymorphism in the progenitor chromosome of deficiency line *Drl-rv28*.

In order to confirm that the *myosinV* and *az2* genes corresponded to loci *43Cb* and *43Cc*, and in an attempt to distinguish between these two unordered loci, it was decided to study X-ray induced alleles of *43Cb* and *43Cc*. X-ray generated mutations tend to include large deletions or rearrangements which give rise to altered banding patterns on Southern analysis. In contrast, EMS generated alleles tend to be point mutations which do not cause altered banding patterns unless they actually occur within a restriction site. Most of the alleles generated by the analysis of Heitzler *et al* (1993) were EMS induced, however an X-ray induced allele existed for both *43Cb* and *43Cc*. These are described in table 7.8.

Table 7.8 X-ray induced alleles of *43Cb* and *43Cc*

Allele	**Genetic Description**	**Source**	**Comments**
$43Cb^{1}$	*l(2)43Cb^{1} cn bw sp / In(2LR)O,Cy dp^{lvl} pr cn^{2}*	Cambridge	X-ray allele
$43Cc^{4}$	*l(2)43Cc^{4} cn bw sp / In(2LR)O,Cy dp^{lvl} pr cn^{2}*	Cambridge	X-ray allele

Genomic DNA was prepared from OrR, *43Cb^{1}* and *43Cc^{4}* flies. DNA was also prepared from lines 579 and 580 which have the same genetic background as *43Cb^{1}* and *43Cc^{4}* and therefore serve as a control for polymorphisms in the progenitor

chromosome. DNA from each prep was digested with *Bam*HI, *Eco*RI or *Xba*I then Southern blotted as previously described. The membrane was initially probed with the X6/X7 probe which hybridised to the expected 6.5kb and 8kb *Bam*HI fragments, the 1kb, 2kb, 5kb and 12kb *Eco*RI fragments and the 6kb and 7kb *Xba*I fragments. However, in the $43Cc^4$ digest the probe hybridised to an additional *Eco*RI fragment of around 15kb. To confirm that this extra band was associated with the upstream region of the *myosinV* gene, the membrane was stripped and reprobed with the pP1X7 probe alone, which contains only *myosinV* sequence. Again this additional 15kb *Eco*RI fragment was detected with allele $43Cc^4$, confirming that it was associated with the *myosinV* gene and not the *az2* gene (fig 7.17). In addition, hybridisation with the pP1X7 probe alone confirmed the upstream *Bam*HI fragment as 6.5kb.

It was possible that the large, additional *Eco*RI fragment detected in allele $43Cc^4$ by the pP1X7 probe could be due to a partial digest of line $43Cc^4$ genomic DNA. To eliminate this possibility, Southern analysis was performed on line $43Cc^4$ genomic DNA which had been digested for 30 minutes, two hours or overnight with *Eco*RI. The digests were blotted as described above then probed with the pP1X7 probe. The pP1X7 probe is known to detect *Eco*RI fragments of 1kb, 2kb and 12kb. Figure 7.18 shows that after a 30 minutes or two hour digest, there was an additional partial digest band at 3kb while the 12kb band was obscured by undigested material. However, after overnight digestion with *Eco*RI, the 3kb partial digest band had almost disappeared but the additional 15kb band was the same intensity as the 12kb band. This indicates that the 15kb band is not due to a partial digest, but to a genuine mutation in $43Cc^4$.

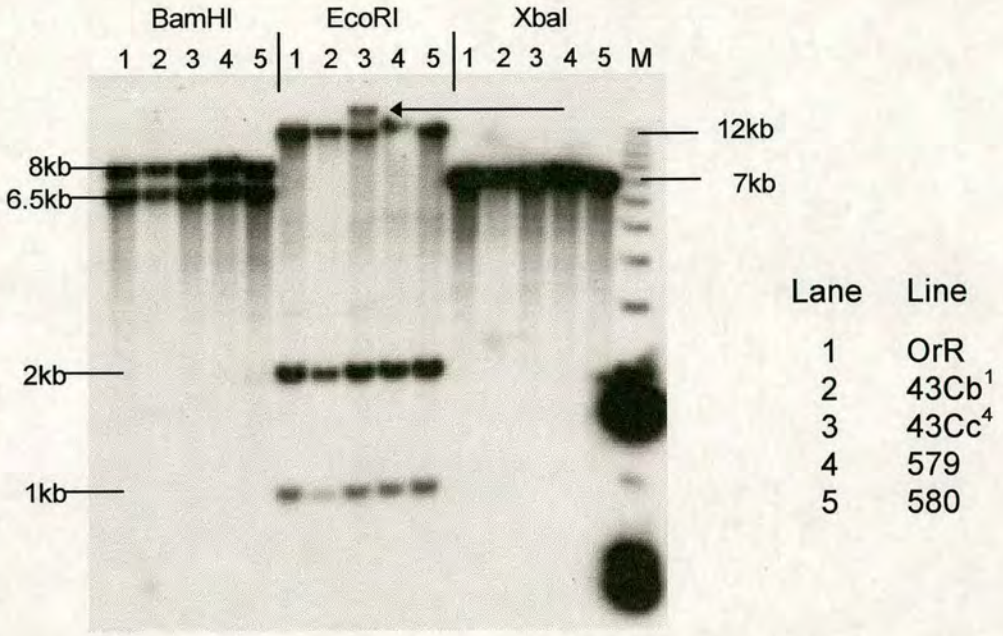

Figure 7.17 Southern blot of genomic DNA from X-ray alleles of *43Cb* and *43Cc*, and control lines *OrR*, 579 and 580, digested with *Bam*HI, *Eco*RI and *Xba*I then probed with the *myosinV* specific pP1X7 probe. The sizes of known restriction fragments are indicated. The $43Cc^4$ X-ray mutation was found to give rise to an additional *Eco*RI fragment of around 15kb. This additional band is marked with an arrow. M: markers.

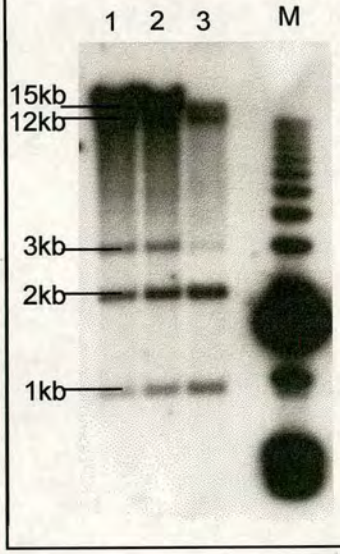

1 30 minute digest
2 2 hour digest
3 overnight digest
M markers

Figure 7.18 Southern blot of $43Cc^4$ genomic DNA digested with *Eco*RI for varying lengths of time, then probed with the pP1X7 probe. The sizes of known restriction fragments are indicated. After a 30 minute or two hour digest, there was an additional partial digest band at 3kb while the 12kb and 15kb bands were obscured by undigested material. However, after overnight digestion with *Eco*RI, the 3kb partial digest band had almost disappeared but the additional 15kb band was the same intensity as the 12kb band.

That the pP1X7 probe detects an additional 15kb *Eco*RI fragment in *43Cc*^{4} genomic DNA, but no additional *Bam*HI fragments, indicates that the *43Cc*^{4} mutation must uncover the *Eco*RI site but map proximal to the *Bam*HI as depicted in figure 7.19. This means that the *43Cc*^{4} mutation maps 3-4kb upstream of known *myosinV* coding sequence. To date, the very 5' end of the *myosinV* gene, including the translational start site, has not actually been cloned. From sequence comparison with other class V unconventional myosins it has been estimated that an additional 150bp remains to be cloned. It is therefore possible that the *myosinV* gene contains a large first intron, in common with related genes such as myosinVI and spectrin. It may be that the *myosinV* gene corresponds to locus *43Cc* and the *43Cc*^{4} mutation affects the first exon, 3-4kb upstream of presently known coding sequence. A large first intron would also explain why it has not been possible to obtain the very 5' end of the *myosinV* gene by 5'RACE from the pP1X7 subclone. Alternatively, the *43Cc*^{4} mutation may map to the upstream regulatory region of the *myosinV* gene.

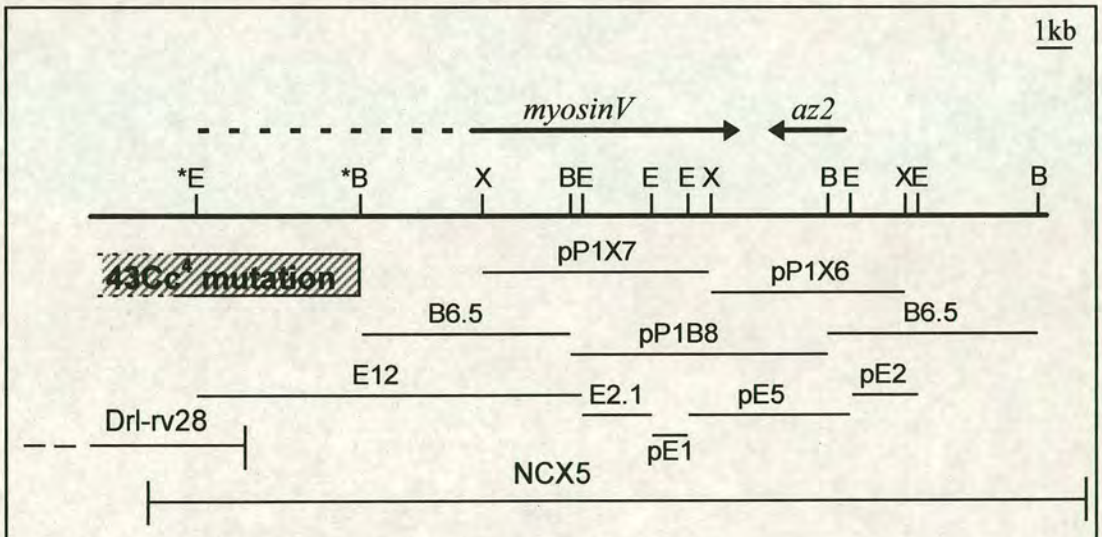

Figure 7.19 Schematic representation of X-ray allele analysis. X-ray allele 43Cc^4 genomic DNA gives an additional ~15kb *Eco*RI fragment, but no additional B*am*HI fragments, when probed with the combined X6/X7 probes. This indicates that the mutation uncovers the **Eco*RI site but is upstream of the **Bam*HI site as depicted above. B: *Bam*HI, E: *Eco*RI, X: *Xba*I.

From the above X-ray allele data alone, it can be concluded that locus *43Cc* either corresponds to the *myosinV* gene or is immediately proximal to the *myosinV* gene. Taking into account the fact that loci *43Cb* and *43Cc* are unordered with respect to each other, this gives four possibilities for the mapping of the *myosinV* and *az2* genes to loci in the 43 region. These possibilities are depicted in figure 7.20A-D. The deficiency analysis of lines *Drl-rv28* and *NCX5* suggested that the *myosinV* and *az2* genes corresponded to loci *43Cb* and *43Cc*. Even if the *Drl-rv28* result is disregarded due to lack of a progenitor chromosome control, two of the possibilities shown in figure 7.20 can be eliminated by the *NCX5* result alone. *NCX5* uncovers loci *43Cb* and *43Cc* (fig 7.4) but was shown not to break between the *myosinV* and *az2* genes, thereby eliminating the possibilities shown in figure 7.20A and 7.20D. Figure 7.20C places the *myosinV* gene at *43Da*, but as the original polytene *in situ* result mapped the *myosinV* gene to 43BC and a P1 dot blot refined this to 43C (Bryce MacIver, personal communication) this seems unlikely. Consideration of all the available data therefore leads to the conclusion that the *myosinV* gene corresponds to locus *43Cc* and the *az2* gene corresponds to *43Cb*, as depicted in figure 7.20B.

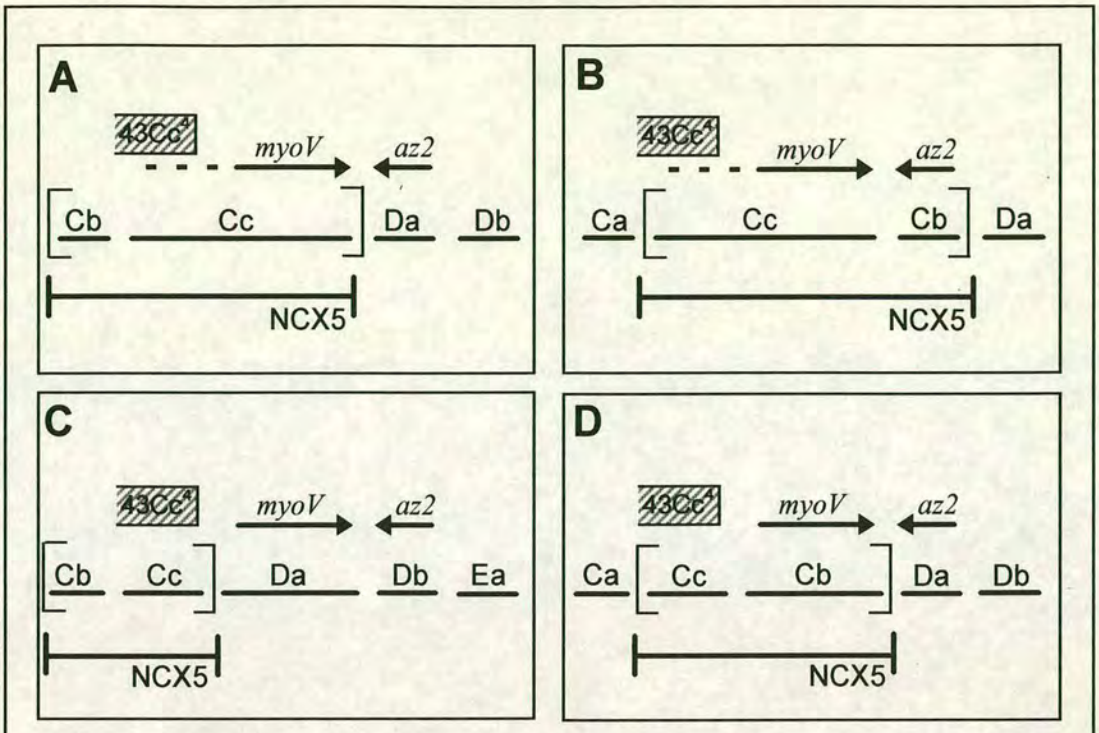

Figure 7.20 Possible interpretations of the X-ray allele analysis. X-ray analysis indicates that the *43Cc*^{4} mutation maps either to the *myosinV* gene or immediately proximal to the *myosinV* gene i.e. the *myosinV* gene is either *43Cc* (A & B) or is immediately distal to *43Cc* (C & D). Loci *43Cb* and *43Cc* are unordered with respect to one another and so *43Cb* may be proximal to *43Cc* (A & C) or distal to *43Cc* (B & D). Deficiency analysis indicates that deficiency *NCX5* does not break between the *myosinV* and the *az2* genes so this rules out possibilities A & D. Polytene *in situ* and P1 mapping place *myosinV* in the 43C region, making possibility C unlikely. The most likely scenario is therefore B i.e. that the *myosinV* gene corresponds to loci *43Cc* and the *az2* gene corresponds to loci *43Cb*. Full discussion in text.

7.2.8 Analysis of the *l(2)43Cc* embryonic lethal phenotype

The *myosinV* gene has been tentatively mapped to *l(2)43Cc*, a locus originally identified by its lethal phenotype in the genetic analysis of the 43A-E region by Heitzler *et al* (1993). To gain further insight into the normal function of the gene, homozygous *l(2)43Cc* arrested embryos were examined for defects. *l(2)43Cc*^{4} homozygous embryos were generated and identified by the same strategy used to generate *l(2)43Bb* homozygotes (7.2.5 and fig 7.13). *43Cc*^{4}/OrR x *43Cc*^{4}/OrR crosses were set up in egg collection cages and those eggs which had failed to hatch

after 24 hours were dechorionated, mounted in Aquamount and examined for defects. The *l(2)43Cc*^{4} homozygotes appeared to have arrested fairly late in embryogenesis and the most striking aspect of the phenotype was the complete lack of segmentation pattern in the dorsal regions of the arrested embryos. Figure 7.21A shows a ventral view of an arrested embryo with the ordered rows of bristles clearly marking the boundaries of the embryonic segments. Figure 7.21B shows a dorsal view of the same embryo where the bristles are still present but are in a disordered array with no suggestion of any segmentation pattern. The contrast between the segmented ventral region and the unsegmented dorsal region can be clearly seen in the lateral view of a *l(2)43Cc*^{4} arrested embryo shown in figure 7.21C. This segmentation defect appeared to be a consequence of dorsal closure failure (fig 7.21D).

The defects observed in *43Cc*^{4}*/43Cc*^{4} arrested embryos suggest that the *l(2)43Cc* gene is required for dorsal closure - the elongation and migration of the lateral epidermal cells to cover the dorsal surface of the embryo after germ band retraction. This phenotype supports the mapping of the *myosinV* gene to the *l(2)43Cc* locus, as an involvement of *l(2)43Cc* in the morphogenetic movements of sheets of epithelial cells is consistent with the accumulation of the *myosinV* transcript in the folds of the ventral furrow and the folds of gastrulation in the early embryo. The 95F class VI unconventional myosin and *Drosophila* non-muscle myosin II have also been shown to be involved in epithelial morphogeneis (Deng and Bownes, paper in preparation; Edwards and Kiehart, 1996), further supporting the mapping of the *myosinV* gene to *l(2)43Cc.*

It would have been desirable to undertake a fuller analysis of the *l(2)43Cc* phenotype by examining the arrested embryos arising from different alleles of *l(2)43Cc*, as was performed for the *l(2)43Bb* locus. Unfortunately, such an analysis was not possible due to time considerations. It would also have been interesting to study the phenotype of *l(2)43Cb* arrested embryos in order to relate it to what is known about the *az2* gene. Again, this was not possible due to lack of time, however further analysis of both genes remains a topic for future study.

Figure 7.21 Defects displayed by *l(2)43Cc*^{4} arrested embryos. A) Ventral view of an arrested embryo reveals rows of bristles (arrows) forming the correct, wild type segmentation pattern in the ventral region of the embryo. B) Dorsal view of the same embryo reveals random arrays of bristles (arrowheads) and a complete lack of any segmentation pattern in the dorsal region of the embryo. C) Lateral view of an arrested embryo clearly demonstrates the difference between the rows of bristles marking segment boundaries in the ventral region of the embryo (arrows) and the random array of bristles in the dorsal region of the embryo (arrowheads). D) An embryo which had failed to complete dorsal closure. Anterior is to the left. D: dorsal, V: ventral.

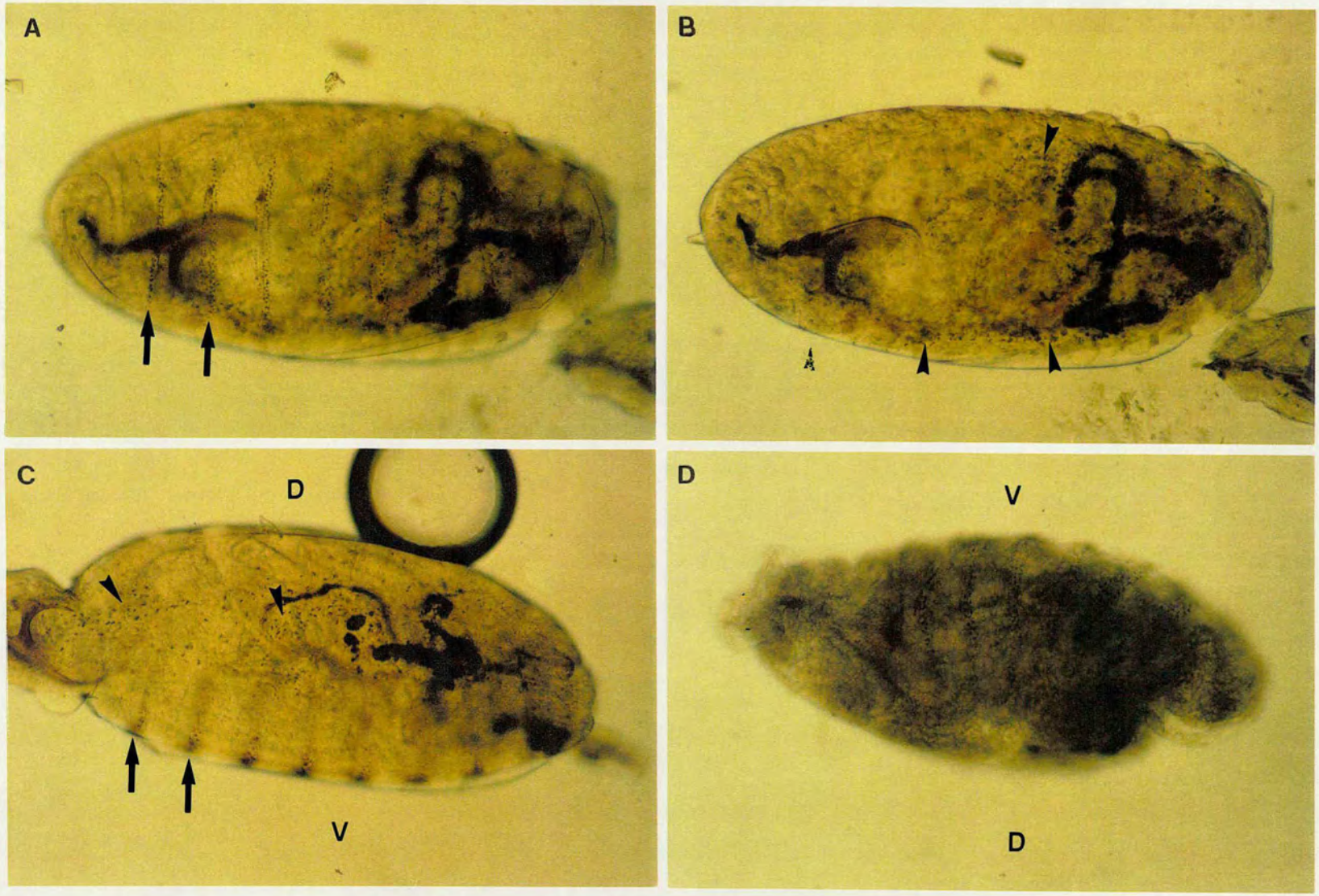
A
B
C
D
V
D
V
D

7.3 Summary

To gain an insight into the normal function of the *myosinV* gene it was necessary to create a mutation in the gene and study the phenotypic effects of loss of function. The initial aim was to create a *myosinV* mutant by local hopping of the two P-elements in the H14 line. One of these two P-elements, which map close to the *myosinV* gene in section 43 of the right arm of the second chromosome, was successfully recombined apart in preparation for a mutagenesis attempt, however, it did not map particularly close to the position of the *myosinV* gene. Since the 43 region had already been the focus of an extensive mutagenesis analysis and it was likely that a mutation in the *myosinV* gene already existed, it was decided to try to map the *myosinV* gene to one of the identified loci in the 43 region.

Initially, the *humilis* gene was a promising candidate to correspond to the *myosinV* gene. *humilis* was the only female sterile mutation recovered in the screen of the 43 region and this corresponded well with the involvement of the *myosinV* gene in oogenesis. A study of the arrested embryos from *humilis* female steriles revealed anterior defects which were also consistent with the anterior oocyte localisation of the *myosinV* transcript. Although the circumstantial evidence was encouraging, it was not possible to conclusively link the *myosinV* gene to the *humilis* gene.

A deficiency mapping analysis was undertaken to refine the position of the *myosinV* gene within the 43 region. Southern analysis detected an altered restriction pattern in deficiency lines 579 and 580, suggesting that the *myosinV* gene mapped to locus *l(2)43Bb* and the adjacent *c34* gene mapped to *l(2)43Bc*. Arrested embryos from several lethal alleles of *l(2)43Bb* were analysed and found to contain defects of the tubule networks such as the gut and trachea. Subsequent evidence showed that the altered restriction pattern observed in lines 570 and 580 was, in fact, due to a polymorphism in the progenitor chromosome from which these deficiency lines were derived. Additionally the *myosinV* gene was discovered to be adjacent to the *az2*

gene while the *c34* gene did not map to the section 43 at all.

A dot blot analysis of P1 cosmids mapped the *myosinV* gene to the 43C region. A combination of deficiency mapping and X-ray allele analysis finally placed the *myosinV* gene at *l(2)43Cc* and the adjacent *az2* gene at *l(2)43Cb*. *l(2)43Cc* homozygous arrested embryos were examined and found to have abnormal segmentation in the dorsal region of the embryo as a consequence of dorsal closure failure. It was therefore postulated that embryonic expression of the *myosinV* gene is required for morphogenetic sheet movements during embryogenesis. A similar phenotypic analysis of the *l(2)43Cb* gene was not possible due to time considerations, but remains a topic for future study.

Figure 7.14 Defects displayed by *l(2)43Bb* arrested embryos. A, B & C - Defects in Bb^{1}/Bb^{1} arrested embryos include A) over developed tracheal system and B) breaks in tracheal system (arrows), while C) darkfield photography reveals that the cuticle segmentation pattern is normal. D, E & F - Bb^{1}/1594 embryos arrest at an earlier stage and show more severe defects including D) failure of tubule networks such as gut and trachae, E) breaks in under-developed tracheal system (arrows) and F) failure of dorsal closure and head involution plus yolk not contained to a gut (arrow). Anterior is to the left.

Chapter 8

Discussion

8.1 Expression of the *myosinV* gene

The *myosinV* gene was discovered serendipitously in the course of an enhancer trap screen to identify genes with interesting expression patterns during oogenesis. Analysis of cDNAs related to the enhancer trap screen led to the discovery of a transcript which was localised during oogenesis but which was unrelated to any enhancer trap pattern. This transcript was localised to the oocyte from the very early stages of oogenesis and was later localised as a band at the anterior margin of the oocyte. The early localisation to the oocyte was similar to that of the *orb*, *oskar* and *gurken* transcripts which all have fundamental roles in oogenesis (Lantz and Schedl, 1994; Ephrussi *et al*, 1991; Neuman-Silberberg and Schupbach, 1993). Localisation at the anterior margin was similar to the *fs(1)K10* and *bicoid* transcripts which have key roles in oogenesis and embryogenesis respectively (Cheung *et al*, 1992; Berleth *et al*, 1988). The transcript localisation pattern was therefore suggestive of an important role in oogenesis or embryogenesis or both. Subsequent cloning and sequencing of the related gene led to the discovery that it encoded a protein with all the features of a class V unconventional myosin - a myosin head domain with ATP-binding and actin binding domains, a neck region consisting of six IQ motifs, and a tail domain predicted to form coiled-coil α-helices. The gene is therefore a *Drosophila* class V unconventional myosin gene and was thus termed *myosinV*.

A developmental profile revealed that the *myosinV* transcript was also abundant in testes and early embryos. The ovarian and early embryo transcript were both sized at around 6kb while the testes transcript was found to be approximately 500bp shorter at 5.5kb. This size difference was postulated to be due to differences in the 3'UTR of the transcripts, as ovarian and testes transcripts were thought unlikely to share the same 3'UTR localisation signals. However, RT-PCR analysis revealed that the ovarian and testes transcripts do share the same 3'UTR, suggesting that the size difference may be due to alternate splicing or differences in the 5'UTR. *in situ* hybridisation revealed that within the early embryo, the *myosinV* transcript was

concentrated at sites of morphogenetic movement, such as the infolds of the ventral furrow, suggesting that the *myosinV* product may be involved in the migration epithelial cell sheets. This early embryo expression was originally presumed to comprise entirely of maternally encoded transcript laid down in the oocyte during oogenesis. The testes transcript was found to be localised to the germ-line derived cells of the testes, just as the ovarian transcript is localised to the germ-line derived cells of the ovary, strongly suggesting that the transcript is germ-line specific. However, a subsequent polyA$^+$ Northern indicated the presence of rare 6kb male and female carcass transcripts and a 2kb female carcass specific transcript. The existence of rare carcass transcripts was verified by RT-PCR and confirms that expression of the *myosinV* gene is not germ-line specific. Subsequent genetic analysis of the *myosinV* gene revealed that it corresponds to one of three essential loci in the 43C region of chromosome 2R, all of which give rise to an embryonic lethal mutant phenotype. Embryonic lethality indicates that there must be some zygotic expression of the *myosinV* gene in the early embryo and that maternal expression is not sufficient to rescue a homozygous mutant zygote. The above data indicates that the *myosinV* gene potentially plays a number of roles during development. Expression and transcript localisation in the germ-line derived cells of the ovary and testes suggests that *myosinV* plays an important role during oogenesis and spermatogenesis, while genetic analysis reveals that *myosinV* has an essential function during embryogenesis.

8.2 Mechanisms of Transcript Localisation

The *myosinV* transcript is one of many transcripts localised to and within the *Drosophila* oocyte during oogenesis. Any mechanism to explain the active, directed transport of mRNAs should include two essential features - a *cis*-acting signal intrinsic to the transcript itself, and the *trans*-acting cellular machinery to interpret the signal and bring about localisation. In almost all cases where a transcript localisation signal has been identified, it has been located to the 3'UTR of the transcript. Examples of

transcripts with 3'UTR localisation signals include *bicoid, oskar* and *orb* (Macdonald and Struhl, 1988; Kim-Ha *et al*, 1993; Lantz and Schedl, 1994). The cellular machinery required to bring about transcript localisation is widely believed to include the oocyte's microtubule cytoskeleton. A number of transcripts have been shown to require an intact microtubule cytoskeleton for their localisation and, in addition, the microtubule network undergoes a series of rearrangements throughout oogenesis which are consistent with a role in transcript localisation (Theurkauf *et al*, 1992). As part of the present study, the 780bp 3'UTR of the *myosinV* transcript was assessed for its ability to direct transcript localisation by the creation of a transgene in which the *myosinV* 3'UTR is fused to a portion of *lacZ*. The importance of an intact microtubule cytoskeleton was also determined by testing the effect of the microtubule depolymerising drug, colchicine, on *myosinV* transcript localisation.

8.2.1 Role of the 3'UTR

The 780bp *myosinV* 3'UTR was fused to a portion of the *lacZ* gene and inserted into the *Drosophila* genome by P-element mediated germline transformation. Only one transformed line was created in this way, however, several more were generated by mobilisation of the inserted P-element. The use of RT-PCR confirmed that the *lacZ/myoV3'UTR* fusion transcript was being expressed in these transformants, but *in situ* hybridisation with a *lacZ* RNA probe was unable to detect transcript localisation, despite being able to detect localisation in control flies transformed with *lacZ* fused to the *Adducin-like* 3'UTR. On the basis of this result, it would appear that the 3'UTR of the *myosinV* transcript does not contain a signal capable of directing transcript localisation during oogenesis. It may therefore be the case that a signal to direct localisation resides in some other region of the *myosinV* transcript, i.e. within the 5'UTR of the transcript or within the *myosinV* coding region itself. As mentioned above, almost all identified transcript localisation signals have been found to reside within the 3'UTR of the localised transcript. However, more recently, the coding region of a transcript has been implicated in its targeting and localisation. The 5'

coding region of the *Drosophila* maternal mRNA *α-yemanuclein* has been shown to be required for its early accumulation in the oocyte and its localisation during oogenesis (Capri *et al*, 1997). At the time these experiments to identify a localisation signal within the 3'UTR of the *myosinV* transcript were undertaken, only the 3' region of the *myosinV* gene had been cloned and there was no precedent for localisation signal existing anywhere but within the 3'UTR. With the subsequent cloning of the 5' region of the *myosinV* gene, and in light of recent evidence, a possibility for future work would be to perform similar experiments to determine whether the 5'UTR or coding region of the *myosinV* transcript are capable of directing transcript localisation during oogenesis.

It is possible that the 3'UTR of the *myosinV* transcript does, in fact, contain a localisation signal but the design of the transformation vector did not allow its detection. The 3'UTR sequence used in the pmyoV3'UTR transformation vector was obtained by PCR cloning from pNMC7b, a sub-clone of pNMC7 which was originally obtained in a screen of a whole body cDNA library. As described in chapter three, a subsequent screen of an ovarian cDNA library was undertaken to ensure that the sequence of pNMC7b represented that of the ovarian transcript. Of the positive clones recovered in this screen, two contained UTR sequence. One of these was identical to the 3'UTR found in pNMC7b. However, at the 3' end of the second cDNA clone, there was an extra seven base pairs of sequence prior to the poly(A) tail. These extra seven base pairs match the sequence of the genomic DNA and so would appear to be genuine, rather than merely a cloning artifact (Bryce MacIver, personal communication). The appearance of seven extra base pairs in one out of three cloned cDNAs could be attributed to the fact that there is no clear polyadenylation consensus signal in the *myosinV* sequence and polyadenylation may therefore occur at a number of sites rather than at one specific site. The consensus signal for polyadenylation is AATAAA (Proudfoot, 1991). Poly(A) polymerases bind to this signal in the primary transcript and stimulate cleavage and polyadenylation at a site usually 10-35 nucleotides downstream of the poly(A) consensus signal. This poly(A) signal appears in the *Adducin-like* 3'UTR within the transformation vector pAdd3'UTR, however,

neither the signal AATAAA or its most common alternative ATTAA appear in the *myosinV* 3'UTR.

The *myosinV* 3'UTR sequence used to construct the transformation vector pmyoV3'UTR was lacking the seven extra base pairs and had no clear polyadenylation signal. It is unlikely that these seven base pairs constitute part of the localisation signal, as previous studies on the 3'UTRs of the *bicoid* and *oskar* transcripts have shown that large regions of the most 3' end can be deleted and replaced by a heterologous polyadenylation signal without any detrimental effect on transcript localisation (Macdonald *et al*, 1993; Kim-Ha *et al*, 1993). However, it is possible that the absence of a polyadenylation signal in pmyoV3'UTR meant that the resulting transcript included much of the *white* gene. The addition of all or part of the *white* transcript to the *lacZ/myoV3'UTR* transcript would almost certainly affect the formation of the secondary structure, which is thought to be a critical factor for the recognition of localisation signals (Macdonald, 1990). Perhaps the introduction of a synthetic polyadenylation signal into pmyoV3'UTR would have prevented the inclusion of the *white* transcript and the *myosinV* 3'UTR would have been found capable of directing localisation of the *lacZ/myoV3'UTR* transcript.

8.2.2 Role of the microtubules

A number of transcripts have been shown to require the microtubule cytoskeleton for their transport and localisation during *Drosophila* oogenesis (Theurkauf *et al*, 1992). In order to determine whether the correct localisation of the *myosinV* transcript requires an intact microtubule cytoskeleton, transcript localisation was assessed in flies which had been fed the microtubule depolymerising drug colchicine. The results showed that *myosinV* transcript localisation deteriorated with increasing exposure to colchicine. Both the early localisation to the oocyte and anterior localisation within the oocyte were ultimately lost on exposure to colchicine, suggesting that an intact microtubule cytoskeleton is required for both stages of localisation.

The microtubules are themselves dynamically localised during oogenesis. In early germarial cysts a microtubule organising centre (MTOC) forms in the pro-oocyte and from stages 1-6 microtubules are anchored at this organising centre by their minus ends and extend their plus ends through the ring canals, into the adjacent nurse cells. At stage 7/8 this MTOC degenerates and from stages 8-10 microtubules originate at the anterior cortex of the oocyte and extend their plus ends towards the posterior pole (Theurkauf *et al*, 1992; Theurkauf, 1994a). It has therefore been proposed that during early oogenesis, mRNAs are transported from the nurse cells to the oocyte via an association with minus-end directed microtubule motor proteins, then, between stages 8-10, mRNAs such as *bicoid* and *Adducin-like* are localised to the oocyte's anterior by minus-end directed motors, while *oskar* mRNA and Staufen protein are localised to the posterior by plus-end directed motors (Theurkauf, 1994; Clark *et al*, 1994).

The *myosinV* transcript is localised to the oocyte from stages 1-6, then accumulates at the oocyte's anterior between stages 8-10. This localisation was found to be dependent on the integrity of the microtubules, suggesting that the *myosinV* transcript may also be localised via an association with a minus-end directed motor protein. However, the results of chapter 4 concerning the localisation of *myosinV* mRNA in *gurken*, *Notch* and *Delta* mutant backgrounds appear to conflict with this conclusion.

The re-organisation of the microtubule cytoskeleton at stage 7/8 requires the function of *gurken* in the germline and *Notch* and *Delta* in the follicle cells. If *gurken*, *Notch* or *Delta* are mutant, the microtubules fail to form a polarised array and instead form a mirror-symmetric cytoskeleton, in which the microtubule plus-ends are in the centre and the minus-ends extend towards both poles (Ruohola *et al*, 1991; Gonzalez-Reyes *et al*, 1995). In *gurken*, *Notch* and *Delta* mutant ovaries, the behaviour of the *bicoid*, *Adducin-like* and *oskar* transcripts is consistent with their directed transport along the microtubules i.e. *bicoid* and *Adducin-like* mRNA localise to both poles of the oocyte while *oskar* mRNA and Staufen protein localise to the oocyte's centre. However, the results of chapter 4 show that localisation of the *myosinV* transcript is unperturbed in

the ovaries of two different *gurken* mutants, suggesting that the localisation of *myosinV* mRNA does not depend on microtubule polarity. *myosinV* mRNA is mis-localised in *Notch* and *Delta* mutants, but not to both poles of the oocyte as would be expected if localisation was towards the minus-ends of the microtubules. *Notch* and *Delta* temperature sensitive mutants are incompletely penetrant and give rise to very variable phenotypes, depending on time and temperature of incubation. The fact that *myosinV* mRNA is not correctly localised in *Notch* and *Delta* mutants could be interpreted to mean that its localisation does depend on microtubule polarity, even though the characteristic mis-localisation pattern is not observed. However, taken together with the normal localisation of *myosinV* mRNA in *gurken* mutants, it would seem certain that localisation of *myosinV* mRNA does not depend on microtubule polarity.

From the loss of *myosinV* mRNA localisation in ovaries treated with the microtubule depolymerising drug, colchicine, it can be concluded that an intact microtubule cytoskeleton is required for localisation of *myosinV* mRNA. However, the failure of *myosinV* mRNA to mis-localise to both poles of *gurken*, *Notch* or *Delta* mutant oocytes would suggest that the mechanism of *myosinV* mRNA localisation is not directed transport via a minus-end directed microtubule motor protein.

Although the *myosinV* gene was initially chosen for further study on the basis of the interesting localisation pattern of its transcript, it may be that the localisation of the transcript has no bearing on the function of the MyosinV protein. Several other transcripts e.g. those of *fs(1)K10*, *orb* and *Adducin-like,* are localised to the oocyte's anterior cortex at the same time as the *myosinV* transcript and it has been postulated since the initiation of this thesis that anterior localisation is not actually a requirement for protein targeting or gene function, but is merely a consequence of mRNA transport from the nurse cells to the oocyte (Serano & Cohen, 1995). This gratuitous mRNA localisation has been demonstrated to be the case for *fs(1)K10* mRNA, which localises to the anterior cortex although its protein is actually localised to the oocyte nucleus. Mutations in *cappuccino* and *spire*, which allow the transport of *fs(1)K10*

mRNA to the oocyte but prevent its subsequent anterior localisation, were shown not to disrupt the synthesis or localisation of K10 protein. In addition, modified *fs(1)K10* transgenes which mislocalise transcripts to the posterior pole, were shown to be still capable of producing localised and functional K10 protein (Serano & Cohen, 1995). It would therefore appear that transcript localisation is not necessarily a prerequisite for protein localisation and is not always indicative of protein function.

Preliminary steps have been taken to generate antibodies to the MyosinV protein in order that its distribution in ovaries can be immunohistochemically determined and compared to that of its transcript (Bryce MacIver, personal communication). A cDNA representing the most 3' 3kb of the gene was cloned into an *E.coli* expression vector and the resulting recombinant protein was used to raise antibodies in rabbits. The antibodies raised were able to detect the recombinant MyosinV protein and also reacted to a band in an ovarian extract on a Western blot. However, it has not yet been possible to detect the wild type protein in whole mount ovaries due to problems with background staining (Bryce MacIver, personal communication). Further refinements of the immunohistochemical techniques will be required to reveal the spatial and temporal distribution of the MyosinV protein during oogenesis. Once this has been achieved, the issue of whether *myosinV* transcript localisation is gratuitous or is indeed necessary for MyosinV protein localisation can be addressed.

8.3 Transcript Localisation in Mutant Backgrounds

The asymmetric localisation of maternal transcripts is a common and important phenomenon during development in *Drosophila*. Numerous events of oogenesis and embryogenesis depend on transcript localisation e.g. oocyte determination, axis specification and anterior embryonic patterning require the localisation of the *Bic-D*, *gurken* and *bicoid* transcripts respectively (Suter and Steward, 1991, Gonzalez-Reyes *et al*, 1995, Berleth *et al*, 1988). Localisation of these transcripts in turn requires the

functions of other genes e.g. correct localisation of the *bicoid* transcript requires the functions of the *exuperantia*, *swallow* and *staufen* genes (St Johnston *et al*, 1989). In order to determine the genetic requirements for the localisation of the *myosinV* transcript, its localisation pattern was studied in a number of flies carrying mutations for genes involved in oogenesis. Mislocalisation of the *myosinV* transcript in a particular mutant background indicates a dependence on that wild type gene product for normal localisation.

Localisation of the *myosinV* transcript was found to require the functions of the *egalitarian*, *Bicaudal-D*, *chickadee*, *exuperantia*, *orb*, *cappuccino*, *spire*, *Notch* and *Delta* genes, but was found not to require the functions of the *swallow*, *staufen*, *gurken*, *fs(1)K10*, *oskar*, *vasa*, *tudor* or *valois* genes. Mutations in the *Bicaudal-D* and *egalitarian* genes result in failure of oocyte determination, while mutations in *chickadee*, *cappuccino*, *spire*, *Notch* and *Delta* all affect aspects of the cytoskeleton, making it seem likely that these mutations affect *myosinV* transcript localisation indirectly. It is probable that only the functions of the *exuperantia* and *orb* genes are specifically required for localisation of the *myosinV* gene. *exuperantia* is one of the genes required for correct anterior localisation of *bicoid* mRNA and the failure to tightly localise *bicoid* mRNA to the oocyte anterior in *exuperantia* mutants is similar to the mislocalisation of the *myosinV* transcript (St Johnston *et al*, 1989). This common dependence on *exuperantia* for *bicoid* and *myosinV* transcript localisation indicates that although *bicoid* and *myosinV* have different localisation patterns, the same localisation factors can be employed for shared intermediate steps. The transient, *exuperantia* dependent, localisation of the *myosinV* to the oocyte anterior at stages 8-10 would suggest that the *myosinV* gene plays a spatially and temporally specific role during oogenesis. However it should be noted that *bicoid* mRNA is localised to the anterior of the oocyte from stage 5 of oogenesis but is not translated until after fertilisation when it is required for anterior embryonic patterning. Again, an antibody to MyosinV will be required to determine whether the protein is actually translated and localised during oogenesis.

The *orb* gene was the only gene whose function was required for the early localisation of the *myosinV* transcript to the oocyte from stage 1 of oogenesis. The *orb* gene encodes a germ-line specific RNA binding protein which has been implicated in the localisation of several mRNAs during oogenesis and has been shown to be required for events such as oocyte determination, pole plasm assembly and establishment of dorsoventral polarity (Lantz *et al*, 1994; Christerson and McKearin, 1994). The Orb protein is proposed to be part of the multiprotein machinery required for the transport and localisation of mRNAs. It would appear that this localisation machinery is required both for transport of the *myosinV* transcript from the nurse cells to the oocyte and for its localisation within the oocyte.

One interesting aspect of *myosinV* transcript localisation is that it does not appear to share the same genetic requirements for localisation as other anterior localised transcripts such as *bicoid, orb, fs(1)K10* and *Adducin-like*. These transcripts are thought to be localised towards the minus ends of microtubules and their localisation depends upon the functions of *gurken*, *Notch* and *Delta* for the correct reorganisation of the oocyte's microtubule cytoskeleton. Mutations in *gurken, Notch* or *Delta* result in the formation of double anterior oocytes with a mirror-symmetric cytoskeleton in which the microtubule plus ends are at the centre of the oocyte and the minus ends extend towards both poles (Ruohola *et al*, 1991; Gonzalez-Reyes *et al*, 1995). In these mutant oocytes *bicoid, orb, fs(1)K10* and *Adducin-like* transcripts are mislocalised to the minus ends of microtubules at both poles of the oocytes. This pattern of mislocalisation is not observed with the *myosinV* transcript which localises normally in *gurken* mutants, mislocalises to one anterior corner of *Notch* mutant oocytes and persists at the posterior of *Delta* mutant oocytes. Although inhibitor studies with colchicine have shown that the microtubules are necessary for *myosinV* transcript localisation, the above results imply that the *myosinV* transcript is not transported along the microtubules by a minus-end directed motor in the same way as the *bicoid, orb, fs(1)K10* and *Adducin-like* transcripts.

To further the understanding of the role of *myosinV* in oogenesis and embryogenesis it

would be interesting to perform the reciprocal experiments to determine which localised transcripts require the function of the *myosinV* gene for their correct localisation during oogenesis. The tentative mapping of *myosinV* to *l(2)43Cc* has brought this possibility closer, however, to study the effects of a *myosinV* mutant during oogenesis would require a female sterile allele of *l(2)43Cc* and such an allele is not presently available.

8.4 Genetic Analysis

To further characterise the *myosinV* gene and elucidate its function, it was essential to study the phenotypic effect of mutations in the gene. The chromosome position of the *myosinV* gene was determined as 43BC by *in situ* hybridisation to polytene chromosomes, while a dot blot analysis of P1 cosmids further mapped the *myosinV* gene to 43C. The 43 region had already been the focus of an extensive genetic analysis by Heitzler *et al* (1993) and provided three candidate loci in the 43C region to correspond to the *myosinV* gene - *l(2)43Ca*, *l(2)43Cb* and *l(2)43Cc*. A combination of deficiency mapping and X-ray allele analysis strongly suggested that the *myosinV* gene corresponds to *l(2)43Cc,* while the adjacent *az2* gene corresponds to *l(2)43Cb*. Mutations at all three loci in the 43C region produce an embryonic lethal phenotype, making it certain that *myosinV* is an essential gene, even if the final mapping to *l(2)43Cc* is inaccurate.

The discovery that mutations in the *myosinV* gene give rise to an embryonic lethal phenotype validates the reverse genetic approach which resulted in the isolation of the gene. The *myosinV* gene is not actually related to an enhancer trap, but it was discovered in the course of an enhancer trap screen designed to identify genes, like *myosinV*, which have interesting expression patterns during oogenesis. The *myosinV* gene would never have been discovered in a classical genetic screen for genes involved in oogenesis, as females carrying homozygous mutations in the gene would

die as embryos, before the maternal effects on oogenesis and embryogenesis could be assessed. The discovery of the *myosinV* gene therefore illustrates the importance of the reverse genetic approach for the identification of genes which are involved in oogenesis, but which have earlier essential functions.

A more detailed analysis of the *l(2)43Cc* embryonic lethal phenotype indicates that *l(2)43Cc*^{4} homozygotes arrest fairly late in embryogenesis. Arrested embryos appear to have failed to complete dorsal closure and as a result they lack signs of segmentation in their dorsal regions while segmentation in their ventral regions is completely normal. Failure of dorsal closure in what is thought to be a *myosinV* mutant suggests that MyosinV protein is normally involved in the morphogenetic movement of epithelial cells as they migrate to completely enclose the embryo. The proposed involvement of MyosinV in the morphogenesis of epithelial cell sheets is consistent with the accumulation of *myosinV* mRNA in the ventral furrow and gastrulation folds of the early embryo and supports the mapping of the *myosinV* gene to the *l(2)43Cc* locus.

The fact that *myosinV* corresponds to a gene which, when mutant, gives rise to an embryonic lethal phenotype, indicates that maternal *myosinV* expression is not sufficient to rescue a homozygous mutant embryo. The developmental profile of *myosinV* expression shows that the transcript is abundant in ovaries and 0-4 hour embryos, but is no longer detectable in 4-16 hour embryos or 16-24 hour embryos. It is likely that the transcript observed in 0-4 hour embryos is maternally encoded transcript, laid down during oogenesis, but which has degraded by four hours of embryonic development. The fact that *l(2)43Cc* homozygous embryos arrest late in embryogenesis suggests that the maternally expressed transcript provides sufficient MyosinV to complete the early epithelial morphogenetic events such as ventral furrow formation and gastrulation. However, it would appear that epithelial sheet movements in the later stages of embryogenesis, such as dorsal closure, require the zygotic expression of the *myosinV* gene. Although obviously essential, this gene must be expressed at very low levels in the zygote, as the transcript is not detectable by

Northern analysis.

8.5 *Drosophila myosinV*

This thesis concerns the study of the expression, localisation and mutant phenotype of a class V unconventional myosin in *Drosophila*. Recent advances have made myosin V one of the best characterised of all the unconventional myosins. Biochemical studies on chick brain actomyosin preparations have revealed that myosin V is a dimeric, actin-activated Mg-ATPase, which can translocate towards the barbed end of actin filaments (Espindola *et al*, 1992; Cheney *et al*, 1993). Meanwhile, analysis of mutant phenotypes in yeast and mice have provided evidence that myosin V is a motor protein which can transport a wide range of cargoes (reviewed by Titus, 1997).

Mutations in the essential yeast class V myosin gene, *MYO2*, give rise to large, vesicle-filled cells which fail to bud, consistent with a role for MYO2 in the transport of vesicles to areas of cell growth (Johnston *et al*, 1991). *MYO2* mutants are also defective in the transport of Chs3p - a chitin synthase, to sites of polarised growth, although the transport of Chs5p - another chitin synthase, is unaffected, suggesting that myosin V transports a distinct subset of molecules. A second yeast class V myosin is encoded by the non-essential *MYO4* gene. Mutations in *MYO4* prevent the directed transport of the Ash1p transcriptional regulator into the daughter cell. Failure to accumulate Ash1p allows the expression of the HO endonuclease in the daughter cell which, in turn, allows the daughter cell to switch mating types (Jansen *et al*, 1996; Bobola *et al*, 1996).

Mutations in the mouse myosin V gene result in the *dilute* phenotype - a lightening of the coat colour caused by failure to transfer the pigment-containing melanosomes, from their site of synthesis in melanocytes, to the growing hair shaft (Silvers, 1979).

Keratinocytes, which go on to form a hair shaft, normally engulf and phagocytose the melanosome-rich dendrites of melanocytes, resulting in a uniform distribution of pigment granules throughout the shaft. However, in *dilute* mice the pigment granules form characteristic clumps that lead to the washed out coat colour. Studies both in cultured cells and *in situ* have shown that the overall morphology of *dilute* melanocytes is normal but the melanosomes are wrongly distributed such that they are concentrated in the cell body and excluded from the dendrites (Wei *et al*, 1997). Immunolocalisation studies in wild-type melanocytes have shown that the myosin V encoded by the *dilute* locus is normally associated with melanosomes (Wu *et al*, 1997). These findings implicate myosin V in the directed transport of melanosomes from the cell body to the tips of the dendrites. A more severe allele of *dilute* causes neurological defects such that homozygous animals suffer nervous seizures and die within a few weeks of birth (Searle, 1952). This indicates that dilute is an essential gene but the basis of the neurological defect is unclear. The overall morphology of a *dilute* brain is again normal, suggesting that the seizures and lethality are due to abnormalities in the intracellular function of neurons. It has been demonstrated that myosin V associates with synaptic vesicles (Prekeris *et al*, 1996), so it may be that myosin V is required for the transport of neurotransmitter-containing vesicles to synaptic sites.

Mutations in the human myosin V gene have recently been linked to Griscelli syndrome - a rare autosomal recessive disorder characterised by partial albinism and variable immunodeficiency, which, in the absence of a bone marrow transplant, usually leads to death in early childhood (Griscelli *et al*, 1978). The Griscelli syndrome locus was found to co-localise with the human myosin-Va gene and mutations in the gene were found in several Griscelli patients (Pastural *et al*, 1997). The partial albinism or pigment dilution is characterised by large clumps of pigment granules in the hair shafts, similar to that observed in the *dilute* mouse. Immunological abnormalities include impaired natural killer cell activity and absent delayed-type hypersensitivity. The apparent requirement for a class V myosin in the immunological system serves to illustrate the diverse functions of this motor protein.

Myosin V is reported to be expressed at low levels in most vertebrate tissues, but is especially abundant in nervous tissue and neurosecretory cells (Espindola *et al*, 1992). Transcripts have also been observed in kidney, spleen, thymus, testis, liver and muscle, but ovarian expression has not been tested (Mercer *et al*, 1991; Zhao *et al*, 1996). The *Drosophila myosinV* gene was isolated and identified by virtue of its strong ovarian expression and interesting transcript localisation pattern. The *myosinV* transcript is also abundant in testes and early embryos. It is likely that the transcript observed in early embryos is maternally encoded transcript carried over from oogenesis, however, as genetic analysis indicates that mutations in the gene produce an embryonic lethal phenotype, there must be some expression from the zygotic genome. RT-PCR indicates that the *myosinV* gene is expressed elsewhere in *Drosophila* but at levels undetectable by Northern analysis.

The *myosinV* transcript is first observed very early in *Drosophila* oogenesis - in the oocyte of stage 1 egg chambers as they bud off from the germarium. This early localisation is similar to that of the *orb* and *Bic-D* transcripts and suggests a role for *myosinV* in oocyte differentiation. MyosinV protein might potentially be involved in the transport of mRNAs and proteins to the pro-oocyte, where they are required for the biochemical and cytological differentiation of the oocyte. However it is important to note that *oskar* mRNA also accumulates in the early oocyte but is not translated until after stage 9 when it is localised at the oocyte's posterior. An antibody to MyosinV will be required for to determine whether the protein is present in early oocytes or not translated until later in oogenesis.

Between stages 8 and 10 of oogenesis the *myosinV* transcript accumulates at the anterior margin of the oocyte. This localisation pattern suggests that MyosinV might be involved in the transport of materials through the ring canals into, and across the oocyte. In 1994, Bohrmann and Biber used time-lapse analysis with video-enhanced contrast microscopy to demonstrate the transport of cytoplasmic particles from the nurse cells, through the ring canals and into the oocyte, between stages 7 and 10A.

The transport process was selective, unidirectional and inhibitable with cytochalasin B but not with microtubule inhibitors. They proposed that particle transport occurred along a polarised scaffold of actin-based cytoskeleton, driven by a myosin-like molecule. The localisation of its transcript makes MyosinV an ideal candidate to mediate this transport process, however, antibody staining is again required to determine whether the distribution pattern of MyosinV protein matches that of its transcript.

The transport of molecules along the microtubule cytoskeleton has been extensively studied in *Drosophila* and other organisms, however, there is increasing evidence to suggest that the actin cytoskeleton is also involved in directed transport and indeed, that the two systems may interact to co-ordinate intracellular transport. There is considerable evidence to suggest that *oskar* mRNA is localised to the posterior of the oocyte by directed transport along the microtubules – *oskar* mRNA localisation is disrupted by microtubule depolymerising drugs (Ephrussi *et al*, 1991) and *oskar* mRNA co-localises with a kinesin:β-gal fusion protein, both in wild-type and mirror-symmetric oocytes (Clark *et al*, 1994). However, recent findings indicate that the posterior localisation of *oskar* mRNA is also dependent on tropomyosin II – an actin crosslinking molecule (Erdelyi *et al*, 1995). Females carrying mutations in this non-muscle tropomyosin gene produce embryos that fail to develop pole cells as a consequence of the specific impairment of *oskar* mRNA localisation. This dependence on both the microtubule cytoskeleton and the actin cytoskeleton suggests an inter-relationship between these two networks. It has been proposed that cytoplasmic tropomyosin II is involved in the delivery of *oskar* mRNA to the microtubule network at the anterior of the oocyte for subsequent transport across the oocyte (Erdelyi *et al*, 1995). Alternatively, tropomyosin II may be required to sequester *oskar* mRNA at the oocyte's posterior. The localisation of tropomyosin II mRNA to the posterior pole of the oocyte makes the latter model more likely (Tetzlaff *et al*, 1996).

An inter-relationship between the actin cytoskeleton and the microtubule network has also been observed in a number of other organisms. Studies on the squid giant axon

have shown that transport particles can move along both the actin and microtubule networks and that single vesicles can switch from one network to another (Kuznetzov *et al*, 1992). In the mouse, the myosin V protein encoded by the *dilute* gene is localised to organelles which can associate with both the actin cytoskeleton and the microtubule network (Evans *et al*, 1997). Microtubule motors and actin-based motors have been found to be present on the same particles and it is thought that microtubules are used for transport over long distances within the cell, while actin filaments are used over shorter distances (reviewed by Langford, 1995). A molecule which may functionally link the actin and microtubule cytoskeletons has recently been reported. The *Drosophila* 95F class VI unconventional myosin was found to co-precipitate with a homologue of cytoplasmic linker protein (CLIP), a protein that links endocytic vesicles to microtubules (Lantz and Miller, 1998). 95F and *Drosophila* CLIP are co-expressed in a number of embryonic tissues including axonal processes and the posterior pole of the early embryo. The close association of these two proteins in regions where both actin and microtubule networks are know to be important, strongly suggests that the CLIP protein may mediate the co-ordination of the two transport systems.

In addition to MyosinV and tropomyosin II, a number of other myosins are known to function during *Drosophila* oogenesis and embryogenesis. The 95F class VI myosin mentioned above is essential during oogenesis for the proper organisation of the syncitial blastoderm (Mermall *et al*, 1994; Mermall and Miller, 1995). Injection of antibodies to 95F results in abnormal furrows and aberrant nuclear morphology suggesting that 95F is required for normal actin-based furrow formation. Work in this lab has shown that 95F is also required for epithelial morphogenesis, both during oogenesis for the morphogenesis of the follicle cells and later in development for the evagination of the imaginal discs (Deng and Bownes, paper in preparation). The class I unconventional myosin, myosin-IB is present in both the apical and basolateral domains of the follicle cells during oogenesis where it may be involved in the secretion of the yolk proteins, the vitelline membrane and the chorion (Morgan *et al*, 1995). Myosin-IB is also found along with myosin-IA in the brush border of the gut during

late embryogenesis. A conventional myosin, non-muscle myosin II, is required for a number of events throughout oogenesis and embryogenesis (Edwards and Kiehart, 1996). During oogenesis the regulatory light chain, encoded by the *spaghetti squash* gene, is required for follicle cell migrations, interfollicular stalk formation and transferal of the nurse cell contents into the oocyte. During embryogenesis, *spaghetti squash* is required for eye and leg imaginal disc development, while the non-muscle myosin II heavy chain encoded by the *zipper* gene is required for epithelial sheet movements (Edwards and Kiehart, 1996).

The *Drosophila myosinV* gene is proposed to correspond to *l(2)43Cc*, an essential locus which gives rise to an embryonic lethal mutant phenotype. The observed dorsal closure defects in *l(2)43Cc* arrested embryos suggests that the MyosinV protein is required for epithelial morphogenesis. As discussed above, non-muscle myosin II and 95F class VI myosin have also been shown to be required for the morphogenesis of epithelial cell sheets. The phenotype of *l(2)43Cc* therefore lends support to the mapping of the *myosinV* gene to this locus. It is also clear from the above discussion that myosins are involved in a diverse range of functions during *Drosophila* development, and that one myosin species may perform several different roles. It will therefore be interesting to further characterise the *Drosophila myosinV* gene and elucidate its function(s) both during oogenesis and embryogenesis.

8.6 Future Studies

One priority for future work on the *Drosophila myosinV* gene is to confirm that it does indeed correspond to the *l(2)43Cc* locus. One way in which this may be possible is to attempt to rescue the *l(2)43Cc* embryonic lethal phenotype by germline transformation with the entire *myosinV* coding sequence. However, at around 6kb, the coding sequence may be too long to be incorporated into a transformation vector and injected into embryos. Even if it transpires that *myosinV* does not correspond to

l(2)43Cc, it is certain that it corresponds to one of the other lethal loci in the 43C region. A more detailed analysis of the embryonic lethal phenotype will required to provide an insight into the potential role of MyosinV during embryogenesis. Study of the role of *myosinV* during oogenesis will require the formation of chimeric germ-line clones or the generation of a female sterile or maternal effect lethal allele. Once a mutant with a defect in oogenesis becomes available it will be interesting to assess the effect of loss of *myosinV* function on egg chamber morphology and the localisation of other transcripts such as *bicoid*, *gurken* and *oskar*. It would also be interesting to mis-express the *myosinV* transcript and mis-localise it to the posterior of the oocyte by fusing it to the 3'UTR of *oskar* mRNA, however, again the length of the coding sequence may prove problematic. An insight into the function of the *myosinV* gene may be obtained by treating ovaries or embryos with microfilament destabilising drugs such as cytochalasin B, but such drastic drug treatment may have pleiotropic effects which are difficult to interpret. An immediate goal for the future study of the *myosinV* gene is the generation of antibodies to MyosinV which are capable of detecting the protein in whole mount ovaries and embryos. Knowledge of MyosinV protein distribution is essential for the understanding of its function. It would also be interesting to inject anti-MyosinV antibody into early embryos to assesses the effects of antibody inhibition. The discovery of a class V unconventional myosin in a genetically amenable organism such as *Drosophila* should greatly facilitate the study of the functions and interactions of these fascinating proteins.

References

Ainger K, Avossa D, Morgan F, Hill SJ, Barry C, Barbarese E, Carson JH. (1993). Transport and localization of exogenous myelin basic protein mRNA microinjected into oligodendrocytes. Journal of Cell Biology 123: 431-441

Artavanis-Tsakonas S, Simpson P. (1991). Choosing a cell fate: a view from the *Notch* locus. Trends in Genetics 7: 403-408

Bahler M, Kroschewski R, Stoffler H-E, Behrmann T. (1994). Rat myr4 defines a novel subclass of myosin I: identification, distribution, localization and mapping of calmodulin binding sites with differential calcium sensitivity. Journal of Cell Biology 26: 375-389

Bakken AH. (1973). A cytological and genetic study of oogenesis in *Drosophila melanogaster*. Developmental Biology 33: 100-122

Banerjee U, Renfranz PJ, Pollock JA, Benzer, S. (1987). Molecular characterization and expression of *sevenless*, a gene involved in neuronal pattern formation in the *Drosophila* eye. Cell 49: 281-291

Bardsley A, McDonald K, Boswell RE. (1993). Distribution of tudor protein in the *Drosophila* embryo suggests separation of functions based on site of localization. Development 119: 207-219

Bellen HJ, O'Kane CJ, Wilson C, Grossniklaus U, Pearson RK, Gehring WJ. (1989). P-element-mediated enhancer detection: a versatile method to study development in *Drosophila*. Genes and Development 3: 1288-1300

Bement WM, Hasson T, Wirth JA, Cheney RE, Mooseker MS. (1994). Identification and overlapping expression of multiple unconventional myosin genes in vertebrate cell-types. Proceedings of the National Academy of Sciences, USA. 91: 6549-6553.

Bement WM, Mooseker MS. (1995). TEDS Rule: a molecular rationale for differential regulation of myosins by phosphorylation of the heavy chain head. Cell Motility and the Cytoskeleton. 31: 87-92

Berleth T, Burri M, Thoma G, Bopp D, Richstein S, Frigerio G, Noll M, Nusslein-Volhard C. (1988). The role of localization of *bicoid* RNA in organizing the anterior pattern of the *Drosophila* embryo. Embo Journal 7: 1749-1756

Birnboim HC, Doly J. (1979). A rapid alkaline lysis extraction procedure for screening recombinant DNA. Nucleic Acids Research 7: 1513-1523

Bobola N, Jansen RP, Shin TH, Nasmyth K. (1996). Asymmetric accumulation of Ash1p in postanaphase nuclei depends on a myosin and restricts yeast mating type switching to mother cells. Cell 84: 699-709

Bohrmann J, Biber K. (1994). Cytoskeleton-dependent transport of cytoplasmic particles in previtellogenic to mid-vitellogenic ovarian follicles of *Drosophila*: time-lapse analysis using video-enhanced contrast microscopy. Journal of Cell Science 107: 849-858

Boswell RE, Prout ME, Steichen JC (1991). Mutations in a newly identified *Drosophila* melanogaster gene, *mago nashi*, disrupt germ cell formation and result in the formation of mirror-image symmetrical double abdomen embryos. Development 113: 373-384

Bownes M, Dale L. (1982). in *A Handbook of* Drosophila *Development*. ed R Ransom. Elsivier Biomedical Press. pp 31-68

Bownes M, Sang JH. (1974). Experimental manipulations of early *Drosophila* embryos II. Adult and embryonic defects resulting from the removal of blastoderm cells by pricking. Journal of Embryology and Experimental Morphology 32: 273-285

Brand AH, Perrimon N. (1993). Targeted gene expression as a means of altering cell fates and generating dominant phenotypes. Development 118: 401-415

Brand AH, Perrimon N. (1994). Raf acts downstream of the EGF receptor to determine dorsoventral polarity during *Drosophila* oogenesis. Genes and Development 8: 629-639

Capri M, Santoni MJ, Thomas-Delaage M, Ait-Ahmed O. (1997). Implication of a 5' coding sequence in targeting maternal mRNA to the *Drosophila* oocyte. Mechanisms of Development 68: 91-100

Chao Y-C, Donahue KM, Pokrywka NJ, Stephenson EC. (1991). Sequence of *swallow*, a gene required for the localization of *bicoid* message in *Drosophila* eggs. Developmental Genetics 12: 333-341

Chasasn R, Anderson KV. (1993). in *The Development of* Drosophila melanogaster. eds Bate M, Martinez-Arias A. Cold Spring Harbour Laboratory Press, New York. pp 387-424

Chen IL, Edwards K, Lin RC, Coats LW, Kiehart DP. (1991). *Drosophila* myosin heavy chain at 35B,C. Journal of Cell Biology 115: 330a (Abstract)

Cheney RE, Mooseker MS. (1992). Unconventional myosins. Current Opinion in Cell Biology 4: 27-35

Cheney RE, Riley MA, Mooseker MS. (1993a). Phylogenetic analysis of the myosin superfamily. Cell Motility and the Cytoskeleton 24: 215-223

Cheney RE, Oshea MK, Heuser JE, Coelho MV, Wolenski JS, Espreafico EM, Forscher P, Larson RE, Mooseker MS. (1993b). Brain myosin-V is a two-headed unconventional myosin with motor activity. Cell 75: 13-23

Cheung H-K, Serano TL, Cohen RS. (1992). Evidence for a highly selective RNA transport system and its role in establishing the dorsal-ventral axis of the *Drosophila* egg. Development. 114: 653-661

Cheung H-K, Serano TL, Cohen RS. (1992). Evidence for a highly selective RNA transport system and its role in establishing the dorsal-ventral axis of the *Drosophila* egg. Development. 114: 653-661

Chowdhury K, Rohdewohld H, Gruss P. (1988). Specific and ubiquitous expression of different Zn finger protein genes in the mouse. Nucleic Acids Research 16 (21): 9995-10011

Chou T-B, Perrimon N. (1992). Use of a yeast site-specific recombinase to produce female germline chimeras in *Drosophila*. Genetics 131 :643-653

Christerson LB, McKearin DM. (1994). *orb* is required for anteroposterior and dorsoventral patterning during *Drosophila* oogenesis. Genes and Development 8: 614-628.

Clark L, Giniger E, Ruohola-Baker H, Jan LY, Jan YN. (1994). Transient posterior localisation of a kinesin fusion protein reflects anterioposterior polarity of the *Drosophila* oocyte. Current Biology 4: 289-300

Cooley L, Theurkauf WE. (1994). Cytoskeletal functions during *Drosophila* oogenesis. Science 266: 590-596.

Cooley L, Verheyen E, Ayers K. (1992). *chickadee* encodes a profilin required for intercellular cytoplasm transport during *Drosophila* oogenesis. Cell 69: 173-184

Dalby B, Glover DM. (1992). 3' non-translated sequences in *Drosophila* cyclin-B transcripts direct posterior pole accumulation late in oogenesis and perinuclear association in syncitial embryos. Development 115: 989-997

Davis I, Francis-Lang H, Ish-Horowicz D. (1993). Mechanisms of intracellular transcript localization and export in early *Drosophila* embryos. Cold Spring Harbour Symposium Quant Biology 58: 793-798

Davis I, Ish-Horowicz D. (1991). Apical localization of pair-rule transcripts requires 3' sequences and limits protein diffusion in the *Drosophila* blastoderm embryo. Cell 67: 927-940

Ding D, Lipshitz HD. (1993). Localized RNAs and their functions. BioEssays 15: 651-658

Ding D, Parkhurst SM, Halsell SR, Lipshitz HD. (1993). Dynamic *Hsp83* RNA localization during *Drosophila* oogenesis and embryogenesis. Molecular and Cellular Biology 13: 3773-3781

Ding D, Parkhurst SM, Lipshitz HD. (1993). Different genetic requirements for anterior RNA localization revealed by the distribution of *Adducin-like* transcripts during *Drosophila* oogenesis. Proceedings of the National Academy of Sciences, USA 90: 2512-2516

Driever W, Nusslein-Volhard C. (1988a). A gradient of bicoid protein in *Drosophila* embryos. Cell 54: 83-93

Driever W, Nusslein-Volhard C. (1988b). The *bicoid* protein determines position in the *Drosophila* embryo in a concentration-dependent manner. Cell 54: 95-104

Driever W, Nusslein-Volhard C. (1989). The *bicoid* protein is a positive regulator of *hunchback* transcription in the early *Drosophila* embryo. Nature 337: 138-143

Driever W, Siegel V, Nusslein-Volhard C. (1990). Autonomous determination of anterior structures in the early *Drosophila* embryo by the bicoid morphogen. Development 109: 811-820

Driever W, Thoma G, Nusslein-Volhard C. (1989). Determination of spatial domains of zygotic gene expression in the *Drosophila* embryo by the affinity of binding sites for the bicoid morphogen. Nature 340, 363-367

Edgar BA, Odell GM, Schubiger G. (1987). Cytoarchitecture and the patterning of *fushi tarazu* expression in the *Drosophila* blastoderm. Genes and Development 1: 1226-1237

Edgar BA, Weir MP, Schubiger G, Kornberg T. (1986). Repression and turnover pattern of *fushi tarazu* RNA in the early *Drosophila* embryo. Cell 47: 747-754

Edwards KA, Kiehart DP. (1996). *Drosophila* nonmuscle myosin II has multiple essential roles in imaginal disc and egg chamber morphogenesis. Development 122: 1499-1511

Elisha Z, Havin L, Ringel I, Yisraeli JK. (1995). Vg1 RNA binding protein mediates the association of Vg1 RNA with microtubules in *Xenopus* oocytes. Embo Journal 14: 5109-5114

Emmons S, Phan H, Calley J, Chen W, James B, Manseau L. (1995). *Cappuccino*, a *Drosophila* maternal effect gene required for polarity of the egg and embryo, is related to the vertebrate limb deformity locus. Genes and Development 9: 2482-2494

Ephrussi A, Dickinson LK, Lehmann R. (1991). *oskar* organises the germ plasm and directs localization of the posterior determinant *nanos*. Cell 66: 37-60

Ephrussi A, Lehmann R. (1992). Induction of germ cell formation by *oskar*. Nature 358: 387-392

Erdelyi M, Michon A-M, Guichet A, Bogucka Glotzer J, Ephrussi A. (1995). Requirement for *Drosophila* cytoplasmic tropomyosin in *oskar* mRNA localization. Nature 377: 524-527

Espreafico EM, Cheney RE, Matteali M, Nascimento MC, De Camilli PV, Larson RE, Mooseker MS. (1992). Primary structure and cellular localization of chicken brain myosin-V, an unconvential myosin with calmodulin light chains. Journal of Cell Biology 119: 1541-1557

Espindola FS, Espreafico EM, Coelho MV, Martins AR, Costa FRC, Mooseker MS, Larson RE. (1992). Biochemical and immunological characterization of p190-calmodulin complex from vertebrate brain: a novel calmodulin binding protein. Journal of Cell Biology 118: 359-368

Evans LL, Hammer J, Bridgman PC. (1997). Subcellular localization of myosin V in nerve growth cones and outgrowth from *dilute-lethal* neurons. Journal of Cell Science 110: 439-449

Fehon RG, Kooh PJ, Rebay I, Regan CL, Xu T, Muskavitch MA, Artavanis-Tsakonas S. (1990). Molecular interactions between the protein products of the neurogenic loci *Notch* and *Delta*, two EGF-homologous genes in *Drosophila*. Cell 61: 523-534

Ferrandon D, Elphick L, Nusslein-Volhard C, St Johnston, D. (1994). Staufen protein associates with the 3'UTR of *bicoid* mRNA to form particles that move in a microtubule-dependent manner. Cell 79: 1221-1232

Fischer-Vize JA, Rubin GM, Lehmann R. (1992). The *fat facets* gene is required for *Drosophila* eye and embryo development. Development 116: 985-1000

Forristall C, Pondel M, Chen L, King ML. (1995). Patterns of localization and cytoskeletal association of two vegetally localized RNAs, Vg1 and Xcat-2. Development 121: 201-208

Francis-Lang H, Davis I, Ish-Horowicz D. (1996). Asymmetric localization of *Drosophila* pair-rule transcripts from displaced nuclei: evidence for directional nuclear export. Embo Journal 15: 640-649

Frigerio G, Burri M, Bopp D, Baumgartner S, Noll M. (1986). Structure of the segmentation gene *paired* and the *Drosophila* PRD gene set as part of a gene network. Cell 47: 735-746

Frohnhofer HG, Lehmann R, Nusslein-Volhard C. (1986). Manipulating the anterioposterior pattern of the *Drosophila* embryo. Journal of Embryology and Experimental Morphology. 97: 169-179

Frohnhoffer HG, Nusslein-Volhard C. (1986). Organisation of anterior pattern in the *Drosophila* embryo by the maternal gene *bicoid*. Nature 324: 120-125

Frohnhoffer HG, Nusslein-Volhard C. (1987). Maternal genes required for the localization of *bicoid* activity in the embryo of *Drosophila*. Genes and Development 1: 880-890

Gans M, Audit C, Masson M. (1975). Isolation and characterization of sex-linked female sterile mutants in *Drosophila melanogaster*. Genetics 81: 683-704

Garner CC, Tucker RP, Matus A. (1988). Selective localization of messenger RNA for cytoskeletal protein MAP2 in dendrites. Nature 336: 674-677

Gibson F, Walsh J, Mburu P, Varela A, Brown KA, Antonio M, Beisel, KW, Steel KP, Brown SDM. (1995). A Type-VII myosin encoded by the mouse deafness gene *shaker-1*. Nature 374: 62-64.

Golumbeski GS, Bardsley A, Tax F, Boswell RE. (1991). *Tudor*, a posterior group gene of *Drosophila melanogaster* encodes a novel protein and a messenger RNA localized during mid-oogenesis. Genes and Development 5: 2060-2070

Gonzalez-Reyes A, St Johnston D. (1994). Role of oocyte position in establishment of anterior-posterior polarity in *Drosophila*. Science 266: 639-642.

Gonzalez-Reyes A, Elliott H, St Johnston D. (1995). Polarization of both major body axes in *Drosophila* by Gurken-Torpedo signalling. Nature 375: 654-658.

Gottlieb E. (1992). The 3' untranslated region of localized maternal messages contains a conserved motif involved in mRNA localization. Proceedings of the National Academy of Sciences, USA 89: 7164-7168

Griscelli C, Durandy A, Guy-Grand D, Daguillard F, Herzog C, Prunieras M. (1978). A syndrome associating partial albinism and immunodeficiency. American Journal of Medicine 65: 691-702

Grossniklaus U, Bellen HJ, Wilson C, Gehring WJ. (1989). P-Element-mediated enhancer detection applied to the study of oogenesis in *Drosophila*. Development 107: 189-200

Hammer JA. (1994). The structure and function of unconventional myosins: a review. Journal of Muscle Research and Cell Motility 15: 1-10

Hasson T, Mooseker MS. (1994). Porcine myosin-VI - Characterization of a new mammalian unconventional myosin. Journal of Cell Biology. 127: 425-440.

Hay B, Ackerman L, Barbel S, Jan LY, Jan YN. (1988). Identification of a component of *Drosophila* polar granules. Development 103: 625-640

Hay B, Jan LY, Jan YN. (1990). Localization of *vasa*, a component of *Drosophila* polar granules, in maternal-effect mutants that alter embryonic anteroposterior polarity. Development 109: 425-433

Hayden SM, Wolenski JS, Mooseker MS. (1990). Binding of brush border myosin I to phospholipid vesicles. Journal of Cell Biology 111: 443-451

Hays TS, Porter ME, McGrail M, Grissom P, Gosch P, Fuller MT, McIntosh JR. (1994). A cytoplasmic dynein motor in *Drosophila*: identification and localization during embryogenesis. Journal of Cell Science 107: 1557-1569

Hedge J, Stephenson EC. (1993). Distribution of *swallow* protein in egg chambers and embryos of *Drosophila melanogaster*. Development 119: 457-470

Heitzler P, Coulson D, Saenz-Robles M-T, Ashburner M, Roote J, Simpson P, Gubb D. (1993). Genetic and cytogenetic analysis of the 43A-E region containing the segment polarity gene *costa* and the cellular polarity genes *prickle* and *spiny-legs* in *Drosophila melanogaster*. Genetics 135:105-115

Hill MA, Gunning P. (1993). Beta and gamma actin mRNAs are differentially located within myoblasts. Journal of Cell Biology 122: 825-832

Horowitz JA, Hammer JA. (1990). A new *Acanthamoeba* myosin heavy chain. Journal of Biological Chemistry. 265: 20646-20652

Huang W-M, Fourquet LR, Wu E, Wu J-Y. (1990). Molecular cloning and amino acid sequence of brain L-glutamate decarboxylase. Proceedings of the National Academy of Sciences, USA 87: 8491-8495

Hulskamp M, Schroeder C, Pfeifle V, Jackle H, Tautz D. (1989). Posterior segmentation of the *Drosophila* embryo in the absence of a maternal posterior organizer gene. Nature 338: 629-632

Illmensee K, Mahowald AP. (1974). Transplantation of posterior pole plasm in *Drosophila*: induction of germ cells at the anterior pole of the egg. Proceedings of the National Academy of Sciences of the USA 71: 1016-1020

Illmensee K, Mahowald AP, Loomis MR. (1976) The ontogeny of germ plasm during oogenesis in *Drosophila*. Developmental Biology 49: 40-65

Ingham PW, Howard KR, Ish-Horowicz D. (1985). Transcription pattern of the *Drosophila* segmentation gene *hairy*. Nature 318: 439-445

Irish V, Lehmann R, Akam M. 1989). The *Drosophila* posterior group gene *nanos* functions by repressing *hunchback* activity. Nature 338: 646-648

Jacob J, Sirlin JL. (1959). Cell function in the ovary of *Drosophila*. I. DNA. Chromosoma 10: 210-228

Jansen R-P, Dowzer C, Michaelis C, Galova M, Nasmyth K. (1996). Mother cell-specific *HO* expression in budding yeast depends on the unconventional myosin myo4p and other cytoplasmic proteins. Cell 84: 687-697.

Johnston GC, Pendergast JA, Singer RA. (1991). The *Saccharomyces cerevisiae MYO2* gene encodes an essential myosin for vectorial transport of vesicles. Journal of Cell Biology 113: 539-551

Jongens TA, Ackerman LD, Swedlow JR, Jan L , Jan YN. (1994). *germ cell-less* encodes a cell-type-specific nuclear pore-associated protein and functions early in the germ-cell specification pathway of *Drosophila*. Genes and Development 8: 2123-2136

Jongens TA, Hay B, Jan LY, Jan YN. (1992). The *germ cell-less* gene product: a posteriorly localized component necessary for germ cell development in *Drosophila*. Cell 70: 569-584

Jung G, Hammer JA. (1994). The actin binding site in the tail domain of *Dictyostelium* myosin IC (myoC) resides within the glycine- and proline-rich sequence (tail homology region 2). FEBS Letters 342:197-202

Kellerman KA, Miller KG. (1992). An unconventional myosin heavy-chain gene from *Drosophila melanogaster*. Journal of Cell Biology 119: 823-834.

Kim-Ha J, Smith JL, Macdonald PM (1991). *oskar* mRNA is localized to the posterior pole of the *Drosophila* oocyte. Cell 66: 23-35

Kim-Ha J, Webster PJ, Smith JL, Macdonald PM. (1993). Multiple RNA regulatory elements mediate distinct steps in localization of *oskar* mRNA. Development 119: 169-178

King R. (1970). in *Ovarian Development in* Drosophila melanogaster. Academic Press, New York

King RC, Koch EA. (1963). Studies on ovarian follicle cells of *Drosophila*. Quarterly Journal of Microscope Science 104: 297-320

Kinkema M, Wang, HY, Schiefelbein J. (1994). Molecular analysis of the myosin gene family in *Arabidopsis thaliana*. Plant Molecular Biology 26: 1139-1153.

Kinkema M, Schiefelbein J. (1994). A myosin from a higher-plant has structural similarities to class-V myosins. Journal of Molecular Biology 239: 591-597.

Kislauskis EH, Zhu X, Singer RH. (1994). Sequences responsible for intracellular localization of beta-actin messenger RNA also affect cell phenotype. Journal of Cell Biology 127: 441-51

Knight AE, Kendrick-Jones J. (1993) A myosin-like protein from a higher plant. Journal of Molecular Biology 231: 148-154

Kobayashi S, Amikura R, Okada M. (1993). Presence of mitochondrial large ribosomal RNA outside mitochondria in germ plasm of *Drosophila* melanogaster. Science 260: 1521-1524

Kobayashi S, Yamada M, Asoaka M, Kitamura T. (1996). Essential role of the posterior morphogen *nanos* for germline development in *Drosophila*. Nature 380: 708-711

Koch EA, King RC. (1966). The origin and early differentiation of the egg chamber of *Drosophila melanogaster*. Journal of Morphology 119: 283-304

Koch EA, Smith PA, King RC. (1967). The division and differentiation of *Drosophila* cystocytes. Journal of Morphology 124: 143-166

Kopczynski CC, Alton AK, Fechtel K, Kooh PJ, Muskavitch MA. (1988). *Delta*, a *Drosophila* neurogenic gene, is transcriptionally complex and encodes a protein related to blood coagulation factors and epidermal growth factor of vertebrates. Genes and Development 2: 1723-1735

Ku M, Melton DA. (1993). Xwnt-11: a maternally expressed *Xenopus* wnt gene. Development 119: 1161-1173

Kuznetsov SA, Langford GM, Weiss DG. (1992). Actin-dependent organelle movement in squid axoplasm. Nature 356: 722-725

Lamarche N, Hall A. (1994). GAPs for rho-related GTPases. Trends in Genetics 10: 436-440

Langford GM. (1995). Actin- and microtubule-dependent organelle motors: interrelationships between the two motility systems. Current Opinion in Cell Biology 7: 82-88

Lantz V, Ambrosio L, Schedl P. (1992). The *Drosophila orb* gene is predicted to encode sex-specific germline RNA-binding proteins and has localized transcripts in ovaries and early embryos. Development 115: 75-88

Lantz V, Chang JS, Horabin JI, Bopp D, Schedl P. (1994). The *Drosophila orb* RNA-binding protein is required for the formation of the egg chamber and establishment of polarity. Genes and Development 8: 598-613

Lantz VA, Miller KG. (1998). A class VI unconventional myosin is associated with a homologue of a microtubule-binding protein, cytoplasmic linker protein-170, in neurons and at the posterior pole of *Drosophila* embryos. Journal of Cell Biology 140: 897-910

Lantz V, Schedl P. (1994). Multiple cis-acting targeting sequences are required for *orb* mRNA localization during *Drosophila* oogenesis. Molecular and Cellular Biology 14: 2235-2242

Larson RE, Espindola FS, Espreafico EM. (1990). Calmodulin binding proteins and calcium/calmodulin-regulated enzyme activities associated with brain actomyosin. Jounal of Neurochemistry 54: 1288 1294

Larson RE, Pitta DE, Ferro JA. (1998). A novel 190 kDa calmodulin-binding protein associated with brain actomyosin. Brazilian Journal of Medical and Biological Research 21: 213-217

Lasko P. (1994). Molecular genetics of *Drosophila* oogenesis. RG Landes and Co, Austin

Lasko PF, Ashburner M. (1990). Posterior localization of *vasa* protein correlates with, but is not sufficient for, pole cell development. Genes and Development 4: 905-921

Lasko PF, Ashburner M. (1988). The product of the *Drosophila* gene *vasa* is very similar to eukaryotic initiation factor-4A. Nature 335: 611-617

Lawrence JB, Singer RH. (1986). Intracellular localization of messenger RNAs for cytoskeletal proteins. Cell 45: 407-415

Lederberg EM, Cohen SN. (1974). Transformation of *Salmonella typhimurium* by plasmid deoxyribonucleic acid. Journal of Bacteriology 119: 1072-1074

Lehmann R, Nusslein-Volhard C. (1986). Abdominal segmentation, pole cell formation, and embryonic polarity require the localized activity of *oskar*, a maternal gene in *Drosophila*. Cell 47: 141-152

Lehmann R, Nusslein-Volhard C. (1987). *hunchback*, a gene required for segmentation of an anterior and posterior region of the *Drosophila* embryo. Developmental Biology 119: 402-417

Lehmann R, Nusslein-Volhard C. (1991). The maternal gene *nanos* has a central role in posterior pattern formation of the *Drosophila* embryo. Development 112: 679-691

Li M, McGrail M, Serr M, Hays TS. (1994). *Drosophila* cytoplasmic dynein, a microtubule motor that is asymmetrically localized in the oocyte. Journal of Cell Biology 126: 1475-1494

Liang L, Diehl-Jones W, Lasko P. (1994). Localization of *vasa* protein in the *Drosophila* pole plasm is independent of its RNA-binding and helicase activities. Development 120: 1201-1211

Lillie S, Brown S. (1992). Suppression of a myosin defect by a kinesin related gene. Nature 356: 358-361

Lin H, Yue L, Spradling A. (1994). The *Drosophila* fusome, a germ-line specific organelle contains membrane skeletal proteins and functions in cyst formation. Development 120: 947-956

Lindsley DL, Zimm GG. (1992). The Genome of *Drosophila melanogaster*. Academic Press Inc, San Diego

Litman P, Barg J, Ginzburg I. (1994). Microtubules are involved in the localization of tau mRNA in primary neuronal cell cultures. Neuron 13: 1463-1474

Luria SE, Burrows JN. (1957). Hybridization between *Escherichia coli* and *Shigella*. Journal of Bacteriology 74: 461-476

MacDonald PM. (1990). *bicoid* mRNA localization signal: phylogenetic conservation of function and RNA secondary structure. Development 110: 161-171

Macdonald P, Kerr K, Smith JL, Leask A. (1993). RNA regulatory element BLE1 directs the early steps of *bicoid* mRNA localization. Development 118: 1233-1243

MacDonald PM, Leask A, Kerr K. (1995). exl protein specifically binds BLE1, a *bicoid* mRNA localization element, and is required for one phase of its activity. Proceedings of the National Academy of Sciences, USA 92: 10787-10791

Macdonald PM, Struhl G. (1988). cis-acting sequences responsible for anterior localization of *bicoid* mRNA in *Drosophila* embryos. Nature 336: 595-598

Mahowald AP, Kambysellis MP. (1980). Oogenesis in *The Genetics and Biology of* Drosophila. ed Asburner M, Wright TRF. Vol 2 Academic Press, New York. pp 141-224

Manseau LJ, Schupbach T. (1989). *cappuccino* and *spire*: two unique maternal-effect loci required for both the anteroposterior and dorsoventral patterns of the *Drosophila* embryo. Genes and Development 3: 1437-1452

Marcey D, Watkins WS, Hazelrigg T. (1991). The temporal and spatial distribution pattern of maternal exuperantia protein: evidence for a role in establishment but not maintenance of *bicoid* mRNA localization. Embo Journal 10: 4259-4266

Marino M, Archidiacono N, Franze A, Rosati M, Rocchi M, Ballabio A, Grimaldi G. (1993). A novel X-linked member of the human zinc finger protein gene family: isolation, mapping, and expression. Mammalian Genome 4 (5): 252-257

Markussen FH, Michon AM, Breitwieser W, Ephrussi A. (1995). Translational control of *oskar* generates short Osk, the isoform that induces pole plasm assembly. Development 121: 3723-3732

Melton DA. (1987). Translocation of a localized maternal mRNA to the vegetal pole of *Xenopus* oocytes. Nature 328: 80-82

Mercer JA, Seperack PK, Strobel MC, Copeland NG, Jenkins NA. (1991). Novel myosin heavy shains encoded by murine *dilute* coat colour locus. Nature 349: 709-713

Mermall V, McNally JG, Miller KG. (1994). Transport of cytoplasmic particles catalyzed by an unconventional myosin in living *Drosophila* embryos. Nature 369: 560-562.

Mermall V, Miller KG. (1995). The 95F unconventional myosin Is required for proper organization of the *Drosophila* syncytial blastoderm. Journal of Cell Biology 129: 1575-1588.

Micklem DR, Dasgupta R, Elliott H, Gergely F, Davidson C, Brand A, Gonzalez-Reyes A, St Johnston D. (1997). The *mago nashi* gene is required for the polarisation of the oocyte and the formation of perpendicular axes in *Drosophila*. Current Biology 7: 468-478

Mische SM, Mooseker MS, Morrow JS. (1987). Erythrocyte adducin: a calmodulin-regulated actin-bundling protein that stimulates spectrin-actin binding. Journal of Cell Biology 105: 2837-2845

Miyata H, Bowers B, Korn ED. (1989). Plasma membrane association of *Acanthamoeba* myosin I. Journal of Cell Biology 109: 1519-28

Moepps B, Conrad S, Schraudolf H. (1993). PCR-dependent amplification and sequence characterisation of partial cDNAs encoding myosin-like proteins in *Anemia phyllitidis* (L.) Sw. and *Arabidopsis thaliana* (L.) Heynh. Plant Molecular Biology 21: 1077-1083

Mohler JD. (1977). Developmental genetics of the *Drosophila* egg. I. Identification of 59 sex-linked cistrons with maternal effects on embryonic development. Genetics 85: 259-272

Mohler J, Wieschaus EF. (1986). Dominant maternal-effect mutations of *Drosophila* melanogaster causing the production of double-abdomen embryos. Genetics 112: 803-822

Montell C, Rubin GM. (1988). The *Drosophila ninaC* locus encodes two photoreceptor cell specific proteins with domains homologous to protein kinases and the myosin heavy chain head. Cell 52: 757-772

Mooseker MS, Cheney RE. (1995). Unconventional myosins. Annual Review of Cell and Developmental Biology 11: 633-675

Morgan, NS, Skovronsky DM, Artavanis-Tsakonas S, Mooseker MS. (1994). The molecular-cloning and characterization of *Drosophila-melanogaster* Myosin-Ia and Myosin-Ib. Journal of Molecular Biology 239: 347-356.

Morgan NS, Heintzelman MB, Mooseker MS. (1995). Characterization of Myosin-1a and Myosin-1b, two unconventional myosins associated with the *Drosophila* brush border cytoskeleton. Developmental Biology 172: 51-71

Morisato D, Anderson KV. (1995). Signaling pathways that establish the dorsal-ventral pattern of the *Drosophila* embryo. Annual Review of Genetics 29: 371-399

Moses K, Ellis MC, Rubin GM. (1989). The *glass* gene encodes a zinc-finger protein required by *Drosophila* photoreceptor cells. Nature 340 (6234): 531-536.

Neuman-Silberberg FS, Schupbach T. (1993). The *Drosophila* dorsoventral patterning gene *gurken* produces a dorsally localized RNA and encodes a TGF alpha-like protein. Cell 75: 165-174

Neuman-Silberberg FS, Schupbach T. (1996). The *Drosophila* TGF-alpha-like protein Gurken: expression and cellular localization during *Drosophila* oogenesis. Mechanisms of Development 59: 105-113

Newmark PA, Boswell RE. (1994). The *mago nashi* locus encodes an essential product required for germ plasm assembly in *Drosophila*. Development 120: 1301-1313

Newmark PA, Mohr SE, Gong L, Boswell RE. (1997). *mago nashi* mediates the posterior follicle cell-to-oocyte signal to organize axis formation in *Drosophila*. Development 124: 3197-3207

Ni B, Rosteck PR, Nadi S, Paul SM. (1994). Cloning and expression of a cDNA encoding a brain-specific Na^+-dependent inorganic phosphate cotransporter. Proceedings of the National Academy of Sciences of the USA 91: 5607-5611

Nusslein-Volhard C, Frohnhofer HG, Lehmann R. (1987). Determination of anteroposterior polarity in *Drosophila*. Science 238: 1675-1681

O'Kane CJ, Gehring WJ. (1987). Dectection *in situ* of genomic regulatory elements in *Drosophila*. Proceedings of the National Academy of Sciences, USA 84: 9123-9127

Oliver TN, Corey DP, Derfler BH, Pennisi CM, Cheney RE. (1996). Myosin-X: An unconventional myosin with PH domains. Molecular Biology of the Cell 7: 227-227.

Perrimon N, Mohler D, Engstrom L, Mahowald AP. (1986). X-linked female-sterile loci in *Drosophila melanogaster*. Genetics 113 : 695-712

Peterson MD, Novak KD, Reedy MC, Ruman JL, Titus MA. (1995). Molecular genetic analysis of myoC, a *Dictyostelium* myosin I. Journal of Cell Science 108: 1093-1103

Pokrywka NJ, Stephenson EC. (1991). Microtubules mediate the localization of *bicoid* RNA during *Drosophila* oogenesis. Development 113: 55-66

Pollard TD, Korn ED. (1973) *Acanthamoeba* Myosin I. Isolation from *Acanthamoeba castellanii* of an enzyme similar to muscle myosin. Journal of Biological Chemistry 248: 4682-4690

Pollard TD, Doberstein SK, Zot HG. (1991). Myosin-I. Annual Review of Physiology 53: 653-681

Pomeroy ME, Lawrence JB, Singer RH, Billings-Gagliardi S. (1991). Distribution of myosin heavy chain mRNA in embryonic muscle tissue visualized by ultrastructural *in situ* hybridization. Developmental Biology 143: 58-67

Porter JA, Hicks JL, Williams DS, Montell C. (1992). Differential localizations and requirements for the two *Drosophila ninaC* kinase/myosins in photoreceptor cells. Journal of Cell Biology 116: 683-693

Pondel MD, King ML. (1988). Localized maternal mRNA related to transforming growth factor beta mRNA is concentrated in a cytokeratin-enriched fraction from *Xenopus* oocytes. Proceedings of the National Academy of Sciences, USA 85: 7612-7616

Porter JA, Montell C. (1993) Distinct roles of the *Drosophila* ninaC kinase and myosin domains revealed by systematic mutagenesis. Journal of Cell Biology 122: 601-612

Prekeris R, Cooper JB, Hernandez RM, Terrian DM. (1996). Myosin V is a synaptic vesicle protein. Molecular Biology of the Cell 7: 317a

Price JV, Clifford RJ, Schupbach T. (1989). The maternal ventralizing locus *torpedo* is allelic to *faint little ball*, an embryonic lethal, and encodes the *Drosophila* EGF receptor homolog. Cell 56: 1085-1092

Proudfoot N. (1991). Poly(A) signals. Cell 64: 671-674

Raff JW, Whitfield WG, Glover DM. (1990). Two distinct mechanisms localise *cyclin B* transcripts in syncytial *Drosophila* embryos. Development 110: 1249-1261

Reinhard J, Scheel AA, Dickman D, Hall A, Ruppert C, Bahler M. (1995). A novel type of myosin implicated in signalling by rho family GTPases.EMBO Journal 14: 697-704

Ruohola H, Bremer KA, Baker D, Swedlow JR, Jan LY, Jan YN. (1991). Role of neurogenic genes in establishment of follicle cell fate and oocyte polarity during oogenesis in *Drosophila*. Cell 66: 433-449

Ruohola-Baker H, Jan LY, Jan YN. (1994). The role of gene cassettes in axis formation during *Drosophila* oogenesis. Trends in Genetics 10: 89-94

Ruppert JM, Kinzler KW, Wong AJ, Bigner SH, Kao F-T, Law ML, Seuanez HN, O'Brien SJ, Vogelstein B. (1988). The GLI-*Kruppel* family of human genes. Molecular and Cellular Biology 8: 3104-3113

Sander K, Lehmann R. (1988). *Drosophila* nurse cells produce a posterior signal required for embryonic segmentation and polarity. Nature 335: 68-70

Sanders G, Lichte B, Meyer HE, Kilimann MW. (1992). cDNA encoding the chicken ortholog of the mouse *dilute* gene product. sequence comparison reveals a myosin I subfamily with conserved C-terminal domains. FEBS Letters 311: 295-298

Sanger F, Nicklen S, Coulson AR. (1977). DNA sequencing with chain-terminating inhibitors. Proceedings of the National Academy of Sciences, USA 74: 5463-5467

Schroder C, Tautz D, Seifert E, Jackle H. (1988). Differential regulation of the two transcripts from the *Drosophila* gap segmentation gene *hunchback*. Embo Journal 7: 2881-2887

Schupbach T. (1987). Germ line and soma cooperate during oogenesis to establish the dorsoventral pattern of egg shell and embryo in *Drosophila* melanogaster. Cell 49: 699-707

Schupbach T, Weischaus E. (1986). Maternal-effect mutations altering the anterior-posterior pattern of the *Drosophila* embryo. Roux's Archives of Developmental Biology 195: 302-317

Schupbach T, Wieschaus E. (1989). Female sterile mutations on the 2nd chromosome of *Drosophila melanogaster* I. Maternal effect mutations. Genetics 121: 101-117

Schupbach T, Wieschaus E. (1991). Female sterile mutations on the 2nd chromosome of *Drosophila melanogaster* II. Mutations blocking oogenesis or altering egg morphology. Genetics 129: 1119-1136.

Schroder C, Tautz D, Seifert E, Jackle H. (1988). Differential regulation of the two transcripts from the *Drosophila* gap segmentation gene *hunchback*. Embo Journal 7: 2881-2887

Schupbach T. (1987). Germ line and soma cooperate during oogenesis to establish the dorsoventral pattern of egg shell and embryo in *Drosophila* melanogaster. Cell 49: 699-707

Searle AG. (1952). A lethal allele of *dilute* in the house mouse. Heredity 6: 395-401

Serano TL, Cohen RS. (1995). Gratuitous mRNA localization in the *Drosophila* oocyte. Development 121: 3013-3021

Siegel V, Jongens TA, Jan LY, Jan YN. (1993). *pipsqueak*, an early acting member of the posterior group of genes, affects *vasa* level and germ cell-somatic cell interaction in the developing egg chamber. Development 119: 1187-1202

Silvers WK. (1979). *Dilute* and *Leaden*, the *p*-locus, *Ruby-Eye*, and *Ruby-Eye-2*. In *Coat Colors of Mice: A Model foe Mammalian Gene Action and Interaction*. ed WK Silvers. New York: Springer Verlag pp 83-89, 104-107

Solc CF, Derfler RH, Duyk GM, Corey DR. (1994). Molecular cloning of myosins from the bullfrog saccular macula: a candidate for the hair cell adaption motor. Aud. Neuroscience 1: 63-75

Southern EM. (1975). Detection of specific sequences among DNA fragments separated by gel electrophoresis. Journal of Molecular Biology 98: 503-517

St Johnston D. (1994). RNA localization. Getting to the top. Current Biology 4: 54-56

St Johnston D. (1995). The intracellular localization of messenger RNAs. Cell 81: 161-170

St Johnston D, Beuchl D, Nusslein-Volhard C. (1991). *staufen*, a gene required to localise maternal RNAs in the *Drosophila* egg. Cell 66: 51-63

St Johnston D, Brown NH, Gall J G, Jantsch M. (1992). A conserved double-stranded RNA-binding domain. Proceedings of the National Academy of Sciences, USA 89, 10979-10983

St Johnston D, Driever W, Berleth T, Richstein S, Nusslein-Volhard C. (1989). Multiple steps in the localization of *bicoid* RNA to the anterior pole of the *Drosophila* oocyte. Development Supplement 13-19

St Johnston D, Nusslein-Volhard C. (1992). The origin of pattern and polarity in the *Drosophila* embryo. Cell 68: 201-219

Steel KP, Brown SDM. (1994). Genes and deafness. Trends in Genetics 10: 428-435
Stephenson EC, Chao Y-C, Fackenthal JD. (1988) Molecular analysis of the *swallow* gene of *Drosophila melanogaster*. Genes and Development 2: 1655-1665

Steward O, Banker GA. (1992). Getting the message from the gene to the synapse: sorting and intracellular transport of RNA in neurons. Trends in Neurosciences 15: 180-186

Storto PD, King RC. (1989). The role of polyfusomes in generating branched chains of cystocytes during *Drosophila* oogenesis. Developmental Genetics 10: 70-86

Struhl G. (1989). Differing strategies for organizing anterior and posterior body pattern in *Drosophila* embryos. Nature 338: 741-744

Struhl G, Struhl K, Macdonald PM. (1989). The gradient morphogen bicoid is a concentration-dependent transcriptional activator. Cell 57: 1259-1273

Sundell CL, Singer RH. (1991). Requirement of microfilaments in sorting of actin messenger RNA. Science 253: 1275-1277

Suter B, Romberg LM, Steward R. (1989). *Bicaudal-D*, a *Drosophila* gene involved in developmental asymmetry: localized transcript accumulation in ovaries and sequence similarity to myosin heavy chain tail domains. Genes and Development 3: 1957-1968

Suter B, Steward R. (1991). Requirement for phosphorylation and localization of the *Bicaudal-D* protein in *Drosophila* oocyte differentiation. Cell 67: 917-926.

Tautz D, Pfeifle C. (1989). A non-radioactive *in situ* hybridization method for the localization of specific RNAs in *Drosophila* embryos reveals translational control of the segmentation gene *hunchback*. Chromosoma 98: 81-85

Tetzlaff MT, Jackle H, Pankratz MJ. (1996). Lack of *Drosophila* cytoskeletal tropomyosin affects head morphogenesis and the accumulation of oskar mRNA required for germ cell formation. EMBO Journal 15: 1247-1254

Theurkauf WE. (1994a). Premature microtubule-dependent cytoplasmic streaming in *cappuccino* and *spire* mutant oocytes. Science 265: 2093-2096

Theurkauf WE. (1994b). Microtubules and cytoplasm organization during *Drosophila* oogenesis. Developmental Biology 165: 352-360.

Theurkauf WE, Alberts BM, Jan YN, Jangens TA. (1993). A central role for microtubules in the differentiation of *Drosophila* Oocytes. Development 118: 1169-1180

Theurkauf WE, Smiley S, Wong ML, Alberts BM. (1992). Reorganization of the cytoskeleton during *Drosophila* oogenesis: implications for axis specification and intercellular transport. Development 115: 923-936

Titus MA. (1997). Myosin V - the multi-purpose transport motor. Current Biology 7: R301-R304

Trapp BD, Moench T, Pulley M, Barbosa E, Tennekoon G, Griffin J. (1987). Spatial segregation of mRNA encoding myelin-specific proteins. Proceedings of the National Academy of Sciences, USA 84: 7773-7777

Tso JY, Sun X-H, Wu R. (1985). Structure of two unlinked *Drosophila melanogaster* glyceraldehyde-3-phosphate dehydrogenase genes. Journal of Biological Chemistry 260: 8220-8228

Wang C, Dickinson LK, Lehmann R. (1994). Genetics of *nanos* localization in *Drosophila*. Developmental Dynamics 199: 103-115

Wang C, Lehmann R. (1991). *Nanos* is the localized posterior determinant in *Drosophila*. Cell 66: 637-647

Wang S, Hazelrigg T. (1994). Implications for *bcd* localization from spatial distribution of *exu* protein in *Drosophila* oogenesis. Nature 369: 400-403

Weeks DL, Melton DA. (1987). A maternal mRNA localized to the animal pole of *Xenopus* eggs encodes a subunit of mitochondrial ATPase. Proceedings of the National Academy of Sciences, USA 84: 2798-2802

Weeks DL, Melton DA. (1987). A maternal mRNA localized to the vegetal hemisphere in *Xenopus* eggs codes for a growth factor related to TGF-beta. Cell 51: 861-867

Wei Q, Wu X, Hammer JA. (1997). The predominant defect in *dilute* melanocytes is in melanosome distribution and not cell shape, supporting a role for myosin V in melanosome transport. Journal of Muscle Research and Cell Motility 18: 517-527

Weil D, Blanchard S, Kaplan J, Guilford P,Gibson F, Walsh J, Mburu P, Varela A, Levilliers J, Weston MD, Kelley PM, Kimberling W J, Wagenaar M, Levi-Acobas F, Larget-Piet D, Munnich A, Steel KP, Brown SDM, Petit C. (1995). Defective myosin VIIA gene responsible for Usher syndrome type IB. Nature 374: 80-81

Weir MP, Kornberg T. (1985). Patterns of *engrailed* and *fushi tarazu* transcripts reveal novel intermediate stages in *Drosophila* segmentation. Nature 318: 433-439

Weischaus E, Szabad J. (1979). The development and function of the female germline in *Drosophila melanogaster* and cell lineage study. Developmental Biology 68: 29-46

Wharton KA, Johansen KM, Xu T, Artavanis-Tsakonas S. (1985). Nucleotide sequence from the neurogenic locus *notch* implies a gene product that shares homology with proteins containing EGF-like repeats. Cell 43: 567-581

Wharton RP, Struhl G. (1989). Structure of the *Drosophila Bicaudal-D* protein and its role in localizing the posterior determinant *nanos*. Cell 59: 881-892

Wheatley S, Kulkarni S, Karess R. (1995). *Drosophila* nonmuscle myosin II is required for rapid cytoplasmic transport during oogenesis and for axial nuclear migration in early embryos. Development 121: 1937-1946

Wilson C, Kurth Pearson R, Bellen HJ, O'Kane CJ, Grossniklaus U, Gehring W. (1989). P-element mediated enhancer detection: An efficient method for isolating and characterizing developmentally regulated genes in *Drosophila*. Genes and Development 3: 1301-1313

Wirth JA, Jensen KA, Post PL, Bement WM, Mooseker MS. (1996). Human myosin-IXb, an unconventional myosin with a chimerin-like rho/rac GTPase-activating protein domain in its tail. Journal of Cell Science 109: 653 661

Wolenski JS, Cheney RE, Mooseker MS, Forscher P. (1995). In vito motility of immunoadsorbed brain myosin-V using a *Limulus* acrosomal process and optical tweezer based assay. Journal of Cell Science 108: 1489-1496

Wolenski JS, Hayden SM, Forscher P, Mooseker MS. (1993). Calcium-calmodulin and regulation of brush border myosin-I MgATPase and mechanochemistry. Journal of Cell Biology 122: 613-621

Wu X, Bowers B, Wei Q, Kocher B, Hammer JA. (1997). Myosin V associates with melanosomes in mouse melanocytes: evidence that myosin V is an organelle motor. Journal of Cell Science 110: 847-859

Xu T, Caron LA, Fehon RG, Artavanis-Tsakonas S. (1992). The involvement of the *Notch* locus in *Drosophila* oogenesis. Development 115: 913-922

Yisraeli JK, Sokol S, Melton DA. (1990). A two-step model for the localization of maternal mRNA in *Xenopus* oocytes: involvement of microtubules and microfilaments in the translocation and anchoring of Vg1 mRNA. Development 108: 289-298

Young PE, Richman AM, Ketchum AS, Kiehart DP. (1993). Morphogenesis in *Drosophila* requires nonmuscle myosin heavy chain function. Genes and Development 7: 29-41

Yue L, Spradling AC. (1992). *hu-li tao shao*, a gene required for ring canal formation during *Drosophila* oogenesis, encodes a homolog of Adducin. Genes and Development 6: 2443-2454

Zhang P, Spradling AC. (1993). Efficient and dispersed local P element transposition from *Drosophila* females. Genetics 133: 361-373

Zhao LP, Koslovsky JS, Reinhard J, Bahler M, Witt AE, Provance DW, Mercer JA. (1996). Cloning and characterization of myr-6, an unconventional myosin dilute/myosin-V family. Proceedings of the National Academy of Sciences,USA 93: 10826-10831.

Appendix

Dev Genes Evol (1998) 208:172–174

EXPRESSION NOTE

Angela McCormack · Bryce MacIver · Mary Bownes

Cloning and expression of *az2*, a putative zinc finger transcription factor from *Drosophila melanogaster*

Received: 9 February 1998 / Accepted: 15 March 1998

Abstract A *Drosophila* gene (*az2*), mapping to a cluster of embryonic lethals at 43BC on the polytene chromosomes, has been sequenced and found to encode a predicted protein with six consecutive C2H2 zinc finger domains. The carboxy-terminus of *az2* is related to a number of *Drosophila* and mammalian transcription factors. The 5' end of the gene is unrelated to genes in the databases. The gene is expressed in the adult female, in both the carcass and ovary, but is most abundant in the ovary. It is expressed in the nurse cells and transported to the oocyte.

Edited by D. Tautz

A. McCormack[1] · B. MacIver[2] · M. Bownes (✉)
Institute of Cell and Molecular Biology, University of Edinburgh, Darwin Building, King's Buildings, Edinburgh, EH9 3JR, UK

Current addresses:
[1] Hannah Research Institute, Ayr, KA6 5HL, UK
[2] Department of Biology, Eberly College of Science, Pennsylvania State University, University Park, PA 16802-5301, USA

Whilst undertaking a chromosome walk in the 43BC region of the *Drosophila* genome we have identified a gene encoding a putative novel zinc finger transcription factor. A cDNA was isolated from a λZAP ovarian cDNA library mapping immediately downstream of a *myosin V* gene (MacIver, McCormack, Slee and Bownes, unpublished) which we are studying. It was subcloned into Bluscript B$^-$Sk$^-$, sequenced and named *az2*. The sequence and the predicted protein sequence is available with accession number AF03768. There is an 'atg' at position 10 which is a potential start site. However, there is a more usual start 'atg' 200 bp upstream in the genomic DNA sequence (Cavener 1987) and thus this could potentially be a truncated cDNA. The best poly(A) site is an AATATA; the consensus sequence is AATAAA (Proudfoot 1991).

Database comparisons of the putative protein showed that the C-terminal domain contained several zinc finger domains. They consist of stretches of approximately 25 amino acids with two cysteine or histidine residues at

```
hshkr1   GE.KPYVCRE CGRGFRQHSH LVRHK.RTHS .GEKP.YICR ECEQGFSQKS
hsznf8   GE.RHHKCSE CGKAFTQKST LRMHQ.RIHT .GERS.YICT QCGQAFIQKA
mmmkr5   GE.KPYECEI CRKAFSHHAS LTQHQ.RVHS .GEKP.FKCK ECGKAFRQNI
mm2nf3   GE.KPFECDH CGKAFPSSSY LNVH.LKIHT .GEKP.FRCT VCGKTFTCSS
dmglas   GEMKPNLCRL CGKTYARPST LKTH.LRTHS .GERP.YRCP DCNKSFSQAA
   az2   QKLK...CEV CEHSFSTDHA LQAHQFRDHK MGDGGWFRCT LCELNFDRKC

hshkr1   HLIRHL.RTH TGEKPYVCTE CGRHFSWKSN LKTHQRTHSG ...VKPYVCL
hsznf8   HLIAH.QRIH TGEKPYECSD CGKSFPSKSQ LQMHKRIHTG ...EKPYICT
mmmkr5   HLASH.WRIH TGEKPFECGE CGKSFSISSQ LATHQRIHTG ...EKPFECK
mm2nf3   YLPVHM.RTH TGGRPFRCII CGRSFLWSSY LRVHMRIHTG ...EKPYVCQ
dmglas   NLTAHV.RTH TGQKPFRCPI CDRRFSQSSS VTTHMRTHSG ...ERPYRCS
   az2   HLQQHSQRVH M.DKSFVCEI CSRSFAFGSQ LAIHKRTHDE KHVAKPFVCE

hshkr1   ECGQCFSLKS NLNKH.QRSH TGEKPFVC..  human Kruppel related[1]
hsznf8   ECGKAFTNRS NLNTH.QKSH TGEKSYICAE  human ZNF81[2]
mmmkr5   VCRKAFRQNI HLASH.WRIH TGEKPFECGE  mouse mkr5[3]
mm2nf3   YCGKAFTEHS GLNKHLRK.H TGEKPYEYKE  mouse mkr3[3]
dmglas   SCKKSFSDSS TLTKHLR.IH SGEKPYQCKL  Drosophila glass[4]
   az2   FCGKCFKQKI QMTTHVTAVH TKIRALQVRH  Drosophila az2
```

Fig. 1 Alignment of zinc finger proteins from several species using the GCG PILEUP program. C2H2-type zinc finger domains consist of the consensus pattern C-X-X-C-X-X-X-[LIVMFYWC]-X-X-X-X-X-X-X-X-H-X-X-X-(X)-H where the two Cs and the two Hs are the zinc ligands. The C-terminal region of the az2 predicted protein contains multiple copies of this consensus in common with regions of the five known zinc finger proteins shown

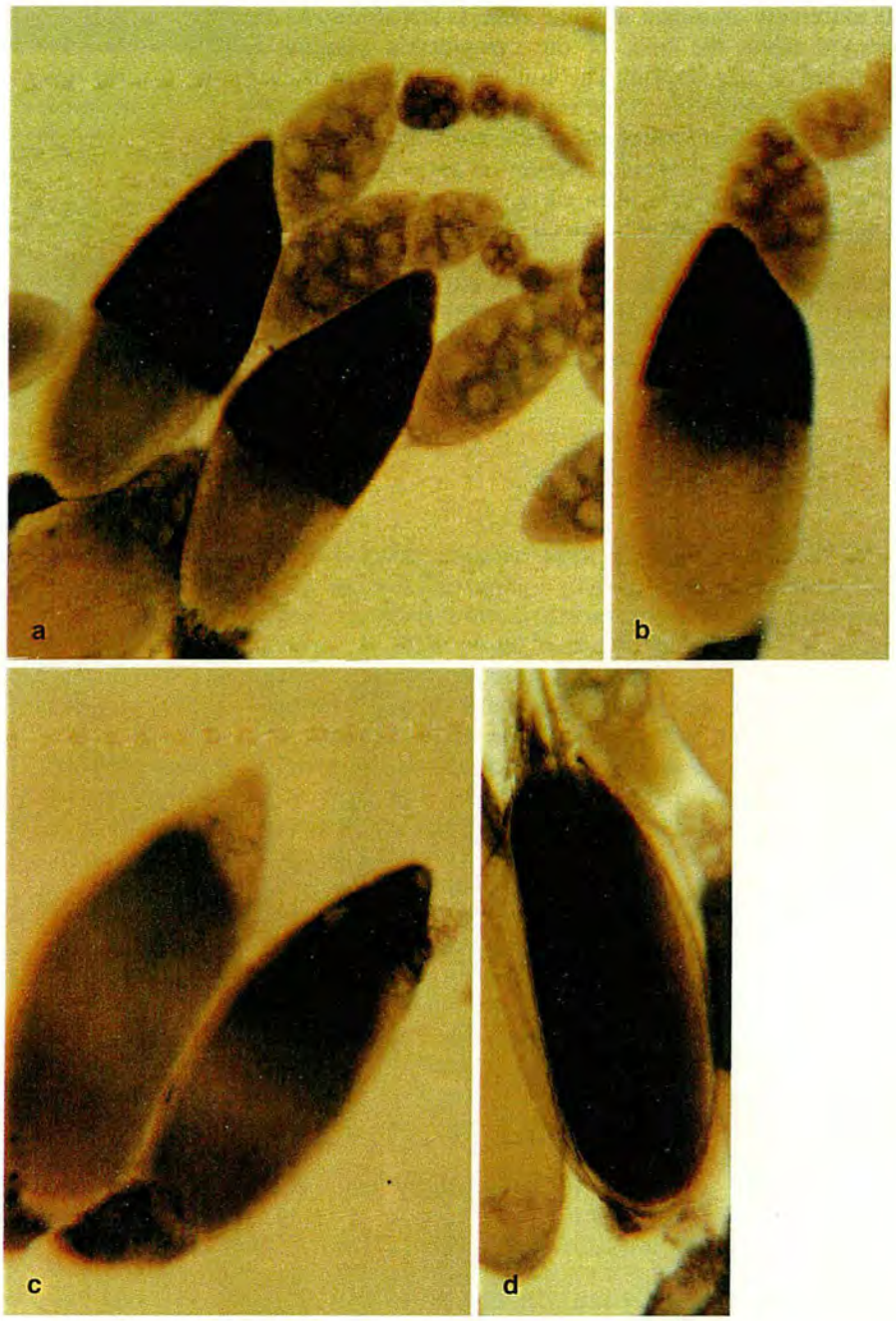

Fig. 2a–d In situ hybridisation to *az2* RNA in the ovaries of *Drosophila*. Transcripts are observed in all cells throughout oogenesis, but become especially abundant in the stage 10 nurse cell. They are then 'dumped' into the oocyte at stages 11 and 12. **a** Stage 1–10; **b** stage 11 a high concentration of transcript is seen at due anterior of due oocyte; **c** stage 12; **d** stage 13 (*n* nurse cells, *o* oocyte)

either end, which are involved in the tetrahedral co-ordination of a zinc atom. This interacts with DNA to mediate transcription. Zinc fingers are classified by the number and position of these cysteine (C) and histidine (H) residues. The C-terminal region of the *az2* gene encodes consecutive C2H2 type domains which have the consensus sequence of C-X-X-C-X-X-X-[LIVMFYWC]-X-X-X-X-X-X-X-X-H-X-X-X-(X)-H. Figure1 shows an alignment of the predicted C-terminal domain of *az2* with five other known zinc finger proteins from *Drosophila*, mouse and humans (Chowdhury et al. 1988; Ruppert et al. 1988; Moses et al. 1989; Marino et al. 1993). The N-terminal region, however, shows no significant homology with any other protein in the database, suggesting *az2* encodes a novel transcriptional regulator.

Northern analysis showed that the *az2* transcript was abundant in ovaries and female carcasses. Since our main interest is in oogenesis we investigated the temporal and spatial expression of the gene during oogenesis using in situ hybridisation with a digoxigenin-labelled fragment of 0.9 kb from the *az2* cDNA. As shown in Fig. 2 the transcript is present at low levels in the nurse cells during early stages of oogenesis, but becomes very abundant at about stage 8 to 9 (following the staging system of King 1970). At stage 10b the transcript, which

is extremely abundant in nurse cells, is transferred to the oocyte when the bulk of the cytoplasmic material is dumped in the oocyte. The transcript therefore is at a higher concentration at the anterior of the oocyte initially and then diffuses throughout the entire mature oocyte and egg. This is a typical expression pattern for mRNAs which are to be utilised in early embryogenesis prior to transcription initiation in the embryo.

Acknowledgements This research was supported by the Wellcome Trust. Angela McCormack was supported by a bbsrc studentship and Bryce MacIver by the Darwin Trust. We are grateful to Sheila Milne for typing the manuscript.

References

Cavener DR (1987) Comparison of the consensus sequence flanking translational start sites in *Drosophila* and vertebrates. Nucleic Acids Res 15:1353–1361

Chowdhury K, Rohdewohld H, Gruss P (1988) Specific and ubiquitous expression of different Zn finger protein genes in the mouse. Nucleic Acids Res 16:9995–10011

King RC (1970) Ovarian development in *Drosophila melanogaster.* Academic Press, New York London

Marino M, Archidiacono N, Franze A, Rosati M, Rocchi M, Ballabio A, Grimaldi G (1993) A novel X-linked member of the human zinc finger protein gene family: isolation, mapping, and expression. Mamm Genome 4:252–257

Moses K, Ellis MC, Rubin GM (1989) The *glass* gene encodes a zinc finger protein required by *Drosophila* photoreceptor cells. Nature 340:531–536

Proudfoot N (1991) Poly(A) signals. Cell 64:671–674

Ruppert JM, Kinzler KW, Wong AJ, Bigner SH, Kao F-T, Law ML, Seuanez HN, O'Brien SJ, Vogelstein B (1988) The *GLI-Kruppel* family of human genes. Mol Cell Biol 8:3104–3113

Eur. J. Biochem. 257, 529–537 (1998)

Identification of an essential gene encoding a class-V unconventional myosin in *Drosophila melanogaster*

Bryce MacIVER[1], Angela McCORMACK[2], Roger SLEE[3] and Mary BOWNES[4]

[1] Department of Biology, Eberly College of Science, Pennsylvania State University, USA
[2] Hannah Research Institute, Ayr, UK
[3] Western General Hospital, Edinburgh, UK
[4] Institute of Cell and Molecular Biology, University of Edinburgh, Edinburgh, UK

(Received 12 May 1998) – EJB 98 0649/2

Class-V myosins are a unique type of myosin motor with roles in intracellular transport. The mouse *dilute* gene was the first member of this class to be cloned, with mutations resulting in lightening of the coat colour or neurogenic defects leading to early death. Further examples of class-V myosins have been described in yeast, chicken and rat. Here, we report the cloning of the first class-V myosin from *Drosophila*. We show that expression of this myosin is predominantly in the adult germ line and early embryo and that the transcript is localised in the oocyte during oogenesis. Genetic and in situ hybridisation experiments have determined that this gene is located in the 43C region. We have evidence that it maps to a mutation in this region with an embryonic lethal phenotype.

Keywords: myosin V; oogenesis; *Drosophila*; developmental genetics.

Myosins are a superfamily of molecules capable of converting chemical energy into mechanical force. More specifically, they are protein complexes composed of one or two heavy chains and varying numbers of light chains. Myosin heavy chains comprise a characteristic head region containing ATP and actin-binding domains and a variable tail (carboxy) region. Comparison of the amino acid sequence of the head region has allowed a phylogenetic relationship between these molecules to be established [1, 2]. Conventional myosins are classified as dimeric filament-forming molecules found in muscle and non-muscle cells. In recent years, an expanding group of unconventional myosins has been described in vertebrates, invertebrates and plants. These unconventional myosins are currently grouped into 12 classifications based on sequence similarity within the myosin-head domain [3].

The mouse *dilute* locus has been shown to encode an unconventional myosin [4] and was the progenitor of a new group of unconventional myosins, now called class V. The class-V myosins are characterised by possessing head regions showing greater similarity to members within this class than to other myosins, a 'neck' region containing six IQ motifs predicted to bind regulatory light chains and a tail domain that has regions that form coiled-coil α-helices and other regions predicted to be of a globular nature. Additional myosin Vs have been cloned from yeast, chicken and rat and degenerate PCR analysis has identified similar genes in humans [5]. A class-V myosin has also been recently described in *Caenorhabditis elegans* [6]. Studies on the mouse and yeast myosin Vs suggest a role in vesicle transport.

The *dilute* locus produces two distinct phenotypes, a lightening of the coat colour and a neurogenic defect resulting in lethality. The lightening of the coat colour was thought to result from abnormal melanocyte morphology [7]; however, recent studies of mutant cell lines have shown that melanocyte morphology is normal, but the melanosomes are incorrectly distributed [8]. Furthermore, immunolocalisation studies show that the *dilute* myosin V is associated with these melanosomes [9]. The cause of the neurogenic defect which causes convulsions and death at 3 weeks postnatal is unknown.

In the budding yeast *Saccharomyces cerevisiae*, two examples of class-V unconventional myosins, *MYO2* and *MYO4*, have been identified. The *MYO2* gene is essential and is required for bud formation [10]. A mutant for this gene shows accumulation of vesicles suggesting that the role of the protein is in transporting material to the bud site. Budding occurs in several stages; bud-site selection, bud-site assembly, cytoskeletal organisation and polarised growth. Mutants for *MYO2* fail to deposit the chitin ring, which is required for bud-site formation, but these mutants are able to complete the cell division when shifted to the restrictive temperature at a late stage, suggesting there is no role for this myosin in cytokinesis or nuclear migration [10]. Myo2p has also been implicated in the inheritance of the vacuole during cell division [11]

In contrast, the *MYO4* gene, isolated by random cloning and sequence comparison is not essential [12]. The *MYO4* gene has also been identified as *SHE1*, one of five genes involved in mating-type switching. In the mother cell, mating type is switched by the *HO* endonuclease during cell division. It is postulated that the *SHE* genes are responsible for transporting an *HO* endonuclease repressor into the daughter cell [13].

The best biochemically characterised class-V myosin is p190 from the chicken brain. This myosin was purified from brain extracts [14] and cDNAs were subsequently obtained from an

Correspondence to M. Bownes, Institute of Cell and Molecular Biology, University of Edinburgh, Edinburgh EH9 3JR, UK
Fax: +44 131 6508650.
E-mail: MBownes@srv0.bio.ed.ac.uk

Abbreviation. GAD, glutamate decarboxylase.

Note. The novel nucleotide sequence presented here has been submitted to the GenBank/EMBL database and is available under accession number Y08160.

expression library [15]. Bacterially expressed IQ motifs were shown to bind calmodulin, although this binding does not appear to have a strict requirement for calcium. Further efforts have shown the stoichiometric relationship between calmodulin and this myosin V to be 4:1 [16], with two additional light chains of 17 kDa and 23 kDa also identified. Visualisation of the myosin by electron microscopy has given clues to the structure of this molecule. A two-headed molecule was observed, suggesting a dimer. The head regions were spaced further apart than those seen in conventional myosin IIs, probably due to the myosin V having six IQ motifs compared with two in myosin II. A stalk domain and a globular domain, consistent with the coiled-coil α-helices and the carboxyl globular domain predicted from the sequence data, were also observed. This study also demonstrated that the p190 protein bound to actin filaments and translocated towards the barbed end of actin in vitro [16].

A second subclass of vertebrate myosin V, *myr6*, has been described in the rat [17] and we have cloned the mouse ortholog (B. MacIver et al., unpublished results). The mouse ortholog is strongly expressed in heart, lung, liver, kidney and testis, with lower levels seen in brain and muscle [17]. The long-term focus of this work is to determine whether there is any functional overlap between the *myr6* ortholog and the *dilute* gene.

Our laboratory investigates the molecular genetics of *Drosophila* oogenesis. We have cloned a gene that encodes a transcript that localises to the oocyte from very early stages of oogenesis, in a pattern similar to that seen for the *orb* and *oskar* [18, 19] genes with essential functions in oogenesis and embryogenesis. We have named this gene *didum* for *dilute*-like *Drosophila* unconventional myosin. We have established that *didum* encodes a class-V unconventional myosin and report the molecular cloning, expression pattern and initial genetic analysis for this gene.

MATERIALS AND METHODS

Fly stocks. Flies were cultured on a cornmeal, yeast and agar medium in vials and bottles. The wild-type line used was *OregonR*, while deficiencies used for PCR analysis were *pk78k* (42E3; 43C3) and *P32* (43A3; 43F6). Other deficiencies used can be found in Heitzler et al. [30].

Library screening and cloning. A 1.6-kb cDNA was initially isolated from a whole-body library in the NM1149 lambdaphage vector. A 0.8-kb *Eco*RI fragment from this cDNA was used to screen an ovarian library in the ZAP II lambdaphage vector with four recombinants containing a 2.2-kb insert (pBMF10). The 2.2-kb cDNA was used as probe for subsequent screens of the Canton S genomic library in the FIX II lambdaphage (Stratagene) and 'mini-libraries' prepared from the recombinant P1 DS00574. Mini-libraries were constructed by digestion of DNA prepared from P1 DS00574 with either *Bam*HI, *Eco*RI or *Xba*I and ligating fragments into appropriately prepared pBluescript SK− (Stratagene).

DNA sequencing. The dideoxy chain determination method [20] was used initially in the form of a Sequenase 2.0 kit (US Biochemicals), followed by automated sequencing on Perkin Elmer ABI 373A and 377A machines, using dye-labelled primers, then dye-labelled terminator reactions. Sequenced fragments were assembled using GCG GELSTART software [21]. Sequence analysis was done with GCG GAP, MAP, FASTA, TFASTA and PILEUP software. Predicted coiled-coil regions were identified with the MacStripe version [22] of the algorithm written by Lupas et al. [23].

Expression analysis. In situ hybridisation to whole-mount ovaries was carried out using a method modified from Tautz and Pfeifle [24]. Dissected ovaries were fixed in freshly prepared 4% (mass/vol.) paraformaldehyde for 1 h at room temperature. Probe was digoxigenin (Boehringer Mannheim)-labelled cDNA used in HS solution [50%vol. formamide, 5× NaCl/Cit (0.15 M sodium chloride, 15 mM trisodium citrate, pH 7), 50 mg/ml heparin, 0.1%vol. Tween-20, 100 μg/ml non-specific DNA]. Alkaline-phosphate-conjugated anti-digoxigenin antibody was used to detect the signal with X-phosphate and nitro-blue tetrazolium salt providing the substrate.

Northern-blot analysis was carried out by preparing total RNA from appropriate developmental stages using the Trizol method (Gibco-BRL). Approximately 10 μg total RNA was loaded in each well of a 0.8% agarose/formaldehyde gel run in Mops buffer. The RNA was then transferred to Hybond N+ (Amersham) and probed with the 2.2-kb cDNA.

Southern blotting. Genomic DNA was prepared from 20–30 adult flies using the method of Ashburner [25]. DNA was digested with restriction endonucleases for several hours in the appropriate buffer, then separated on 0.8% agarose gels in Tris/EDTA buffer (89 mM Tris/HCl, 89 mM boric acid, 2.5 mM EDTA, pH 8.3) before transfer to Hybond N (Amersham). Probes used were a variety of ^{32}P-labelled cDNA and genomic fragments.

PCR analysis. PCRs were performed in a Hybaid thermocycler using Promega *Taq* polymerase and supplied buffer with Mg^{2+} concentration of 2 mM. Reverse transcription PCR utilised BRL Superscript II reverse transcriptase as suggested by the manufacturer prior to PCR. Oligonucleotide primers were designed using the GCG PRIME program and those used were:

did3 5′-AGTTTGGAGCGGTAAACC-3′
did4 5′-TTCCGCTAAATCCTCCAC-3′

for reverse transcription PCR,

1806 5′-GGCCACGTCGATTGGAGC-3′
2800 5′-TACAAGGTTTAGGCAAGG-3′

for PCR of the *didum* gene,

did12 5′-CGATACGCTCGGATTATG-3′
did6 5′-GTTTCGCCCTTGACAACA-3′

for 5′ RACE of the *didum* gene, and

So1 ATGTTACAGCATCCCGCCAC
So4 AACACGATATTTGCCACCAG
1241 GCAAACTAAAATCCGTA
1240 TATATCGACCAACGGCG

for control PCRs of the *sine oculis* gene and kinase gene on the third chromosome.

RESULTS

Identification, cloning and sequencing. An adult female fly has a pair of ovaries with each ovary consisting of 15–20 ovarioles joined at their ends by terminal filaments [26]. At the tip of each ovariole are 1–4 germ line-derived stem cells, which divide to produce a daughter stem cell and a cystoblast. The cystoblast undergoes a series of four further mitotic divisions, during which cytokinesis is incomplete, to produce a cyst of 16 cells (cystocytes) connected by intercellular bridges called ring canals. One of these 16 cells differentiates to become the oocyte, while the remaining 15 become polyploid nurse cells, which supply material to the developing oocyte. Somatically derived follicle cells migrate to surround the cystocyte to form an egg chamber. These follicle cells produce yolk proteins, the vitelline membrane and the chorion and have essential roles in establish-

Fig. 1. Whole-mount in situ hybridisation to *Drosophila* ovaries showing *didum* transcript localised to the oocyte. Whole-mount in situ hybridisation to *Drosophila* ovaries showing *didum* transcript localised to the oocyte from early stages beginning at stage 1 in the germarium and becoming an anterior band at mid stages (6−8). Later stages (9−10) show high levels of expression, with signal apparent in the nurse cells and loss of the anterior banding pattern. Later still, the transcript is dumped into the oocyte. A brief description of oogenesis follows: each ovary consists of 15−20 ovarioles joined at their ends by terminal filaments [26]. At the tip of each ovariole are 1−4 germ line-derived stem cells, which divide to produce a daughter stem cell and a cystoblast. The cystoblast undergoes a series of four further mitotic divisions, during which cytokinesis is incomplete, to produce a cyst of 16 cells (cystocyte) connected by intercellular bridges called ring canals. One of these 16 cells differentiates to become the oocyte while the remaining 15 become polyploid nurse cells, which supply material to the developing oocyte. Somatically derived follicle cells migrate to surround the cystocyte to form an egg chamber. These follicle cells produce yolk proteins, the vitelline membrane and the chorion and have essential roles in establishing polarity within the developing oocyte.

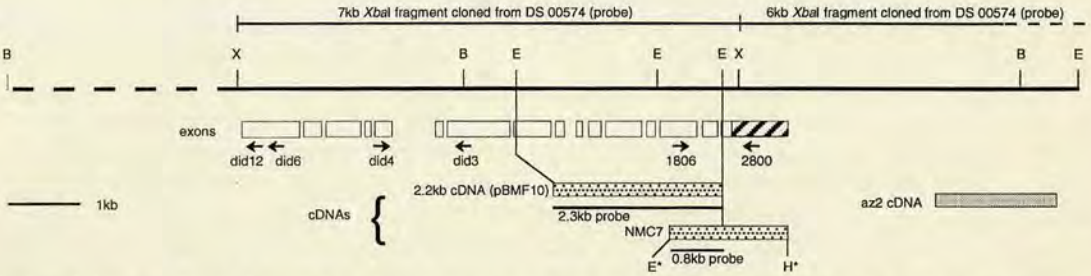

Fig. 2. Organisation of the gene. Physical map of the genomic region. The solid line represents cloned DNA, the dashed line represents an upstream *Bam*HI restriction fragment. Open boxes represent exons, with the cross-hatched section representing the 3′ untranslated region, while shaded boxes represent cDNAs. The *az2* gene maps 3′ to the *didum* gene and encodes a putative zinc-finger-containing protein. Thin lines represent the cDNA and genomic fragments used as probes. Restriction endonucleases: B, *Bam*HI; E, *Eco*RI; H, *Hin*dIII; X, *Xba*I. The sites in cDNA NMC7 marked with an asterisk (*) are part of the vector cloning sites.

ing polarity within the developing oocyte. Our laboratory is investigating the molecular mechanisms involved in oogenesis by examining a number of enhancer trap lines for interesting patterns of reporter-gene expression.

One enhancer trap line exhibited a temporal and spatial expression pattern in subsets of follicle cells. As these lines were *P*[*lacZ*;*rosy*] insertions, a genomic library was prepared with clones that spanned the P element. In this way, DNA flanking the insertion was isolated and used to screen a λNM1149 whole-body cDNA library and a number of independent cDNAs were obtained. One cDNA of 1.6 kb, called NMC7, was used to perform in situ hybridisation on whole-mount ovaries, with the result shown in Fig. 1. The expression pattern observed was unrelated to the original reporter gene expression pattern from the enhancer trap line. However, it did reveal a transcript localised to the oocyte from an early stage (germarial stage 2), with the localisation confined to the anterior margin of the oocyte during middle stages (6−8) of development. Later vitellogenic stages (9−11) showed strong expression in the nurse cells and a loss of anterior localisation in the oocyte. This expression pattern is similar to that seen for *orb* [18] and the early localisation in the oocyte suggested possible roles in oocyte determination and maturation.

Examination of the enhancer trap line by in situ hybridisation to the polytene chromosomes showed two P element insertions on the third chromosome, whereas the cloned gene was localised to chromosome 2 by the same method (see later). It remains unclear how NMC7 was identified via the enhancer trap procedure; however, the expression pattern it generated was of interest and we therefore pursued an analysis of this cDNA.

The NMC7 cDNA insert was 1.6 kb and was subcloned into pBluescript as a 0.8-kb *Eco*RI fragment, pNMC7a and a 0.8-kb *Eco*RI-*Hin*dIII, pNMC7b (Fig. 2). The 0.8-kb fragment from pNMC7a was used to screen an ovarian cDNA library in λZAP II. The largest recombinant plasmids contained cDNA inserts of 2.2 kb (pBMF10). Sequence information determined from the ends of these plasmids showed that they overlapped with NMC7, as shown in Fig. 2. All cDNAs isolated from the λZAP library terminated at the *Eco*RI site within NMC7, suggesting that the *Eco*RI sites of the cDNA inserts had been restricted during construction of the ovarian λZAP library.

In total, these cDNAs represented 3.2 kb of this gene. The DNA sequence was determined on both strands by subcloning overlapping fragments from the cDNAs into pBluescript and by the use of several oligonucleotide primers. An incomplete open reading frame encoding 816 amino acids and the 3′ untranslated region of 661 nucleotides were observed. Database searches revealed significant similarity to the class-V unconventional myosins.

A Northern blot showed that the transcript from this gene was about 6.5 kb in size, strongly suggesting that this gene would encode a full-length unconventional myosin (result not shown). Extensive screening of cDNA libraries prepared from embryonic, larval, and adult testes tissue failed to provide any additional cDNAs. Therefore, a strategy to clone and sequence genomic DNA and to determine the cDNA sequence by reverse transcription PCR was adopted. The chromosome position had been identified as 43BC from in situ hybridisation to polytene chromosomes (result not shown). From this information, a number of P1 recombinant phage containing *Drosophila* genomic DNA were obtained from the *Drosophila* sequencing/mapping project [27] that mapped to this region. DNA was prepared from these P1s and analysed by dot blotting, with the 2.2-kb cDNA showing hybridisation to P1 DS00574. Mini-libraries

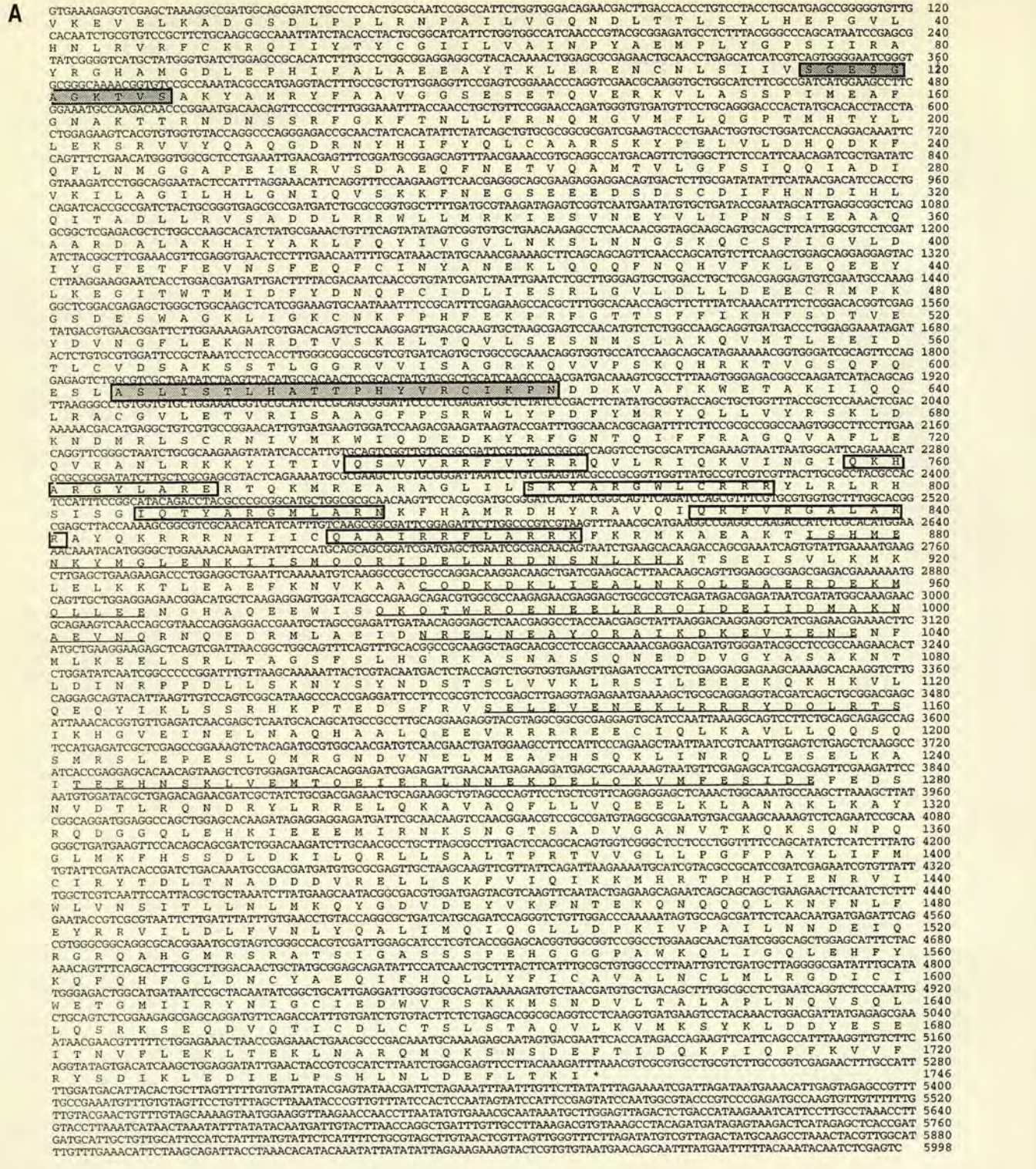

Fig. 3. Sequence and IQ motifs. Partial DNA sequence and deduced protein translation for the *didum* gene. The ATP-binding domain is shown in the shaded box, while a dashed underline shows the actin-binding domain. The central, defining portions of the IQ motifs are shown in the open boxes. Regions predicted to form coiled-coil α-helices are underlined. The IQ motifs are also shown aligned separately.

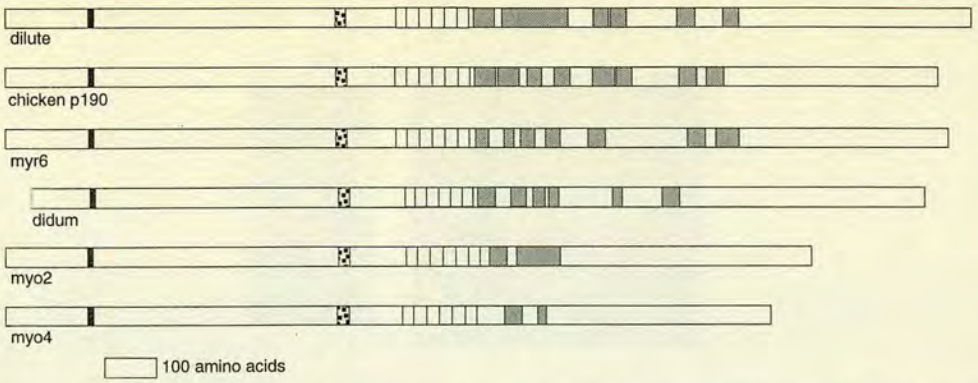

Fig. 4. Comparison of unconventional class-V myosins. Schematic representation of the class-V unconventional myosins; mouse *dilute* (X57377), chicken p190 (Z11718, X67251), rat *myr6* (U60416), yeast *MYO2* (M35532), yeast *MYO4* (M90057), *C. elegans hum-2* (U52516) and the new *Drosophila* sequence, *didum* (Y08160). The black shaded box represents the ATP-binding site, the hatched box represents the actin-binding domain. IQ motifs are represented by six adjacent open boxes. Coiled-coil domains are represented by shaded boxes and were predicted by the MacStripe program [22] using a window of 21 amino acids.

Table 1. Percentage sequence similarity and identity at the amino acid level of members of the class-V myosins. Full-length sequences aligned using GCG GAP program with gap weight = 12, length weight = 4 (program defaults).

	Didum	*dilute*	*myr6*	p190	myo2	myo4
Drosophila didum	–					
Mouse *dilute*	53/42	–				
Rat *myr6*	52/41	72/62	–			
Chicken p190	54/42	94/92	72/63	–		
Yeast myo2	44/34	44/34	44/36	46/35	–	
Yeast myo4	42/33	44/34	44/33	44/34	60/52	
C. elegans hum-2	46/36	49/38	48/37	49/38	41/30	41/30

were prepared from P1 DS00574 using the restriction enzymes *Bam*HI, *Eco*RI and *Xba*I with a 7-kb *Xba*I fragment isolated by hybridisation to the 2.2-kb cDNA. Further fragments have been isolated from all three mini-libraries which span the 3′ end of the myosin V and an additional, previously unreported, gene encoding a putative zinc-finger-containing protein, which we have named *az2*, was also isolated [28].

DNA sequence information from the 7-kb *Xba*I fragment showed, upon translation, that this fragment contained most of the missing 5′ sequence related to the myosin V. A cDNA fragment was produced by designing primers to the known cDNA and genomic sequences and performing reverse transcription PCR. The DNA sequence was then determined by designing further primers and "walking" along the PCR-generated cDNA fragment. Attempts were made to obtain the estimated 500-bp of missing 5′ cDNA sequence by 5′ RACE (Gibco-BRL), using both total RNA and poly(A)-rich RNA, but have not generated the missing region yet. A summary of the physical map is shown in Fig. 2, while the cDNA sequence with deduced translation is shown in Fig. 3.

Sequence analysis. All myosins have a head region comprising an ATP-binding domain and an actin-binding domain. Class-V myosins are further distinguished by six 'IQ' repeats, which are believed to bind regulatory light chains, and a tail domain with regions predicted to form coiled-coil α-helices and yet other regions predicted to form globular domains of unknown function. All these features can be identified in the deduced peptide sequence demonstrating that this gene encodes a class-V myosin in *Drosophila* (Fig. 4). A comparison of the deduced peptide

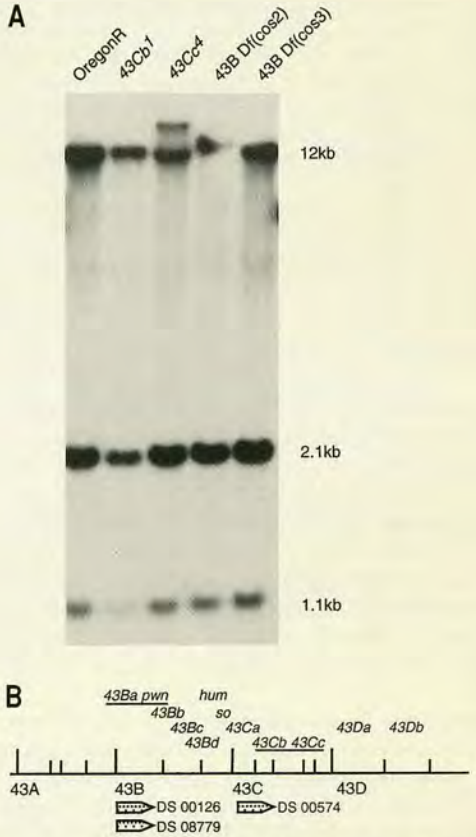

Fig. 5. Genetic analysis of *didum*. (A) Southern blot of genomic DNA digested with *Eco*RI from lines with similar chromosomal background (*43Cb*[1], *43Cc*[4], *cos*[2] and *cos*[3] from Heitzler et al. [30] and *OregonR* wild type). An additional band is visible at a high molecular mass in the *43Cc*[4] lane. Extended incubation (not shown) indicates that this result is not due to partial digestion. Probe used for this result was the 7-kb *Xba*I genomic fragment, which spans most of the myosin-V coding sequence. (B) Schematic map of the 43 region based on the results of [30]. Genes are shown above the main line, with those underlined being unordered with respect to each other. P1-cloned genomic DNA is shown below the main line.

sequence to other members of the myosin-V class shows that the *didum* gene product has significant sequence similarity and is shown in Table 1.

We also observed significant similarity to a murine cDNA encoding a 723-amino acid protein described as a glutamate de-

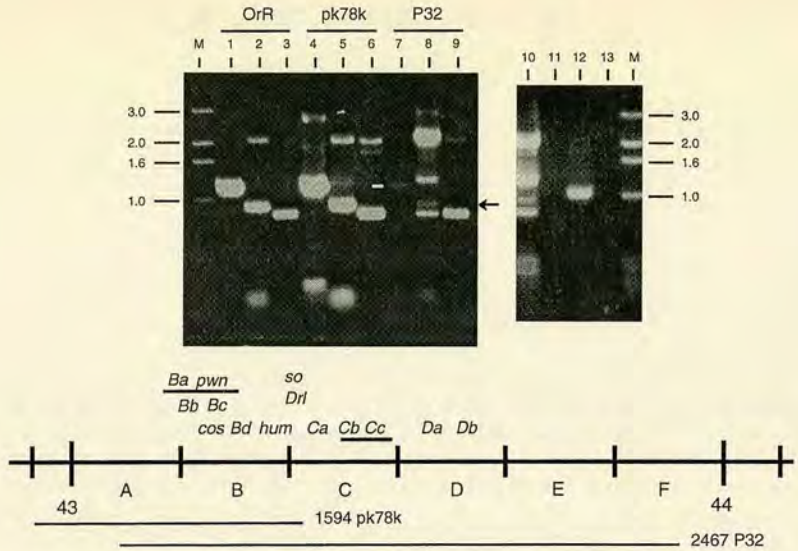

Fig. 6. PCR analysis of putative *didum* mutants. PCR results from genomic DNA derived from homozygous deficient embryos (P32 and pk78k) and wild type (*OregonR*). Lanes 1, 4 and 7 are *didum*-derived products using primers 1806 and 2800. Lanes 2, 5 and 8 are products from the *sine oculis* (*so*) gene. Lanes 3, 6 and 9 are PCR products for a kinase gene located on chromosome 3 used as positive control. Lane 7 shows significant reduction of *didum* product in deficiency line P32 (white line). Lane 8 shows similar reduction of the specific *so* gene product (black arrow); however, large amounts of spurious PCR products are also observed in lane 8. Lanes 10 and 11 show PCR from this deficiency (P32) with individual *so* primers, so1 and so4, respectively. Lane 12 is a *didum* cDNA plasmid control with primers 1806 and 2800, while lane 13 is a control without template DNA. DNA marker sizes shown are in kb. A schematic map of the 43BC region and the regions covered by the deficiencies is also shown.

carboxylase (GAD) [29]. However, this gene is most likely to be a truncated cDNA from a second class-V myosin in the mouse. We have isolated a 4.5-kb murine cDNA using PCR primers based on the sequence of Huang et al. [29] and can identify an actin-binding domain and IQ motifs within the translated sequence (B. MacIver et al., unpublished results). In parallel, recent work has shown an ortholog in rat (*myr6*) which encodes a full-length myosin V [17] and is 96% identical at the DNA level to the 'GAD' cDNA.

The consensus sequence for the 'IQ' motif includes the residues IQXXXRGXXXRR; however, we note that the third motif shows sequence variation in that the defining 'IQ' is replaced by LS. Sequence variation is observable in other class-V myosins at the 'I' position, but not at the 'Q' position. An alignment of these 'IQ' motifs is shown in Fig. 3.

Genetic analysis. As mentioned earlier, the chromosome position of the *didum* gene is 43BC, as determined by in situ hybridisation to polytene chromosomes. The P1 DS00574, in which *didum* is located, was mapped to 43C by the *Drosophila* Genome Sequencing Project [27]. The 43 region has been extensively analysed for complementation groups at the genetic level and 27 complemetation groups have been identified [30]. Genes in the 43BC region include the frequently used marker *pawn*, the maternal effect gene *humilis* and the gene encoding a homeobox-containing protein required for eye development, *sine oculis* [31], in addition to seven uncharacterised embryonic lethal genes (*43Ba*, *43Bb*, *43Bc*, *43Bd*, *43Ca*, *43Cb* and *43Cc*). We have examined all available deficiency lines and X-ray-derived mutations from the 43BC region by Southern analysis using genomic fragments spanning the *didum* gene as a probe (7-kb and 6-kb *Xba*I fragments, as shown in Fig. 2). We observe a band shift associated with the $43Cc^4$ mutation (X-ray induced), as shown in Fig. 5. This band shift maps at least 4 kb 5′ of the cloned genomic DNA and, thus, from this result alone, we cannot be absolutely confident that the *didum* gene is *43Cc*. The observed band shift is not due to polymorphisms as the shift is not observed in other lines from this study with the same chromosomal background. We did not observe any band shifts associated with deficiencies or mutated genes from the 43B region, although there are polymorphisms in this region.

We have confirmed by PCR that the *didum* gene maps to 43C on genomic DNA from homozygous embryos deficient for 43C (line P32) and 43B (line pk78 k) using primers 1806 and 2800 in the 3′ region (Fig. 2). The deficiency lines were crossed to wild-type *OregonR* flies to remove the balancer chromosomes, then embryos that failed to hatch were collected for DNA preparation. DNA from line P32 showed a much reduced level of product (Fig. 6, lane 7) compared with the controls. We propose that the low level of *didum* product observed in lane 7 resulted from natural death in a small number of *OregonR* embryos.

Expression profile. In addition to observing the expression pattern by in situ hybridisation in whole-mount ovaries, we have analysed the expression of the *didum* gene by Northern blotting. We observe strong expression only in adult ovaries and testes, with the testes transcript slightly smaller than that from the ovary (Fig. 7A). We observe expression in the early embryo, which is likely to be due to the stored maternal mRNA transferred to the oocyte in late oogenesis. However, all genes corresponding to the chromosomal position 43C, are essential genes and show an embryonic lethal phenotype and we infer from this observation that the *didum* gene is expressed in the embryo even though levels of expression must be too low to detect on the Northern blots. To resolve this anomaly, a reverse transcription PCR strategy was employed and we established that low levels of expression can be detected in non-gonadal tissues (Fig. 7C). We examined *tudor* flies, which have a mutation which results in loss of the germ line, and observed a band corresponding to the transcript. This band was also observable in the carcass from female *OregonR* flies. Thus, the *didum* is also expressed in the embryo and in adult somatic cells at low levels.

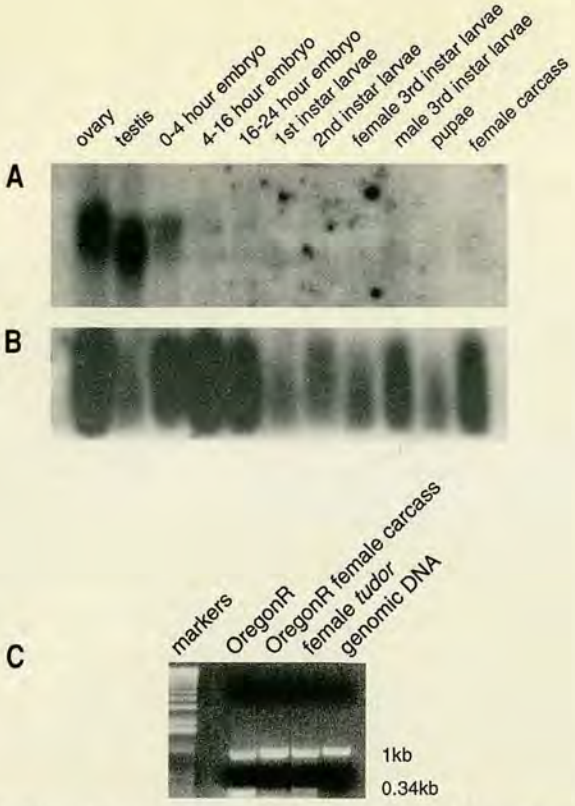

Fig. 7. Expression of *didum* during development. (A and B) Developmental profile. Northern blot with total RNA from various developmental stages hybridised with a ^{32}P-labelled 2.2-kb cDNA probe. (A) The approximate 6.5-kb *didum* transcript. (B) An ~600-bp RP49 transcript used as loading check. The lengthening of the bands is due to the high amounts of total RNA used, as it has not been observed on other Northern blots which have used less RNA. (C) Reverse transcription PCR result performed with primers did3 and did4, which span the largest intron (Fig. 2). The transcript produces a 343-bp band, whereas genomic DNA produces a 1000-bp band. Markers are Gibco-BRL 1-kb ladder.

DISCUSSION

Our results demonstrate that *Drosophila melanogaster* possesses a class-V myosin. We identified this gene by observing a transcript localised to the oocyte during early stages of oogenesis. This localisation pattern was similar to that seen for the *orb* and *oskar* [32] genes, which have fundamental roles in oogenesis and embryogenesis, respectively.

The deduced protein has all the required characteristics of a class-V myosin; the myosin-head region with its ATP and actin-binding domains, the six 'IQ' repeats and a tail domain with regions showing a very high probability of forming coiled-coil α-helices. It is interesting to note that the 'IQ' residues in the third IQ repeat are replaced by LS (leucine, serine) and that this substitution is unique to the *Drosophila* protein. Further functional studies on light-chain binding will determine the significance of this substitution.

The early expression of this gene suggests an involvement in oocyte differentiation, perhaps by localising specific factors within the oocyte. Mid stages of oogenesis show anterior localisation of the myosin-V transcript, again suggesting a role in oogenesis. Later stages of oogenesis show strong levels of expression in the nurse cells and a transfer of transcripts to the oocyte suggesting a subsequent role in embryogenesis. We know that during oogenesis mRNA/protein complexes are transported to the posterior of the oocyte where they become localised. We speculate that this transport could be similar to the vesicle transport role observed in mouse and yeast and involve myosin V. Most investigations of transportation systems within the oocyte have focused on the microtubule network with all localised RNAs showing a dependence on this network. Indeed, *didum* transcript's localisation is affected by depolymerising the microtubule network (A. McCormack and M. Bownes, unpublished results). There is also increasing evidence that transportation and localisation of molecules and organelles involves both the microtubule network and actin filaments [33]. Recent results in *Xenopus* [34] and fish [35] lend further support to this hypothesis, which showed myosin-V protein localised to microtubule-binding melanosomes in *Xenopus*. We can envisage that microtubule-dependent localisation is used to transport material from the nurse cells to the oocyte, then specific actin-based transport is used to refine the localisation or is involved in anchoring the organelles or perhaps, in this case, complexes of RNAs and proteins. Further insights into the oocyte-specific role of the *didum* gene will be ascertained when mutant germ-line clones in this gene have been generated.

Both the *dilute* gene and the *myr6* ortholog are widely expressed in mouse [4, 17], with transcripts observed in brain, kidney, spleen, thymus, testis, liver and muscle; we are currently investigating whether these genes are expressed in the ovary. We observe high levels of *didum* expression in the germ line of *Drosophila*, moderate levels of transcript in early embryos and very low levels in somatic cells at other developmental stages.

Several other myosins are known to function in oogenesis. The *myosin-Ib* gene is expressed in the follicle cells during oogenesis, initially in all follicle cells, but by stage 10, only in the columnar cells surrounding the oocyte [36]. Antibody detection shows that this myosin has a basolateral location followed later by an apical location within the follicle cells. This apical location may be associated with the actin-containing microvilli that extend from the follicle cells into the perivitelline space and is possibly associated with secretion of yolk proteins, the vitelline membrane and the chorion.

The 95F class-VI myosin has essential functions during embryogenesis [37, 38]. Work in our laboratory has also shown that this myosin functions in oogenesis with disruption of the gene resulting in defects in follicle cell migration (W.-M. Deng and M. Bownes, unpublished results). Follicle cell movements are also dependent on non-muscle myosin II, a conventional myosin [39]. Non-muscle myosin II forms bipolar filaments and is thought to drive cellular contractile events. Mutations in the regulatory light chain gene, *spaghetti squash*, of this myosin complex affect the centripetal migration of the follicle cells that surround the anterior of the developing oocyte [39]. Strong staining of this myosin is also seen in the border cells. The *spaghetti squash* mutation also produces a 'dumpless' phenotype, where the nurse cells fail to transfer their cytoplasm into the oocyte, showing that non-muscle myosin functions within the germ line [40].

Two distinct class-V myosin genes have been described in the budding yeast, a lower eukaryote. There are also two distinct genes in the mouse (*dilute* and the *myr6* ortholog) and it is probable that orthologs of these genes have been identified in humans [41]. It will be interesting to see whether a second myosin-V gene can be isolated in *Drosophila* and to investigate the functions of both molecules within this class of unconventional myosins.

Our results show that *didum* maps to the 43C region with analysis of all available aberrations in this region, suggesting *didum* corresponds to *43Cc*. The aberration seen in *43Cc* maps several kilobases 5′ of our cloned genomic DNA but, as yet, we have a small region of 5′ DNA missing from the cDNA and there is the potential for further introns. The *43Cb* and *43Cc*

genes are unordered in the genetic analysis, suggesting that they map very close together. This observation correlates well with our isolation of the *az2* zinc-finger-encoding gene, which maps close to, and immediately 3′ of *didum* [28]. It is necessary to isolate further mutations to ensure that *didum* corresponds with *43Cc*. The best option would be to locate a lethal P insertion in or near the gene; this would allow us to confirm insertion in the gene by plasmid rescue and sequencing of the DNA flanking the insertion. We could then confirm the genetic position by complementation mapping with the P insertion and the 43C alleles available. However, should it be found that *didum* actually corresponds to an adjacent gene, it is still the case that it is an essential gene, since all the nearby genes are embryonic lethals. Now that a myosin V is at hand in a genetically amenable organism such as *Drosophila*, further progress can be made in the understanding of the functions and molecular interactions of these intriguing molecules.

We would like to thank Adrian Bird and Vicki Clark for use of an automated sequencing facility and Nicola Preston for further automated sequencing. B. M. received a studentship from the Darwin Trust of Edinburgh, A. M. received a studentship from the Biotechnology and Biological Sciences Research Council. R. S. was supported by a Wellcome Trust project grant to M. B. This research project was funded by grants from the Wellcome Trust.

REFERENCES

1. Goodson, H. V. & Spudich, J. A. (1993) Molecular evolution of the myosin family: relationships derived from comparisons of amino acid sequences, *Proc. Natl Acad. Sci. USA 90*, 659–663.
2. Cheney, R. E., Riley, M. A. & Mooseker, M. S. (1993) Phylogenetic analysis of the myosin superfamily, *Cell Motil. Cytoskeleton 24*, 215–223.
3. Mooseker, M. S. & Cheney, R. E. (1995) Unconventional myosins, *Annu. Rev. Cell Dev. Biol. 11*, 633–675.
4. Mercer, J. A., Seperack, P. K., Strobel, M. C., Copeland, N. G. & Jenkins, N. A. (1991) Novel myosin heavy-chain encoded by murine dilute coat colour locus, *Nature 349*, 709–713.
5. Bement, W. M., Hasson, T., Wirth, J. A., Cheney, R. E. & Mooseker, M. S. (1994) Identification and overlapping expression of multiple unconventional myosin genes in vertebrate cell-types, *Proc. Natl Acad. Sci. USA 91*, 6549–6553.
6. Baker, J. P. & Titus, M. A. (1997) A family of unconventional myosins from the nematode *Caenorhabditis elegans*, *Mol. Biol. 272*, 523–535.
7. Silvers, W. K. (1979) *The coat colors of mice.* Springer, Berlin Heidelberg New York.
8. Provance, D. W., Wei, M., Ipe, V. & Mercer, J. A. (1996) Cultured melanocytes from dilute mutant mice exhibit dendritic morphology and altered melanosome distribution, *Proc. Natl Acad. Sci. USA 93*, 14554–14558.
9. Wu, X., Boweres, B., Wei, O., Kocher, B. & Hammer, J. A. (1997) Myosin V associates with melanosomes in mouse melanocytes: evidence that myosin V is an organelle motor, *J. Cell Sci. 110*, 847–859.
10. Johnston, G. C., Pendergast, J. A. & Singer, R. A. (1991) The *Saccharomyces cerevisiae MYO2* gene encodes an essential myosin for vectorial transport of vesicles, *J. Cell Biol. 113*, 539–551.
11. Hill, K. L., Catlett, N. L. & Weisman, L. S. (1996) Actin and myosin function in directed vacuole movement during cell division in *Saccharomyces cerevisiae*, *J. Cell Biol. 135*, 1535–1549.
12. Haarer, B. K., Petzold, A., Lillie, S. H. & Brown, S. S. (1994) Identification of *MYO4*, a second class V myosin gene in yeast, *J. Cell Sci. 107*, 1055–1064.
13. Jansen, R. P., Dowzer, C., Michaelis, C., Galova, M. & Nasmyth, K. (1996) Mother cell-specific HO expression in budding yeast depends on the unconventional myosin myo4p and other cytoplasmic proteins, *Cell 84*, 687–697.
14. Espindola, F. S., Cheney, R. E., Matteoli, M., Nascimento, A. A. C., Decamilli, P. V., Larson, R. E. & Mooseker, M. S. (1992) Biochemical and immunological characterization of p190-calmodulin complex from vertebrate brain: a novel calmodulin binding protein, *J. Cell Biol. 119*, 1541–1557.
15. Espreafico, E. M., Cheney, R. E., Matteali, M., Nascimento, M. C., De Camilli, P. V., Larsen, R. E. & Mooseker, M. S. (1992) Primary structure and cellular localization of chicken brain myosin-V, an unconvential myosin with calmodulin light chains, *J. Cell Biol. 119*, 1541–1557.
16. Cheney, R. E., O'Shea, M. K., Heuser, J. E., Coelho, M. V., Wolenski, J. S., Espreafico, E. M., Forscher, P., Larson, R. E. & Mooseker, M. S. (1993) Brain myosin-V is a two-headed unconventional myosin with motor activity [see comments], *Cell 75*, 13–23.
17. Zhao, L. P., Koslovsky, J. S., Reinhard, J., Bähler, M., Witt, A. E., Provance, D. W. & Mercer, J. A. (1996) Cloning and characterization of myr-6, an unconventional myosin dilute/myosin-V family, *Proc. Natl Acad. Sci. USA 93*, 10826–10831.
18. Lantz, V., Ambrosio, L. & Scheds, P. (1992) The *Drosophila orb* gene is predicted to encode sex-specific germline RNA-binding proteins and has localised transcripts in ovaries and early embryos, *Development 8*, 598–613.
19. Kim-Ha, J., Smith, J. L. & Macdonald, P. M. (1991) *oskar* mRNA is localised to the posterior pole of the *Drosophila* oocyte, *Cell 66*, 23–25.
20. Sanger, F., Nicklen, S, & Coulson, A. R. (1977) DNA sequencing with chain-terminating inhibitors, *Proc. Natl Acad. Sci. USA 74*, 5463–5467.
21. Devereux, J., Haeberli, P. & Smithies, O. (1984) A comprehensive set of sequence analysis programs for VAX, *Nucleic Acids Res. 12*, 387–395.
22. Knight, A. E. (1994) *The diversity of myosin-like proteins* (PhD thesis), University of Cambridge.
23. Lupas, A., van Dyke, M. & Stock, J. (1991) Predicting coiled coils from protein sequences, *Science 252*, 1162–1164.
24. Tautz, D. & Pfeifle, C. (1989) A non-radioactive in situ hybridization method for the localization of specific RNAs in *Drosophila* embryos reveals translational control of the segmentation gene *hunchback*, *Chromosoma 98*, 81–85.
25. Ashburner, M. (1989) *Drosophila, a laboratory handbook*, Cold Spring Harbor Laboratory Press, Cold Spring Harbor.
26. King, R. (1970) *Ovarian development in Drosophila melanogaster*, Academic Press, New York.
27. Hartl, D. L., Nurminsky, D. I., Jones, R. W. & Lozovskaya, E. R. (1994) Genome structure and evolution in *Drosophila*: applications of the framework P1 map, *Proc. Natl Acad. Sci. USA 91*, 6824–6829.
28. McCormack, A., MacIver, B. & Bownes, M. (1998) Cloning and expression of *az2*, a putative zinc finger transcription factor from *Drosophila melanogaster*, *Dev. Genes Evol. 208*, 172–174.
29. Huang, W.-M., Fourquet, L. R., Wu, E. & Wu, J.-Y. (1990) Molecular cloning and amino acid sequence of brain L-glutamate decarboxylase, *Proc. Natl Acad. Sci. USA 87*, 8491–8495.
30. Heitzler, P., Coulson, D., Saenz-Robles, M.-T., Ashburner, M., Roote, J., Simpson, P. & Gubb, D. (1993) Genetic and cytogenetic analysis of the 43A-E region containing the segment polarity gene costa and the cellular polarity genes *prickle* and *spiny-legs* in *Drosophila melanogaster*, *Genetics 135*, 105–115.
31. Serikaku, M. A. & O'Tousa, J. E. (1994) *sine oculis* is a homeobox gene required for *Drosophila* visual system development, *Genetics 139*, 1137–1150.
32. Kim-Ha, J., Webster, P. J., Smith, J. L. & Macdonald, P. M. (1993) Multiple RNA regulatory elements mediate distinct steps in localization of *oskar* mRNA, *Development 119*, 169–178.
33. Langford, G. M. (1995) Actin- and microtubule-dependent organelle motors: interrelationships between the two motility systems, *Curr. Opin. Cell Biol. 7*, 82–88.
34. Rogers, S. L. & Gelfand, V. I. (1998) Myosin cooperates with microtubule motors during organelle transport in melanophores, *Curr. Biol. 8*, 161–164.
35. Rodionov, V. I., Hope, A. J., Svitkina, T. M., Borisy, G. G. (1998) Functional coordination of microtubule-based and actin-based motility in melanophores, *Curr. Biol. 8*, 165–168.
36. Morgan, N. S., Heintzelman, M. B. & Mooseker, M. S. (1995) Characterization of myosin-1a and myosin-1b, two unconventional

myosins associated with the drosophila brush border cytoskeleton, *Dev. Biol. 172*, 51–71.

37. Mermall, V., McNally, J. G. & Miller, K. G. (1994) Transport of cytoplasmic particles catalysed by an unconventional myosin in living *Drosophila* embryos, *Nature 369*, 560–562.
38. Mermall, V. & Miller, K. G. (1995) The 95F unconventional myosin is required for proper organization of the *Drosophila* syncytial blastoderm, *J. Cell Biol. 129*, 1575–1588.
39. Edwards, K. A. & Kiehart, D. P. (1996) *Drosophila* nonmuscle myosin II has multiple essential roles in imaginal disc and egg chamber morphogenesis, *Development 122*, 1499–1511.
40. Karess, R. E., Chang, X. J., Edwards, K. A., Kulkarni, S., Aguilera, I. & Kiehart, D. P. (1991) The regulatory light chain of nonmuscle myosin is encoded by *spaghetti-squash*, a gene required for cytokinesis in *Drosophila*, *Cell 65*, 1177–1189.
41. Hasson, T., Skowron, J. F., Gilbert, D. J., Avraham, K. B., Perry, W. L., Bement, W. M., Anderson, B. L., Sherr, E. H., Chen, Z. Y., Greene, L. A., Ward, D. C., Corey, D. P., Mooseker, M. S., Copeland, N. G. & Jenkins, N. A. (1996) Mapping of unconventional myosins in mouse and human, *Genomics 36*, 431–439.